Design, Performance and Fit of Fabrics for Female Body Armour

A thesis submitted to the University of Manchester for the degree of
Doctor of Philosophy
in the Faculty of Engineering and Physical Sciences

2011

Dan Yang

School of Materials

List of Contents

Words Count: 42555

List of Tables

List of Figures

List of Publications

Journals

Chen, X. and Yang, D., Use of 3D Angle-interlock Woven Fabric for Seamless Female Body Armour: Part I: Ballistic Evaluation, *Textile Research Journal*, 2010. **80**(15): p.1581-1588.

Chen, X., and Yang, D., Use of 3D Angle-interlock Woven Fabric for Seamless Female Body Armour: Part II: Mathematical Modelling, *Textile Research Journal*, 2010. **80**(15): p. 1589-1601.

Conferences

Chen, X., and Yang, D., Pattern Design for Female Body Armour Based on Mouldable Ballistic Fabrics, *International Foundation of Fashion Technology Institutes Conference*, Taipei (Taiwan), 2010.

Yang, D., Pattern Making and Grading for Female Body Armour Panels, *First World Conference on Software for the Textile and Clothing Industries*, Manchester (UK), 2009.

Yang, D., Design and Performance of Continuous and Conformable Fabric Panels for Female Body Armour, *Postgraduate Conference at the University of Manchester*, Manchester (UK), 2009.

Abstract

This thesis focuses on the development of a new technique which enables a novel type of front panel for female body armour to be engineered, providing female contour, high level protection, and therefore comfort in wearing.

The traditional cutting and stitching method can be used to form a dome shape to accommodate the bust area but it gives rise to weakness against projectile impact at the seams. A novel type of fabric with the advantage in mouldability is needed as an alternative to the conventional plain woven fabric in making female body armour without the need of cutting or folding but ease in manufacture. Dome-shaped fabric and angle-interlock woven fabric are two potential candidates. The analysis and comparisons determine the selection of the fabric with superior dome depth which is more suitable for the female body armour application.

Ballistic evaluations on the selected fabric were carried out from two aspects: the overall ballistic performance investigation and the parametric study. The result provided a better understanding of kinetic energy absorption capability of single-piece selected fabrics. Additionally, the ballistic performance of fabric panels was further evaluated in the factory in order to ensure the selected fabric could achieve the commercial requirement.

After the investigations of mouldability and ballistic resistance of the selected fabric, a mathematical model was created, which determines the pattern geometry for the front panel of the female body armour. This mathematical model takes the body figure size and bra size as the input, and the output is the profile of the front panel of female body armour. This work enables the speedy creation of a front panel of the female body armour in the selected fabric. This is an important advance and a novel approach for making seamless female body armour with satisfactory ballistic performance.

Declaration

No portion of the work referred to in the thesis has been submitted in support of an application for another degree or qualification of this or any other university or other institution of learning. To the best of my knowledge and belief, this thesis contains no material previously published or written by another person, except where due deference has been made.

Copy Statement

I. The author of this thesis (including any appendices and/or schedules to this thesis) owns any copyright in it (the 'Copyright') and she has given The University of Manchester the right to use such Copyright including for administrative purposes.

II. Copies of this thesis, either in full or in extracts and whether in hard or electronic copy, may be made **only** in accordance with the Copyright, Designs and Patents Act 1988 (as amended) and regulations issued under it or where appropriate, in accordance with licensing agreements which the University has from time to time. This page must be from a part of any such copies made.

III. The ownership of certain Copyright, patents, designs, trade marks and other intellectual property (the 'Intellectual Property') and any reproductions of copyright works in the thesis, for example graphs and tables ('Reproductions'), which may be described in this thesis, may not be owned by the author and may be owned by third parties. Such Intellectual Property and Reproductions cannot and must not be made available for use without the prior written permission of the owner of the relevant Intellectual Property Rights and/or Reproductions.

IV. Further information on the conditions under which disclosure, publication and commercialisation of this thesis, the Copyright and any Intellectual Property and/or Reproductions described in it may take place is available in the University IP Policy (seehttp://www.campus.manchester.ac.uk/medialibrary/policies/intellectualproperty.pdf), in any relevant Thesis restriction declarations deposited in the University Library, The University Library's regulations (see http://www.manchester.ac.uk/library/aboutus/regulations) and in The University's policy on presentation of Theses.

Acknowledgements

My deep sincere gratitude and thankfulness go first and foremost to my supervisor, Dr. Xiaogang Chen, for his constant encouragement and great guidance throughout the whole project. Without his consistent and illuminating instruction, this thesis could not have reached its present form.

I also wish to thank Mr. Leslie Downes for his technical help in weaving fabrics. I am also deeply impressed by his considerable expertise and humour personality, and I believe the precious friendship between him and me will be cherished and kept in heart forever.

Grateful recognition is directed towards Dr. Richard Kennon whose constructive suggestions and advices motivate me to finish this research as well as possible. I also would like to acknowledge the support of Mr. Nick Clarke, Ms. Wendy Moody and Dr. Pammi Sinha at the School of Materials for pattern making.

My sincere thankfulness also extends to all my colleagues in the Textiles and Paper division at the School of Materials for providing friendly and pleasant working atmosphere. Special thanks go to Dr. Danmei Sun, who helps me to improve my arguments, encourages and inspires me. Dr. Ying Wang and Dr. Fuyou Zhu are also gratefully acknowledged for their great support and advice.

Parents are always the persons I need to extend my great appreciation to for their selfless support, boundless love and endless encouragement.

Last but not the least, special acknowledgement is made to all my friends, and with whom, I have experienced a wonderful and pleasurable life in Manchester.

To all those concerned, thank you very much...

With love and gratitude to my dearest parents

Chapter 1

Introduction

The police and members of armed forces may be deployed in extremely dangerous situations and face the risk of serious injury or fatal wounding, whilst carrying out their duties. Unfortunately civil safety does not have a positive outlook and is seriously threatened by violent crime. In the UK the British Crime Survey demonstrated that crime rose steadily from 1981 to the early 1990s, peaking in 1995. Then crime dropped and showed little overall change though an exception of a statistically significant reduction of 10% occurred in 2007/2008. The frequency of weapon usage in violent crimes has been stable over the past decade, about one in five (21%); though it decreased in recent years due to a reduction in the use of limitation weapons, a rise of 2% of violent crimes was found in the use of shotguns as well as handguns in 2008/2009 [1]. The situation was even worse in the US. Based on the data from the Graduate Institute of International and Development Studies, and US Bureau of Justice Statistics, there were 3.6 firearms homicides per 100,000 population in the US, which was 30 times more than in the UK and 8 times more than in Germany in 2000 [2]. The firearms offence had not changed for almost ten years: it remained 7% of all violent crimes from 1999 to 2008 in the US, reported by US Bureau of Justice Statistics [3].

The civil safety is confronted with even bigger challenges as modern conflicts and warfare are more likely to take place in congested urban streets than war zones, and some of them have become serious terrorist attacks (e.g. the September 11th 2001 New York Attacks, the October 12th 2002 Bali Bombings and the July 7th 2005 London Bombings). Military soldiers are to cooperate with the police officers to guard the civil safety instead of only appearing in the battlefields.

Civil safety has raised the concerns about the importance of body armour, which could improve the potential to save lives during conflicts. Body armour is an integral part of the fighting kit of a wearer as it plays a key role in protecting police or military personnel from enemy threats, warfare tactics and military systems [4-10]. The National Institute of Justice has reported that the risk of fatality from firearms assaults is 14 times higher for officers who are not wearing body armour than those wearing body armour. Figure 1.1 indicates that American police officers have significantly benefited from the introduction and development of body armour, as shown by a decline in the officer deaths [11].

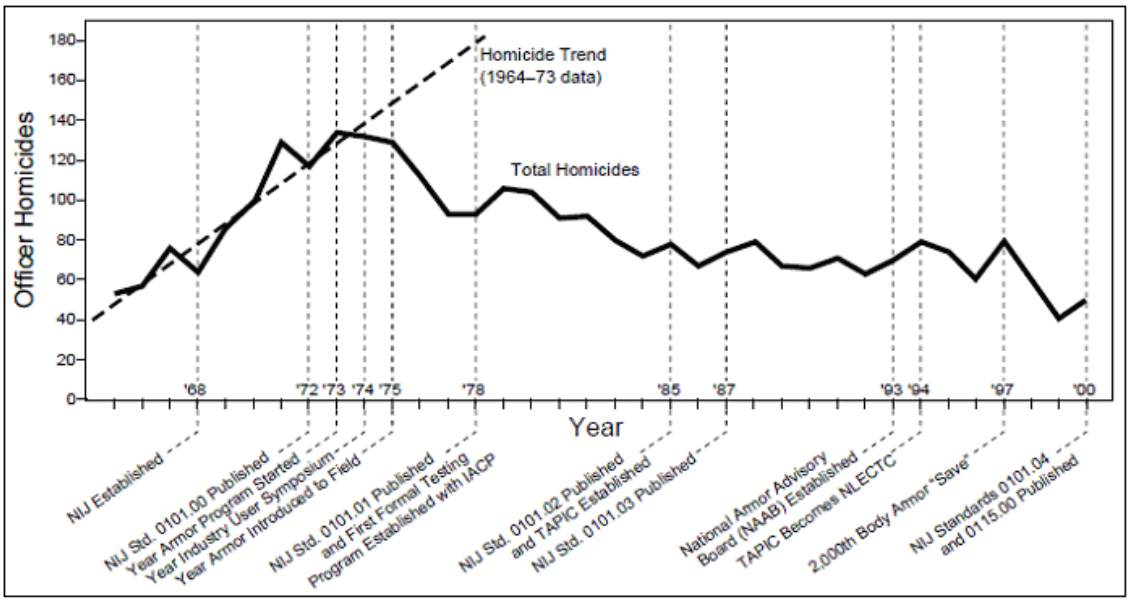

Figure 1.1 Trends in officer homicides in the US, 1965-2000 [11]

1. 1 The Problem

It is true that females have become an important force for guarding the national safety which cannot be ignored. For example, in Europe the percentage of female law enforcement officers in service increased from 20% of the force in 1996 to between 30% and 50% in 2004. The US has already closed to achieving parity between men and women in service [12]. In terms of the percentage of women serving in the military, the ratio approached 9.1% in 2006 in the UK [13]. The US saw the ratio rise dramatically from 1.6% in 1973 to 10.8% in 2007 [14]. Women have been breaking barriers in civil guards and military organisations and will continue to break barriers. However, even though considerable efforts have been made to improve the performance of body armour in various aspects (such as ballistic protection, breathability and comfort to the wearer in response to operational requirements and experiences of police and military forces [15-25]), most of them are primarily concerned for male wearers. Nevertheless, as more and more female police officers and soldiers are exposed to hostile conditions and environments, the need to protect their lives becomes increasingly important.

On the other hand, female body armour has not been improved in parallel. The apparent reflection is that most female officers and soldiers still wear unisex body armour but with smaller sizes. This is obviously unsuitable due to the physiological differences between women and men; incorporating the female torso into a male-based system, may result in disproportionate protective and functional sacrifices. It has been acknowledged that breasts are very sensitive organs; they can be bruised easily but recover slowly. Breast injuries can result in dystrophic calcifications (calcification of degenerated or necrotic tissue), lesions (localised pathological changes in a bodily organ or tissue) or the death of the breast organ; therefore the wounded female may lose a breast or even her life if extensive internal bleeding occurs [26]. Moreover, without a good customised

fit, body armour can become a distraction to the duties of female wearer (as she may feel uncomfortable or even pain on some parts), which will obstruct her mobility and leave her life in danger.

The traditional cutting and stitching method would form dome shapes to accommodate the contour of a female bust. Nevertheless, seams employed in garment production are easily penetrated by small projectiles or fragments at close ranges. Butted seams are particularly vulnerable [27]. Overlapping seams are much stronger in fabric stitching (due to more friction between the fabrics and threads); however, the small ballistic missiles still can break them directly by penetrating and severing the loop of threads among the seams. Fabric folding is another way to form the dome shape but the downside is that there are too many layers which are folded under the armpits, which apparently leads to discomfort in wear. In addition, the weakness of stitches against the projectile impact still exists as many stitches are required during the folding procedure. Therefore, an improved method for making protective and comfortable female body armour is imperative.

1.2 Aims and Objectives

The aim of this project was to research for a new technique to enable a novel type of female body armour to be engineered, which would provide the high level of protection associated with the female contour thus making it fit and comfortable to wear without the need for cutting and stitching.

The first objective was the selection of the techniques that would develop domed fabrics with no requirement for cutting or folding. Three-dimensional dome-shaped fabrics and

angle-interlock woven fabrics were mainly considered. The former type, characterised by dome shapes woven directly from the loom, could be taken into account in the design of the bust area; the latter, classified as one of typical three-dimensional woven structure fabrics, possessed good mouldability and consequently could integrally form the required crater shape. Their deformation depth was studied and compared in order to select the better type. A series of experiments were performed to achieve this purpose.

1) Experimental investigations was undertaken to observe the correlation between the deformation depth of three-dimensional dome-shaped fabrics and the relevant governing parameters - weaves, dome size, radius ratio, number of circles, weft linear density, weft density and shrinkage. The outcome could provide important empirical understanding of the dome formability of the dome-shaped fabrics.

2) The dome formability of angle-interlock woven fabrics was also studied. The results were compared with that of dome-shaped fabrics for the purpose of distinguishing which one possessed better deformation depth. The comparisons would be worthwhile in the selection of techniques for engineering the novel female body armour.

The second objective focused on the ballistic evaluation of the selected fabrics. The single-piece fabrics as well as fabric panels were experimentally evaluated, in order to understand the ballistic-resistant properties of the selected fabrics.

1) By using the ballistic range at the University of Manchester, the overall ballistic performance of the single-piece selected fabrics was evaluated via the comparisons of kinetic energy absorption between the selected fabrics and other different fabrics. Additionally, the ballistic performance of the selected fabrics was extensively investigated under the parametric studies.

2) Fabric panels were evaluated in the ballistic tests to investigate if they could qualify in the commercial market for the NIJ standard. The whole test was strictly carried out at the in-house range of the collaborating factory and the result provided valuable evidence if the selected fabric qualified.

The third objective was to work out a procedure of pattern cutting for the front panel of the female body armour based on the fabric type selected. Mathematical modelling was carried out to determine the pattern geometry. The body size and bra size were taken as the input, and the profile of the front pattern of the female body armour was the output. With this procedure, the front panel of the female body armour was quickly created. This indicated that a novel approach for making a seamless front panel of female body armour, with the satisfactory ballistic performance, could be established.

1.3 Thesis Layout

Chapter 1 is the introductory chapter. Introduction of body armour, ballistic performance of body armour, and current and potential female body armour technologies are mainly reviewed in Chapter 2. The current main technologies include unisex tailoring, cutting and sewing, folding, overlapping, and moulding. But these technologies have different drawbacks in the shape performance, protection, wear ability or comfort so that alternative routes- three-dimensional dome-shaped fabrics and angle-interlock woven fabrics are taken into account.

In Chapter 3, preliminary work on the female body armour technology with the application of three-dimensional dome-shaped fabrics is illustrated. The relationships between the dome formability of dome-shaped fabrics and the relevant governing parameters (e.g. weaves, dome size) are investigated.

Chapter 4 focuses on investigating the mouldability of angle-interlock woven fabrics. Analysis and comparison between dome-shaped fabrics and angle-interlock woven fabrics also have been exhibited in order to select the type with the better deformation depth. Based on this, more extensive study of the selected fabrics' ballistic performance is investigated, as illustrated in Chapter 5.

Chapter 6 presents the pattern creation for the front female body armour panel. On the basis of employing the selected fabric which has good dome formability as well as satisfactory ballistic performance, a mathematical model simulating pattern geometry for the front panel of female body armour has been established, which would lead to

quick creation of front female body armour panel based on the input of the body figure and bra sizes. Chapter 7 ends the thesis with conclusions and future work.

Chapter 2

Literature Review

This chapter mainly aims to review the following aspects: (1) introduction of body armour, (2) ballistic performance of body armour and (3) the current and potential female body armour design technologies. Two important types of fabric, dome-shaped fabric and angle-interlock woven fabric, are also reviewed because of the possibility to be used for female body armour.

2.1 Introduction of Body Armour

2.1.1 History

Body armour is a virtual requirement for police and soldiers especially when anti-social behaviour and global terrorism seem to dominate the headlines of today's news in recent years. Inadequate safety measures could put frontline professionals at unnecessary risk and cause intolerable injuries or harm. In fact, the inclination to wear body armour is nothing novel; various types of materials have been used to protect humans from injuries in battles and other dangerous situations throughout history. Ancient tribes used animal skins and other natural materials to protect their bodies. The warriors of ancient Rome and medieval Europe covered their torsos in metal plates

before going into battles [28]. With the development of civilisations, body armour was advanced and mainly classified into the following three categories [29]:

- Armour made of leather, fabric, or mixed layers of both, sometimes reinforced by quilting or felt;
- Chain mail, made of interwoven rings of iron or steel;
- Rigid armour made of metal, horn, wood, plastic, or some other similar tough and resistant material

However with the advent of more effective weapons e.g. guns and cannons in the 15th century, body armour had to be highly improved against projectiles at high speed. Utilising traditional body armour seemed impossible as most of them were not reliable enough against firearms. Silk, which was already considered by the Japanese in the medieval period, was not recorded as the first use of soft body armour in the USA until the late 19th century. However, the soft body armour made of silk was only effectively against low-velocity bullets travelling at 400 metres per second or less, but not new generation ammunitions travelling at more than 600 metres per second at that time [30]. In the First World War various experiments were carried out to develop soft body armour; linen, tissue, cotton and silk were concerned in the padded neck defence and vests in the UK. The Americans developed bullet-proof body armour by using overlapping steel plates sewn to strong fabric garments against pistol projectiles around the 1920s and 1930s, such body armour could offer good protection but was quite heavy and uncomfortable [29]. The body armour with effective protection against ammunition fragments known as flak jacket was developed in the Second World War. However, the flak jacket was not good enough against most pistol and rifle threats. In addition, as the

flak jacket was sewn with steel plates, the disadvantages in weight and lack of conformability blocked it to be applied widely [30]. A technical breakthrough of body armour research appeared in the 1960s, during which the first ballistic nylon was invented. This newly invented armour which was made of ballistic nylon had reduced weight but improved ballistic protection [29].

The revolution in modern body armour generation was brought about by DuPont after the introduction of its new aramid fibre called Kevlar® in 1965. This kind of fibre, which is five times stronger than steel on an equal weight basis, is widely applied in reliable lightweight bullet-proof body armour [31]. Nowadays, such high-strength and high-performance materials in the application of body armour are fairly popular around the world.

2.1.2 Categories

Body armour mainly functions to protect the human torso from firearm-fired projectiles and fragments from explosions. They can be divided into two main categories based on ballistic threats, i.e. soft body armour and hard body armour as detailed below [32-35].

2.1.2.1 Soft body armour

Soft body armour is used to absorb the impact energy from small calibre handguns and shotgun projectiles, and small fragments from explosives such as hand grenades [36]. Soft body amour is constructed of many layers of flexible woven or laminated fabrics or other ballistic resistant fabrics. The number of layers is around 7-50 layers based on protection levels and fabric styles. The areal density of fabrics is around 90-250 g/m^2 in which condition the ballistic performance could be accurately demonstrated. Those

layers of fabrics are assembled into a ballistic panel. The ballistic panel is in turn inserted into a carrier, an outer layer of garment fabrics with no general ballistic resistance which provides a means of supporting and securing the armour garment to the user. The ballistic panel may be retained or removed from the carrier [37]. The whole armour garment is generally manufactured in the form of vest in consideration of the wearer's mobility during anti-crime activities or military tasks. Covert vest and overt vest are the two main styles [38], as shown in Figure 2.1. The covert vest is concealable, worn underneath a shirt, sweater or casual hoodie, and the overt vest is worn over the uniform.

(a) **(b)**

Figure 2.1 Body armour: (a) covert vest; (b) overt vest [38]

The fabric of soft body armour is made from synthetic polymeric lightweight fibrous materials that exhibit greatly improved ballistic resistance performance [29]. The two main types of fibres used in soft body armour are aramid and high-performance polyethylene. Well-known brands of aramid fibres are Kevlar® registered by DuPont,

Twaron® and Technora® by Teijin Aramid. Dyneema® by DSM and Spectra® by Honeywell belong to the high-performance polyethylene group. In contrast to aramid fibres, the polyethylene fibres, characterised by higher strength but lower specific density, have good resistance to moisture, UV-rays and abrasion. Other important ballistic fibres are ballistic nylon and PBO, albeit they are rarely used in today's market. More details will be demonstrated in the following section. The energy absorption properties of ballistic fibres have been illustrated in Figure 2.2 [39].

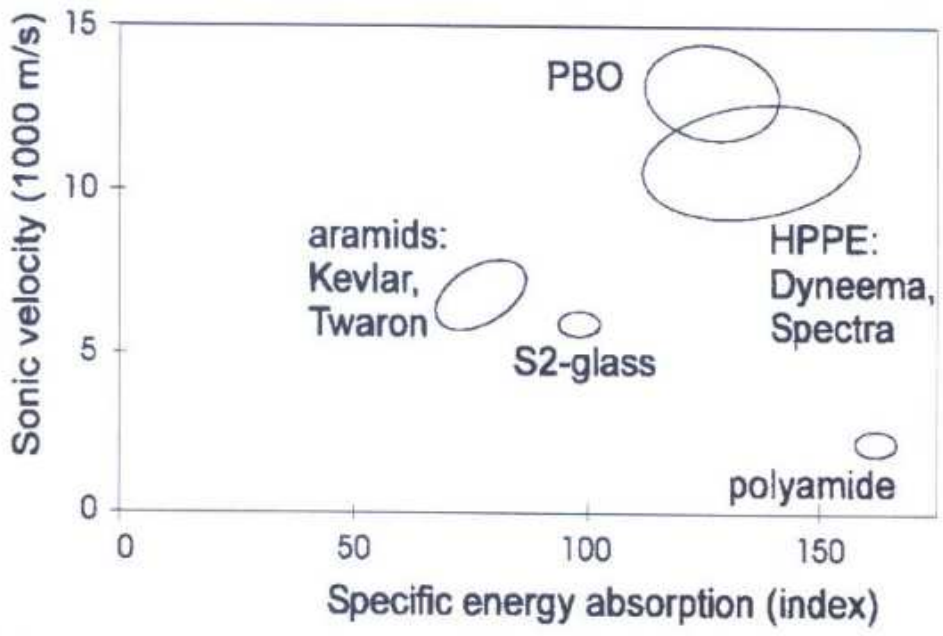

Figure 2.2 Energy absorption properties of high performance fibres [39]

Para-aramid fibres

A para-aramid fibre consists of long synthetic polyamide chains in which at least 85% of the amide linkages are attached directly to two aromatic rings. The polyamide, known as para-phenylene terephalamide, is produced from the reaction between para-phenylendiamine and terephthaloyl chloride at low temperature in a dialkyl amide solvent including hexamethylphosphoramide, N-methyl pyrrolidone and dimethyl acetamide [40]. These highly oriented chains with strong inter-chain bonding largely determine para-aramid fibre's unique chemical and physical properties, such as light

weight, high impact resistance, high strength, excellent thermal and dimensional stability, flame resistance and cut resistance. These excellent characteristics make para-aramid fibres superior in many protective applications. The molecular structure [41] and the scanning electron micrograph (SEM) [40] of typical para-aramid fibre- Kevlar are shown in Figure 2.3.

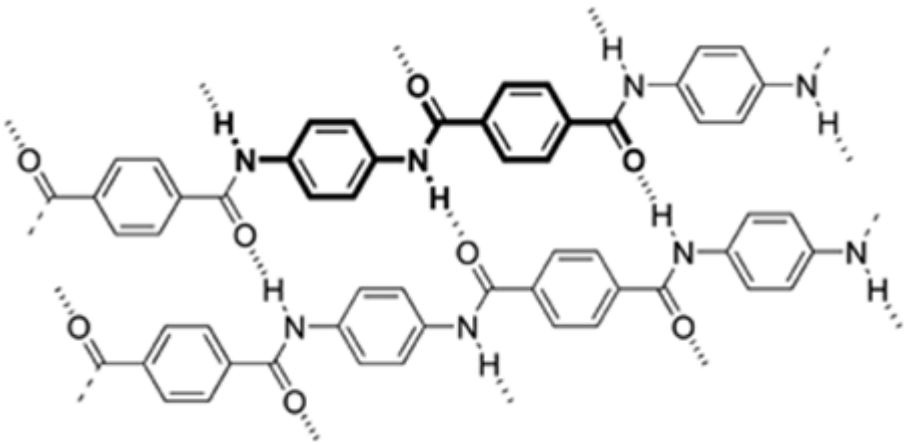

(a)

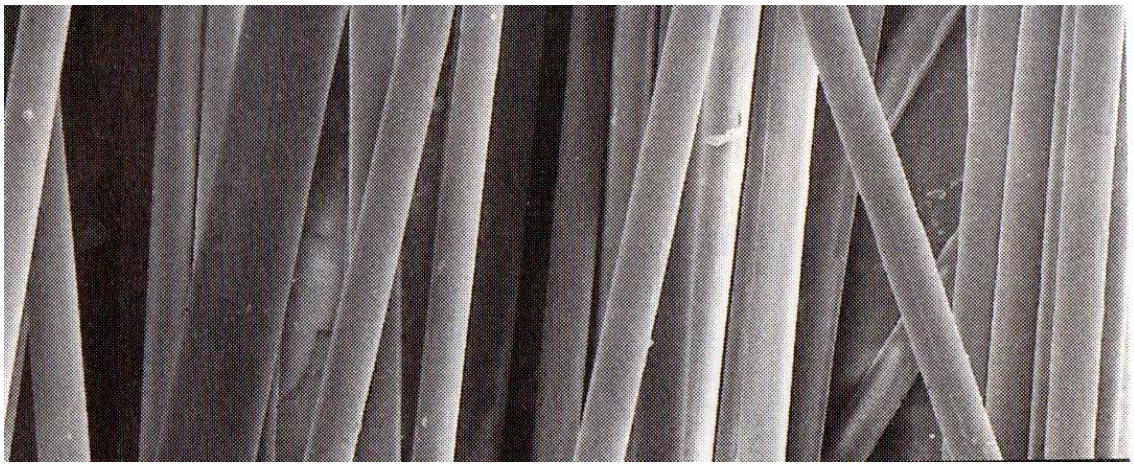

(b)

Figure 2.3 Kevlar: (a) molecular structure [41]; (b) filaments SEM [40]

Kevlar® is a trade mark of para-aramid fibre registered by the DuPont Company. The first Kevlar known as Kevlar® 16 was invented in 1965. Over the four decades of innovations, high tenacity and light weight of Kevlar have been dramatically improved. Currently the most common types used in ballistic applications are Kevlar® 29, Kevlar® 49 and Kevlar® 129. Kevlar® 29 was the first and is now still the original family product

type used in life protection. Kevlar® 49 is a well-known type of high modulus fibre and Kevlar® 129 is renowned for its high tenacity. Their material properties are listed in Table 2.1 [31]. The fibre types with the most used weave structures in the fabric panels for soft body armour are listed in Table 2.2 [42].

Table 2.1 Mechanical properties of various fabrics [31]

		Kevlar® 29 Standard tenacity, andard modulus	Kevlar® 49 High modulus	Kevlar® 129 High tenacity
Decitex		1670	1580	1670
Density	(g/cm^3)	1.44	1.44	1.44
Tenacity	(cN/tex)	207	201	238
	(Gpa)	3000	2900	3427
Modulus	(cN/tex)	5160	7517	6810
	(Gpa)	74	105	95
Elongation at break	(%)	3.5	2.5	3.4
Decomposition temperature in air	(ºC)	427-482	427-482	427-482

Table 2.2 Weave structures [42]

Weave	Linear density warp×weft (denier)	Fabric density warp×weft (per inch)	Thickness (mm)	Areal density (g/m^2)	Breaking strength warp×weft (kg/cm)
Kevlar® 29 and Kevlar® 129					
Plain	840×840	31×31	0.3048	220.59	161×170
Plain	1500×1500	24×24	0.4318	319.00	197×214
Plain	1000×1000	31×31	0.3810	281.67	161×166
Plain	840×840	26×26	0.2540	196.83	134×143
Plain	1500×1500	17×17	0.3048	223.98	139×145
Plain	1420×1420	17×17	0.2794	220.59	152×152
Plain	1000×1000	22×22	0.2540	281.67	116×130
Plain	400×400	32×32	0.1524	108.60	80×77
2×2 Basket	1500×1500	35×35	0.5842	468.32	322×325
2×2 Basket	1420×1420	35×35	0.5842	464.93	349×357
Plain	200×200	40×40	0.1270	71.27	60×58
Plain	3000×3000	17×17	0.6096	461.53	286×322

8×8 Basket	1500×1500	48×48	0.8128	638.00	393×411
4×4 Basket	3000×3000	21×21	0.7620	546.37	357×357
4×4 Basket	3000×3000	24×24	0.7620	610.85	416×447
Kevlar® 49					
Plain	1420×1420	17×17	0.3048	217.19	125×134
Crowfoot	195×195	34×34	0.0762	57.69	38×38
8H satin	380×380	50×50	0.2032	166.29	118×116
Plain	195×195	34×34	0.0762	57.69	46×46
Plain	380×380	22×22	0.1016	74.66	53×53
Plain	1140×1140	17×17	0.2540	169.68	112×115
Crowfoot	1140×1140	17×17	0.2286	169.68	111×114
Plain	1420×1420	13×13	0.2540	162.89	102×107
4×4 Basket	1420×1420	28×28	0.4826	363.12	243×232
4×4 Basket	2130×2130	27×22	0.6350	461.53	326×263
8×8 Basket	1420×1420	40×40	0.6604	509.04	327×320

Polyethylene fibres

Polyethylene fibre consists of ultra high molecular weight polyethylene (UHMWPE) by gel spinning due to thermoplastic characteristic. UHMWPE has a structure composed of extremely long molecule chains with n (number of the repeat unit) greater than 100,000. The molecular structure is shown in Figure 2.4 [43]. The highly parallel oriented molecule chains are the main characteristic of the fibre microstructure of UHMWPE fibres which give its property of high strength and high modulus but low density.

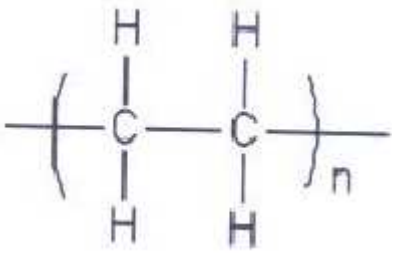

Figure 2.4 Polyethylene molecule [43]

Others

Ballistic nylon is a polyamide fibre which has been used in ballistic applications for a long time. The history of nylon fibre usage dates back to the Second World War. As para-aramid and polyethylene fibres become dominant in protective applications

nowadays due to their superior mechanical properties, nylon fibre is stepping down from the stage of history.

PBO is a new high tenacity fibre under the trademark Zylon® by Toyobo which has extraordinary high compressive strength. It consists of rigid-rod chain molecules of poly (p-phenylene-2, 6-benzobisoxazole). The molecule is shown in Figure 2.5 [44]. It has strength and modulus almost double that of para-aramid fibre and shows the 100ºC higher decomposition temperature than para-aramid fibre. However, it may degrade under UV light and visible light so rapidly that it has become controversial to use body armour made of PBO fibres especially after the incidence of it failing to protect police officers in 2003. In 2005, Zylon was banned from use in the ballistic applications by the National Institute of Justice of U.S. government [44].

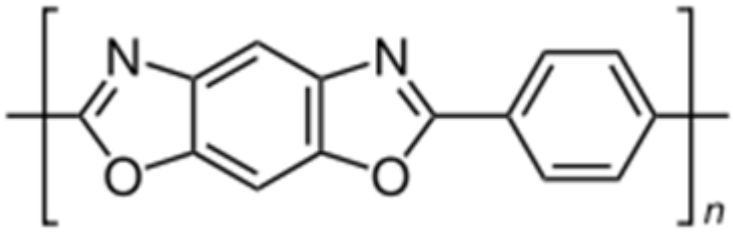

Figure 2.5 Poly (p-phenylene-2, 6-benzobisoxazole) molecule [44]

2.1.2.2 Hard body armour

Hard body armour is used against higher level threats, such as rifle rounds and metallic components. It is constructed by inserting ceramic, metal or plastic plates into the pocket which is on the inside or the outside of the soft body armour to provide additional protection. Nowadays, armour grade ceramics include aluminium oxide, silicon carbide and boron carbide. The materials of those plates possess additional stab-resistant or puncture-resistant abilities due to their tough and rigid properties [29].

Hard body armour is much more weighty and bulkier than soft body armour because it contains rigid ceramic or other types of plates required in front and back of the human torso (though it could offer higher ballistic protection from bursts of fire from submachine guns). Due to its weight and bulkiness, it is impractical for routine use by police officers but is more likely to be worn by military personnel for short periods in the battle against high level threats. Soft body armour is more suitable for routine tasks as it is much more lightweight and comfortable.

2.1.3 Functions

The main function the body armour should possess is ballistic resistance as the most frequent threat faced by police and members of armed forces is from firearms and fragments. Furthermore, stab resistance is important because pointed and sharp-edged weapons are notable fatal threats to the police and military personnel, especially the prison officers, due to the large amount of attacks with such weapons during their duties [45]. Other additional functions of body armour are also considered in order to protect wearers as much as possible.

2.1.3.1 Ballistic resistance

The ballistic resistance of body armour is demonstrated in the form of absorbing the kinetic energy coming from a flying projectile. Body armour consists of multiple layers of very strong fibres, which can absorb and disperse the energy of the impact across a general area when a projectile strikes it. Additional energy is absorbed by each successive layer of material until the projectile has been stopped or the projectile may penetrate all layers if it possesses very strong kinetic energy. Multiple layers also assist in reducing the effects of blunt trauma, caused by the force of the impacting projectile

against the armour, resulting in non-penetrating internal injuries such as bruises, broken ribs or other injuries to internal organs. The typical test apparatus for ballistic testing has been shown in Figure 2.6 [46].

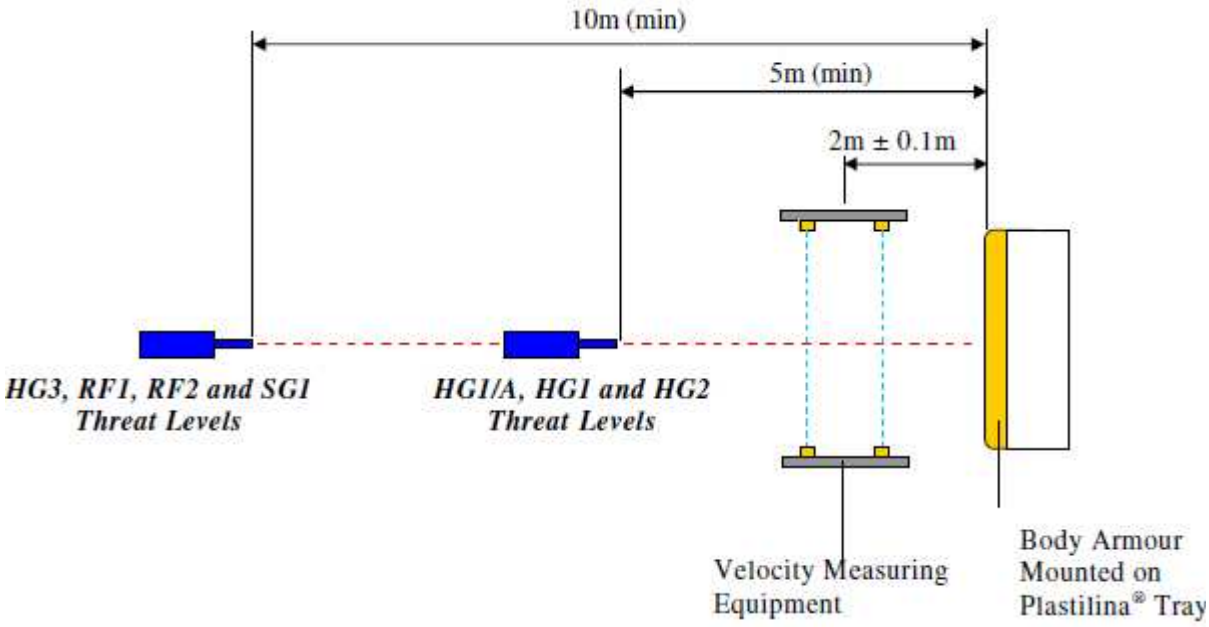

Figure 2.6 Typical test apparatus for ballistic testing [46]

The two most important ballistic test standards are the NIJ standard–0101.04 produced by the US National Institute Justice (NIJ) [47] and the HOSDB standard [46] for the UK police, published by the Home Office Police Scientific Development Branch (HOSDB) at the request of the Self Defence and Restraint Sub-Committee of the Association of Chief Police Officers (ACPO). Seven formal ballistic-resistant body armour classification types have been established in accordance to the NIJ Standard–0101.04, which are listed in Table 2.3 [47]. In the HOSDB standard, the ballistic body armour is classified into five categories as shown in Table 2.4 [46]. Additionally, most countries have their own ballistic standards to correlate with the **c**orresponding national security systems, some of which have been demonstrated in Table 2.5 [48]. In all standards, the body armour protection is evaluated on the ability to stop projectiles with the smallest possible depth of the back face signature.

Table 2.3 NIJ standard-0101.04 P-BFS performance test summary [47]

Test Variables						Performance Requirements					
Armour Type	**Test Round**	**Test Bullet**	**Bullet Weight**	**Reference Velocity (±30 ft/s)**	**Hits Per Armour at 0° Angle of Incidence**	**BFS Depth Maximum**	**Hits Per Armour at 30° Angle of Incidence**	**Shots Per Panel**	**Shots Per Sample**	**Shots Per Threat**	**Total Shots Req'd**
I	1	0.22 calibre LR LRN	2.6g 40gr.	329m/s (1080 ft/s)	4	44mm (1.73 in)	2	6	12	24	48
	2	0.380 ACP FMJ RN	6.2g 95gr.	322m/s(1055 ft/s)	4	44mm (1.73 in)	2	6	12	24	
IIA	1	9mm FMJ RN	8.0g 124gr.	341m/s (1120 ft/s)	4	44mm (1.73 in)	2	6	12	24	48
	2	40 S&W FMJ	11.7g 180gr.	322m/s (1055 ft/s)	4	44mm (1.73 in)	2	6	12	24	
II	1	9mm FMJ RN	8.0g 124gr.	367m/s (1205 ft/s)	4	44mm (1.73 in)	2	6	12	24	48
	2	357 Mag JSP	10.2g 158gr.	436m/s(1430 ft/s)	4	44mm (1.73 in)	2	6	12	24	
IIIA	1	9mm FMJ RN	8.2g 124gr.	436m/s (1430 ft/s)	4	44mm (1.73 in)	2	6	12	24	48
	2	44 Mag SJHP	15.6g 240gr.	436m/s (1430 ft/s)	4	44mm (1.73 in)	2	6	12	24	
III	1	7.62 mm NATO FJ	9.6g 148gr.	847m/s (2780 ft/s)	6	44mm (1.73 in)	0	6	12	12	12
IV	1	0.30 calibre M2 AP	10.8g 166gr.	878m/s (2880 ft/s)	1	44mm (1.73 in)	0	1	2	2	2
Special	*	*	*	*	*	44mm (1.73 in)	*	*	*	*	*

*** User Specified**

- **Panel = Front or back component of typical armour sample**
- **Sample = Full armour garment, including all component panels (F & B)**
- **Threat = Test ammunition round by calibre.**

Table 2.4 HOSDB ballistic performance levels [46]

Performance Level	Calibre	Ammunition Description	Bullet Mass(g)	Minimum Range (m)	Upper Prediction Limit (mm)	Velocity (m/s)
HG1/A	9mm	9mm FMJ Dynamit Nobel DM11A1B2	8.0 (124grain)	5	44	365 ± 10
	0.357" Magnum	Soft Point Flat Nose Remington R357M3	10.2 (158grain)	5		390 ± 10

HG1	9mm	9mm FMJ Dynamit Nobel DM11A1B2	8.0 (124grain)	5	25	365 ± 10
	0.357” Magnum	Soft Point Flat Nose Remington R357M3	10.2 (158grain)	5		390 ± 10
HG2	9mm	9mm FMJ Dynamit Nobel DM11A1B2	8.0 (124grain)	5	25	430 ± 10
	0.357” Magnum	Soft Point Flat Nose Remington R357M3	10.2 (158grain)	5		455 ± 10
HG3	Carbine 5.56×45 NATO 1 in 7” Twist	Federal Tactical Bonded 5.56mm(.223) LE223T3 Law Enforcement Ammunition	4.01 (62grain)	10	25	750 ± 15
RF1	Rifle 7.62mm 1 in 12” Twist	BAE Systems Royal Ordnance Defence Radway Green NATO Ball L2 A2	9.3 (144grain)	10	25	830 ± 15
RF2	Rifle 7.62mm 1 in 12” Twist	BAE Systems Royal Ordnance Royal Ordnance Defence Radway Green NATO Ball L40 A1 7.62×51mm High Power (HP)	9.7 (150grain)	10	25	850 ± 15
SG1	Shotgun 12 gauge True Cylinder	Winchester Loz. Rifled Lead Slug 12RS15 or 12RSE	28.4 (437grain)	10	25	435 ± 25

Table 2.5 Ballistic standards: (a)German Schutzklassen; (b) Russia-Gost 50744-95; (c) CEN prEN ISO 14876-2 [48]

(a)

Performance Level	**Ammunition Description**	**Bullet Mass(g)**	**Velocity (m/s)**	**Maximum Back face Deformation (mm)**
SKL	9mm×19 FMSJ DM 41SR Ruag	8.0	365 ± 5	18-22
SK1	9mm×19 FMSJ DM 41SR Ruag 9mm×19 QD-PEP MEN 9mm×19 Action 4 Ruag	8.0 5.9 6.1	410± 10 475± 10 460± 10	18-22 (36-44 for contact shot)
SK2	0.357 Mag BFM Dynamit Nobel	7.1	580 ± 10	18-22
SK3	5.56mm×45 FMJ + P SS109 FNB 7.62mm×51 FMJ DM111 MEN	4.0 9.55	920± 10 830± 10	18-22

SK4	7.62×51 FMJ AP P80 FNB	9.75	820 ± 10	18-22

(b)

Performance Level	Ammunition Description	Bullet Mass(g)	Velocity (m/s)	Maximum Back face Deformation (mm)
1	9mm Makarov PM 7.62mm Nagan	5.9 6.8	290-315 265-285	17
2	5.45mm PSM 7.62mm Tokarev TT	2.5 5.5	310-325 415-455	17
2a	18.5mm 12 gauge	35.0	390-410	17
3	5.45mm AK 74 7.62mm AKM	3.4 7.9	870-890 710-725	17
4	5.45mm AK 74 7.62mm SVD	3.4 9.6	870-890 820-835	17
5	7.62mm AKM Steel Core	7.9	710-725	17
6	7.62 SVD	9.6	820-835	17

(c)

Performance Level	Ammunition Description	Bullet Mass(g)	Velocity (m/s)	Maximum Back face Deformation (mm)
1	9mm×19 FMSJ	8.0	360 ± 10	44
2	9mm×19 FMSJ	8.0	415± 10	44
3	9mm×19 FMSJ 0.357 Mag FMJ	8.0 10.2	425 ± 10 430± 10	44
4	5.56mm×45 M193 7.62mm×51 NATO Ball	3.6 9.4	970± 15 830± 15	44
5	7.62×51 AP Hardened Steel Core	9.7	820 ± 15	44

S	12/70 gauge Brenneke Solid Lead Slug	32	425± 25	44

2.1.3.2 Stab resistance

Stab resistance of body armour is generally improved using very tightly woven fabrics or very closely spaced laminated layers, in order to counteract the high impact forces of stab threats coming from pointed knives, ice picks or spikes [37]. As the threat impacts the armour, the materials either deflect the threats, or slightly stretch before breaking or being severed (due to their very high levels of tensile strength and cut/tear resistance) while the impact force is distributed over a larger area of armour. Multiple layers are also used to dissipate the impact energy from stab threats. Typical test apparatus for knife and spike testing is shown in Figure 2.7 [49].

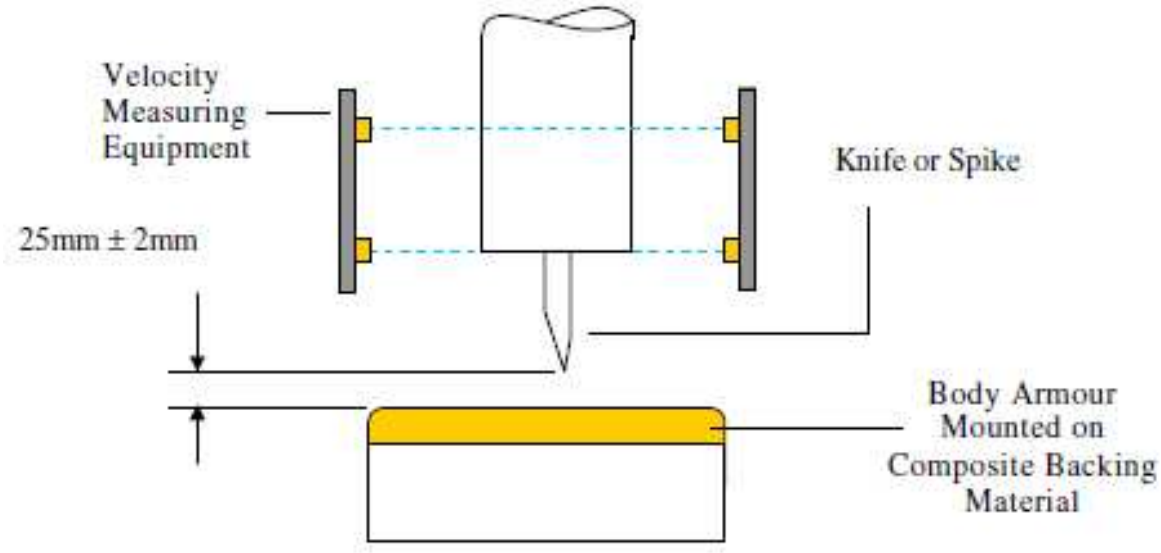

Figure 2.7 Typical test apparatus for knife and spike testing [49]

Stab-resistant body armour was placed into two categories, based on the kind of threats it is designed to shield [37]. The first category is designated the ‘edged blade’ class; it shields engineered or high-quality blades. The second category, which is named the ‘spike’ class, protects from the types of improvised weapons commonly found in

correctional facilities. Within each of these two categories, there are three levels of protection from low to high based on the energy that would impact the body armour during an attack. The titles of these levels have been given according to the HOSDB body armour standards for the UK police (2007), known as KR1 & KR1+SP1 (the low protection level), KR2 & KR2+SP2 (the medium protection level) and KR3 & KR3+SP3 (the high protection level), as shown in Table 2.6 [49].

Table 2.6 Description of Knife and Spike Protection Levels [49]

Protection Levels	Energy Level E1 (joules)	Maximum Penetration at E1 (mm)	Energy Level E2 (joules)	Maximum Penetration at E2 (mm)
KR1	24	7	36	20*
KR1+SP1	24	KR1=7,SP1=0*	KR1=36,SP1=N/A	KR1=20*,SP1=N/A
KR2	33	7	50	20*
KR2+SP2	33	KR2-7,SP2=0*	KR2=50,SP2=N/A	KRA=20*,SP2=N/A
KR3	43	7	65	20*
KR3+SP3	43	KR3=7,SP3=0*	KR3=65,SP3=N/A	KR3=20*,SP3=N/A

2.1.3.3 Other functions

Apart from the aforementioned, body armour may also need to have additional functions e.g. UV resistance, heat resistance, flameproof or waterproof, to accommodate the harsh environment associated with armed combat, chemical and biological warfare and extreme climates. Many manufacturers are competing with each other by providing functional materials in order to enhance the various properties of the body armour. For example, Milliken & Company has released Abrams® fabric, which is an innovative flame-resistant fabric for protective vests by providing higher protection against flames and burns in a more durable, printable fabric with the benefits of improved light-

fastness and strength [50]. TenCate also produces flame-resistant fabrics (Defender M Fabrics) to be used in military applications [51]. With regard to waterproof functions, the water-repellent treatment on the ballistic material could be provided by using GoreTex®. According to the manufacturer, GoreTex® is a water-resistant fabric made of expanded Teflon®, which allows perspiration to evaporate but prevents moisture from reaching the ballistic material [37]. Fierce competition prevails in the market of body armour application; manufacturers may need to develop different technologies to ensure their superiorities. More current research of body armour is reviewed in the following section.

2.2 Ballistic Performance of Body Armour

As the major function of body armour is to protect against firearm-fired projectiles and fragments from explosions, numerous studies have been carried out to investigate the ballistic performance of body armour in the last two decades [52-74]. Materials and structures are the two main aspects scientists and researchers have focused on.

2.2.1 Materials

2.2.1.1 Aramid

A lot of investigations have been performed on the damage and energy absorption behaviour of para-aramid armour plates as aramids are regarded as the most widely used ballistic protective materials. Silva *et al* [75] investigated the ballistic resistance of Kevlar® 29 reinforced vinylester armour plates experimentally and theoretically. A study done by Hayhurst *et al* [76] investigated the damage and energy dissipation behaviour of para-aramid armour plates with different ply numbers under high velocity impacts with heavy particles. Akdemir *et al* [77] examined the effect of production

parameters upon the terminal ballistic properties of para-aramid composite armour under different conditions. Additionally, Simons *et al* [78] used finite element analysis modeling to investigate the damage behaviour of para-aramid armour under various threats. Clegg *et al* [79] discussed the damage behaviour on the para-aramid armour plate which consists of 19 plies subjected to threats of 1.1 g weight under ballistic impact. Further, Riewald *et al* [80] produced armour plates and helmets made from para-aramid materials and tested their ballistic performance under a water immersed condition. Colakoglu [81] studied the ballistic performance of two different polymer matrix composites for armour design. And finally in addition to that, Lim *et al* [82] also researched the damage behaviour of para-aramid armour plates under ballistic impact of four different projectile geometries by using electron microscopy.

The state-of-art technology is often more interesting and worthwhile to be paid attention. DuPont has just released a new type of ballistic material known as Kevlar® XP™ which is announced to provide 15% reduction in backface deformation and 10% reduction in overall weight, whereas to maintain its performance in extreme field conditions that officers face (e.g. heat, humidity and mechanical wear) [31]. However, as this is the latest ballistic innovation of DuPont, the cost, the quality guarantee and the service life are still requested to stand the test of time.

Dupont's strong competitor Teijin Aramid, promotes Twaron CT Microfilament® which is a highly resistant aramid yarn made from 1,000 individual filaments with an extremely fine filament diameter. 50% more filaments are used in this type of yarn than traditional aramid yarn [83]. The body armour with the usage of Twaron CT

Microfilament® which is quite lightweight and comfortable has been accepted by the law enforcement and military soldiers.

2.2.1.2 High-performance polyethylene

DSM introduced Dyneema® HB50 in 2007, which was an ultra-strong and lightweight polyethylene material. The panels made with Dyneema® HB50 were able to absorb the impact rifle threats such as AK47 and Nato Ball. It was upgraded to HB80 in 2009 was claimed as the highest ballistic performance unidirectional (UD) product on today's market [84]. However, DSM is often trapped in patent infringement issues; this apparently negatively affects the development of new ballistic materials. There is still a long and harsh way to go for DSM to well defend its state-of-the-art technologies.

Honeywell has updated ballistic materials from Spectra Shield® II SA-3113 to Spectra Shield® II SA-1211, which has strong protection against NIJ threats and substantial reduction in blunt trauma. The state-of-the-art technology of Honeywell is Gold Shield® GN-2117 promoted in 2009 which has demonstrated up to 10% reduction in weight but provided higher surface durability and chemical resistance in comparison with Honeywell traditional Gold Flex® material [85]. However, it is of interest to notice that this innovation combines Honeywell's patented Shield technology with aramid fibre not its own polyethylene fibre. The advantages of aramid fibre in respect of higher melt temperature and friction coefficient may be the factors to enlighten Honeywell on this innovation. Nevertheless, the invention of Gold Shield GN-2117 will obviously expand Honeywell's portfolio of ballistic materials for advanced armour systems.

2.2.1.3 Potential materials

Nanomaterials

Nanotechnology is predicted to produce revolutionary changes via bringing far-reaching consequences in various areas, in which nanostructured materials have been considered to have great potential in replacing the traditional counterparts in order to make stronger lightweight armour [86]. But it is unclear whether this type of material could provide improvements over heavy armour. Nevertheless, nanofibre-based garments are now considered to provide protection against projectiles.

The new type of carbon nanotube fibre exemplified by the development carried out by a group from the Department of Materials Science and Metallurgy at the University of Cambridge is an example as shown in Figure 2.8. This fibre which is made up of millions of tiny carbon nanotubes is very strong, lightweight and good at absorbing energy at very high velocity. Researchers from the group declared that their material is already several times stronger, tougher and stiffer than fibres currently used to make protective armour. The super-strong body armour for the law enforcement and military personnel could be incorporated with this type of fibre [87]. However, the daily output of this product is very low and it is hard to meet the industrial demand. Further research is required to increase the productivity.

Figure 2.8 lightweight but super-strong carbon nanotube filaments [87]

Wool

The incorporation of wool fibres into aramid fabrics is verified to make positive contributions to the ballistic performance of the fabrics as more energy is absorbed because of the increase of friction between yarns [88]. The blending-in of wool also can benefit wearer comfort and excess moisture management. The downside is that the wool is incorporated as yarn at the weaving stage rather than as fibre at the spinning stage due to the large difference in fibre properties between wool and aramid. The connection between wool and aramid is not strong and a special loom is required to insert them together as parallel yarns to make fabrics.

Ramie

There also has been a suggestion to use ramie in the making of bulletproof panels as it is one of the strongest natural cellulose fibres [89]. The bulletproof panels made from ramie fibre reinforced composites are lighter in weight and much cheaper than conventional counterparts made from ceramic plates, aramid composites or steel-based materials. The ballistic testing of bulletproof panels made from ramie fibre reinforced composites for NIJ level II, IIA and IV was preliminarily investigated and the results were promising.

There are large scales for potential ballistic materials to develop. Nevertheless, synthetic materials (aramid and high-performance polyethylene) are currently still the primary ballistic materials which are commercially applied in body armour designed to defeat high velocity ballistic impacts of projectiles.

2.2.2 Structures

Not only materials but also structures could influence the ballistic performance of body

armour, in which woven, nonwoven and multi-component structures are mainly used in the application of body armour.

2.2.2.1 Woven structures

It has been acknowledged that woven structures especially plain weave is the most widely used in body armour applications. The ballistic performance of layered woven fabrics can be influenced by weave structure, yarn count, warp×weft construction. The corresponding parametric studies have been extensively investigated by Ashok [42] and the results are shown in Table 2.2. Plain weave with linear density 1420 denier and fabric density 17×17 (picks/inch × ends/inch) is the optimal setting as a compromise among breaking strength, weight and cost savings.

Apart from that, boundary conditions affect the ballistic performance of woven fabrics. Shockey *et al* [90] found the ballistic performance of fabric can be increased by clamping on two opposing sides of fabrics. Cunnif [91] investigated the influence of fabric sample dimensions on ballistic properties using Kevlar® and Spectra® fabric samples. The result was shown that the fabric samples with smaller dimensions could provide higher energy absorption capability. Cork and Foster [92] developed the narrow fabrics which were empirically conformed to absorb more energy than wider fabrics against ballistic impacts, especially when gripped in a two-sided configuration. However, narrow fabrics introduced lines of weakness between strips when incorporated into a fabric panel. Another problem was the difficulty of producing the whole fabric panels using the narrow fabrics. It was suggested to glue fabrics to an insubstantial mounting frame made from simple polystyrene composite. However, it was a time-consuming procedure and the related ballistic performance of fabric panels

still needed to be verified as no systematical investigations have been carried out. But generally speaking, those researches may encourage further theoretical and empirical work on the effects of boundary conditions.

It also has been noticed that the ballistic performance of a woven fabric can be improved by using weft yarns which have higher tenacity than warp yarns, suggested by Chitrangad [93]. The weft crimp is often lower than the warp crimp during the weaving process [94]. Therefore in the fabric construction weft yarns exhibit more tension than warp yarns and are easier to be stretched to break against the ballistic impact. With the tenacity increases in weft yarns, equal warp and weft crimps can be expected and therefore the same amount of deformation in warp and weft directions will be achieved. Such fabric construction enhances the energy absorption to a higher level.

Stitching is another important factor influencing the ballistic performance of the layered woven fabrics [95-97]. Karahan *et al* [98] developed three stitches types which were used to combine the fabric layers with different numbers to form the panels, as shown in Figure 2.9. A dramatical reduction of 6.7% in trauma depth was observed with type c stitching compared to the type a under the situation of same fabric ply number. Bilisik and Turhan [99] made a further study of this aspect by introducing multidirectional arrangement of fabric layers. Unstitched and stitched were defined as two classifications. Both of them were further made of four structure types. The first two were totally layered Kevlar® 29 fabric and Kevlar® 129 fabric; then came the third one with half layered Kevlar® 29 and half layered Kevlar® 129. The last one was 12-layer Kevlar® 29 fabric oriented ±45º to the fabric axis and 2-layer Kevlar® 129 at the bottom. The conclusion of trauma depth positively affected by stitching was verified again as lower value was found on multi-axis stitched structures though there was no apparent energy

dissipation difference between multi-axis stitched and unstitched structures. However it came into notice that stitching cannot be too dense as dense stitching increased the rigidity of fabric panel which made wearer uncomfortable if such fabric panel was inserted into the carrier for making the body armour.

(a) (b) (c)

Figure 2.9 Stitching types: (a) sewn only 2.5cm inside from the edges; (b) sewn 2.5cm inside from the edges and in diamond shape;(c) sewn 2.5cm inside from the edges and then with 5cm intervals in bias type [99]

2.2.2.2 Nonwoven structures

Unidirectional fabric structure (a kind of nonwoven structure) is also used in the body armour applications. The unidirectional fabric is generally composed of laminating layers of fabric at right angles. The layer of fabric is just made of yarns paralleling together densely. As there are no interlacements in the structure of the unidirectional fabric, the energy absorption of unidirectional fabric should be different from woven fabric. Karahan [98] did the comparisons of energy absorption between unidirectional Kevlar® fabrics and woven Twaron® fabrics, and the result showed that the former one could absorb 12.5%-16.5% more energy. However, this could not give a definite conclusion that unidirectional fabric is better than woven fabric regarding the ballistic performance as aramid fabrics from different companies are used. As Dyneema® is normally used in unidirectional fabric, the comparison of ballistic energy absorption between unidirectional Dyneema® fabrics and woven Dyneema® fabrics are more worthwhile, which will be a part of the research demonstrated in Chapter 5.

2.2.2.3 Multi-component structures

The state-of-the-art technology of body armour research is to use multi-component structure instead of only using same material structures in making ballistic fabric panels, as multi-component structures show advantages in ballistic performance. Howard [100] found that the structure of using a nonwoven facing on a woven fabric instead of Spectra® shield alone could provide a stronger capability against projectiles fired from handguns at the speed of 350-430 m/s. Unlike plain weave fabrics constructed from many interlaced points which could cause stress wave reflection and in turn the addition of stress waves may contribute to fibre breaking ahead of time, nonwoven fabrics do not have interlaced points and thus are structurally bulky compounds. Ballistic performance could be highly improved by using nonwoven fabrics to compose the cushion layers. Cushion layers together with impact layers compose the ballistic fabric panels. Cushion layers are the inner layers which are close to human torso with the function to prevent non-penetrating damage (blunt trauma); impact layers are the outer layers which make a key role to resist bullet penetration and thus are normally made of bulletproof fibres. Lou *et al* [101] considered to design impact layers and cushion layers to resist bullet penetration and non-penetrating damage respectively. The study offered a new solution to buffer the non-penetrating damage using the elastic cushioning structure combined with nonwoven fabric and chloroprene rubber. This combination could help dissipate impact energy through the friction between the chloroprene rubber and fibres. Lin [102] also suggested enhancing the ballistic performance using cushion layers. But the novel compound cushion materials were made by needled punching and thermal calendering on the basis of a sandwich structure. The sandwich structure was composed of polyester filaments laid on the pre-punching polyamide web with low-melting point polyester staple fibres. It was demonstrated that apparent buffer effect can be achieved by using

this type of cushion layer. Optimistic view was taken to enhance the ballistic performance of a bulletproof vest by replacing the original cushion layer with this novel counterpart.

2.2.3 Others

Coating is also an important way to improve the ballistic property of fabrics. Ahmad *et al* [103] suggested that natural rubber coatings on high modulus can be used to improve ballistic performance. Gadow *et al* [104] studied ceramic and cermet plasma coatings on fibre fabrics which are supposed to enhance protective performance of the lightweight protection. High performance polyethylene (HPPE) fabric coated with elastomer has been analysed and it claims to have enhanced multi-hit fire performance [105]. Additionally, Kevlar® fabrics are suggested to be sprayed on with STF(shear thickening fluid) in very thin coats for the purpose of creating liquid body armour. STF is a material containing nanoparticles which solidifies instantly against sudden impact [106]. A complete protection can be provided instead of just covering vital organs by using this liquid body armour. Moreover, fibres coated with zinc oxide nanowires could also be considered in the development of fabrics which could produce power from body movements. Such kind of fibres is supposed to stimulate muscles and give wearers greater strength for physical movements [106]. The body armour made by this kind of fabric could enable soldiers or police officers to march faster, lift heavier objects and carry more weapons.

Apart from that, Rao and Singh [107] developed the polymer nanocomposite transparent panel and tested its impact resistance behaviour experimentally and theoretically. It was shown that the use of nano-particulate reinforced polymeric

adhesives exhibits enhanced impact resistance. Lee and his colleagues [108] researched the influence of the particle size of silica on the ballistic performance of fabrics impregnated with silica colloidal suspension. The result indicated that silica colloidal suspension impregnated fabric with smaller particles exhibits a lager increment of inter-yarn friction at the onset shear strain for shear thickening.

This section mainly reviews the current technologies of ballistic performance of body armour. However, most of the studies seem to serve male armed forces as body armour panels are normally researched in the form of flat pieces. As female police and soldiers become more important in civil and national safety, special technologies of female body armour to address the problem of unique female torso are imperative in recent years.

2.3 Female Body Armour Design Technologies: State-of-the-art

The female body armour technologies need to provide the right shape together with the right ergonomics for the benefit of female wearers in terms of protection, wearability and comfort. The current main technologies to design female body armour are unisex tailoring, cutting and sewing, folding, overlapping, and moulding.

2.3.1 Unisex tailoring

This technology, which is the most traditional and convenient route, has been used since the invention of body armour. Such methods put little emphasis on the difference in torso between male and female, and the similar style and specification are employed during manufacture. Obviously, well-fitted female body armour could not be produced by this method. It has apparent drawbacks but still owns a large market because of easy

operation and wide acceptance for quite a long time. Actually some accommodations have been adopted nowadays, such as enlarging the armhole openings for more spaces to avoid restricting movement for female officers. However, the weakness in fitting the female torso still exists. Other ways to improve the shape performance while to guarantee the protections are currently being sought.

2.3.2 Cutting and stitching

Apart from the said method, most companies may prefer to cut and stitch the composites to create the bust cups to enhance comfort for female wearers. The full coverage body offered by the American Security.net is a typical example [109]. Detailed female size measurements are often demanded, i.e. the charts provided by the Second-Choice Company, as shown in Figure 2.10 [110].

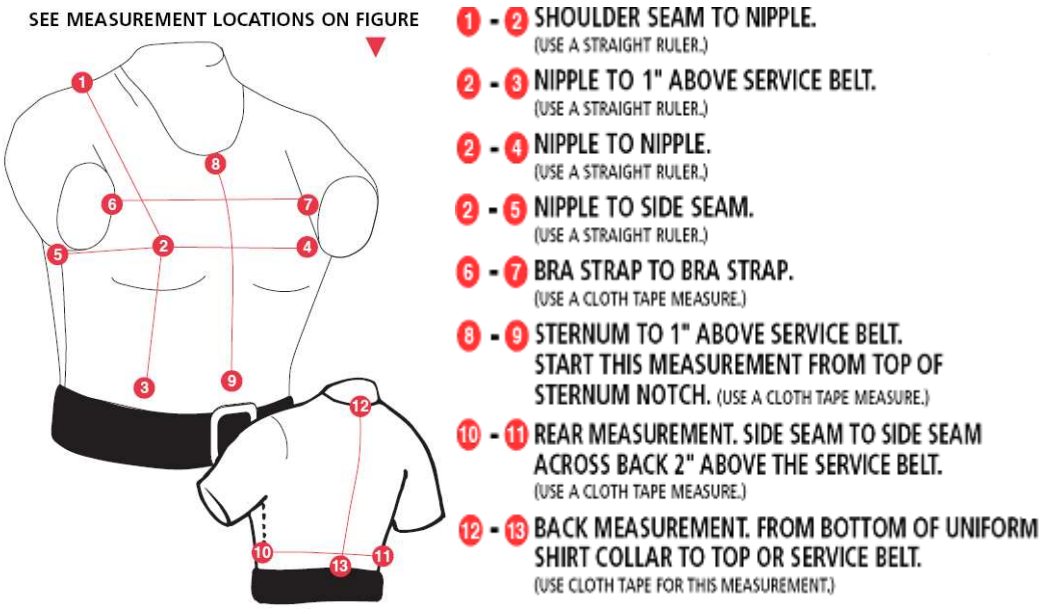

Figure 2.10 Female size measurements [110]

However, such a method also has its negative aspect: the seam that is created by stitching the materials to shape the bust area always becomes the weakest point against

impact due to the discontinuous yarns on that area sharply reducing the armour's ballistic-resistant ability. The laboratory is often instructed to locate such a place to test the minimum level of ballistic protection.

2.3.3 Folding

The TruFit 2 series of body armour from PACA is a classical example of female body armour manufactured by folding, as shown in Figure 2.11 [111]. The two-dimensional reinforcement could shape a three-dimensional form by folding, namely, bending one part to lie on another according to the certain axis.

Figure 2.11 Female body armour by folding [111]

As with cutting and stitching, folding creates discontinuities in the structure, which decreases the torso protection ability. Additionally, wearers may feel uncomfortable under their armpits where ridges may be sharpened by folding many layers.

2.3.4 Overlapping

This female body armour comprises a contoured front protective panel composed of a plurality of superimposed layers of protective piles of ballistic fabric made of aramid polymer yarns. The front protective armour panel is contoured by providing overlapping seams joining two side sections to a central section of the panel so as to cause the front protective armour panel to be contoured to the curvature of the bust of a female wearer of the body armour garment to impart good ballistic protection and comfort to the wearer. Hook and eyes fasteners are attached to fabric tapes at the top edges of the front and rear sections so that the garment is thereby made easily adjustable in length to fit various sized female busts and torsos [112].

The usual means of cutting and seaming fabrics may fail in producing torso protecting body armour having good ballistic protection properties as well as being comfortable to wear for long periods of time because seams employed in the making of clothing are easily penetrated by small arms missiles at close range. For this overlapping method, the close seams having conventional numbers of overlapping layers would permit small projectiles that impact directly at the seam edges to penetrate through the body armour by getting under the edges of the overlapping seam and following a path more or less parallel to the overlapped and seamed portions of fabric.

2.3.5 Moulding

The method now used is a kind of deep drawing process, where the specimen is mounted against a support medium, which mimics the compliance of a human torso. The process requires no additional finishing operations or the use of chemicals to fix the deep drawn shape. Subsequently, the moulded fabric layers are placed on top of each

other to form a garment part and joined by a seam located in the middle of the panel, for instance. The positive point of this system is that the high wear comfort of non-stitched bullet-resistant body armour is fully preserved, as shown in Figure 2.12 [12]. Apart from that, (BA105-23) Ballistic, Knife, Spike, Syringes & Slash, HG1/KR1+SP1 female covert body armour invented by the MC PRODUCTS company also is a typical example, which features a moulded bust area, as shown in Figure 2.13 [113].

Figure 2.12 Female body armour by moulding, produced by Twaron [12]

Figure 2.13 Female body armour by moulding, produced by MC PRODUCTS [113]

On the other side, moulding method also has apparent drawbacks, such as unbalanced density in different areas, shear deformation, extension in the yarns, crimp loss, sliding

of fibres and local wrinkles [114]. Additionally, such a method also incorporated the limitation in the size-choice of bust area of female body armour.

These aforementioned five technologies have been widely applied nowadays but their own individual shortcomings block them from developing further; a new method of producing the female body armour with bust area shape using continuous yarns is required.

2.4 Possible Technologies for Potential Female Body Armour

The difference in chest between men and women requires the fabric to cover the curvaceous female torso naturally without wrinkles or creases. However, the traditional plain woven fabric, widely used in the female body armour application, hardly achieves this requirement as it has limitations to shape the three-dimensional structure because it is formed by intersecting weft yarns with warp yarns in-plane. Therefore, cutting and sewing, folding are necessary to be adopted when this two-dimensional fabric forms a three-dimensional shape to match the bust area. However, these methods have different disadvantages, as mentioned above, so that a new route is being investigated. Three-dimensional dome-shaped fabrics and angle-interlock woven fabric could be two major considerations since both of them could form an entire crater shape due to the particular weaving procedures. More details would be demonstrated as follows.

2.4.1 Three-dimensional dome-shaped fabrics

This bust area design could be taken into account as the design of making three-dimensional dome-shaped patterns. There are mainly three methods to make 3D shells: shaping weaving, varying take-up rate and employing different woven structures. The

former two have an apparent problem of inconvenient operation on the loom so that the latter one is treated as the major consideration. Their working procedures, principles and other relevant information will be reviewed.

2.4.1.1 Shape weaving

Shape weaving allows the first time fabrication of ‘tailor-made’ reinforcements with continuously running filament yarns. The purpose of this process is to produce the three-dimensional dome-shaped fabrics by varying the warp and weft thread spacing combined with a novel interlacing technique. Under such a circumstance the jacquard is not only used for the design but also for producing different surface areas and interspersing these. Areas that are woven ‘too large’ are placed in an environment that is ‘too small’ and they bulge out to form an obvious three-dimensional shape [115].

The specific process is: firstly, a jacquard machine is chosen to make such fabrics because it is preferable for making any desired pattern at any place on the woven three-dimensional shell. The next step is the yarn arrangement for getting the pattern. There are two sets of yarns, the warp yarn and weft yarn. Interlacing these two mutually perpendicular sets of yarns forms a resulting plain fabric. The running warp yarns should be parallel to each other and different fibre lengths are used according to the geometrical shape of three-dimensional domes. Then weft yarns are inserted between the individual lowered and raised warp yarns on a jacquard machine. In order to move any yarn in a predetermined position before weft insertion, the warp yarn passes a special beating up device. A specially controlled segment taking up device is used to manufacture the woven fabric with inserted three-dimensional domes. During this process, the key point lies in the coordination between the mechanical motion and the

additional installed elements, and the operation of a steering computer, which controls the weft insertion data for the shape and the pattern [115]. Figure 2.14 shows the result.

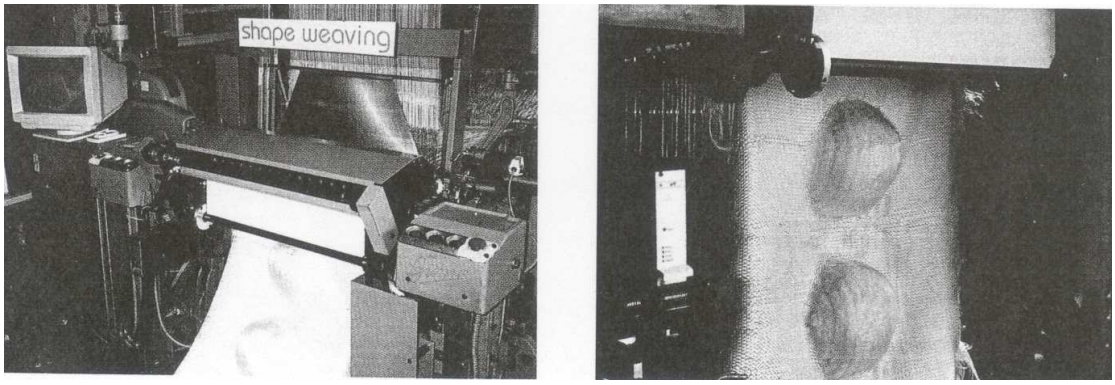

Figure 2.14 Shape weaving [115]

Shape weaving has many advantages in making three-dimensional shell fabrics; it has low weight, high mechanical properties and homogeneous surfaces with no seams. It can also reduce personnel costs, minimise waste of material and improve reproductive power and better quality control. It seems to be a good new solution to enhance quality, reduce costs and potentially increase domestic employment. Nevertheless, the big problem is that such woven fabrics should be fabricated on certain machines, which indicates the restriction against the popularisation of this state-of-the-art technology, especially compared with the moulding route, where almost all shuttle looms could weave two-dimensional fabrics without special operations and specialist knowledge, which then are moulded to become the three-dimensional domes.

2.4.1.2 Varying take-up rate

Altering weft density by varying the take-up rate to obtain relaxation and change in yarns configurations in the fabric is also an effective method to make three-dimensional dome-shaped fabrics. With the introduction of the profile roller (a profile roller is a facility fixed in the front of the loom to help shape the dome effect), the take-up rate can

continuously increase while leading to a decrease in the weft density in the applied area; after the peak profile, the take-up rate starts to decrease, which causes a raise in the weft density. Eventually, a higher take-up rate in the middle of the fabric causes concavity - when viewed from the front of the loom – a curved fell line while the profile is still in contact with the fabric, which is shown in Figure 2.15 [116]. When a dome-shaped fabric is placed onto a flat surface, which is not its natural alignment, the weft yarns are curved into the most relaxed positions, as shown in Figure 2.16 [116].

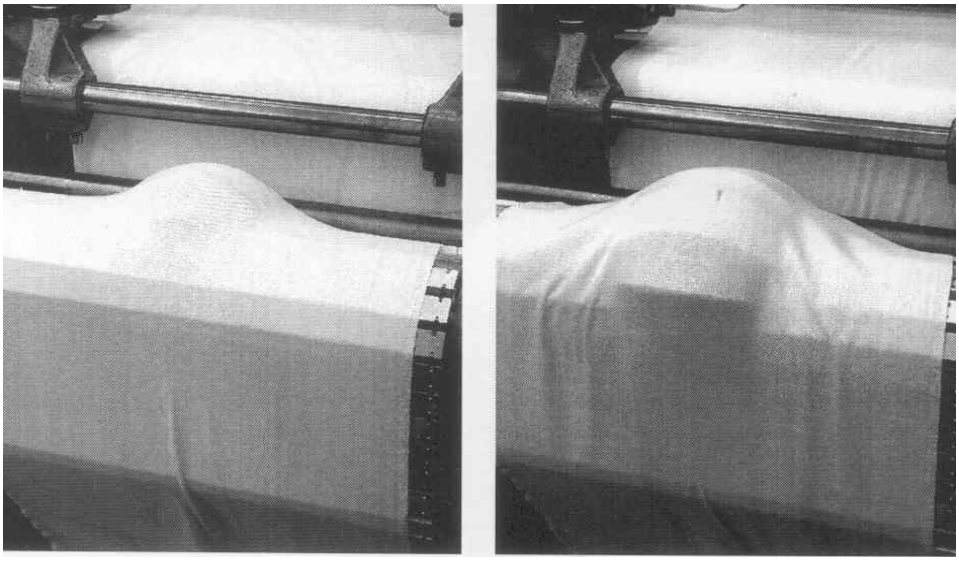

Figure 2.15 Fabric contact with the profile at its beginning and top positions [116]

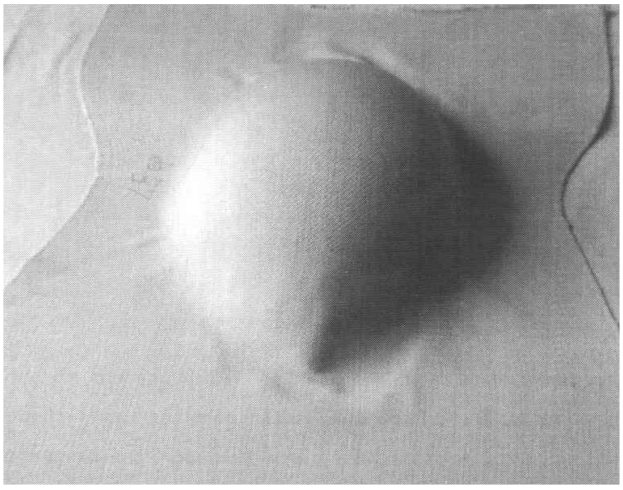

Figure 2.16 A dome-shaped hardened fabric [116]

The dome shown in Figure 2.16 is a little oval-shaped in the warp direction because of yarns having already interlaced to weave before the introduction of the profile roller and still under weaving after the usage of profile roller. The profile roller is the most important assistance in manufacturing this three-dimensional shell, which fundamentally determines the size and the shape of dome. However, the specific relationship among the specification of profile roller, the take-up rate and the dome effect has been little researched, and many complicated calculations and experiments still require to be done. It is hard to manufacture the dome-shaped fabrics according to certain prescribed patterns. A new profile roller may need to be produced for which cost also needs to be taken into account.

2.4.1.3 Employing woven structures

Employing different woven structures is another route to make dome-shaped fabrics. This has been researched and presented by Tayyar, who made the three-dimensional dome-shaped fabric using plain, $\frac{2}{2}$ twill, twilled hopsack, 8-end sateen weaves arranged from outer to centre ring, as shown in Figure 2.17 [116]. This arrangement is inspired by the principle of the honeycomb weave. More details would be demonstrated in the following section. Although the plain, $\frac{2}{2}$ twill, twilled hopsack and 8-end sateen weaves were used in the above mentioned research, the plain, $\frac{2}{2}$ twill and 5-end satin weaves, the three most typical weaves will be used in the current research.

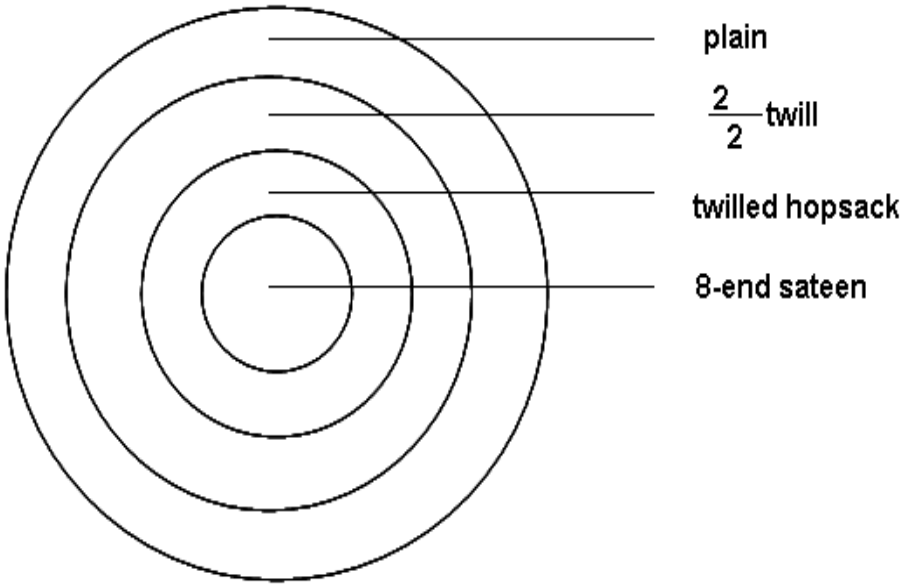

(a)

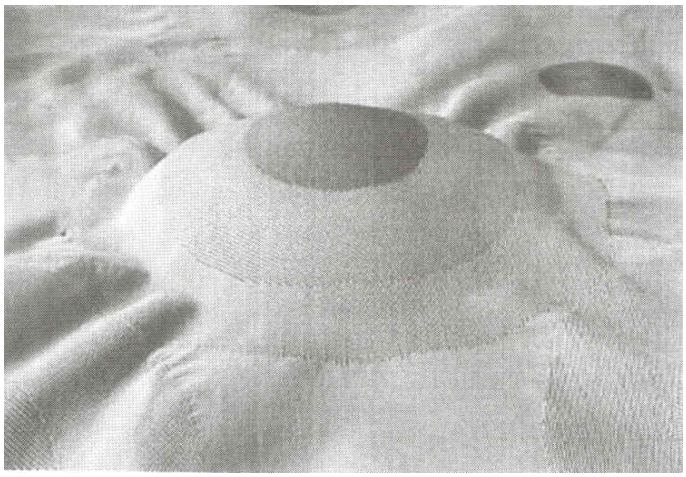

(b)

Figure 2.17 Dome made of plain, $\frac{2}{2}$ twill, twilled hopsack, 8-end sateen weaves: (a) schematic diagram; (b) fabric sample [116]

Principle of honeycomb weaves

Honeycomb weaves are a group of weaves forming an embossed cell-like appearance of fabric, as shown in Figure 2.18. The surface of the weave looks like the honeycomb cells made of wax by the bees. These so called 'cellular' fabrics are characterised by orderly distribution of hollows and ridges. The shorter floats of warp and weft threads show hollows, and the longer floats of warp and weft threads show the ridges of the

honeycomb [117]. The shorter the float, the tighter the area, where it is easier to extend or invade because of the higher tension formed; on the other side, the longer the float, the looser the area, where it tends to shrink. Based on this principle, the dome will swell out on the surface by employing weave structures with long and short floats in a weave. Namely, weaves of different floats and tensions could be used to make domes.

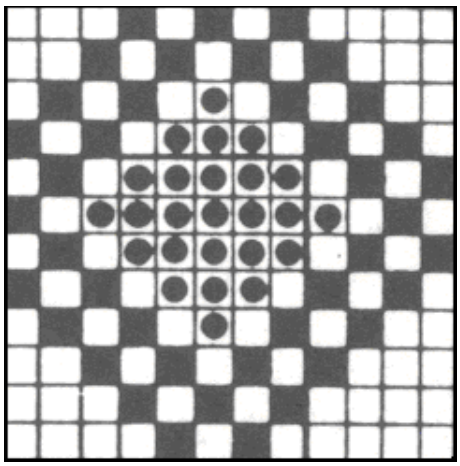

Figure 2.18 Honeycomb weave structure [117]

Types of weaves to make dome-shaped fabrics

Three typical types of weave — plain, twill, and satin/sateen are used to make three-dimensional dome-shaped fabrics, based on the length of float. Plain, $\frac{2}{2}$ twill and 5-end satin weaves are used and their structures are shown in Figure 2.19 [118]:

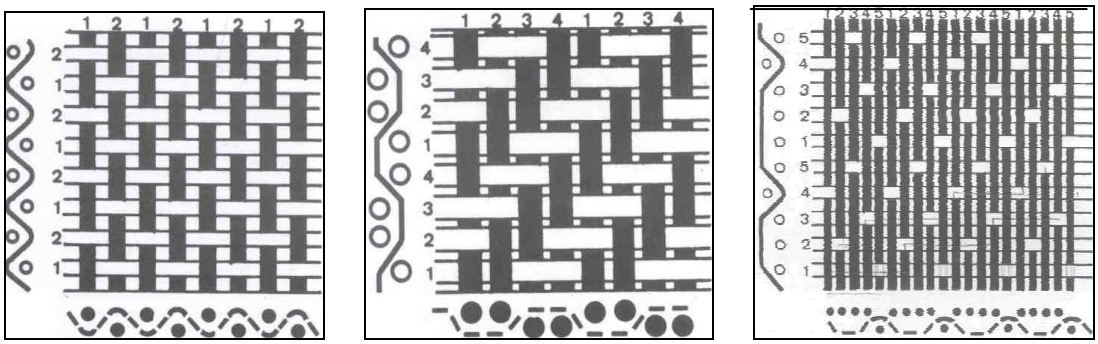

(a) **(b)** **(c)**

Figure 2.19 Weave structure: (a) plain; (b) $\frac{2}{2}$ twill; (c) 5-end satin [118]

Plain weave is the simplest but tightest basic weave, which is formed by repeating on two ends and two picks. The first end passes over the first pick and under the second pick; the second end reversed this action, and weaves one down and one up. The weave is executed by passing each filling yarn successively over and under each warp yarn, alternating each row. This weave provides the greatest number of intersections and shortest average float length in a given space, which has the largest possibility to invade other areas.

Twill weave is characterised by a diagonal rib, or twill line. Each end floats over or under at least two consecutive picks and the points of intersection move one outward and one upward, or downward, on succeeding picks, to produce the diagonal line. Compared with plain weave, this weave has longer floats and smaller tensions.

Satin weaves have the longest floats and the smallest number of intersections, in which the most apparent shrinking phenomenon could be observed. The tension difference among different weaves will lead to the centre of the design to grow out of the fabric plane. These three weaves and their arrangements are employed in the design plan of this research and more information demonstrated in Chapter 3.

2.4.2 Angle-interlock woven fabric

2.4.2.1 Structure

Angle-interlock woven fabric is also an alternative of the traditional woven fabric in shaping three-dimensional domed-pattern since it has advantages in good formability, indicating it could form 3D bust area without cutting and sewing. The angle-interlock woven fabric consists of layers of weft yarns that are laid straight and bound by a single

layer of warp yarns to lock the layers of weft yarns together [119-121]. The stuffers (warp yarns) are oriented along the longitudinal direction. The fillers (weft yarns) are oriented transverse to the loom feed direction, and are inserted between layers of stuffers. The stuffers and fillers form an orthogonal array.

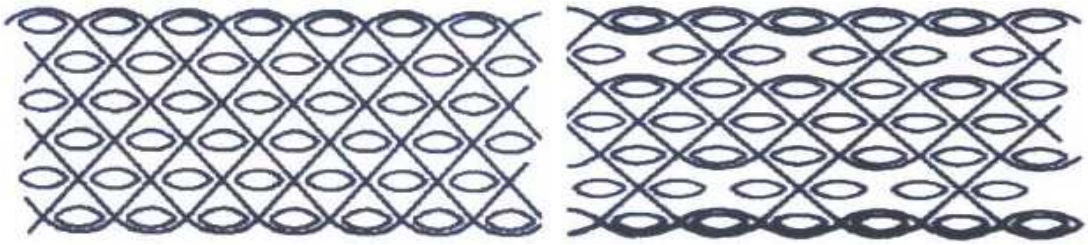

(a) **(b)**

Figure 2.20 Angle-interlock woven fabric: (a) through-the-thickness; (b) layer-to-layer [121]

Various types may exist in the geometry of 3D angle-interlock preform, depending on the number of layers interlaced, the pattern of repeat and the presence of laid-in yarns. Basically, there are two main types of angle-interlock weaves: through-the-thickness angle-interlock weave (TTAW) and layer-to-layer angle-interlock weave (LLAW). The TTAW is a multilayered weave in which warp weaves travel from one surface of the preform to the other, holding together all the layers of the preform. The LLAW is a multilayered preform in which warp weaves travel from one layer to the adjacent layer, and back. A set of warp weaves together hold all the layers of the perform [120, 122-125]. The schematic arrangements of TTAW and LLAW with ideal geometry are shown in Figure 2.20 [121]. The present study focuses on the through-the-thickness angle-interlock woven fabrics with no suffer yarns as they are characterised by low shear rigidity, which make them widely application in many technical applications [125].

2.4.2.2 Properties

As one of the prospective woven structures studied for textile composites, angle-interlock fabrics have attracted considerable research attention, ranging from mechanical analysis to CAD/CAM studies of such fabrics.

Sun and co-workers [126] focused on the research of compressive behaviour of 3-D angle-interlock woven fabric composites at various strain rates. The results showed that the stress-strain curves are rate sensitive and compressive stiffness, maximum compressive stress and corresponding compressive strain are also sensitive to the strain rate. Naik *et al* [120] presented a three-dimensional woven composite strength model for predicting the failure behaviour of three-dimensional angle-interlock woven composites under on-axis uniaxial static tensile loading and shear loading. Sheng and Hoa [127] put forward a three-dimensional geometric model for predicting elastic constants of 3D angle-interlock woven fabric composites. Good agreement was shown between the prediction and the experimental results. Nie *et al* [128] developed a new fractional formula to describe the angle-interlock woven fabric construction in a more concise and efficient way for the computer-aided design (CAD). The weaving plan of angle-interlock woven fabric with a large number of layers could be easily and simply characterized by this method. Chen *et al* [129] established mathematical models on the purpose of visualizing their 2-D and 3-D in CAD/CAM software. The study served as a first attempt to enable evaluation of their physical and other properties. Apart from that, mouldability behaviour is important to mention as this property is closely related to the current study. Chen *et al* [120, 130-131] also investigated this aspect extensively and verified that this kind of fabric owns highly advantageous mouldability properties.

2.4.2.3 Mouldability

Among various properties of the angle-interlock woven fabric, mouldability is quite attractive in the female body armour application as it allows the fabrics to be perfectly crater shaped without wrinkles or folding traces or stitches from cutting and stitching [121], as shown in Figure 2.21. Mouldability is defined as 'the fabric's ability to deform into a 3-D shape' [120]. The aim of moulding is to obtain a smooth fibre alignment over a doubly curved surface in order to meet the mechanical and geometrical requirements; this capability of fabrics is referred to as 'mouldability' [125]. The mouldability of woven fabrics depends greatly on shear deformation resistance, which comes from friction between the warp and weft yarns at the crossovers [120], and bending and compression of the yarns.

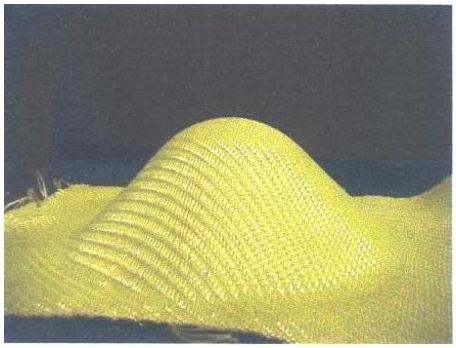

Figure 2.21 the deformed fabric [121]

Compared with multilayer woven fabrics, angle-interlock woven fabric owns lower value on shear rigidity. It can be seen in Table 2.7 and 2.8, the two structures of angle-interlock fabrics, KF3-A and KF3-B, have a lower shearing modulus and a lower Young's modulus than their multi-layer counterparts with similar frequency of stitching f [130]. This can be explained from the fact that the angle-interlock woven fabric has substantially fewer crossover points per unit area than the equivalent layered fabrics, which reduces friction between the warp and weft yarns at the crossovers. Moreover, the angle-interlock structure requires less bending and compression of yarns for shear

deformation [120,125,130,131]. This property makes the angle-interlock woven fabric potential in the application of well fit female body armour.

Table 2.7 3-layer fabric: stitching frequency f [130]

Fabric	KF3-1	KF3-2	KF3-3	KF3-4	KF3-5	KF3-6
f	$1/6$ (0.167)	$2/8$ (0.250)	$1/4$ (0.250)	$2/6$ (0.333)	$1/8$ (0.125)	$3/8$ (0.375)

Table 2.8 Test results [130]

Fabric	f	E_X ($MP\alpha$)	E_Y ($MP\alpha$)	G_X ($g/cm.\deg$)	G_y ($g/cm.\deg$)
KF3-1	0.167	2120	2200	0.85	0.89
KF3-2	0.250	1930	2630	1.19	1.15
KF3-3	0.250	1830	2390	1.11	1.23
KF3-4	0.333	1680	2330	1.48	1.39
KF3-5	0.125	2080	2560	0.91	0.91
KF3-6	0.375	1460	2680	1.49	1.50
KF3-A	0.167	1720	2130	0.53	0.53
KF3-B	0.250	1560	2290	0.64	0.61

2.4.2.4 Ballistic resistance

Apart from the consideration of mouldability, ballistic-resistant property could be another requirement if the fabric is applied in the female body armour. In the angle-interlock weave structure, yarns can be arranged crosswise, lengthwise and in the thickness direction resulting in strength in three individual directions, their interlacing warp yarns between adjacent weft yarns layers enhance strength and stiffness in through-the-thickness direction, and also leads to an increased impact and fracture resistance [125]. This theoretically explains that angle-interlock woven fabric owns ballistic resistance. However, ballistic experiments are necessary to be carried out to investigate if angle-interlock woven fabrics are able to be used as ballistic materials.

2.5 Remarks

This chapter has mainly reviewed the important aspects of body armour (history, categories and functions), the ballistic performance of body armour, and current and potential female body armour technologies. On the purpose of the compliance of the female torso, different methods have been applied, such as cutting and sewing to create the bust cups, folding, overlapping or moulding. These methods could provide more flexibility and comfort to female wearers and therefore better protection could be predicted. However, those technologies are not perfect but accompanied with various negative factors. For example, the downside of the cutting and sewing method is that the yarns are discontinuous in certain areas as the whole fabric is required to trim in order to make the three-dimensional block to fit the curvaceous female torso. Those areas are often very weak and fragile and thus against the projectile hardly. The female body armour owning the structural integrity made with continuous yarns is required. Three-dimensional dome-shaped fabrics and angle-interlock woven fabrics are considered as both of them could form an entire crater shape without traces or wrinkles. The former is shaped based on the honeycomb principle and the latter is mouldable due to low shear rigidity. Their dome formability will be further investigated in order to select the more suitable type in the application of female body armour.

Chapter 3

Preliminary Work: Dome-shaped Fabrics for Female Body Armour Panels

As mentioned in Chapter 2, dome-shaped fabrics could be taken into account when novel solutions are required in the application of female body armour. Dome-shaped fabrics have acknowledged advantages in low wastage of materials, high performance and mechanical properties (e.g. light weight, good resistance to pressure), and satisfactory appearance to make 3D dome shape without seaming and cutting marks to reduce the possibility of breakage. Therefore this type of fabric is suitable for making armours by fitting female curvaceous torso properly.

In this chapter, seven groups of experiments have been set up to demonstrate the correlations between the deformation depth of dome-shaped fabrics and the relevant governing parameters. The more understanding of the relationships, the more suitable the dome formability could be estimated; therefore the better front female body armour panel could be predicted. ScotWeave CAD software plays a key role in designing dome-shaped fabrics.

3.1 Design Principle

Dome-shaped fabric could be produced by a mixture of weaves with long and short float lengths as an analogy to honeycomb weave structures. The formation of honeycomb weaves requires long floats of warp and weft yarns to make the ridges of the honeycomb, the short floats of warp and weft yarns to show hollows, which lie in a lower plane. This is because short-float weaves make a tight area where it is easy to expand and long-float weaves make a loose area where is easy to shrink. Therefore, a dome shape could be formed by using such a weave combination.

Tayyar [116] has produced a dome-shaped fabric sample to demonstrate the principle of honeycomb weaves, as mentioned in section 2.4.1.3 of Chapter 2. Nevertheless, it has been noticed that Tayyar utilised this principle but not obeyed it rigidly. Based on the structure of honeycomb weaves, long and short floats are supposed to arrange in outer and inner ring respectively to create the dome-shaped fabric. However, Tayyar's experiments demonstrated the opposite arrangement of weaves in concentric rings of the dome-shaped pattern. Her dome-shaped fabric was made by arranging plain, $\frac{2}{2}$ twill, twilled hopsack and 8-end sateen weaves from outer to centre ring. The lack of conformity between the honeycomb structure principle and Tayyar's experiments may be attributed to 1) the shape of dome and 2) more warp and weft yarns required when weaving dome-shaped fabrics. The tension is unbalanced in different directions of the dome shape and in turn the layout of warp and weft yarns is also unbalanced to make the dome-shaped fabric. Additionally, unlike honeycomb weaves in which only a few yarns are required to interlace with each other to form one repeat of the structure, many more yarns are required to finish one repeat of a dome-shaped weave structure.

Therefore, the principle of the honeycomb weave is not simply feasible in the production of dome-shaped fabrics.

3.2 Design of Dome-shaped Fabrics

This preliminary work aims to investigate the influence of different parameters on dome formability of dome-shaped fabrics on the basis of Tayyar's research. The weave parameter is taken into account as it is a fundamental element of the fabric construction. As the weave arrangement in concentric rings of the dome-shaped pattern is currently unclear, it is necessary to investigate this aspect first, i.e. the dome shape could be produced in the form of long and short floats arranged in outer and inner concentric rings respectively or the opposite counterpart or both. Additionally, six other important parameters (e.g. size of dome-shaped pattern, radius ratio, number of concentric rings of the dome-shaped pattern) have been set up to study their effect on dome formability. All these parameters are established on the basis of fabric settings with the assistance of ScotWeave CAD software.

3.2.1 Fabric settings

3.2.1.1 Warp and weft densities of fabrics

A Saurer 4×4 box pick& pick shuttle loom was used to make the dome-shaped fabrics, as shown in Figure 3.1. 100% polyester with 33 tex was used for the warp with density 100 ends per inch and 100% polyester with 62.8 tex was used for the weft with density 40 picks per inch. Because the linear density of weft roughly was twice than that of warp, 4×8 design paper was used to draw rings to guarantee the circular shape. The dome effect was not perfectly round, but was still acceptable.

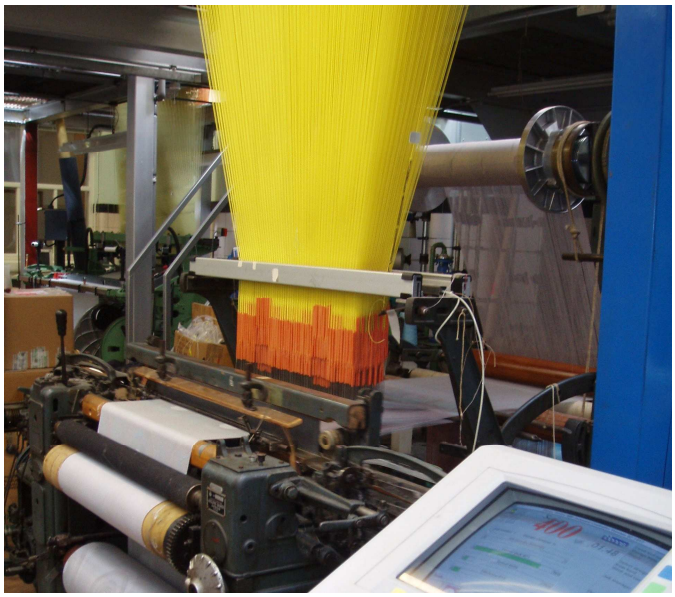

Figure 3.1 Saurer 4×4 box pick & pick shuttle loom

3.2.1.2 Arrangements of dome-shaped patterns on the fabric

It seemed inappropriate for single domes to weave line by line or side by side along the cloth width (shown in Figure3.2 (a)) as each weave demanded different warp length causing unbalanced warp tension. Therefore it was suggested to reduce this problem by shifting the patterns in the weave design, i.e., combining one pattern at the top and two symmetric halves at the bottom. The integral pattern at the bottom would form when the second repeat came, as shown in Figure 3.2 (b).

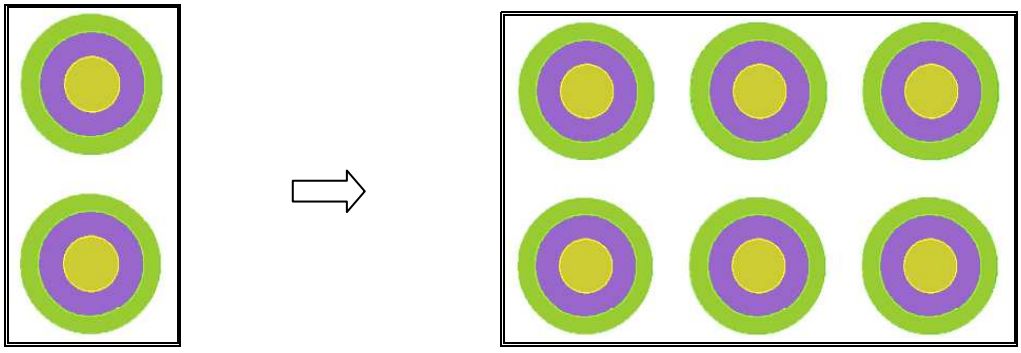

(a)

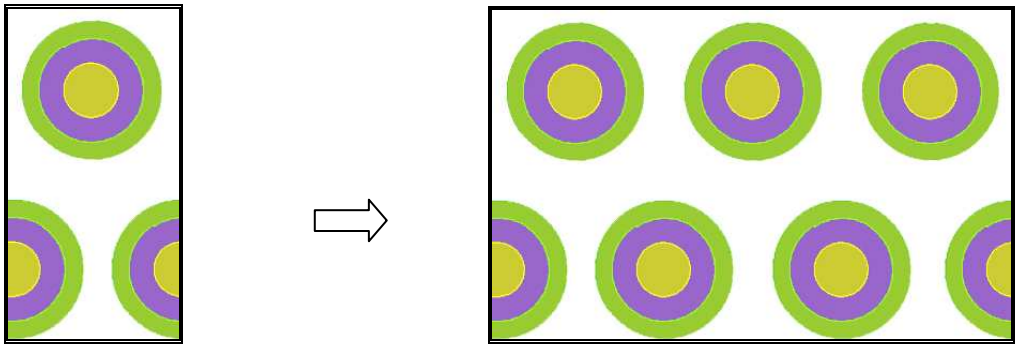

(b)

Figure 3.2 Arrangements of dome-shaped patterns

3.2.2 ScotWeave CAD software

The design was accomplished assisted with the program ScotWeave Version 0043, shown in Figure 3.3, was used to design the dome-shaped fabrics. Artwork Designer and Jacquard Designer were two main programs. In the former program, the basic data, such as the image size, base weave size, appropriate weft/warp repeats and repeat height/width, were set up; the numeric input and weft/warp yarns and dissimilar weaves for different areas were set up in the latter program. All the set-up information was recorded on a floppy disk, which was inserted into the computer for manufacturing, as shown in Figure 3.4. This software would also play a key role in the weave structure and dome-shaped design.

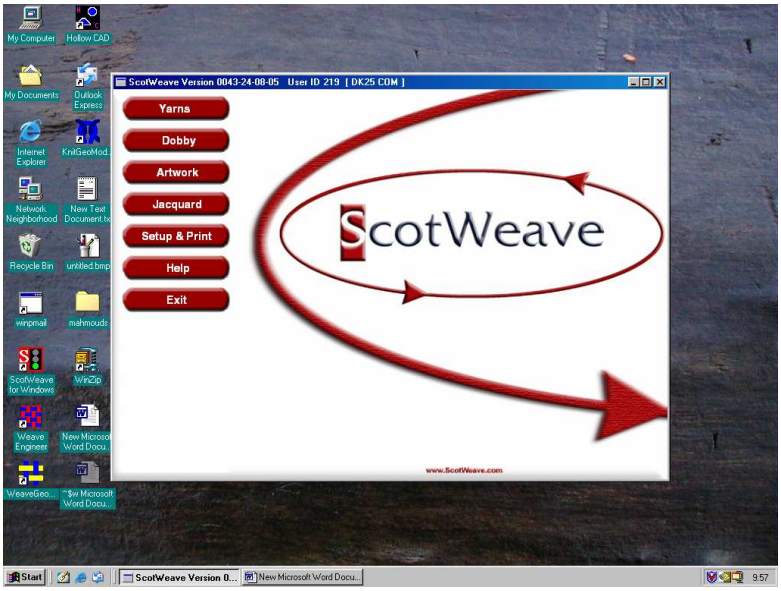

Figure 3.3 ScotWeave version 0043

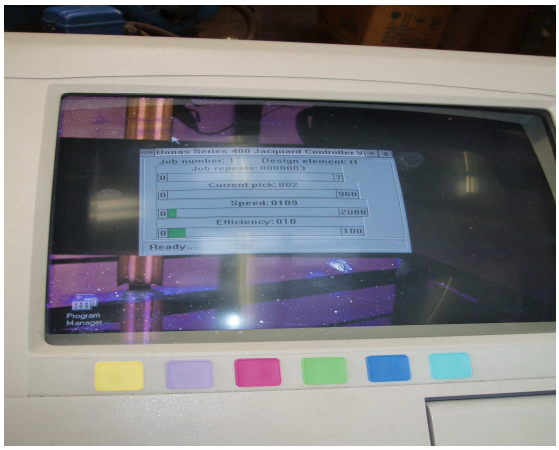

Figure 3.4 Loom control unit

3.2.3 Setting of dome-shaped pattern

3.2.3.1 Size of dome-shaped pattern

The size of the dome-shaped pattern was practically determined by three factors - the scope of weaving capability of the loom, the test scope of the dome tester and the apparent test results expected.

The Saurer 4×4 box pick & pick dobby loom was used in this research. It had a 60.7 cm reed width to determine the cloth width, and three beams behind to offer warp yarns and control the warp tension. The reed setting was not changed during the whole procedure of weaving. As shown in Figure 3.5, the circle base of the mouldability tester has the diameter 29.21 cm (11.5 inch), based on which, rings with the diameter 7.62 cm (3 inch), 15.24 cm (6 inch) and 22.86 cm (9 inch) were determined for the dome-shaped patterns. They were used to form different groups to demonstrate variance according to the various parameters employed. The same three patterns for every design were woven to obtain an average value. All the average values in the group would be analysed to obtain the experimental results.

Figure 3.5 Mouldability tester

3.2.3.2 Design groups

For the purposes of convenience of operation and obtaining results for comparison, the premise has been hypothesised as follows:

In the design of these experiments, the concentric rings' number is 3 and the radius ratio 1:2:3 is arranged from the centre ring to the outer. Plain, $\frac{2}{2}$ twill and 7-end satin are

employed to form the dome and the ground weave of the fabric is granite 8s. Additionally, the dome with the diameter of 9 inches, namely, 22.86 cm, is used as the original one when comparing other domes under different parameter considerations. Because 'inch' is the unit applied in the ScotWeave program, it is used to design the patterns, but converted into 'cm' to keep uniform with other data in test results. Other specifications or alternatives will be mentioned in exceptional circumstances.

In total, there are 24 different patterns designed, categorised into 6 groups, on the basis of varying single parameter one by one:

- 12-Patterns in group one, by changing the weaves;
- 3-Patterns in group two, by changing the size of dome;
- 3-Patterns in group three, by changing the radius ratio;
- 4-Patterns in group four, by changing the ring numbers;
- 3-Patterns in group five, by changing the weft linear densities;
- 3-Patterns in group six, by changing the weft densities.

The correlation between the dome formability and the shrinkage is also under consideration but no new patterns need to be specified.

Changing weaves

Weaves are the fundamental part of the woven fabrics; alternation of weaves would give an influence on the dome effect of the fabric. 15 weave structures have been used to investigate this influence, shown in Figure 3.6.

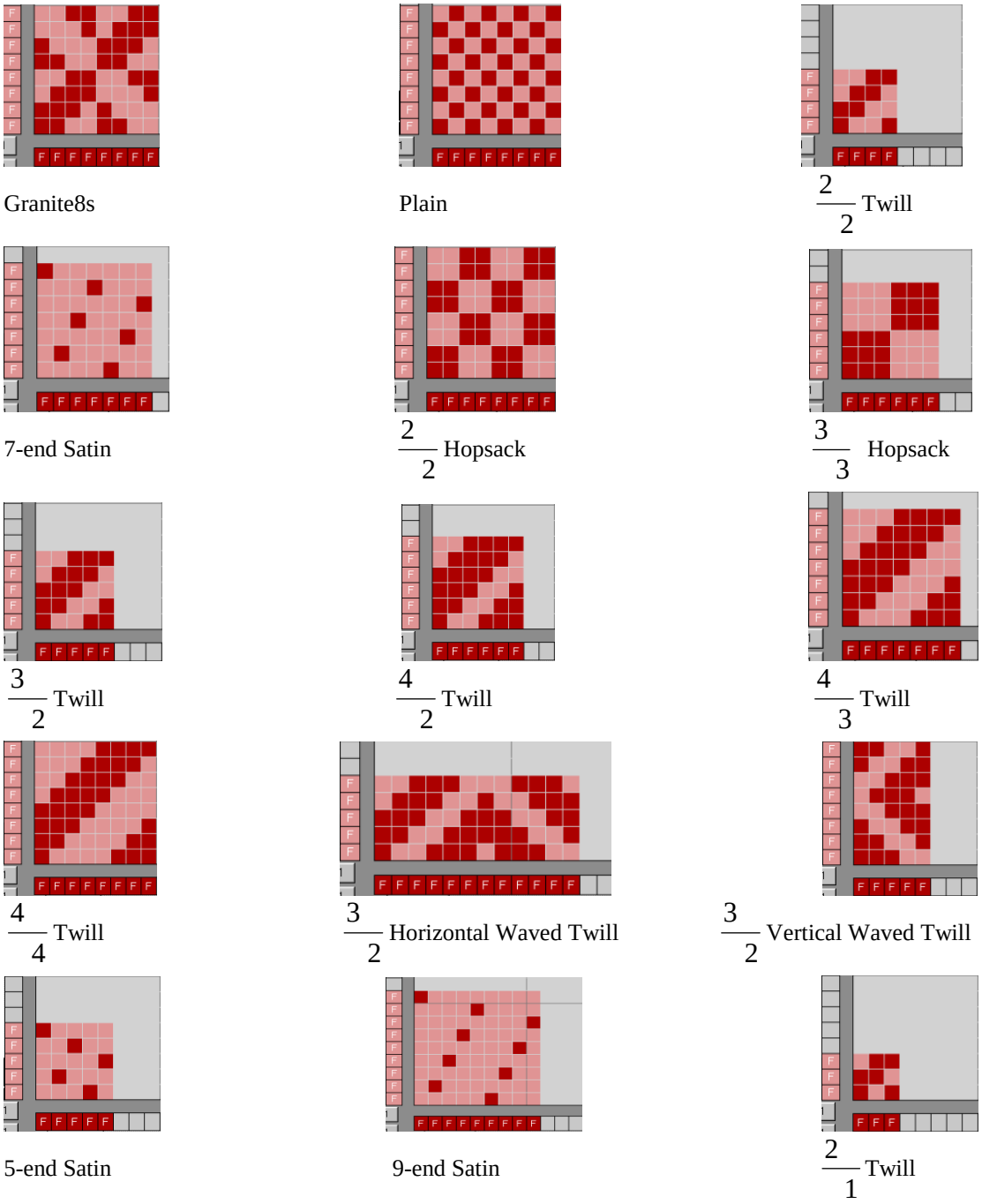

Figure 3.6 Weave structures

Sequence of weaves

The principle of the honeycomb is applied to determine the sequence of weaves, which has been mentioned in Literature Review: the tight weaves makes the fabric to expand and the loose weaves makes the fabric to shrink; based on these, domes could be shaped by means of making weaves with different floats.

The sequence of weaves from outer ring to centre ring is investigated firstly. One group of concentric rings with the same diameter 9 inches and the same number 3, given plain, $\frac{2}{2}$ twill and 7-end satin from outer ring to centre was drawn on the design paper, and the other with the same weaves but in an opposite sequence, as shown in Figure 3.7.

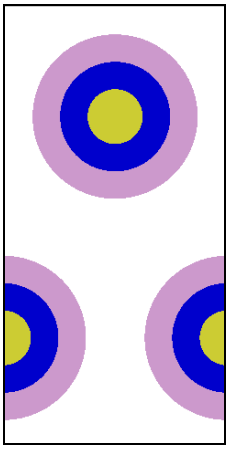

(a)

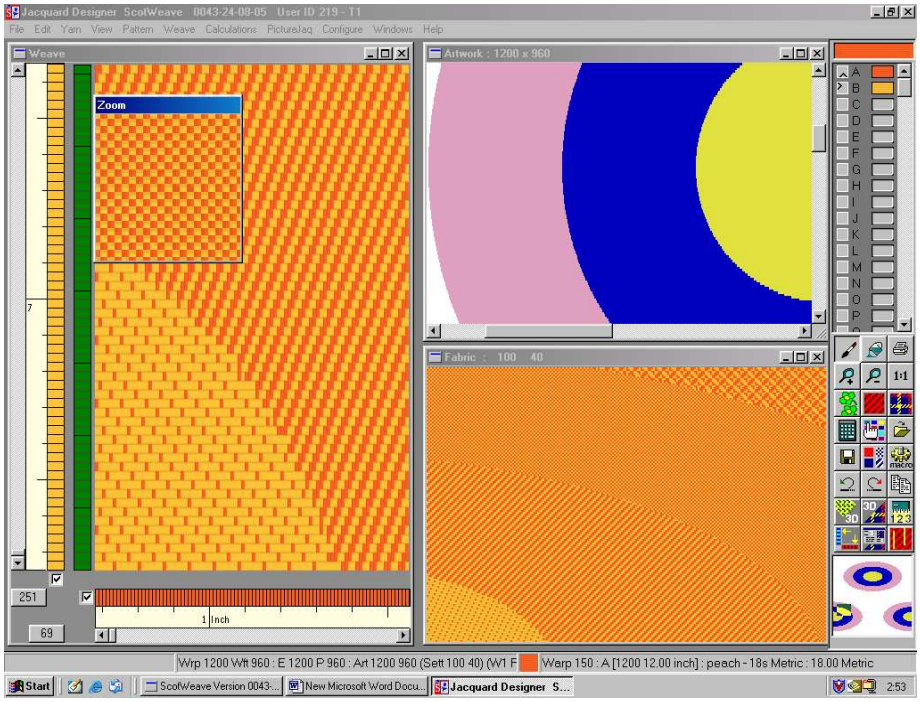

(b)

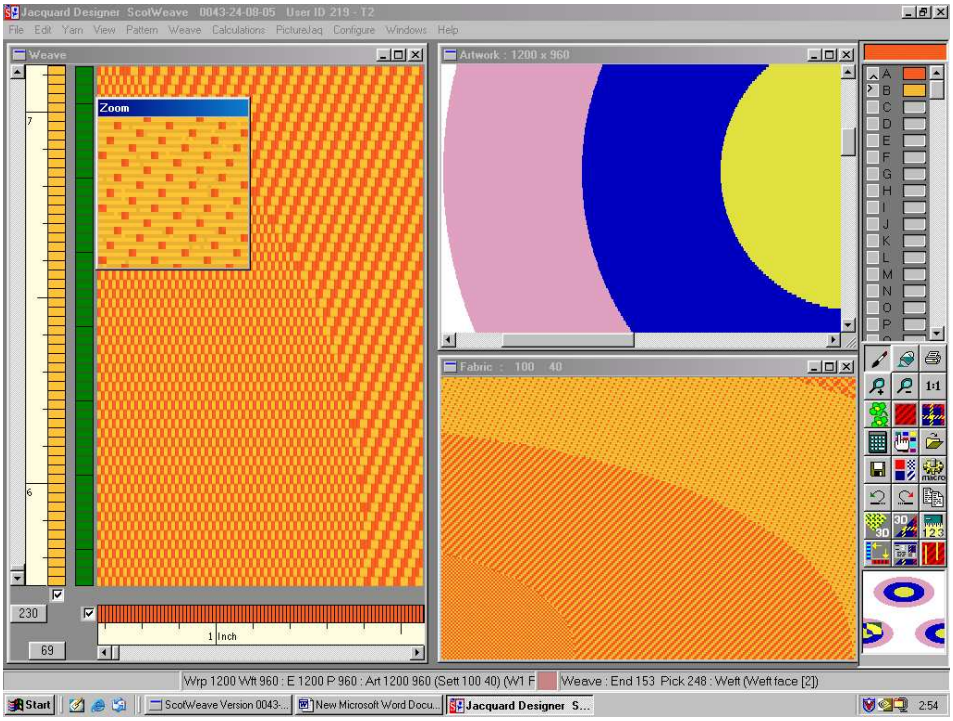

(c)

Figure 3.7 Sequences of weaves: (a) a repeat designed in artwork; (b) plain, $\frac{2}{2}$ twill and 7-end satin arranged from outer ring to centre; (c) 7-end Satin, $\frac{2}{2}$ twill and plain arranged from outer ring to centre

The consideration of the twill weaves employed in the outer ring or the centric place could be neglected because twill weaves do not have the shortest or longest floats, and therefore cannot show the apparent changes compared with plain or satin weaves. The design in Figure 3.7 (b) will be treated as the fundamental model when parameters vary on the basis of Tayyar's practical result in which the dome-shaped fabric is produced by weaves with short and long floats arranged from outer to inner ring. The weaves with the shortest float to the longest float will be employed from the outer ring to the centre, regardless of which types of weaves are employed and how many concentric rings compose a pattern. The production from the transference to the loom will be shown in the next section of manufacture.

Weaves are primarily divided into three categories: plain, twill and satin/sateen. Each of them has sub-branches, which could be applied to weave different dome-shaped fabrics. The major method is that two types of weaves unchange while the third is replaced by its representative derivatives in order to observe the difference on the dome depth of the fabrics.

1) Plain and plain derivatives

In this section, plain weave is replaced by its derivatives - $\frac{2}{2}$ Hopsack and $\frac{3}{3}$ hopsack respectively in the outer ring, as shown in Figure 3.8. The difference in the dome depth will be observed after manufacturing and will be analysed later.

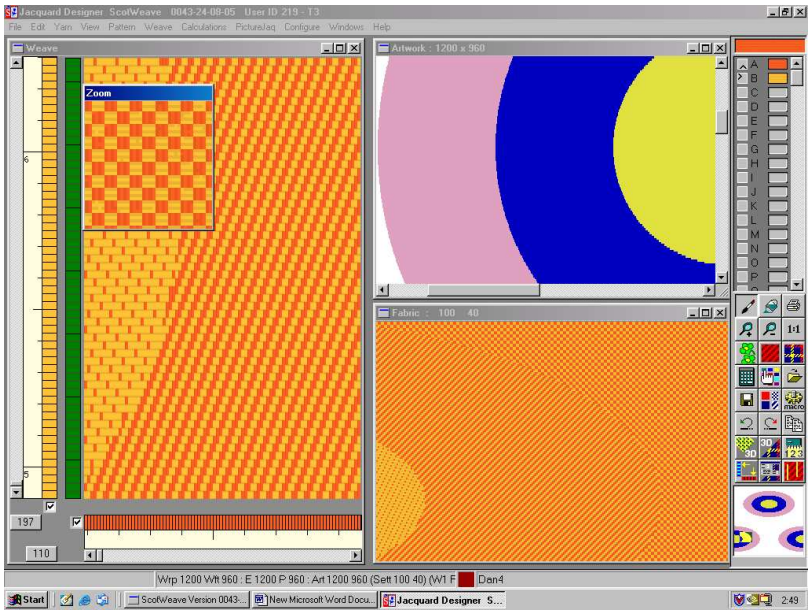

(a)

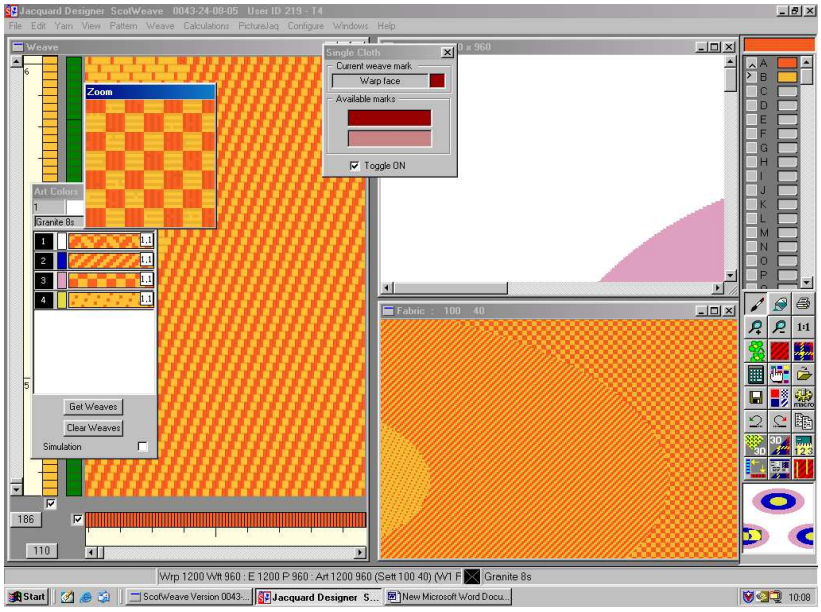

(b)

Figure 3.8 Plain and plain derivatives: (a) $\frac{2}{2}$ hopsack arranged in the outer ring; (b) $\frac{3}{3}$ hopsack arranged in the outer ring

2) Twill and Twill Derivatives

$\frac{2}{2}, \frac{3}{2}, \frac{4}{2}, \frac{4}{3}, \frac{4}{4}, \frac{3}{2}$ horizontal waved weave and $\frac{3}{2}$ vertical waved weave twills are selected for employing in the middle circle of the dome, while maintaining plain and satin unchanged. The patterns with the middle circle of $\frac{2}{2}$, $\frac{3}{2}$ and $\frac{4}{2}$ twills respectively were divided into the same groups based on lengthening the float on the surface; the domes with the middle circle made of $\frac{4}{2}$, $\frac{4}{3}$, $\frac{4}{4}$ respectively were compared based on lengthening the float on the back; the

dome with common $\frac{3}{2}$ twill were compared with the one with 3/2 horizontal waved weave and the other with $\frac{3}{2}$ vertical waved weave twills in another group.

3) Satins

5-end satin, 7-end satin and 9-end satin are used in the centre of the dome in succession. Their influence on the differences in depth of the dome will be listed later.

Size of domes

The domes with the diameters of 3 inches, 6 inches and 9 inches were used when taking into account the relationship between the dome formability and the size of dome. Their weave sequences in the domes were the same, still plain, $\frac{2}{2}$ twill and 7-end satin arranged from outer circle to inner circle.

Radius ratio

Different circle area ratios affect the dome formability. In this part, three domes with different circle area ratios were designed for comparison. The first one was the original one (3 circles, 9 inches) with the radius ratio-1: 2:3 from inner circle to outer. The radius ratios of the other two were 1:3:6 and 3:5:6 respectively. All the weave sequences remained unchanged.

Number of concentric rings

Here the domes with 3 rings, 4 rings, 5 rings and 6 rings were given in succession. Weaves with a gradual increase in the length of float would be arranged from the outer circle to inner circle separately, as shown in Figure 3.9.

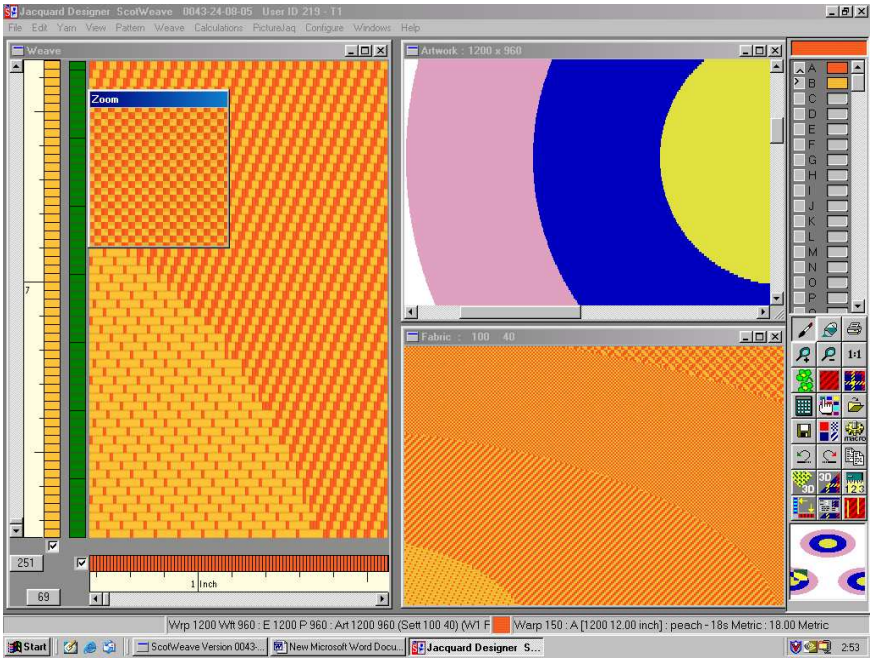
Jacquard Designer ScotWeave 0043-24-08-05 User ID 219 - T1
Weave
Zoom
Artwork : 1200 x 960
Fabric : 100 40
Wrp 1200 Wft 960 : E 1200 P 960 : Art 1200 960 (Sett 100 40) (W1 F
Warp 150 : A [1200 12.00 inch] : peach - 18s Metric : 18.00 Metric

(a)

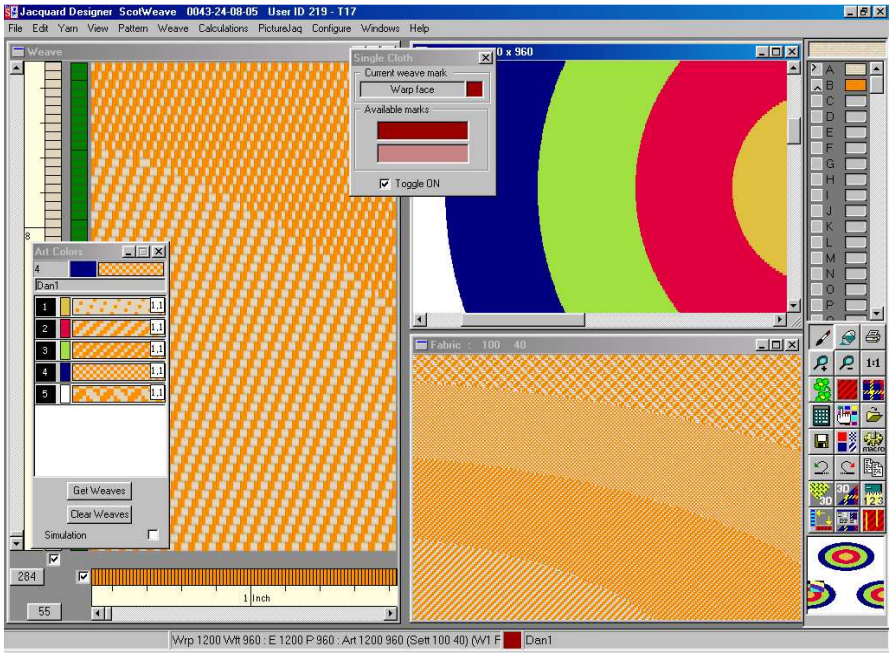
Jacquard Designer ScotWeave 0043-24-08-05 User ID 219 - T17
Weave
Single Cloth
Current weave mark
Warp face
Available marks
Toggle ON
Art Colors
Get Weaves
Clear Weaves
Simulation
Fabric : 100 40
Wrp 1200 Wft 960 : E 1200 P 960 : Art 1200 960 (Sett 100 40) (W1 F
Dan1

(b)

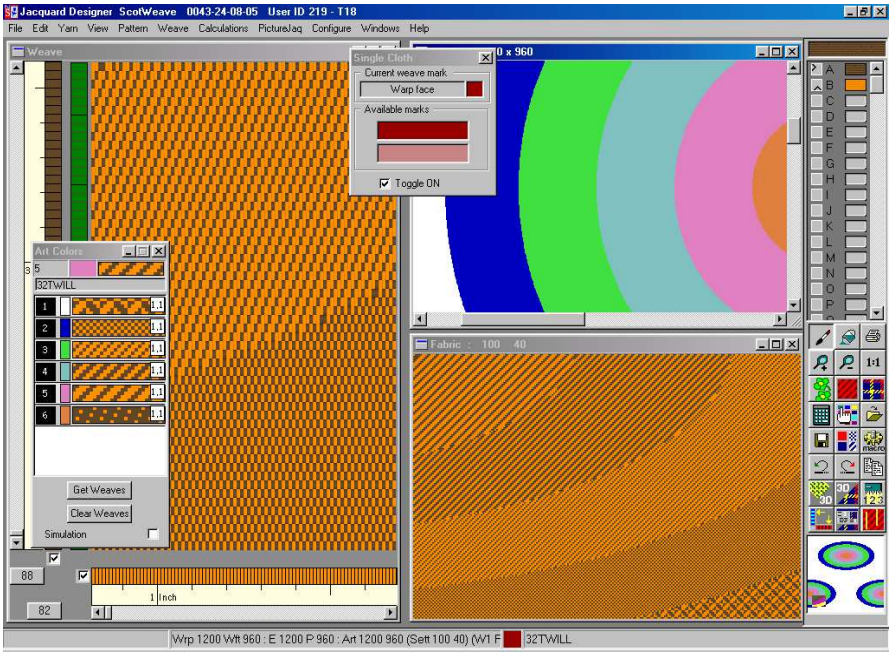

(c)

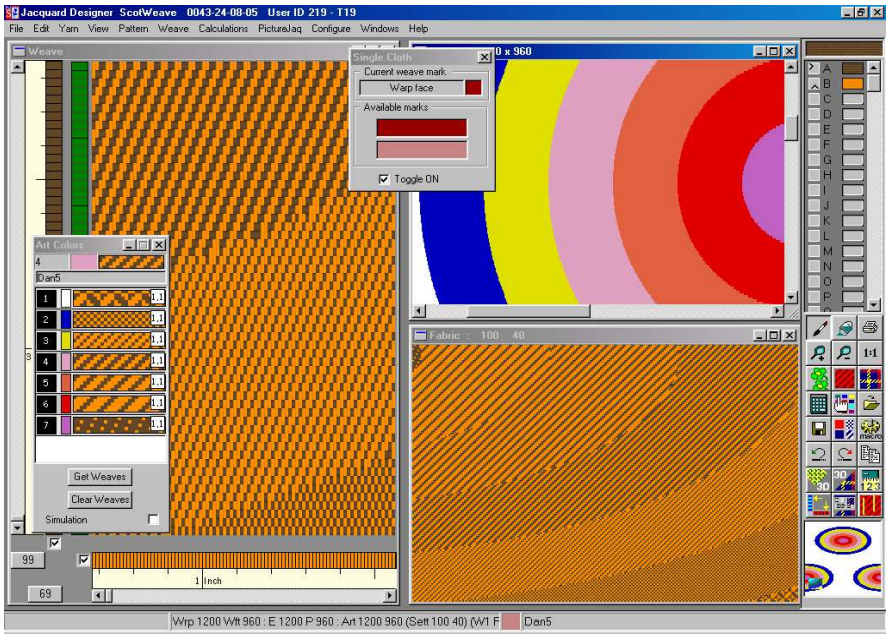

(d)

Figure 3.9 Numbers of concentric rings: (a) design of the dome with 3 rings; (b) design of the dome with 4 rings; (c) design of the dome with 5 rings; (d) design of the dome with 6 rings

Linear density

In this section, yarns with different weft linear densities 62.8 tex, 49.2 tex, 32.8 tex and 24.6 tex, decreasing one by one, were employed respectively in weaving the dome-shaped fabrics. The information of dome-shaped fabric design in Figure 3.7 (b)

was used – a group of concentric rings composed the design. The related specification includes the radius ratio1: 2:3; the diameter of the outer circle is 9 inches; plain, $\frac{2}{2}$ twill, 7-end satin were arranged from outer circle to centre.

Weft density

Within the same design, the variation in weft density leading to the difference in dome formability is also an important aspect to investigate. Weft densities—15.7 picks/cm, 12.6 picks/cm and 9.6 picks/cm would be used as examples.

Shrinkage

Apart from the aforementioned parameters, shrinkage would have an effect on the dome depth and their relationship will be disclosed by observing the difference in the length of picks/ends and the depth of dome before and after the washing process.

Broadly speaking, seven groups were established. All the experimental results will be demonstrated and analysed in the section 3.6 Measurement and Analysis of Dome Formability.

3.3 Manufacture

The Saurer 4×4 box pick & pick shuttle loom with the electronic jacquard was used for weaving the fabrics, and 33 tex and 62.8 tex polyester yarns were used for warp and weft respectively. The designs of the fabrics created by using ScotWeave software were stored on a disk, as already mentioned in section 3.2. The information on the disk was transferred to the jacquard loom for weaving. Figure 3.10 shows the loom from different

angles. It could be observed that two weaver's beams were used for weaving these fabrics.

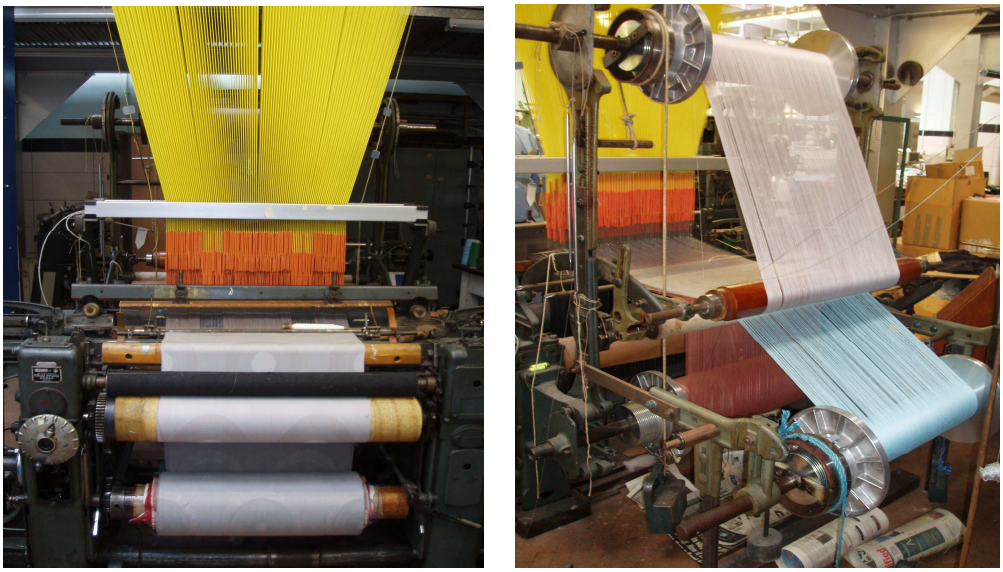

Figure 3.10 Weaving

3.4 Manufacturing Phenomenon

A total of 24 different fabric samples were manufactured from the designs described in section 3.2. The problems and solutions associated with weaving these fabrics are described below.

3.4.1 Curved cloth fell

The first phenomenon was in the curved cloth fell. The same new pick was not beaten up to the same horizontal line when the weaves were different across the fabric width, as shown in the two photographs in Figure 3.11. The fabric area made of plain weave tends to expand most obviously, especially in the vertical direction, followed by the twills and then the satin weaves. Such effect may prove the principle of honeycomb structure, i.e. shorter-float weaves lead to tighter fabric and longer-float weaves make looser fabric. When tighter and looser fabrics are produced side by side, the tighter fabric section tends to invade into the looser fabric sections. For the plain weave, the

weft yarn interlaces with the warp yarn so compactly that the tension inside is greater than that within twill and satin weaves. Therefore, the plain weave has the tightest structure and inclines to expand. Whereas satin weaves, in an opposite situation, have the least number of intersections and tend to produce fabric sections which can be easily pushed in or shrink. This is a general occurrence when weaving almost all fabrics with different weaves in this research.

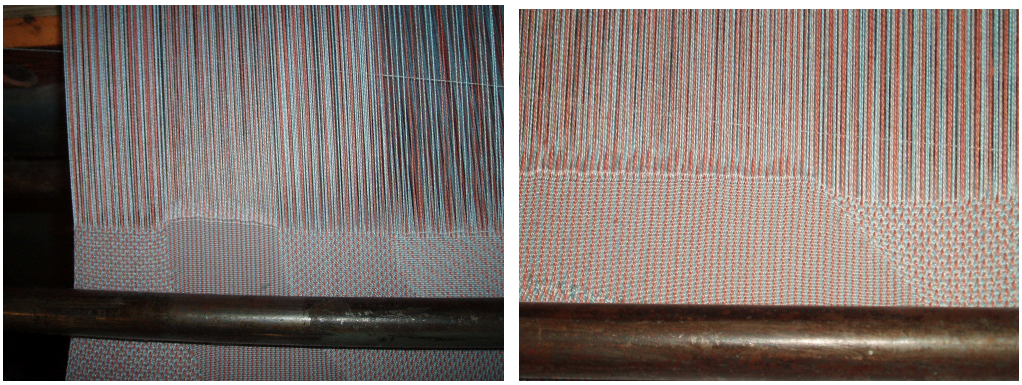

Figure 3.11 Curved cloths fell phenomenon

3.4.2 Slack warp ends

The slack warp ends were observed during the weaving process. The warp ends responsible for forming the satin fabric section become slack after a while, because of fewer intersections compared to other fabric sections. In contrast, the warp ends for the plain fabric section becomes over tight. The tension increase and decrease in the warp ends can be compensated by shifting the patterns in the weave design, which has been demonstrated in section 3.2.

3.4.3 Loose selvedges

Loose selvedge is another apparent phenomenon observed during the weaving process, i.e. bulging selvedge is more likely to be produced when certain weaves (especially hopsack weaves) are applied. Figure 3.12 illustrates this situation: when $\frac{3}{3}$ hopsack

weave combined with other weaves to construct the fabric, the selvedge section created by the hopsack weave expands out and becomes quite loose. This is because the hopsack weave structure does not allow the warp ends to be bundled together enough, and the result only could be expanded out. However, this makes little influence on the patterns used for the measurement because all the valid patterns would be chosen away from the selvedge.

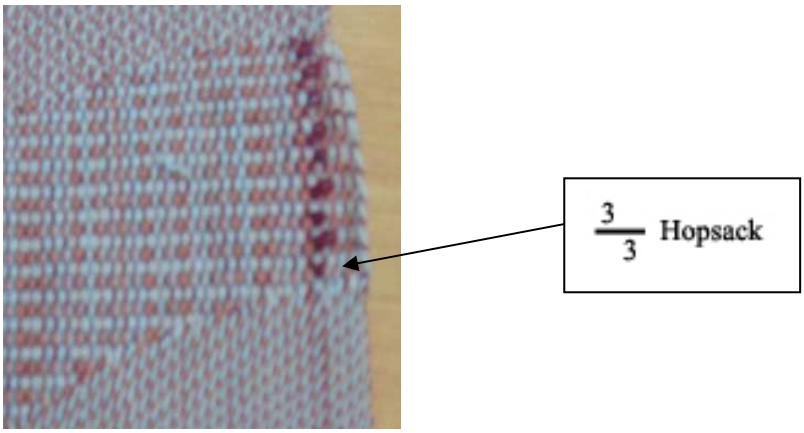

Figure 3.12 Loose selvedge

3.4.4 Weave compatibility

Figure 3.13 (a) shows some longer floats formed on the surface of the fabrics. This is because of the different woven structures used, leading to the longer floats appearing on the intersection connecting the twill weaves with the plain weaves, as shown in Figure 3.13 (b). This weave compatibility problem, which has smaller effect on the relationship between the dome formability and different parameters than the appearance of the fabrics. Adding more intersections could avoid this problem if required, as shown in Figure 3.13 (c).

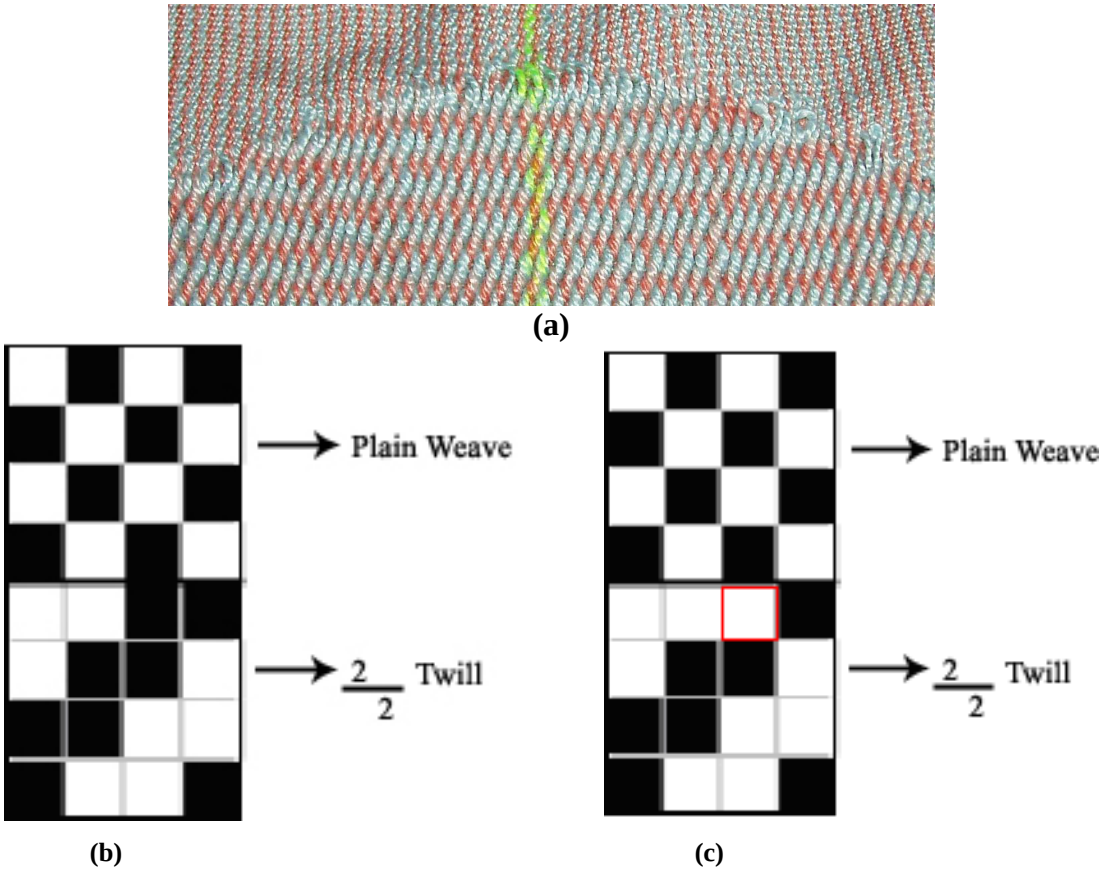

Figure 3.13 Weave compatibility: (a) longer float phenomenon; (b) intersection connection; (c) add intersection

3.5 Manufactured Fabrics

Twenty four different woven fabrics were made for this research. Figure 3.14 shows two examples of fabrics, which were woven based on the designs about weave sequence in the first group mentioned in section 3.2. The fabric showed in Figure 3.14 (a) uses the plain, $\frac{2}{2}$ twill and 7-end satin weaves from the outer ring to the centre; while the fabric shown in (b) uses the opposite sequence of these weaves. Analysis is demonstrated in section 3.6.

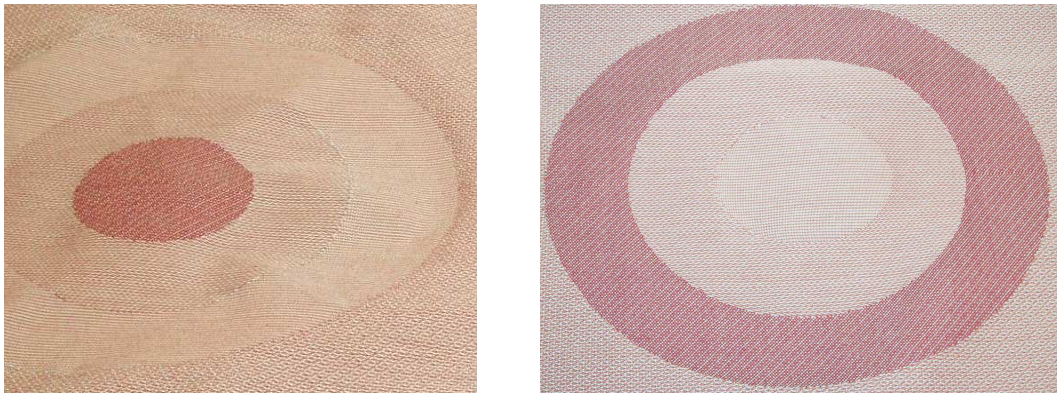

(a) **(b)**

Figure 3.14 Production sample: (a) plain, $\frac{2}{2}$ twill and 7-end satin weaves from the outer ring to the centre; (b) 7-end satin, $\frac{2}{2}$ twill and plain weaves from the outer ring to the centre

The fabrics manufactured were washed at a temperature of 45°C for 65 minutes with no detergent then naturally dried for 24 hours. Measurement of dome effect was taken before and after washing. Results and analysis for the relationship between the dome formability and different fabric parameters are presented below.

3.6 Measurement and Analysis of Dome Formability

This section describes the measurement and analysis of dome effect of the fabrics produced. The yarn used for making the fabrics was 100% polyester with the linear density of 62.8 tex for the warp and 33 tex for the weft. The fabrics were allowed to relax under standard laboratory conditions (20±2°C and 65±2% R.H.). The fabrics were washed at a temperature of 45°C for 65 minutes with no detergent. Measurements were taken before washing and after washing. In order to obtain the data with reasonable accuracy, each design was woven three times, named as a, b and c, and their average values were calculated.

The dome depth and the diameters (of the designed circular area in both warp and weft directions) were measured to find out the relationship between the dome formability and

different structural parameters. As has been explained, the fabrics were measured twice, i.e. before washing and after washing. For the former purpose, more attention would be paid to the dome depth after washing, because the samples reached the permanent geometry; for the latter purpose, the samples would be compared before washing and after washing.

3.6.1 Tools for measurement

A tape was used for the measurement of diameters in warp and weft directions, and the dome mouldability tester for measuring the dome depth.

The mouldability tester has been shown in Figure 3.5. The base has a groove that engages with the ridge to grip the fabric during measuring. The probe with a scale is to measure the depth of the dome. To test the deformation depth, the fabric is placed evenly on the base without extending, and the top is then placed gently on it. At the same time, the groove and the ridge are engaged, holding the fabric. Then the probe is gently pushed down to deform the fabric. The top of the tester is lifted slightly while the fabric is being pushed downwards to permit the fabric to enter the ring. Just before the fabric starts to wrinkle, the scale value is read, which is regarded as the depth of the fabric deformation. The depth is then used as an index of the fabric's mouldabiltiy [119].

3.6.2 Sample details

In total, 24 samples have been woven which are named as S1, S2 … up to S24. The specifications for all samples are listed in Table 3.1. The woven structures have been demonstrated in the section 3.2.3.

Table 3.1 Specification of all samples

Sample Name	Dome Diameter in warp direction (cm)	Weave(outer to inner)	Radius Ratio (outer to inner)	Linear Density (warp × weft) (tex)	Fabric Density (warp × weft) (per cm)
S1	22.86	**Plain,** $\frac{2}{2}$ **Twill,**7**-end Satin***	3:2:1	33×62.8	39.4×15.7
S2	22.86	7**-end Satin,** $\frac{2}{2}$ **Twill, Plain**	3:2:1	33×62.8	39.4×15.7
S3	22.86	$\frac{2}{2}$ **Hopsack,** $\frac{2}{2}$ Twill,7-end Satin	3:2:1	33×62.8	39.4×15.7
S4	22.86	$\frac{3}{3}$ **Hopsack**, $\frac{2}{2}$ Twill, 7-end Satin	3:2:1	33×62.8	39.4×15.7
S5	22.86	Plain, $\frac{3}{2}$ **Twill**,7-end Satin	3:2:1	33×62.8	39.4×15.7
S6	22.86	Plain, $\frac{4}{2}$ **Twill**, 7-end Satin	3:2:1	33×62.8	39.4×15.7
S7	22.86	Plain, $\frac{4}{3}$ **Twill**, 7-end Satin	3:2:1	33×62.8	39.4×15.7
S8	22.86	Plain, $\frac{4}{4}$ **Twill**, 7-end Satin	3:2:1	33×62.8	39.4×15.7
S9	22.86	Plain, $\frac{3}{2}$ **Horizontal Waved Twill**, 7-end Satin	3:2:1	33×62.8	39.4×15.7
S10	22.86	Plain, $\frac{3}{2}$ **Vertical Waved Twil**l, 7-end Satin	3:2:1	33×62.8	39.4×15.7
S11	22.86	Plain, $\frac{2}{2}$ Twill, 5**-end Satin**	3:2:1	33×62.8	39.4×15.7
S12	22.86	Plain, $\frac{2}{2}$ Twill, 9**-end Satin**	3:2:1	33×62.8	39.4×15.7
S13	**7.62**	Plain, $\frac{2}{2}$ Twill, 7-end Satin	3:2:1	33×62.8	39.4×15.7
S14	**15.24**	Plain, $\frac{2}{2}$ Twill, 7-end Satin	3:2:1	33×62.8	39.4×15.7
S15	22.86	Plain, $\frac{2}{2}$ Twill, 7-end Satin	**6:3:1**	33×62.8	39.4×15.7

S16	22.86	Plain, $\frac{2}{2}$ Twill, 7-end Satin	**6:5:3**	33×62.8	39.4×15.7
S17	22.86	Plain, $\frac{2}{1}$ **Twill,** $\frac{2}{2}$ Twill, 7-end Satin	**4:3:2:1**	33×62.8	39.4×15.7
S18	22.86	Plain, $\frac{2}{1}$ **Twill**, $\frac{2}{2}$ Twill, $\frac{3}{2}$ **Twill,**7-end Satin	**5:4:3:2:1**	33×62.8	39.4×15.7
S19	22.86	Plain, $\frac{2}{1}$ **Twill**, $\frac{2}{2}$ Twill, $\frac{3}{2}$ **Twill,** $\frac{4}{2}$ **Twill,**7-end Satin	6:5:4:3:2:1	33×62.8	39.4×15.7
S20	22.86	Plain, $\frac{2}{2}$ Twill, 7-end Satin	3:2:1	33×**49.2**	39.4×15.7
S21	22.86	Plain, $\frac{2}{2}$ Twill, 7-end Satin	3:2:1	33×**32.8**	39.4×15.7
S22	22.86	Plain, $\frac{2}{2}$ Twill, 7-end Satin	3:2:1	33×**24.6**	39.4×15.7
S23	22.86	Plain, $\frac{2}{2}$ Twill, 7-end Satin	3:2:1	33×62.8	39.4×**12.6**
S24	22.86	Plain, $\frac{2}{2}$ Twill, 7-end Satin	3:2:1	33×62.8	39.4×**9.6**
***The bold characters indicate that parameters have changed.**					

3.6.3 Investigations

3.6.3.1 Categories of groups

For the purpose of investigating the relationship between fabric parameters and the depth of domes, 7 groups of fabrics have been organised to observe the influence of the following structural parameters on the dome formability;

(1) Weave selections and weave sequence,

(2) Dome size,

(3) Radius ratio,

(4) Number of circles,

(5) Weft yarn count,

(6) Weft density in fabrics,

(7) Shrinkage.

Table 3.2 lists the details of these 7 groups of fabric samples.

Table 3.2 Categories of groups

GROUPS	PARAMETERS		ROUTES
The relationship between weaves and the dome formability	Sequence of weaves		Comparing sample 1 and sample 2
	Choice of weaves	1.Weaves of outer circle-plain and plain derivatives (plain, $\frac{2}{2}$ Hopsack and $\frac{3}{3}$ Hopsack)	Comparing sample 1, sample 3 and sample 4
		2.Weaves of middle circle-twills ($\frac{2}{2}$ twill, $\frac{3}{2}$ twill, and $\frac{4}{2}$ twill)	Comparing sample 1, sample 5 and sample 6
		3.Weaves of middle circle-twills ($\frac{4}{2}$ twill, $\frac{4}{3}$ twill, $\frac{4}{4}$ twill)	Comparing sample 6, sample 7 and sample 8
		4.Weaves of middle circle-twills ($\frac{3}{2}$ twill, $\frac{3}{2}$ horizontal waved twill, and $\frac{3}{2}$ vertical waved twill)	Comparing sample 5, sample 9 and sample 10

		5.Weaves of inner circle-sateen and satins (5-end satin, 7-end satin, and 9-end satin)	Comparing sample 11, sample 1 and sample 12
The relationship between size of dome and the dome formability	Diameter of domes-7.62cm, 15.24cm, 22.86cm		Comparing sample 13, sample 14 and sample 1
The relationship between radius ratio and the dome formability	Radius ratio 1: 2:3,1:3:6, and 3:5:6		Comparing sample 1, sample 15 and sample 16
The relationship between the number of circles and the dome formability	Number of circles- 3, 4, 5 and 6		Comparing sample 1, sample 17, sample 18 and sample 19
The relationship between the weft linear density and the dome formability	Weft linear densities-62.8 tex, 49.2 tex, 32.8 tex and 24.6tex		Comparing sample 1, sample 20, sample 21 and sample 22
The relationship between the weft density and the dome formability	Weft densities-15.7 picks/cm, 12.6 picks/cm and 9.6 picks/cm		Comparing sample 1,sample 23 and sample 24
The relationship between the shrinkage and the dome formability	Shrinkage in both warp and weft direction		Comparing sample1,sample3 and sample4 before and after washing; Comparing sample13, sample 14 and sample 1 before and after washing.

	5.Weaves of inner circle-sateen and satins (5-end satin, 7-end satin, and 9-end satin)	Comparing sample 10, sample 1 and sample 11
The relationship between size of dome and the dome formability	Diameter of domes-7.62cm, 15.24cm, 22.86cm	Comparing sample 12, sample 13 and sample 1
The relationship between radius ratio and the dome formability	Radius ratio 1: 2:3,1:3:6, and 3:5:6	Comparing sample 1, sample 14 and sample 15
The relationship between the number of circles and the dome formability	Number of circles- 3, 4, 5 and 6	Comparing sample 1, sample 16, sample 17 and sample 18
The relationship between the weft linear density and the dome formability	Weft linear densities-62.8 tex, 49.2 tex, 32.8 tex and 24.6tex	Comparing sample 1, sample 19 sample 20 and sample 21
The relationship between the weft density and the dome formability	Weft densities-15.7 picks/cm, 12.6 picks/cm and 9.6 picks/cm	Comparing sample 1,sample 22 and sample 23
The relationship between the shrinkage and the dome formability	Shrinkage in both warp and weft Direction	Comparing sample1,sample 2 and sample 3 before and after washing; Comparing sample12, sample 13 and sample 1 before and after washing.

3.6.3.2 Group 1. weaves V.S. dome formability

Sequence of weaves

Samples S1 (woven sequence: Plain, $\frac{2}{2}$ Twill, 7-end satin from outer to inner circle) and S2 (woven sequence: 7-end satin, $\frac{2}{2}$ Twill, Plain from outer to inner circle) were compared. The data obtained is shown in Table 3.3.

Table 3.3 Data on dome depth when the weave sequence was changed

Before Washing				
	Depth of Dome (cm)			
Sample	a	b	c	Average
S1	2.00	2.00	2.00	**2.00**
S2	2.50	2.40	2.60	**2.50**

After Washing				
	Depth of Dome (cm)			
Sample	a	b	c	Average
S1	3.20	3.20	3.10	**3.17**
S2	3.40	3.70	3.50	**3.53**

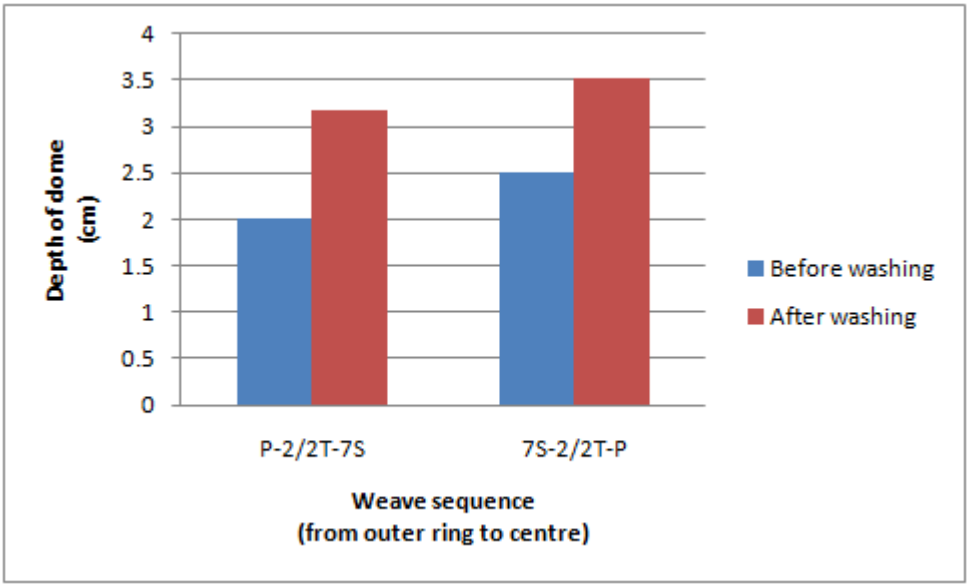

Symbols	Sample
P-2/2T-7S	S1
7S-2/2T-P	S2

Figure 3.15 Comparisons of Sample 1 and Sample 2

S1 represents the weave sequence of plain, $\frac{2}{2}$ twill and 7-end satin arranged from outer circle to inner circle based on Tayyar's experiments and S2 represents the weave sequence of 7-end satin, $\frac{2}{2}$ Twill, Plain from outer to inner circle according to the principle of the honeycomb weave structure. As shown in Figure 3.15, firstly it could be observed that weaves with different floats could make dome-shaped fabrics no matter which weave sequence is selected, i.e. short and long floats are arranged in the outer and inner rings respectively or in the opposite way. Secondly, the dome depth of S1 is smaller that that of S2, this may indicate the fabric with the weave sequence according to the principle of a honeycomb weave structure could offer better dome formability. The dome effect was more apparent when the loose weave was applied in the outer ring for shrinkage performance and the tight weave applied in the inner ring for expansion performance. Theoretically, the shorter the float, the tighter the fabric, which tends to

expand; the longer the float, the looser the fabric, which tends to shrink. The dome will bulge out with different weave combinations.

Choice of weaves

1) Changing the weave for the outer circle

To understand the behaviour of the dome with the different outer ring weaves, samples S1, S3 and S4 were compared, as they are the same in all aspects except for their outer circle weaves: S1 uses plain weaves, S3 $\frac{2}{2}$ Hopsack, and S4 $\frac{3}{3}$ Hopsack (listed in Table 3.1).

The dome depths for all these fabric samples, before and after washing, are listed in Table 3.4.

Table 3.4 Data on dome depth when the weaves of the outer ring were changed

Before Washing				
	Depth of Dome (cm)			
Sample	a	b	c	Average
S1	2.00	2.00	2.00	**2.00**
S3	2.50	2.50	2.60	**2.53**
S4	3.00	3.00	3.00	**3.00**

After Washing				
	Depth of Dome (cm)			
Sample	a	b	c	Average
S1	3.20	3.20	3.10	**3.17**
S3	3.50	3.40	3.60	**3.50**
S4	3.90	4.00	3.80	**3.90**

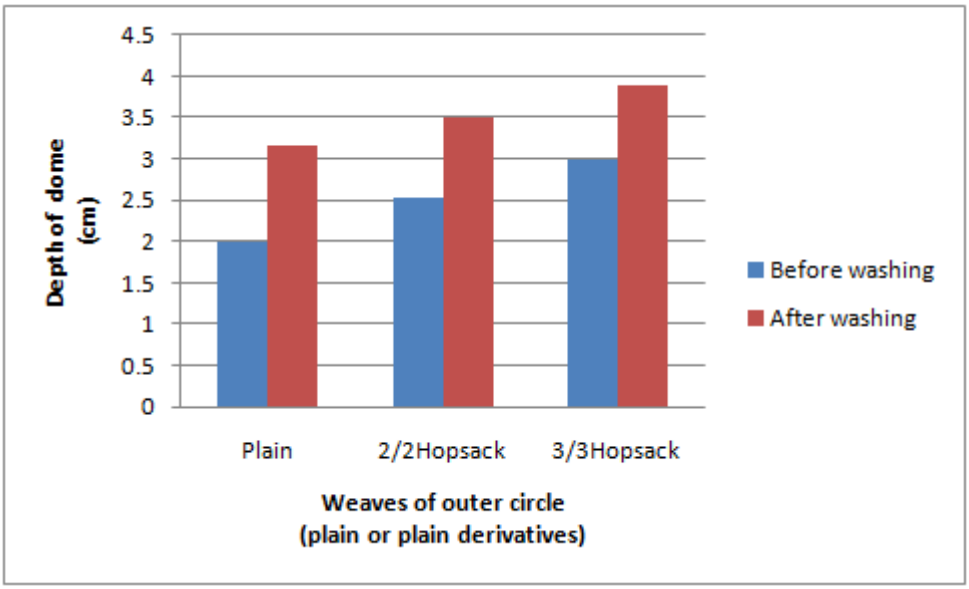

Symbols	Sample
Plain	S1
$\frac{2}{2}$ Hopsack	S3
$\frac{3}{3}$ Hopsack	S4

Figure 3.16 Comparisons of Sample1, Sample2 and Sample 3

It can be observed that S4 has the largest depth of dome, while S1 has the lowest depth of dome. For S4, $\frac{3}{3}$ hopsack weaves were used for the outer circle. For S1, plain weaves were used for the outer circle. The woven structure of $\frac{3}{3}$ hopsack weaves have larger float lengths than plain weaves, demonstrating that, whenever the longer float weave is used in the ringed structure, the longer average float length tends to contribute more to the dome depth. Besides, the washing treatment could have a dominant effect on the dome depth; all domes become larger after washing.

2) Changing the weaves for the middle circle

To understand the behaviour of the dome with the different middle circle weaves, samples S1, S5, S6, S7, and S8 were compared. The study was divided into two parts. In the first part, face floats were varied only in the middle ring weaves: Samples S1, S5 and S6 were compared, $\frac{2}{2}$ twill weaves for S1, $\frac{3}{2}$ twill weaves for S5 and $\frac{4}{2}$ twill weaves for S6 were used for the middle circles (listed in Table 3.1).

In the second part, back floats were varied only in the middle circle: Sample S6, S7 and S8 were compared, $\frac{4}{2}$ twill weaves for S5, $\frac{4}{3}$ twill weaves for S6 and $\frac{4}{4}$ twill weaves for S8 were used for the middle circles (listed in Table 3.1). The dome depths for these fabric samples, before and after washing, are listed in Table 3.5 and Table 3.6.

Table 3.5 Data on dome depth when the weaves of the middle ring were changed for Sample 1, 5 and 6

Before Washing				
	Depth of Dome (cm)			
Sample	**a**	**b**	**c**	**Average**
S1	2.00	2.00	2.00	**2.00**
S5	2.10	2.10	2.10	**2.10**
S6	2.10	2.20	2.20	**2.17**

After Washing				
	Depth of Dome (cm)			
Sample	**a**	**b**	**c**	**Average**
S1	3.20	3.20	3.10	**3.17**
S5	3.30	3.20	3.20	**3.23**
S6	3.35	3.30	3.30	**3.32**

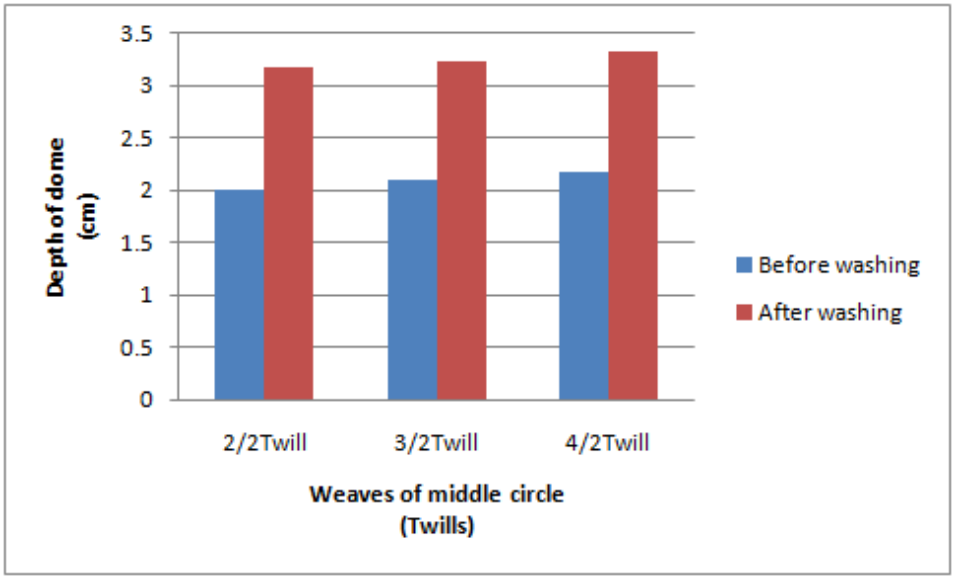

Symbols	Sample
$\frac{2}{2}$ Twill	S1
$\frac{3}{2}$ Twill	S5
$\frac{4}{2}$ Twill	S6

Figure 3.17 Comparisons of Sample 1, Sample 5 and Sample 6

Figure 3.17 shows the difference in the dome depth by changing the face float length of the twill weaves for the middle ring. It can be observed that the depth of the dome increases as the average float of the weaves increases both before and after washing. However, the increase in dome depth is less apparent by lengthening the float of the twill weaves for the middle circle than by lengthening the float of plain weaves for the outer circle, compared with the situation in Figure 3.16.

Table 3.6 Data on dome depth when the weaves of the middle ring were changed for Sample 6, 7 and 8

Before Washing				
	Depth of Dome (cm)			
Sample	a	b	c	Average
S6	2.10	2.20	2.20	**2.17**
S7	2.20	2.20	2.30	**2.23**
S8	2.20	2.30	2.30	**2.27**

After Washing				
	Depth of Dome (cm)			
Sample	a	b	c	Average
S6	3.35	3.30	3.30	**3.32**
S7	3.30	3.40	3.40	**3.37**
S8	3.50	3.40	3.50	**3.47**

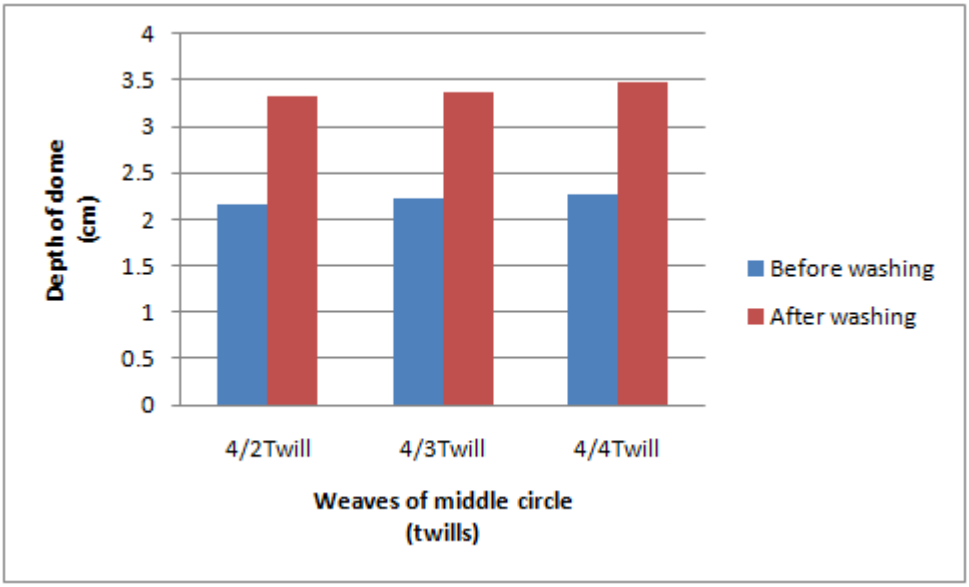

Symbols	Sample
$\frac{4}{2}$ Twill	S6
$\frac{4}{3}$ Twill	S7
$\frac{4}{4}$ Twill	S8

Figure 3.18 Comparisons of Sample 6, Sample 7 and Sample 8

Figure 3.18 illustrates a similar trend as shown in Figure 3.17. The depth of dome tends to increase when the average back float becomes longer. The change in the dome depth is also not obvious.

In addition, the variation of dome depth by employing the weaves with the same float length but different woven structures was also investigated. $\frac{3}{2}$ twill weaves,

$\frac{3}{2}$ horizontal weaved twill weaves, and $\frac{3}{2}$ vertical waved twill weaves for the middle circle were used in S5, S9 and S10 respectively.

Table 3.7 Data on dome depth when the weaves of the middle circle were changed for Sample 5, 9 and 10

Before Washing				
	Depth of Dome (cm)			
Sample	**a**	**b**	**c**	**Average**
S5	2.10	2.10	2.10	**2.10**
S9	1.90	1.90	2.00	**1.93**
S10	2.10	2.00	2.00	**2.03**

After Washing				
	Depth of Dome (cm)			
Sample	**a**	**b**	**c**	**Average**
S5	3.30	3.20	3.20	**3.23**
S9	3.20	3.10	3.25	**3.18**
S10	3.30	3.20	3.15	**3.22**

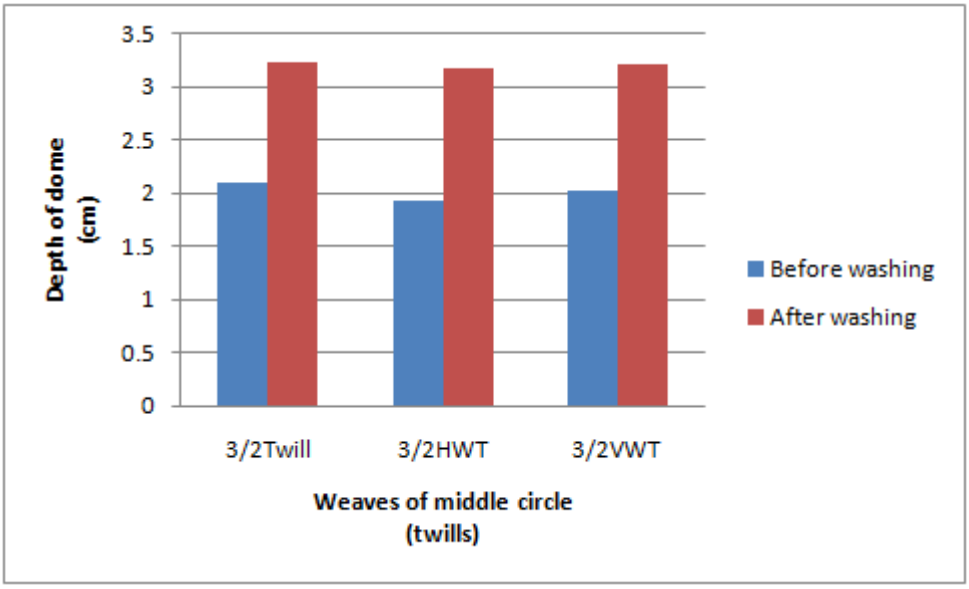

Symbols	Sample
$\frac{3}{2}$ Twill	S5
$\frac{3}{2}$ HWT($\frac{3}{2}$ Horizontal Waved Twill)	S9
$\frac{3}{2}$ VWT($\frac{3}{2}$ Vertical Waved Twill)	S10

Figure 3.19 Comparisons of Sample 5, Sample 9 and Sample10

This chart indicates that the weaves with the same float length could affect the depth of the domes differently. In Figure 3.19 the dome woven with $\frac{3}{2}$ horizontal waved twills weaves for the middle circle has the lowest depth compared with the domes with $\frac{3}{2}$ twill and $\frac{3}{2}$ vertical waved twill as their middle weaves. The difference in dome depth between S5 and S10 is not very apparent. The same tendency could be observed before and after washing.

3) Changing the weaves for the inner circle

To understand the behaviour of the dome with the different inner circle weaves, samples S11, S1 and S12 were compared, as they are same in all aspects expect for their inner circle weaves: S11 woven with 5-end satin, S1 with 7-end satin, and S12 with 9-end satin (listed in Table 3.1).

The dome depths for all these fabric samples, before and after washing, are listed in Table 3.8.

Table 3.8 Data on dome depth when the weaves of the inner ring were changed

Before Washing				
	Depth of Dome (cm)			
Sample	a	b	c	Average
S11	1.80	1.80	1.90	**1.83**
S1	2.00	2.00	2.00	**2.00**
S12	2.10	2.20	2.00	**2.10**

After Washing				
	Depth of Dome (cm)			
Sample	a	b	c	Average
S11	2.80	2.95	2.90	**2.88**
S1	3.20	3.20	3.10	**3.17**
S12	3.10	2.90	3.00	**3.00**

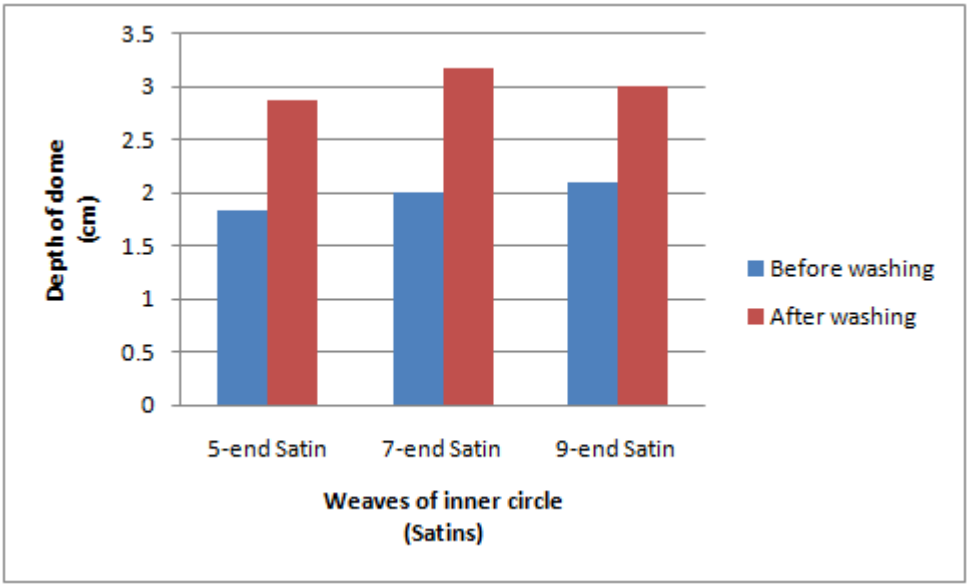

Symbols	Sample
5-end Satin	S11
7-end Satin	S1
9-end Satin	S12

Figure 3.20 Comparisons of Sample 11, Sample 1 and Sample 12

Figure 3.20 shows the changes in the dome depth affected by changing the weaves for the inner circle. Before washing, the dome with 9-end satin weaves has the largest depth, indicating that weaves with the longer average float affect on the depth of the dome. But after washing, depth of the dome, consisting of 7-end satin, increases and the comparison shows that its depth is higher than the domes consisting of 5-end satin and 9-end satin respectively. This indicates that dome made from weaves with suitable average float lengths could make a deep dome, while too short or too long floats are hard to shape a dome.

To conclude, it is clear from the above discussions that the float length directly affects the height of the dome. The longer average float tends to contribute more to the dome depth, whenever the longer float weave is used in the ringed structure. The dome depth becomes deeper by increasing the weaves' float length for the outer circle than for the middle circle or the inner circle. It also has shown that the dome made from weaves with the same length of float can have the different depth. Figure 3.20 is a typical example, where different results are obtained by using twills of the same float length but different structures for the middle circle. In addition, the float which is too long or too short may have a negative effect on the dome depth after washing treatment, as demonstrated in Figure 3.21.

3.6.3.3 Group 2. size of dome V.S. dome formability

In this section, the influence of the dome size on the dome depth was investigated by choosing the outer ring with the diameter of 7.62 cm (3 inch), 15.24 cm (6 inch) and 22.86 cm (9 inch) for S13, S14 and S1 respectively. The weave arrangements of domes

are all the same – 7-end satin, $\frac{2}{2}$ twill and plain weaves are arranged from the inner circle to the outer circle.

Table 3.9 Data on dome depth when the size of dome was changed

Before Washing				
	Depth of Dome (cm)			
Sample	a	b	c	Average
S1	2.00	2.00	2.00	**2.00**
S13	1.50	1.40	1.40	**1.43**
S14	1.80	1.70	1.70	**1.73**

After Washing				
	Depth of Dome (cm)			
Sample	a	b	c	Average
S1	3.20	3.20	3.10	**3.17**
S13	2.90	2.90	2.90	**2.90**
S14	3.00	3.00	3.10	**3.03**

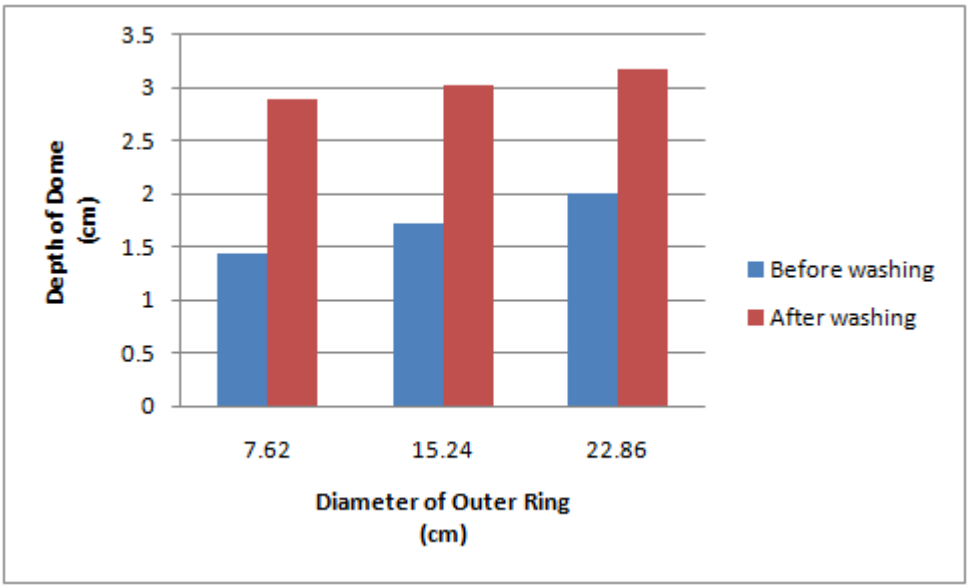

Symbols	Sample
7.62	S13
15.24	S14
22.86	S1

Figure 3.21 Comparisons of Sample 14, Sample 13 and Sample 1

It is clear that the depth of dome increases along with the increase in the dome diameter. Larger is the size of the dome, the deeper is the depth. Figure 3.21 shows that this phenomenon is more apparent before washing than after washing. Besides, the smaller dome is easier to shrink, more influenced by the washing. S13 has the smallest outer ring. Its dome depth increases most after washing.

3.6.3.4 Group 3. radius ratio V.S. dome formability

In this group, the relationship between the radius ratio and the dome depth is investigated. Three samples (S1, S15 and S16) with different radius ratios (from centre ring to outer ring) are used in this study, namely, 1:2:3, 1:3:6 and 3:5:6 respectively. The measured data is listed in Table 3.10.

Table 3.10 Data on dome depth when the radius ratio was changed

Before Washing				
	Depth of Dome (cm)			
Sample	a	b	c	Average
S1	2.00	2.00	2.00	**2.00**
S15	1.70	1.60	1.50	**1.60**
S16	2.20	2.30	2.30	**2.27**

After Washing				
	Depth of Dome (cm)			
Sample	a	b	c	Average
S1	3.20	3.20	3.10	**3.17**
S15	2.80	2.80	2.90	**2.83**
S16	3.40	3.30	3.40	**3.37**

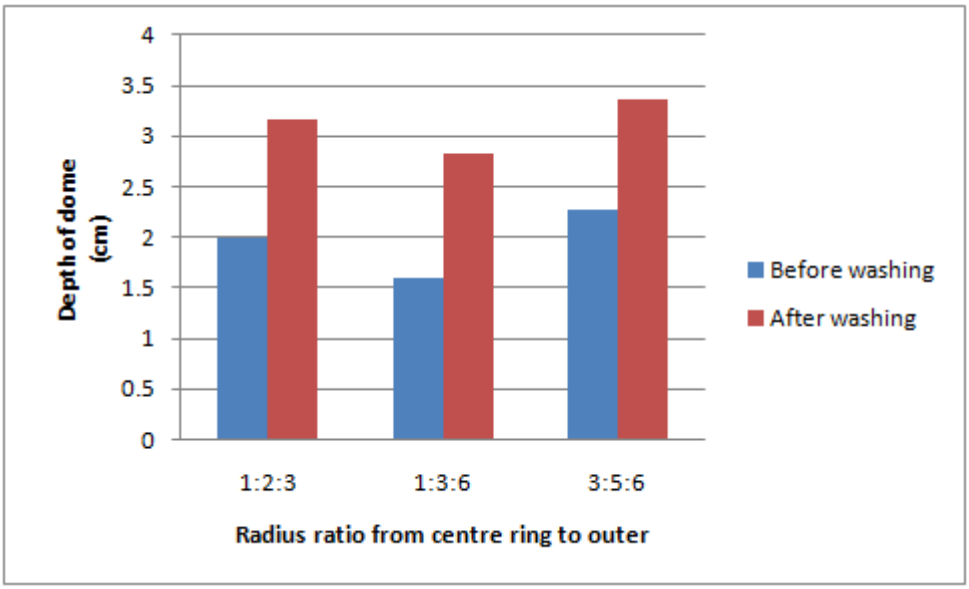

Symbols	Sample
1:2:3	S1
1:3:6	S15
3:5:6	S16

Figure 3.22 Comparisons of Sample 1, Sample 15 and Sample 16

The same trend before and after washing is shown in Figure 3.22. The dome with the radius ratio 1:3:6 from the centre ring to the outer ring has the lowest depth while the dome with the radius ratio 3:5:6 reaches the largest depth. In this group the data suggests that the dome composed of a larger inner ring and a smaller outer ring tends to have the larger depth.

3.6.3.5 Group 4. numbers of circles V.S. dome formability

In this group, the number of circles is increased to observe the difference in the depth of dome. Four samples S1, S17, S18, and S19 were used, each of them are of same size (diameter 22.86 cm for the outer ring) but consisting of different number of circles (3, 4,

5, and 6). As number of circles increase, the float lengths in the dome weave gradually increase from outer ring to inner ring. The results are shown as follows:

Table 3.11 Data on dome depth when the number of rings was changed

Before Washing				
	Depth of Dome (cm)			
Sample	a	b	c	Average
S1	2.00	2.00	2.00	**2.00**
S17	2.20	2.20	2.10	**2.17**
S18	2.30	2.30	2.40	**2.33**
S19	2.50	2.50	2.60	**2.53**

After Washing				
	Depth of Dome (cm)			
Sample	a	b	c	Average
S1	3.20	3.20	3.10	**3.17**
S17	3.00	3.00	3.00	**3.00**
S18	3.10	3.20	3.10	**3.13**
S19	3.00	3.30	3.20	**3.17**

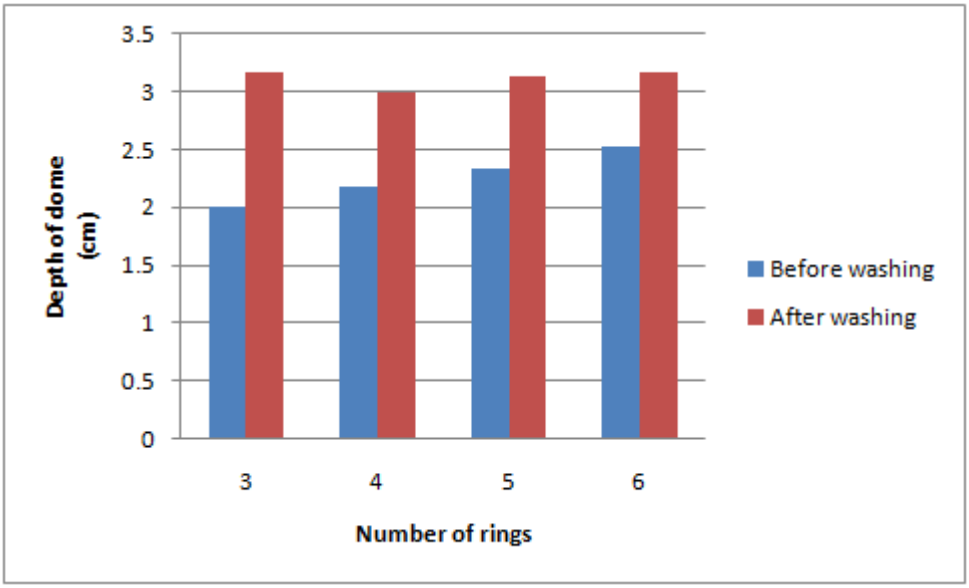

Symbols	Sample
3	S1
4	S17
5	S18
6	S19

Figure 3.23 Comparisons of Sample 1, Sample 17, Sample18 and Sample 19

Figure 3.23 indicates that the washing has a big effect to the depth of dome, reflecting not only on shrinking the fabrics to shape a deeper dome, but also on rearranging the order.

The depth of the dome increases as number of the rings are increased, when the dome shaped fabrics are not washed, However, after washing, the dome with 3 rings shows the higher depth than all the domes tested, even surpassing the depth of the dome with 5 rings and that with 6 rings. This may be an exception or error happened in the experiment. Broadly speaking, the more rings are used; the larger is the dome depth, both before and after washing.

3.6.3.6 Group 5. weft linear density V.S. dome formability

In this section, 3 kinds of different dome-shaped fabrics were woven with the weft linear densities 49.2 tex, 32.8 tex and 24.6 tex. The corresponding samples are named as S20, S21 and S22 respectively (listed in Table 3.1).

Table 3.12 Data on dome depth when the weft linear density and the diameter of outer circle in the warp direction were changed

Before Washing				
	Depth of Dome (cm)			
Sample	a	b	c	Average
S20	2.40	2.40	2.50	**2.43**
S21	2.60	2.70	2.50	**2.60**
S22	2.60	2.70	2.50	**2.60**

	Diameter of Outer Circle in the Warp Direction (cm)			
Sample	**a**	**b**	**c**	**Average**
S20	26.50	26.50	26.50	**26.50**
S21	26.30	26.20	25.80	**26.10**
S22	26.00	26.00	25.90	**25.97**

After Washing				
	Depth of Dome (cm)			
Sample	**a**	**b**	**c**	**Average**
S20	3.20	3.20	3.10	**3.17**
S21	3.40	3.30	3.30	**3.33**
S22	3.40	3.50	3.50	**3.47**
	Diameter of Outer Circle in the Warp Direction (cm)			
Sample	**a**	**b**	**c**	**Average**
S20	23.60	23.50	23.10	**23.40**
S21	23.40	23.40	23.20	**23.33**
S22	23.20	23.20	23.00	**23.13**

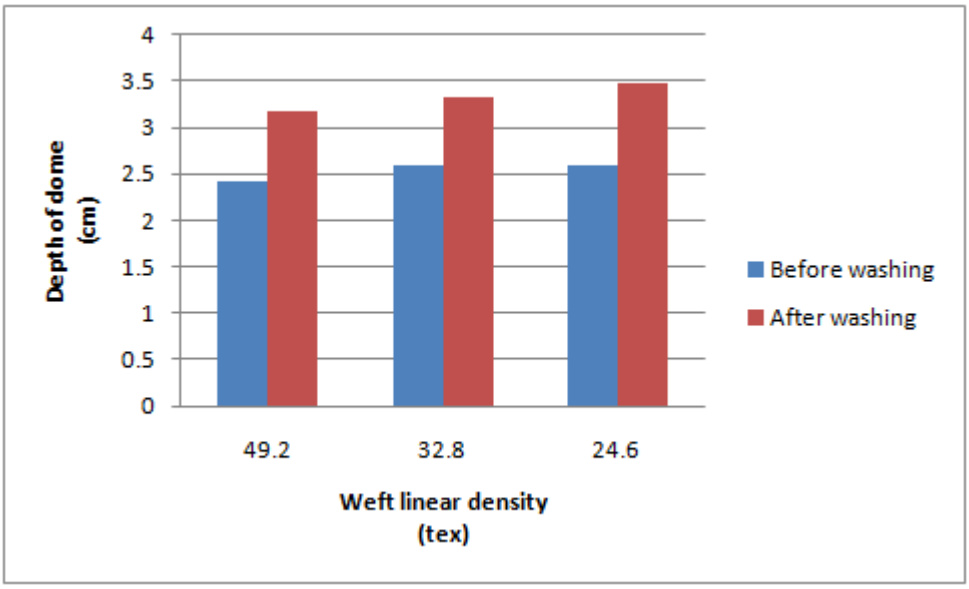

(a)

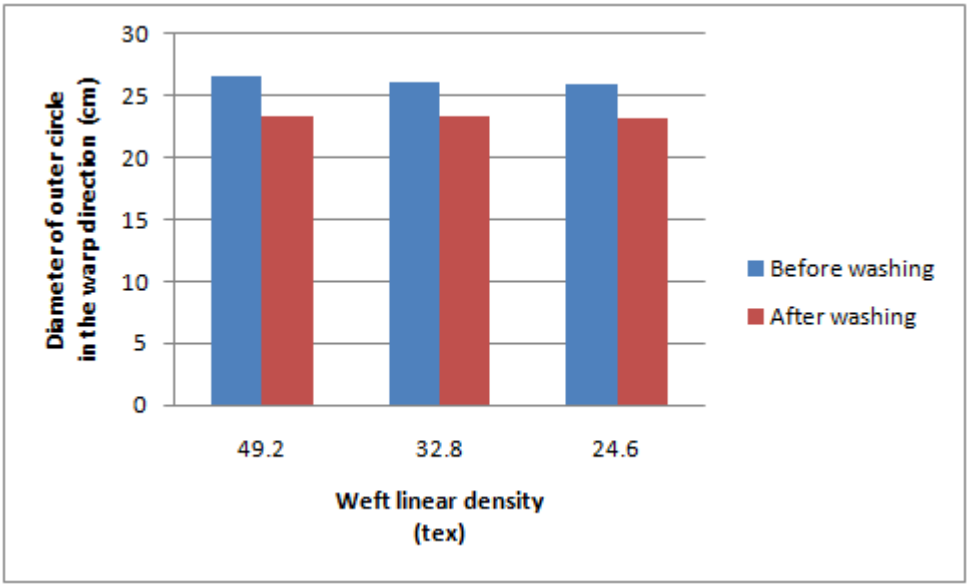

(b)

Symbols	Sample
49.9	S20
32.8	S21
24.6	S22

Figure 3.24 Comparisons of Sample 20, Sample 21 and Sample 22

In terms of dome formability, the depth of dome becomes deeper when finer yarns are employed. The lower the linear density, the deeper the dome will be. Figure 3.24 (a) shows that the dome made from thicker weft yarns tends to have a lower depth than the dome made from thinner weft yarns. Compared with the finer yarns, the thicker yarns lack elasticity and flexibility to form a deeper dome. More friction needs to be overcome when the coarser yarns are beaten up into the fabrics. In addition, it is well known that the weaves with the shorter float tends to expand while the weaves with the longer float tends to shrink. Dome-shaped fabrics are shaped using the weaves with short float in the inner circle and the weaves with long float in the outer circle. The usage of thick picks makes the weaves' expansion and shrinkage motions difficult because of little spaces left among the neighbouring picks. Therefore, it is hard to shape the deep depth of the dome.

For the longer length in the warp direction, as shown in Figure 5.24 (b), it is mainly because of different warp and weft densities, and different warp and weft linear densities used. The warp density is set as 100 ends/inch and the weft density is set as 40 picks/inch to balance the tension between the warp and weft yarns. The dome-shaped fabric is acceptable round. In this section, the variation of weft linear densities make this elongated effect more apparent, which demonstrates again that the weft linear density has an effect on the dome shape. The larger is the weft linear density, the more elongated is the warp direction of the dome.

3.6.3.7 Group 6 weft density V.S. dome formability

In this section, the relationship between the weft density and the dome formability was observed. 15.7 picks/cm, 12.6 picks/cm and 9.6 picks/cm are applied for S1, S23 and S24 respectively (listed in Table 3.1).Test results are shown in the Table 3.13:

Table 3.13 Data on dome depth when the weft density was changed

Before Washing				
	Depth of Dome (cm)			
Sample	a	b	c	Average
S1	3.20	3.20	3.10	**2.00**
S23	2.30	2.30	2.30	**2.30**
S24	2.80	2.90	2.80	**2.83**

After Washing				
	Depth of Dome (cm)			
Sample	a	b	c	Average
S1	3.20	3.20	3.10	**3.17**
S23	3.20	3.30	3.30	**3.27**
S24	3.40	3.50	3.50	**3.47**

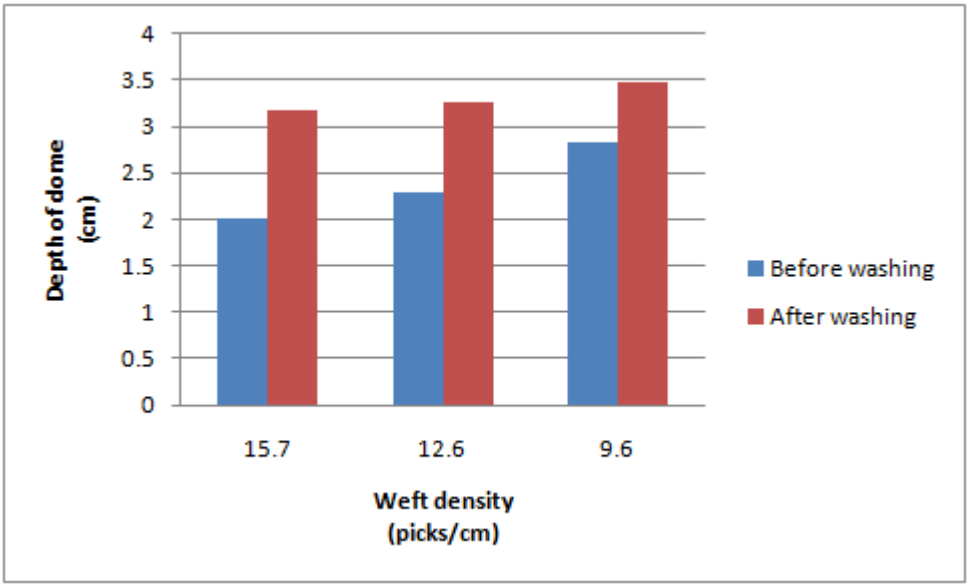

Symbols	Sample
15.7	S1
12.6	S23
9.6	S24

Figure 3.25 Comparisons of Sample 1, Sample 23 and Sample 24

Figure 3.25 indicates that the lower the weft density, the deeper the dome formability is. It is because the expansion of weaves with a short float and the shrinkage of weaves with a long float, make the dome-shaped fabrics. Due to the low weft density, there are more spaces among the neighbouring warp yarns, resulting in more convenience in such expansion and shrinkage motions. Therefore, the dome with the larger depth could be formed.

3.6.3.8 Group 7. shrinkage V.S dome formability

All of the fabrics have shrunk after washing. It is observed that for all dome-shaped fabrics: (a) the shrinkage is always larger in the warp direction than in the weft direction and (b) the dome becomes more obvious in the three-dimensional shape after washing. The previous group of changing the weaves for the outer circle-plain and plain derivatives is used as an example.

Table 3.14 Diameters in warp and weft direction for Sample 1, Sample 3 and Sample 4

Before Washing				
	Diameter of Outer Circle in the Warp Direction (cm)			
Sample	a	b	c	Average
S1	26.10	26.40	26.20	**26.23**
S3	24.90	25.00	25.00	**24.80**
S4	24.20	24.20	24.20	**24.97**
	Diameter of Outer Circle in the Weft Direction (cm)			
Sample	a	b	c	Average
S1	21.60	22.10	21.90	**21.87**
S3	24.90	25.00	25.00	**24.97**
S4	24.20	24.20	24.20	**24.20**

After Washing				
	Diameter of Outer Circle in the Warp Direction (cm)			
Sample	a	b	c	Average
S1	23.90	23.90	24.00	**23.93**
S3	22.40	22.50	22.60	**22.50**
S4	21.40	21.80	21.90	**21.70**
	Diameter of Outer Circle in the Weft Direction (cm)			
Sample	a	b	c	Average
S1	21.70	22.10	22.20	**22.00**
S3	21.70	22.00	22.10	**21.93**
S4	21.50	22.20	22.20	**21.97**

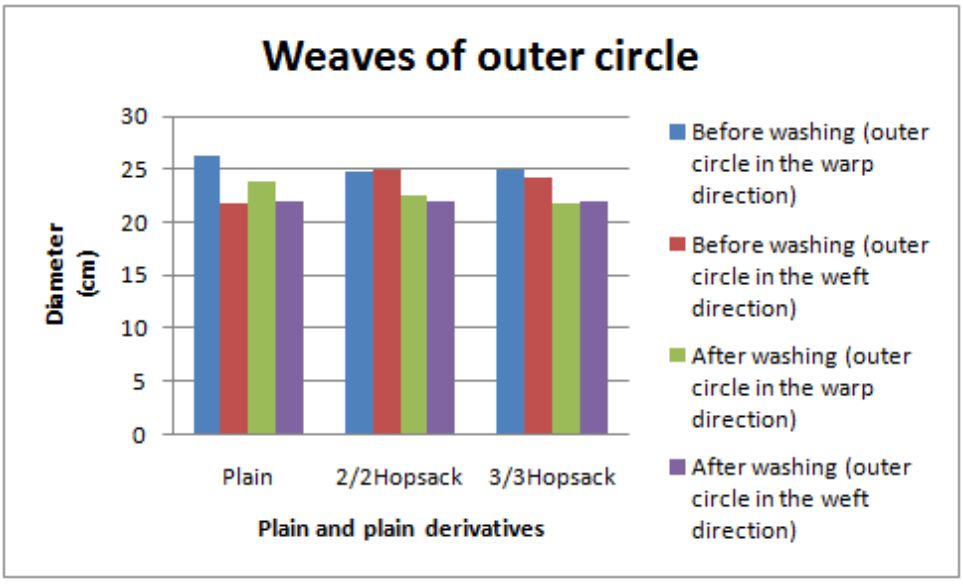

(a) Diameter changes

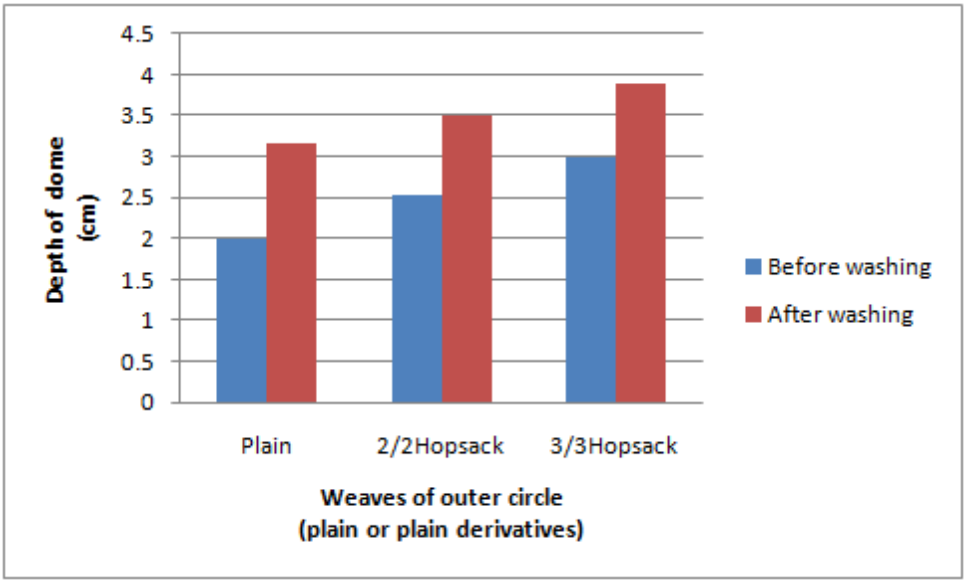

(b) Dome depth changes

Symbols	Meanings
Plain	S1
2/2 Hopsack	S3
3/3 Hopsack	S4

Figure 3.26 Two charts about the group of Sample 1, Sample 3 and Sample 4

In terms of shrinkage, more apparent changes happened in the warp direction than in the weft direction, as shown in Figure 3.26 (a). This indicates that washing gives more influence on warp yarns. The washing treatment helps largely in the removal of warp and weft tension in the fabrics. Because the higher warp density but the lower warp linear density employed to weave the fabrics, the yarn crimp distribution is much more apparent in the warp direction than in the weft direction. This results in a larger shrinkage in warp direction.

The graph in Figure 3.26 (b) has been analysed in the section of choice of weave in the first group. A comparison of graphs X and Y shows that there is a similar trend between the dome depth and the shrinkage of warp yarns. The depth of the dome-shaped fabrics becomes large when the shrinkage of its warp yarns becomes large; the depth of the dome-shaped fabrics becomes small when the shrinkage of its warp yarns becomes

small. More yarns are required to bend the shape resulting in more curved dome effect. On the other side, more curved dome makes the shrinkage more apparent. However, there is no direct relationship between them. The variation of both dome depth and the shrinkage result from the washing treatment.

In conclusion, after washing, yarns shrink in both warp and weft directions and this change reflects more in the warp direction. Besides, washing treatment makes the dome becoming deeper in its depth. This is a universal result that could be demonstrated by almost all experiments in this research.

3.7 Remarks

In this part of the research work, the variation of formability of dome-shaped fabrics woven on a conventional loom was extensively investigated by varying different parameters (i.e. woven structure, size, radius ratio, number of rings, weft linear density and weft density). Nevertheless, an apparent phenomenon which could not be neglected is that the dome depth of such fabric specimens is very limited, which may severely restrict the range of female figure sizes that might be accommodated. The deformation test results for all the dome-shaped fabrics are shown in Figure 3.27, and the main results are listed as follows:

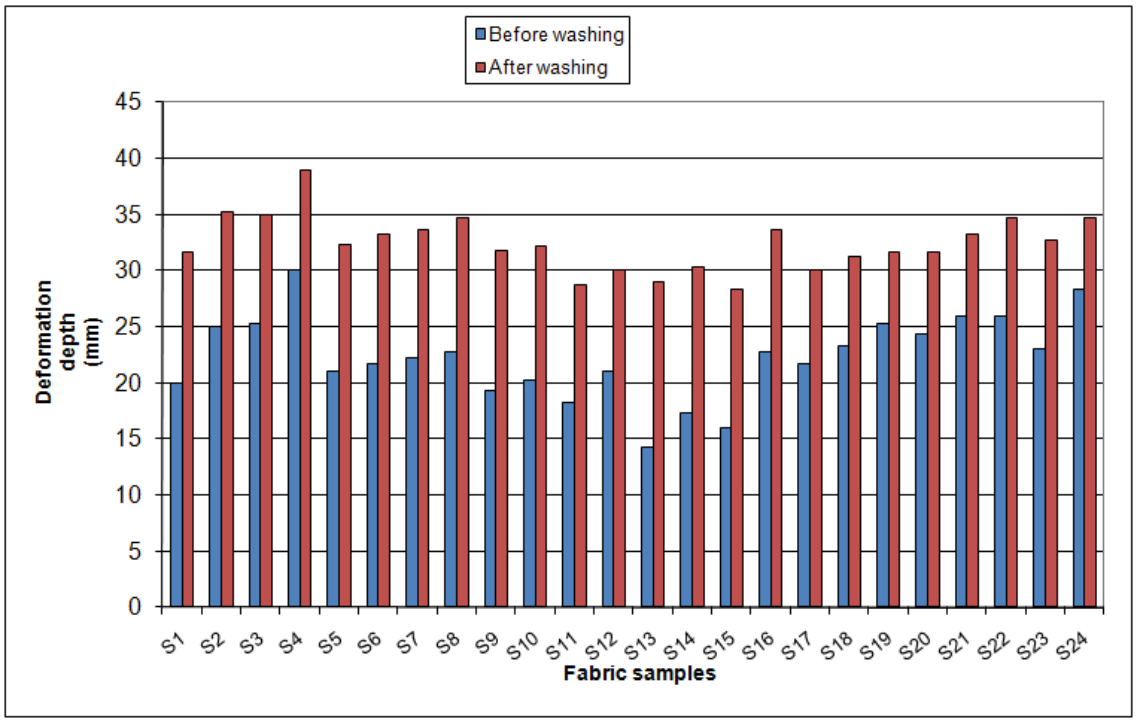

Figure 3.27 Deformation test results of dome-shaped fabrics

1. Dome-shaped fabrics could be made using weave combinations with different floats both in the weave sequence of long and short floats arranged in outer and inner concentric rings respectively and in the opposite sequence. The former weave sequence would offer a larger dome depth, which however is not sufficiently pronounced, just 2.5 cm and only increases to 3.53 cm even after laundering and relaxation. This could be used for the slight female figure, but obviously not satisfactorily produce a bust cup for the larger female sizes.

2. Domes made from weaves with a longer float give greater dome depth. The dome depth is more sensitive to changes in the outer than the inner circle. But this shaping was not always reliably created. Under certain circumstances, the dome made from weaves with the same length of float can have a different depth. If the float is too long or too short, the dome depth cannot deepen enough. The dome depth of specimens measured in this group is around 3 to 4 cm and specimen S4 is

the deepest (3.9 cm) after laundering and relaxation. The dome volume provided here is still quite limited to be used for bust area especially with the large size would lead to a poor fit and a lack of comfort for female wearers.

3. For the relationship between the size of dome and the dome formability, it could be observed that the bigger dome is easier to form to a greater depth. Besides, the smaller dome is easier to shrink, more influenced by the washing treatment. However, it is guessed this result is available in a certain range, beyond which, the size is hard to form a dome, or it would show a different trend. This is an aspect needed to be investigated in the future. The dome depth of specimens is still very limited, only 3.17 cm, 2.9 cm and 3.03 cm respectively after laundering and relaxation. Laundering and relaxation could give positive influence on shaping deeper domes on the basis of the original volume. But the results are still not good enough as the range of female figure sizes will be restricted.

4. For the relationship between circle areas and the dome formability, it may safely be concluded that a deeper dome could be obtained by enlarging the centre area of the dome rather than the outer area of the dome. Like the aforementioned results, there may be a limitation beyond which that this principle is unavailable. The dome depth of specimens in this group changes from 2cm, 1.6cm, 2.27cm to 3.17cm, 2.83cm and 3.37 cm respectively after laundering and relaxation. The dome depth is still very limited.

5. For the relationship between the number of circles and the dome formability**,** the dome depth may be regarded as rising when the rings increase no matter whether it

is before or after washing. The dome depth of specimens is around 3cm after laundering and relaxation.

6. For the relationship between the linear density and the dome formability, weft yarns with lower linear densities could lead to the creation of fabrics which may form deeper domes, because there is more space among the neighbouring warp yarns making the weaves' expansion and shrinkage motion easy. Therefore, a deeper dome is more readily formed. In addition, the weft linear density has an effect on the dome shape. The larger is the weft linear density, the more elongated is the warp direction of the dome. The dome depth of specimens is 3.17cm, 3.33cm and 3.47cm respectively after laundering and relaxation. These still could only be used for slight female figures.

7. For the relationship between the weft density and the dome formability, it is seen that the lower the weft density, the greater the dome formability is. The dome effect is not apparent, around 3cm to 3.5cm after laundering and relaxation.

8. For the relationship between shrinkage and the depth of domes, it can be observed that the shrinkage of yarns and the depth of domes becomes larger or smaller at the same time. But both of them are influenced by the washing treatment and actually there is no direct relationship between them. Washing affects the warp yarns more apparently than the weft yarns; namely, the warp yarn shrinkage is greater than the weft yarn shrinkage. Besides, it is observed that almost all domes become larger after washing than before washing.

The aforementioned conclusions derive from the experimental investigation analysis and could be regarded as general suggestions in weaving dome-shaped fabrics, which will give a positive influence to the study and design of fabrics for the bust area of female body armour. However, it has been noticed that only a limited depth of dome could be obtained from the shaping of fabrics by manipulating the weaving process even after laundering and relaxation. The dome depth of fabric in these specimens is around 1.5cm to 2.5cm and increases to only 2.5cm to 4cm after laundering and relaxation. Specimen S4 has the deepest dome 3.9cm among all specimens after laundering and relaxation which however is still only suitable for the slight female figure. The limited dome volume would apparently restrict the range of female figure sizes. The geometrical limitations of this technique necessitate a change of approach and hence angle-interlock fabrics will be investigated.

Angle-interlock woven fabric offers good mouldability as mentioned in Chapter 2, which may compensate for the weakness in respect of the comparative shallow dome depth provided by the dome-shaped fabric. Thus, the angle-interlock woven fabric would be considered on the research of female body armour. The mouldability of angle-interlock woven fabric would be further investigated and which will be compared with that of dome-shaped fabric in the next chapter.

Chapter 4

Mouldability of Angle-interlock Woven Fabrics and Its Comparison with Dome-shaped Fabrics

The three-dimensional bust area near net shaped with continuous yarns to make the front panels of female body armour could be provided not only by dome-shaped fabrics, but also by angle-interlock woven fabrics, because the latter have good mouldability. The mouldability of angle-interlock woven fabrics has been briefly introduced in Chapter 2. This chapter aims to provide a more comprehensive investigation on this issue from both theoretical and experimental points of view. Shearing, locking angle and shear rigidity are believed to be essential concepts that influence the fabric mouldability [125]. The angle-interlock woven fabric is compared with the dome-shaped woven fabric in order to select the type with the better deformation depth for making the front panel of female body armour. Obviously, the larger the deformation depth, the more apparent bust area could be formed. The selected fabric would be further considered for the ballistic evaluation in this female body armour research.

4.1 Theoretical Analysis

4.1.1 Shearing

The mouldability of angle-interlock woven fabrics has been generally analysed in Chapter 2 of Literature Review. It is known that the mouldability of woven fabrics depends greatly on shear deformation resistance. Shearing is one of the important aesthetic characteristics of fabrics: when a fabric is fitted to a surface, it conforms mainly by a shearing of the angles between warp and weft yarns [132]. This shearing angle relates to the shear strain, which occurrence indicates a deformation of a material substance in which parallel internal surfaces slide past one another. The shear strain is induced by a shear stress in the fabrics, which is derived from the force acting tangentially on a plane in the material or along a line in the case of a two-dimensional sheet. Equal force in the opposite direction is required to balance [132].

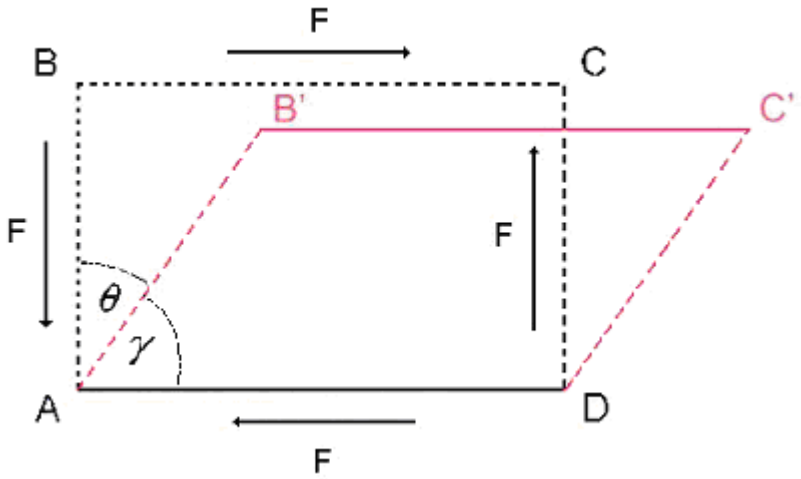

Figure 4.1 Simple shear deformation in a unit cell [132]

Figure 4.1 depicts the shearing behaviour of woven fabrics. $ABCD$ represents a simple square-constructed fabric, whose sides are initially perpendicular and parallel to the direction of the simple shear. $\overline{AB}$ and $\overline{CD}$ represent the warp yarns and $\overline{AD}$ and $\overline{BC}$ represent the weft yarns. When two equal and opposite forces F are applied parallel to the sides of the fabric, shear stress would occur, which induces the shear strain,

illustrated as $\tan\theta$, indicating the deformation conforming to the shearing behaviour.

4.1.2 Locking angle

θ is influenced by γ, which annotates the angle between warp and weft yarns after shearing, as shown in Figure 4.1. Before any deformation occurs, the shearing angle, γ, is 90° for woven fabrics. When shearing starts to happen, the angle γ reduces. As a matter of fact, $\gamma = 90° - \theta$, where $\tan\theta$ indicates the shear strain. The locking angle is the shearing angle achieved just before the maximum shear strain happens, i.e., the yarns begin to jam thus preventing further shear deformation in the fabric. Any further increase of shear load would cause wrinkles to happen [133-135]. In this context, $\gamma_{LockingAngle} = 90° - \theta_{\max}$, where $\tan\theta_{\max}$ indicates the maximum shear strain.

The locking angle is used as a characteristic value for predicting a fabric's ability to conform to a particular surface, namely, fabric mouldability. Maximum shear strain may happen due to structural jamming in warp, weft, or both yarns. Roedel [125] has researched this aspect of angle-interlock woven fabrics comprehensively. Important results are listed as follows:

- locking angle strongly depends on the individual fabric density;
- a decrease in warp and weft yarn density leads to smaller locking angle resulting in better mouldability;
- weft yarn locking mechanism dominates the fabric jamming for angle interlock fabrics;
- for a given overall weft density of the angle interlock fabric, an increase in weft yarn layers improves mouldability.

4.1.3 Shear rigidity

Shear rigidity is an expression of the fabric's initial resistance to shear deformation, and it is induced by the frictional interactions at the inter-yarn contact points. The reversal points between warp and weft yarns where undulation happens over and under each other, often become the highest frictional resistance areas as the yarns produce large contact areas with each other [125]. As the through-the-thickness angle-interlock woven fabrics have few reversal points considering the weave repeat and the total number of weft yarns per unit length, it is understandable that such designs would lead to low shear rigidity. This has already been mentioned in the explanation of the test results of shear rigidity when comparing the angle-interlock woven fabrics to its multi-layer counterparts in Chapter 2. This could also be demonstrated by comparing the cross-sections of the 4-layer through-the-thickness angle-interlock woven fabric and the plain woven fabric, as shown in Figure 4.2.

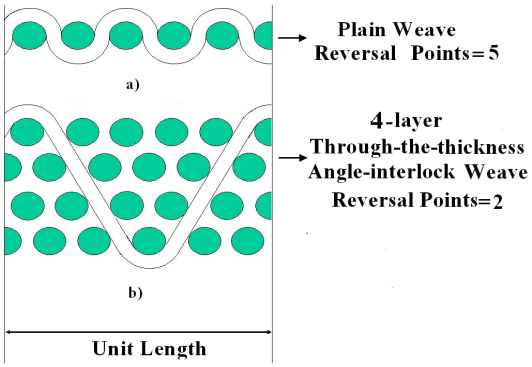

Figure 4.2 Warp yarn path per unit length, cross-sectional view

It is seen in Figure 4.2 that there are 5 reversal points in the plain weave structure whereas there are only 2 reversal points in the angle-interlock structure over the same length. This indicates that the shear rigidity offered by the latter fabric is much lower than that offered by the plain woven fabric. Thus, the angle-interlock fabric provides much better mouldability than its plain counterpart, which verifies the theory that a fabric with low shear resistance would lead to good mouldability. This argument

supports the possibility of replacing the plain woven fabric by the angle-interlock woven fabric in making the front panels of female body armour.

4.2 Empirical Analysis

The mouldability of angle-interlock woven fabrics has been studied theoretically by calculating the locking angle from the structural parameters of the fabrics [125]. Experimental investigation is another way of studying the moulding performance based on the structural parameters. The dome, shaped by angle-interlock woven fabrics due to its mouldability is compared with that of the dome-shaped fabrics to identify the more suitable fabric for female body armour.

Extensive research on angle-interlock woven fabrics has been empirically investigated by Chen *et al* [119] who have systematically designed and produced angle-interlock woven fabrics with different structural parameters, and assessed their mouldability. For this investigation, a total of 42 angle-interlock woven fabrics were made on a conventional dobby loom with a maximum of 16 heald frames. 100% polyester yarns of 65.4 tex were used for both warp and weft. The warp and weft densities for these fabrics are listed in Table 4.1. The details have been expanded on the basis of strictly obeying to the original data for more clear demonstration. The empirical work has illustrated that increases in weft density lead to decreases of deformation depth for all fabrics. It also indicates that the fabric becomes more mouldable as the number of weft yarn layers increases. These results will be compared with those of dome-shaped fabrics. However, as the angle-interlock woven fabrics and dome-shaped fabrics are different types, it is important to take into account their linear densities and areal densities when generally comparing their dome depths. The areal densities of angle-interlock woven fabrics have

not been included in the original document, but which could be calculated and the results have been demonstrated in Table 4.1. As linear density in tex indicates the mass of yarns in grams per 1000 meters and warp/weft density indicates the number of warp/weft yarns per cm, the areal density (g/m^2) can be calculated based on the following equation:

$$W = \frac{T}{10}\left[n_1(1+C_1)+n_2\right] \tag{4.1}$$

Where, W = areal density,

T = yarn linear density,

n_1 = warp density,

n_2 = weft density,

C_1 = warp yarn crimp, which is assumed to be 10% for the angle-interlock woven fabrics considered.

Table 4.1 Angle interlock fabrics made from polyester fibres [119]

Weft layers	Warp density (ends/cm)	Weft density (picks/cm)	Areal density (g/m^2)
2	21.6	7.9	207.06
		9.4	216.87
		11	227.33
		12.6	237.79
		14.2	248.26
2	23.6	7.9	221.44
		9.4	231.25
		11	241.72
		12.6	252.18
		14.2	262.65
2	25.6	7.9	235.83
		9.4	245.64
		11	256.11
		12.6	266.57
		14.2	277.03
3	21.6	15.7	258.07
		18.9	279.00
		22.1	299.92
		24.4	314.97

		27.6	335.89
3	23.6	15.7	272.46
		18.9	293.38
		22.1	314.31
		24.4	329.35
		27.6	350.28
3	25.6	15.7	286.84
		18.9	307.77
		22.1	328.70
		24.4	343.74
		27.6	364.67
4	21.6	23.6	309.73
		28.3	340.47
		33.1	371.86
		37.8	402.60
4	23.6	23.6	324.12
		28.3	354.86
		33.1	386.25
		37.8	416.99
Linear density: 65.4 tex for both warp and weft yarns **Yarn crimp is assumed as 10% which only happens for warp yarns**			

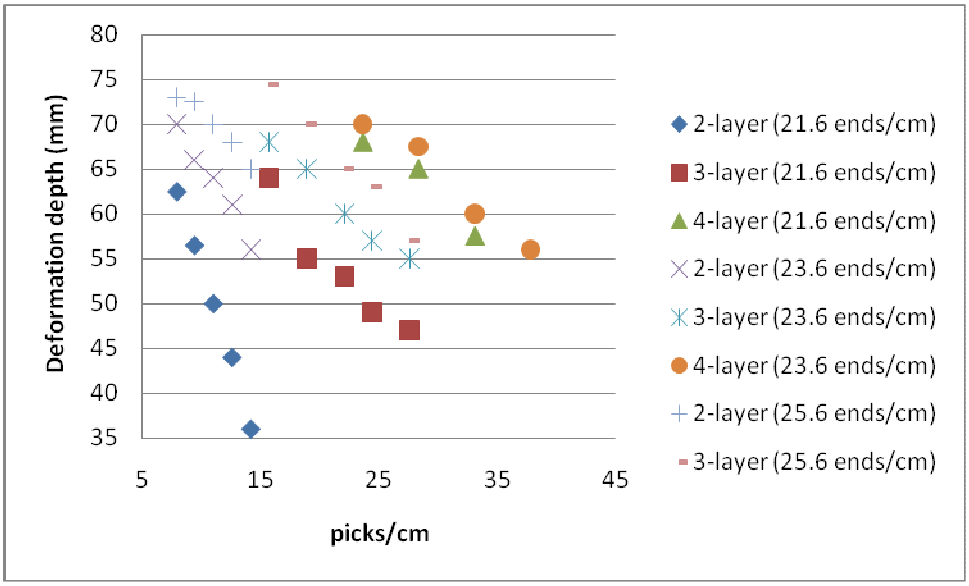

Figure 4.3 Effects of fabric parameters on deformation depth [119]

As mentioned in Chapter 3, dome-shaped fabrics have been systematically designed and researched in order to investigate their dome formability. The deformation depth results of these fabrics are shown in Figure 3.27. All fabrics were also woven from 100% polyester yarns. Their areal densities also are calculated based on the equation (4.2) and the results are listed in Table 4.2.

$$W = \frac{1}{10}[n_1 T_1 (1 + C_1) + n_2 T_2 (1 + C_2)] \quad (4.2)$$

Where, W = areal density,

n_1 = warp density,

n_2 = weft density,

T_1 = warp linear density,

T_2 = weft linear density,

C_1 = crimp of warp yarns, which is assumed to be 4% in 2D fabrics considered,

C_2 = crimp of weft yarns, which is assumed to be 4% in 2D fabrics considered.

Table 4.2 Dome-shaped fabrics made from polyester yarns

Sample	Dome diameter in warp direction (cm)	Weave (outer to inner)	Radius ratio (outer to inner)	Warp density (ends/cm)	Weft density (picks/cm)	Areal density (g/m²)
S1	22.86	**Plain,** $\frac{2}{2}$ **Twill,7-end Satin***	3:2:1	39.4	15.7	237.76
S2	22.86	7**-end Satin,** $\frac{2}{2}$ **Twill, Plain**	3:2:1	39.4	15.7	237.76
S3	22.86	$\frac{2}{2}$ **Hopsack,** $\frac{2}{2}$ Twill,7-end Satin	3:2:1	39.4	15.7	237.76
S4	22.86	$\frac{3}{3}$ **Hopsack**, $\frac{2}{2}$ Twill, 7-end Satin	3:2:1	39.4	15.7	237.76
S5	22.86	Plain, $\frac{3}{2}$ **Twill**,7-end Satin	3:2:1	39.4	15.7	237.76
S6	22.86	Plain, $\frac{4}{2}$ **Twill**, 7-end Satin	3:2:1	39.4	15.7	237.76
S7	22.86	Plain, $\frac{4}{3}$ **Twill**, 7-end Satin	3:2:1	39.4	15.7	237.76
S8	22.86	Plain, $\frac{4}{4}$ **Twill**, 7-end Satin	3:2:1	39.4	15.7	237.76
S9	22.86	Plain, $\frac{3}{2}$ **Horizontal Waved Twill**, 7-end Satin	3:2:1	39.4	15.7	237.76

S10	22.86	Plain, $\frac{3}{2}$ **Vertical Waved Twil**l, 7-end Satin	3:2:1	39.4	15.7	237.76
S11	22.86	Plain, $\frac{2}{2}$ Twill, 5-**end Satin**	3:2:1	39.4	15.7	237.76
S12	22.86	Plain, $\frac{2}{2}$ Twill, 9-**end Satin**	3:2:1	39.4	15.7	237.76
S13	**7.62**	Plain, $\frac{2}{2}$ Twill, 7-end Satin	3:2:1	39.4	15.7	237.76
S14	**15.24**	Plain, $\frac{2}{2}$ Twill, 7-end Satin	3:2:1	39.4	15.7	237.76
S15	22.86	Plain, $\frac{2}{2}$ Twill, 7-end Satin	**6:3:1**	39.4	15.7	237.76
S16	22.86	Plain, $\frac{2}{2}$ Twill, 7-end Satin	**6:5:3**	39.4	15.7	237.76
S17	22.86	Plain, $\frac{2}{1}$ Twill, $\frac{2}{2}$ Twill, 7-end Satin	**4:3:2:1**	39.4	15.7	237.76
S18	22.86	Plain, $\frac{2}{1}$ Twill, $\frac{2}{2}$ Twill, $\frac{3}{2}$ Twill,7-end Satin	**5:4:3:2:1**	39.4	15.7	237.76
S19	22.86	Plain, $\frac{2}{1}$ Twill, $\frac{2}{2}$ Twill, $\frac{3}{2}$ Twill, $\frac{4}{2}$ Twill,7-end Satin	**6:5:4:3:2:1**	39.4	15.7	237.76
S20	22.86	Plain, $\frac{2}{2}$ Twill, 7-end Satin	3:2:1	39.4	15.7	215.55
S21	22.86	Plain, $\frac{2}{2}$ Twill, 7-end Satin	3:2:1	39.4	15.7	188.78
S22	22.86	Plain, $\frac{2}{2}$ Twill, 7-end Satin	3:2:1	39.4	15.7	175.39
S23	22.86	Plain, $\frac{2}{2}$ Twill, 7-end Satin	3:2:1	39.4	**12.6**	217.51
S24	22.86	Plain, $\frac{2}{2}$ Twill, 7-end Satin	3:2:1	39.4	**9.6**	197.92

***The bold characters indicate parameters where changes occurred.**
Linear density: 33 tex for warp yarns and 62.8 tex for weft yarns, except 49.2 tex, 32.8 tex and 24.6 tex were used for weft yarns of sample S20, S21and S22 respectively.
Yarn crimp is assumed to be 4% for both warp and weft yarns

Figure 4.3 indicates that the deformation depth of angle-interlock woven fabrics is around 55-75 mm and Figure 3.27 suggests that the deformation depth of dome-shaped fabrics is around 15-30 mm (before washing) and 25-35 mm (after washing). It can be observed that the angle-interlock woven fabrics generally have larger dome depth than the dome-shaped fabrics considering the similarities in areal densities (237 g/m^2). It can also be seen in Figure 4.3 that heavier angle-interlock woven fabrics (e.g. 386 g/m^2, 402 g/m^2 and 417 g/m^2) still lead to large deformation depth. The principle of moulding angle-interlock woven fabrics is different from that for dome-shaped fabrics. The mouldability of angle-interlock woven fabric is basically determined by its structure consisting of layers of straight weft yarns and a single layer of warp yarns binding the layers of weft yarns together. This unique 3D structure demonstrates fewer cross-over points which lead to lower shear rigidity of the fabric, as has been demonstrated in Section 4.1.3. As a result, the angle-interlock woven fabric is easy to be shear-deformed even though it has higher areal density. On the other hand, the dome-shaped fabric is formed by organising different weave structures in a concentric circles based on the honeycomb principle. In 2D fabrics, short yarn floats contribute to a tight fabric area which tends to extend or invade into the adjacent fabric area because of the high frequency of yarn intersection. Similarly, long floats would lead to a loose fabric area and this area can be pushed to shrink if it is beside a tight fabric area. Based on this principle, the dome swells out on the surface by employing weave structures with appropriately arranged weaves with long and short floats. The dome has already formed when the dome-shaped fabric is taken off the loom. This is different from angle-interlock woven fabric for which additional force is required to deform into a dome. However, the comparisons in Figure 4.3 and Figure 3.27 have demonstrated that the weave structure of angle-interlock woven fabrics permits the formation of larger domes.

As a matter of fact, angle-interlock woven fabric is a very mouldable type of fabric, which can even be shaped into an integral helmet shell [125]. Angle-interlock woven fabrics are more suitable than the dome-shaped fabrics for making the curvaceous front panel of female body armour by conforming to 3D female torso.

For the application of female body armour, a kind of Kevlar® fibre (Kevlar® 49) is used for making angle-interlock woven fabrics. The mouldability of this type of fabric is studied as Kevlar® is the most widely accepted material for soft body armour applications. The experimental results show that the angle-interlock woven fabrics from Kevlar® yarns create dome depth over 70mm tested using the Dome Tester, and this can been seen in Figure 4.4(a). This is comparative to the deformation depth from their polyester counterparts, which are shown in Figure 4.3. Angle-interlock fabrics made from Kevlar® are more mouldable than those made from polyester fibres because of the lower friction between Kevlar® yarns. It is also seen in Figure 4.4(b) that the dome depth of Kevlar® angle-interlock woven fabrics decreases when the weft density increases, as seen in polyester angle-interlock fabrics. The increase in weft density reduces the spacing between the weft yarns and hence affects the fabric locking angle [125].

Table 4.3 Angle-interlock woven fabrics made from Kevlar® fibres

Weft layer	Warp density (ends/cm)	Weft density (picks/cm)	Areal density (g/m^2)
3	6.7	20.8	439.17
4	12	26	609.02
4	12	28	640.58
4	12	30	672.13
4	12	32	703.69
5	12	34	735.24

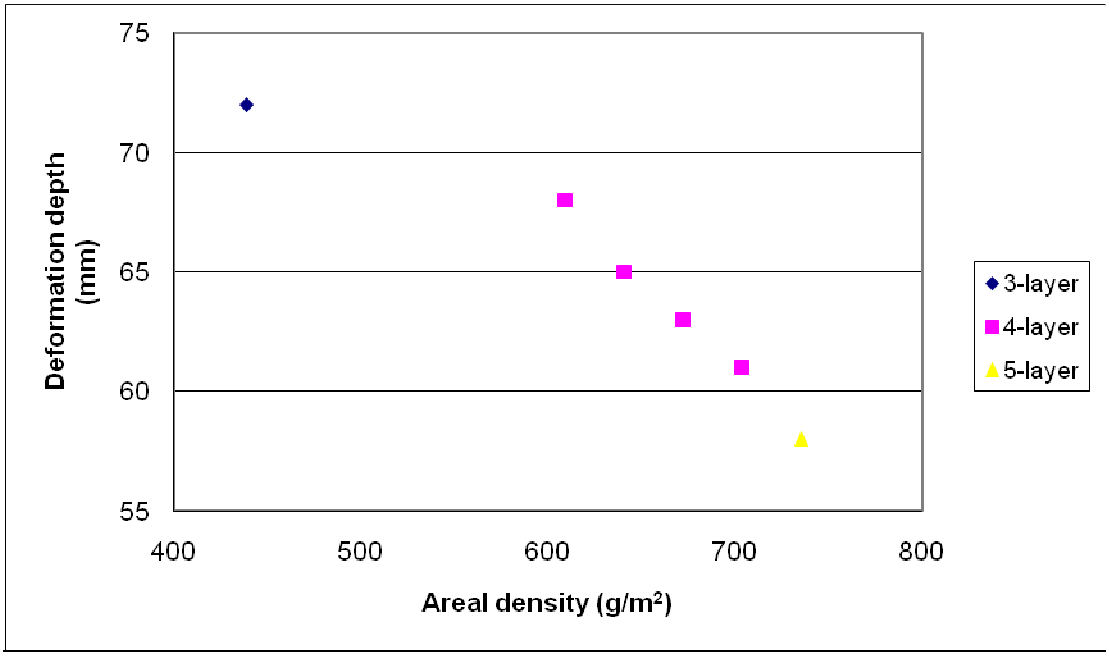

(a)

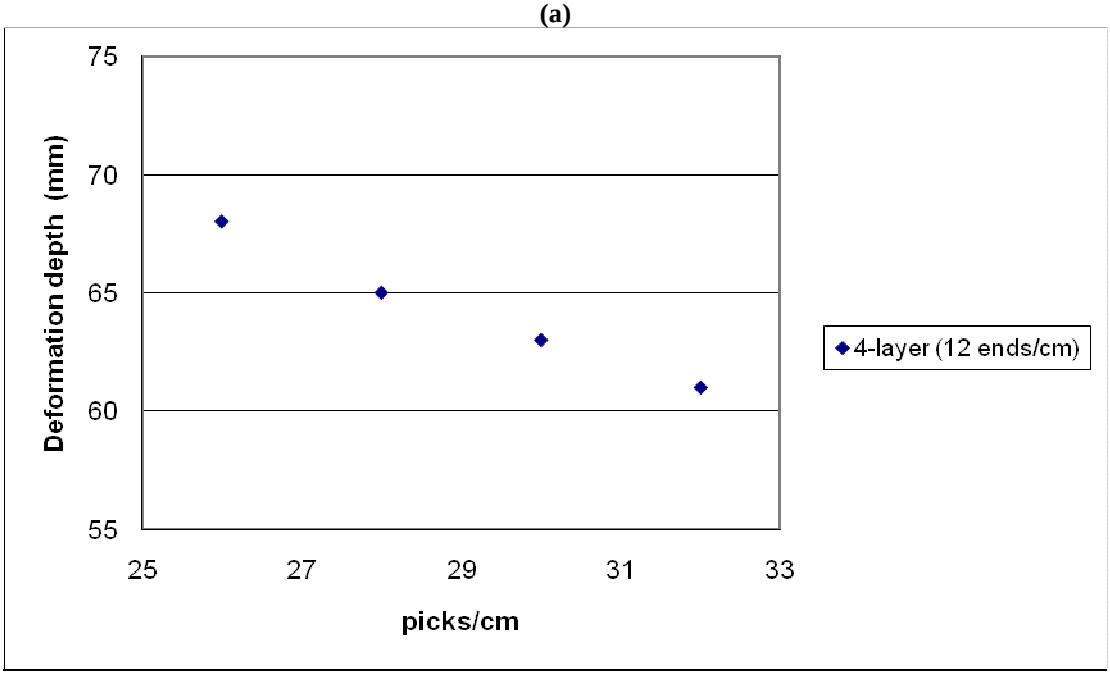

(b)

Figure 4.4 angle-interlock woven fabrics made of Kevlar® yarns: (a) deformation depth V.S. areal density; (b) deformation depth V.S. weft density

4.3 Remarks

Angle-interlock woven fabrics have been theoretically and empirically demonstrated to have good mouldability. In addition, angle interlock fabrics are simple and easy to make. This is an advantage the dome-shaped fabrics do not have. Therefore, angle-interlock woven fabrics become a good candidate for making female body armour based on this

mouldability. However, there is no knowledge of angle interlock fabrics' ability in ballistic protection. Satisfactory body armour must be able to resist the penetration of high velocity projectiles and at the same time allow minimal transverse deformation, to reduce blunt trauma [136]. The ballistic resistant effectiveness of angle-interlock woven fabrics will be evaluated and analysed in the next chapter.

Chapter 5

Ballistic Performance of Angle-interlock Woven Fabrics

The previous chapter has identified the angle-interlock woven fabric as a candidate fabric type for female body armour from the perspective of mouldability of the fabric. As a continuation of this research, the ballistic performance of angle-interlock woven fabrics will be examined. Three objectives are set for this work, which are (i) a study of energy absorption characteristics of single piece of angle-interlock woven fabrics, (ii) a parametric study on angle-interlock woven fabrics for ballistic performance, and (iii) an evaluation of fabric panels made from angle-interlock woven fabrics against the NIJ standard.

5.1 Background

The manner in which the fabric responds to impact loading and dissipates the kinetic energy of an impacting projectile is a complex issue, which varies under different impact conditions. In simple terms, an impact with the same impact energy may happen with two separate situations: low velocity impact by a large mass (drop weight) and

high velocity impact by a small mass (debris, bullet, etc.). The former is generally simulated using a falling weight or a swinging pendulum and the latter using a gas gun or some other ballistic launcher [137]. In this research the ballistic performance of angle-interlock woven fabric will be assessed under the high velocity impact.

5.1.1 Energy absorption mechanism

When the projectile hits the fabric, two waves take place [92]. One is the longitudinal wave travelling in the plane of the target plate. This wave travels through the yarns which are directly hit by the projectile, known as primary yarns. The yarns not directly hit by the projectile are known as secondary yarns, which are also travelled through by this wave because they interact with the primary yarns [138]. Another wave, known as the transverse wave, propagates outward from the impact zone to make deformation in the perpendicular direction to the fabric plane. The fabric deformation due to the transverse wave is shaped like a cone with the impact point at its vertex [92]. Figure 5.1 depicts the propagation of the two waves [139].

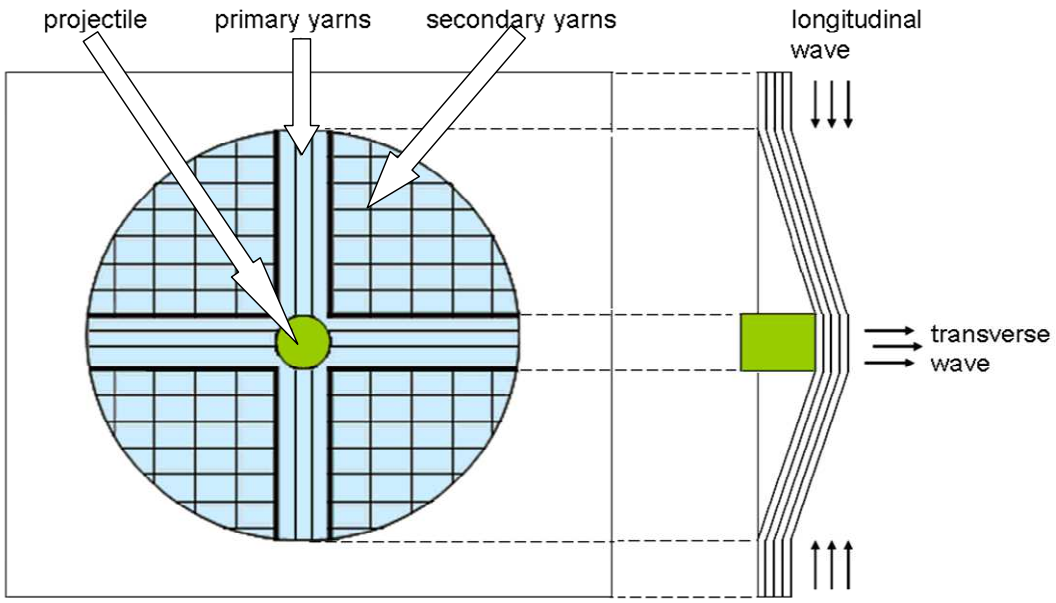

Figure 5.1 Impact wave propagation: (a) top view; (b) side view [139]

Impact energy could be converted into various forms, including yarn failure, fibre pull-out, fibre fracture, cone formation on the back face of the target [137, 138, 139]. The impact energy conversion is governed by several factors, such as the material properties of the constituent fibres, boundary conditions of the sample fabric, projectile geometry, and so on. Among all these, friction between yarns is quite important. The increase of friction between yarns may require more impact energy to overcome and therefore will lead to the increase in the ability to absorb the impact energy [140]. However, it must also be noticed that if the friction is so high that the relative movement of yarns is impossible, the fabrics' capability of absorbing impact energy could be correspondingly reduced. This is because the yarn movement is also an important way of absorbing the impact energy [141].

5.1.2 Loss of kinetic energy

In principle, the energy absorbed by the target fabric on penetration assessing the ballistic performance of the fabric is measured by the decrease in projectile kinetic energy, which is determined from the projectile impact velocity and the exit velocity. The overall loss of kinetic energy of the projectile is defined as [92]:

$$\Delta E = \frac{1}{2}(mV_0^2) - \frac{1}{2}(mV_1^2) \tag{5.1}$$

where ΔE is the loss of kinetic energy

m is the projectile mass

V_0 is the impact velocity

V_1 is the exit velocity

The impact velocity V_0 can be calculated from the flying time of the projectile t_0 between two detectors placed at d_0 distance apart. The impact velocity V_0 can be then calculated from

$$V_0 = \frac{d_0}{t_0} \tag{5.2}$$

The exit velocity V_1 can be achieved using the same method, by measuring projectile flying time t_1 between the two detectors with a distance d_1 between them behind the target fabric. After that, the overall loss of kinetic energy carried by the projectile can be

calculated according to Equation (5.1). The energy loss of the projectile is an effective way to measure a fabric's capability of absorbing energy, which is difficult, if not impossible, to measure directly.

5.2 Energy Absorption of Angle-interlock Woven Fabrics in Comparison to Other Fabric Structures

The purpose of this section is to investigate the energy absorption of different fabric structures to benchmark the overall ballistic performance of angle-interlock woven fabrics by the energy loss test. In addition to the angle-interlock woven structure, four other weave structures have been involved in this investigation.

5.2.1 Fabrics

5.2.1.1 Structures

Plain weave

Plain weave is the simplest weave, characterised by the tightest woven structure as has been detailed in Literature Review. It is the most widely used woven structure in the body armour application.

Plain weave with leno insertions

Leno weave is a type of structure in which a pair of warp yarns is intertwined by embracing a pick of weft yarn in each of the interstices [142]. It has a firmer gripping on the weft yarns and can be produced easily in broad fabrics. The primary purpose of such structure is to limit yarn movement, and therefore the fabrics with stable dimensions can

be formed. Plain weave fabrics with leno insertions are expected to have better dimensional stability than those without leno insertions, and should have better restraining of the weft yarns. Figure 5.2 shows the leno weave structure.

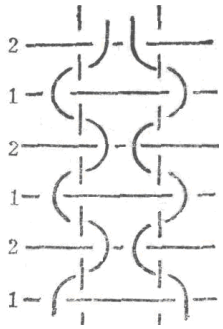

Figure 5.2 Illustration of leno weave

Plain weave with weft yarn cramming

Weft yarn cramming in weaving is performed by stopping take-up, at the same time keeping all other actions as usual during weaving. Fabric weave structure keeps the same. When weft yarn cramming takes place weft yarn density increases.

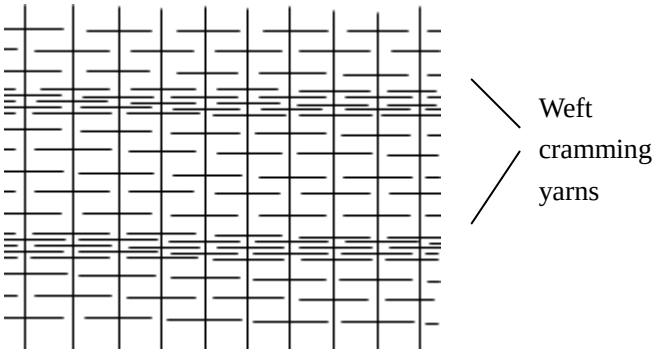

Figure 5.3 Weft yarn cramming

Four-layer cellular fabric

The four-layer cellular fabric with plain weave structure is shown in Figure 5.4. This is performed by connecting the adjacent two layers together in the evenly spaced intervals. 8 warp yarns and 104 weft yarns compose one repeat unit of the weave structure. The conjunction area is characterised by 8 weft yarns and twice the yarn density in both

warp and weft directions.

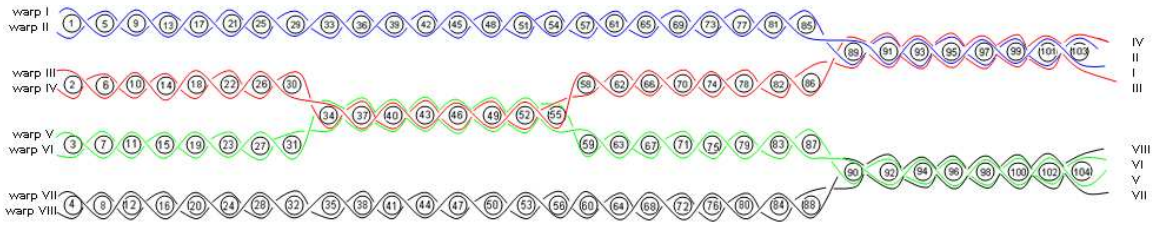

Figure 5.4 Four-layered cellular fabric

5.2.1.2 Specimen details

As a joint effort in the Protective Textiles Research Group, twenty-one different woven fabrics have been designed and manufactured in the University of Manchester. The detailed specifications are listed in Table 5.1.

Table 5.1 Specifications of various fabrics

Fabrics	Fibre type	Yarn densities		Yarn counts		Weave structure
		warp (ends/cm)	weft (picks/cm)	warp (tex)	weft (tex)	
F1	Kevlar® 49	7.5	7.5	158	158	Broad plain woven fabric (one layer)
F2	Kevlar® 49	7.5	7.5	158	158	Broad plain woven fabric (two layers)
F3	Kevlar® 49	7.5	7.5	158	158	Broad plain woven fabric (four layers)
F4	Kevlar® 49	7.5	7.5	158	158	Broad plain woven fabric with leno insertions in every 2cm intervals
F5	Kevlar® 49	7.5	7.5	158	158	Broad plain woven fabric with leno insertions in warp and cramming yarns in weft both in every 2cm intervals
F6	Kevlar® 49	7.5	7.5	158	158	Broad plain woven fabric with leno insertions in every 4cm intervals
F7	Kevlar® 49	7.5	7.5	158	158	Broad plain woven fabric with leno insertions in warp and cramming yarns in weft both in

						every 4cm intervals
F8	Kevlar® 49	7.5	7.5	158	158	Broad plain woven fabric with leno insertions in every 6cm intervals
F9	Kevlar® 49	7.5	7.5	158	158	Broad plain woven fabric with leno insertions in warp and cramming yarns in weft both in every 6cm intervals
F10	Kevlar® 49	7.5	7.5	158	158	Broad plain woven fabric with leno insertions in every 8cm intervals
F11	Kevlar® 49	7.5	7.5	158	158	Broad plain woven fabric with leno insertions in warp and cramming yarns in weft both in every 8cm intervals
F12	Kevlar® 49	7.5	7.5	158	158	Broad plain woven fabric with leno insertions in every 10cm intervals
F13	Kevlar® 49	7.5	7.5	158	158	Broad plain woven fabric with leno insertions in warp and cramming yarns in weft both in every 10cm intervals
F14	Kevlar® 49	7.5	7.5	158	158	Broad plain woven regular two-layer fabric
F15	Kevlar® 49	7.5	7.5	158	158	Broad plain woven interchange two-layer fabric
F16	Kevlar® 49	7.5	7.5	158	158	Broad plain woven regular four-layer fabric
F17	Kevlar® 49	7.5	7.5	158	158	Hand loom made plain woven fabric with weft winding in every 6cm intervals
F18	Kevlar® 49	**12***	**26**	158	158	Four layer angle interlock fabric with densities 12ends/cm and 26picks/cm
F19			**28**			Four layer angle interlock fabric with densities 12ends/cm and 28picks/cm
F20			**30**			Four layer angle interlock fabric with densities 12ends/cm and 30picks/cm
F21			**32**			Four layer angle interlock fabric with densities 12ends/cm and 32picks/cm
F22	**Dyneema®**	**6.73**	**6.73**	**176**	**176**	Broad plain woven fabric

F23						Broad plain woven fabric with leno insertions in every 4cm intervals
F24						Broad unidirectional fabric
***The bold characters indicate that parameters have changed.**						

The fabrics were then cut into the size of 24 cm by 24 cm, clamped by a pair of metal clamps for an energy loss test. As shown in Figure 5.5, needles, which were planted onto one part of the clamp around an aperture with the diameter of 15.2 cm, were used to lock the target area by penetrating the fabric. The target area was further guaranteed by screwing the two clamps together in the four corners. This full-clamped state was suggested to offer the same condition for all the tests.

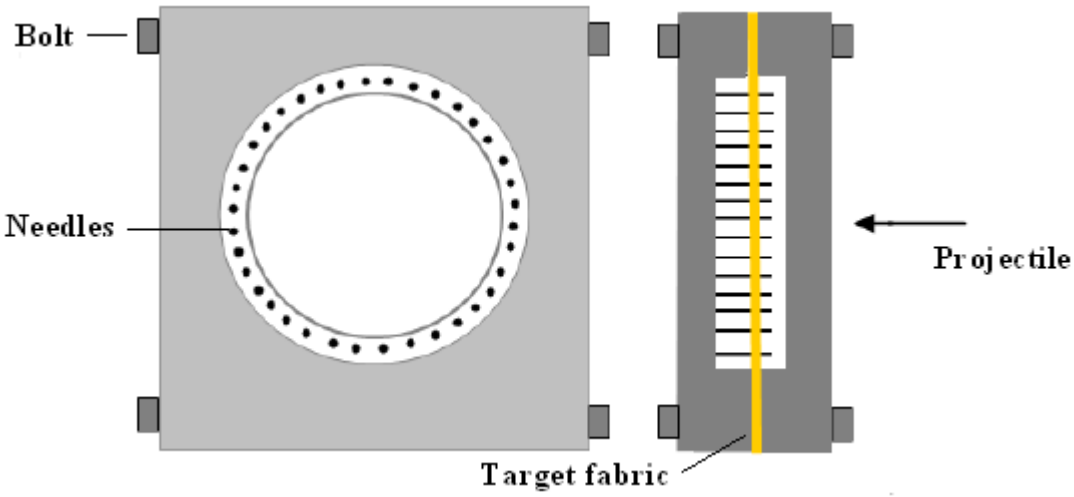

Figure 5.5 Fabric clamp

5.2.2 Experiments

5.2.2.1 Energy loss test

The energy loss test was used to investigate the fabrics' ballistic performance. The firing range for energy loss test consists of a firing device with a 7.6 mm rifle barrel, target holder, and velocity detectors. These are arranged in an enclosed environment and the

firing apparatus is shown in Figure 5.6.

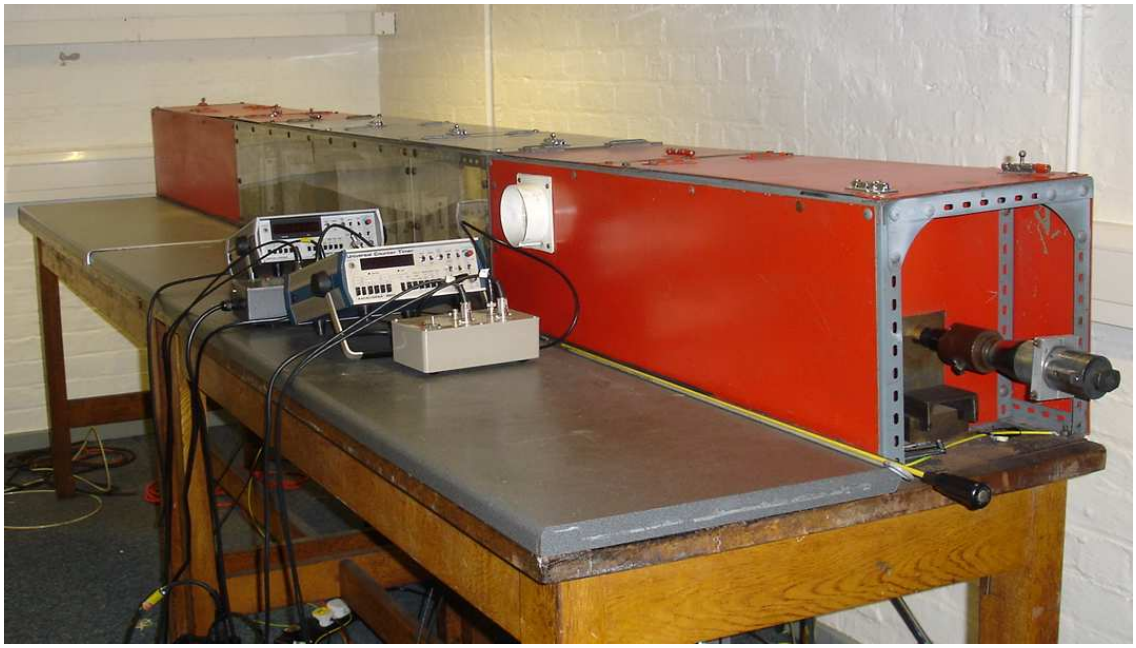

Figure 5.6 Testing apparatus

A blank cartridge was used to propel the projectile held in a sabot. The projectile is a steel cylinder with a diameter and a length of being both 5.56 mm, weighing 1.06 g, as shown in Figure 5.7(a). Pulling the trigger causes the projectile to be forced out from the barrel towards the target fabric at a high velocity, typically 480m/s. The time detectors then picked up the travelling time of the projectile before and after the fabric target. The loss in kinetic energy carried by the projectile after going through the fabric can be calculated using Equation (5.1). In this set-up, the distances between the two pairs of time detectors were 47 cm (front) and 36.2 cm (rear) respectively. Figure 5.7(c) sketches the construction of this firing range.

(a) (b)

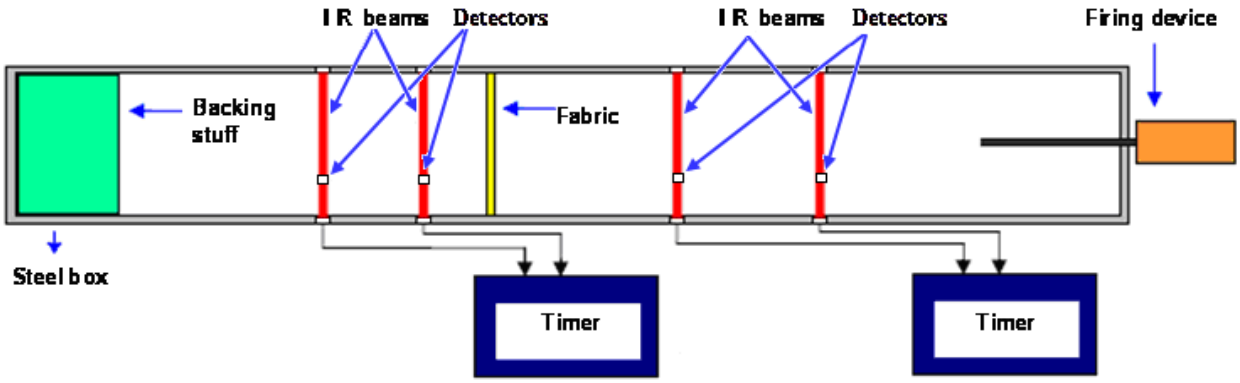

(c)

Figure 5.7 Construction of the testing apparatus:
(a) steel projectile; (b) plastic sabot; (c) schematic diagram

5.2.3 Test results and analysis

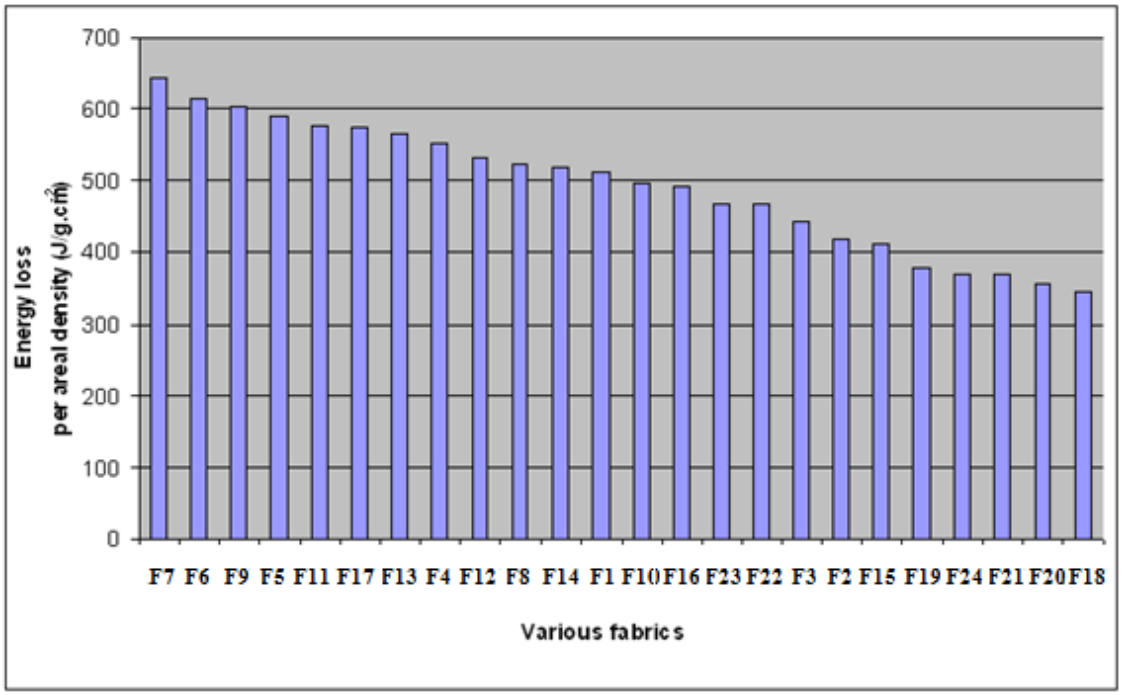

Figure 5.8 Energy absorption of various fabrics normalized by per areal density

Figure 5.8 shows the results of energy loss test for all fabrics. To indicate the energy loss caused by the same amount of materials, the projectile energy loss in Figure 5.8 is normalised by dividing the fabric areal density (in g/cm^2). Relatively speaking, the overall ballistic performance of angle-interlock woven fabrics is quite low as F18, F20, F21 and F19 are ranked as the 1^{st}, 2^{nd} ,3^{rd} and 5^{th} respectively from the bottom. All the 2D woven fabrics have shown capabilities to absorb more energy than the 3D angle-interlock woven fabrics. This is believed to be due to the difference of the number of interlacements contained in the fabrics, which is directly related to the yarn gripping effect. More interlacements lead to tighter yarn gripping. There are more yarn interlacements in a 2D woven fabric compared to a 3D angle-interlock woven fabric; and the interlacements help to transfer energy to the adjacent yarns. Consequently, the

stress wave in a 2D plain woven fabric propagates to a larger area of woven fabric whereas that in a 3D angle-interlock woven fabric tends to be more localised. As a result, the 2D plain woven fabric would absorb more projectile impact energy than the 3D angle-interlock woven fabrics.

As the plain woven fabric is the conventional type in the body armour application, it is of interest to compare the angle-interlock woven fabrics with the plain woven fabrics to benchmark the ballistic performance of the angle-interlock woven fabrics. As can be seen in Figure 5.8, the plain woven fabrics absorb more kinetic energy than the angle-interlock woven fabrics. The top view of structures of plain and 4-layer angle-interlock weaves are shown in Figure 5.9 (a) and (b) respectively. It could be observed that in the same unit area, there are more interlacements in the plain weave than the 4-layer angle-interlock weave. Additionally, the former also has shown more interlacements than the latter in the cross section, which already has been illustrated in Chapter 4 where the shear rigidity of the angle-interlock woven fabric is investigated. Furthermore, the energy loss is normalised by dividing the fabric areal density for the purpose of comparison based on the same amount of material. Interlacements are quite important for the fabric to absorb the impact energy. Interlacements serve like pivot points to stabilise the structure in order to enhance the yarn gripping by increasing friction between yarns. When the fabric receives an impact, the impact energy will dissipate among the warp and weft yarns, and will be distributed on interlacements for further dissipation. More interlacements may make the energy distribution and

dissipation more effectively because better gripping of yarns in the fabric helps the impact energy to propagate to a larger area of fabric. Nevertheless, the energy absorption mechanism is a complicated procedure influenced not only by friction but also by other factors. It is necessary to mention that if the friction between yarns is too high, e.g. to a level that blocks the yarn movement in the fabric, the impact energy absorption by yarns displacement will be minimised, and the mechanism for the energy to be absorbed is left to the yarn breakage only. This is the reason that the unidirectional fabric (F14) made from high performance polyethylene demonstrated lower energy absorption on weight basis than the single layer woven fabrics (e.g.F23, F22 and etc.) and even than a certain type of angle-interlock woven fabrics (F19), as shown in Figure 5.8.

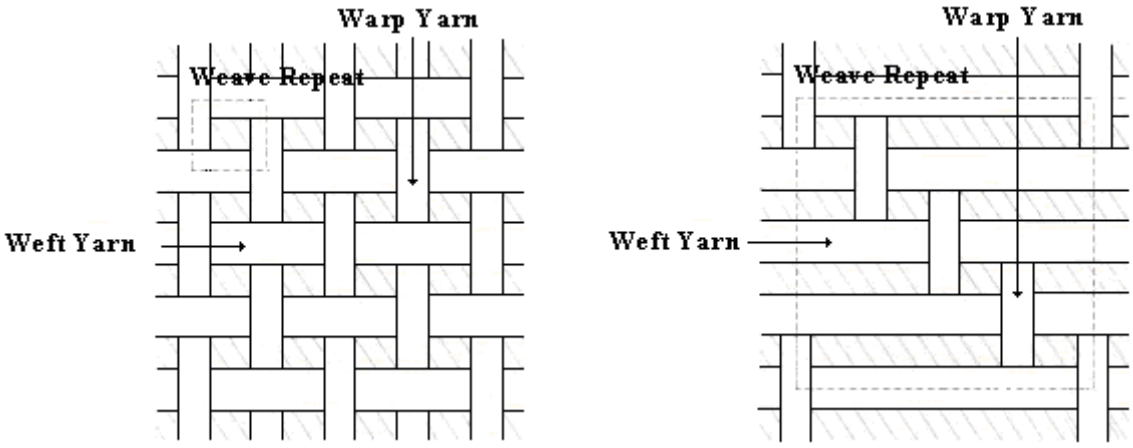

Figure 5.9 Weave structure: (a) plain; (b) 4-layer angle-interlock

Additionally, based on all the designed and manufactured fabrics so far, comparisons are also made on other various fabrics' ability in absorbing impact energy. Important findings are listed as follows:

- Fabrics with leno insertions in warp and cramming yarns in weft show better performance of impact energy absorption than their counterparts without weft yarn cramming. F7 (Broad plain woven fabric with leno insertions in warp and cramming yarns in weft both in every 4cm intervals) is the best in terms of impact energy absorption. This is because weft yarn cramming could also improve the yarn gripping effect to increase friction among weft yarns by increasing weft density. More kinetic energy is consumed against this additional friction. However for BPLWC (Broad plain woven fabric with leno insertions in warp and cramming yarns in weft) fabric itself, optimal setting exits; in this research, fabrics with 4cm insertion intervals are better than other settings. Further investigations may be required in this specific region.

- F17 (Hand loom made plain woven fabric with weft winding in every 6cm intervals) performs better than F8 (the fabric with same insertion intervals of leno weave). This may because much tighter warp yarns grip the winding weft yarns compared to leno weave structure.

- 3D cellular fabrics and the same layer 2D plain fabric: The two and four layered cellular fabrics perform better than the assembly with the same layer 2D plain woven fabric of similar yarn densities.

- Dyneema® plain woven fabrics absorb less impact energy compared to their Kevlar® counterparts. These results may verify that the low surface friction of Dyneema® fibre affects its ballistic-resistant performance.

- For the unidirectional and woven Dyneema® fabrics, the former one shows reduced ballistic performance that the latter one, but may have better trauma proof ability.

5.3 Parametric Study of Ballistic Performance of Angle-interlock Woven Fabrics

The above-mentioned section mainly focused on the overall ballistic performance of angle-interlock woven fabrics and it showed that this kind of fabric demonstrates relatively low capabilities against the ballistic impact. For the purpose of better understanding of the ballistic resistance of angle-interlock woven fabrics, a parametric study of the angle interlock fabrics on the ballistic performance was carried out.

5.3.1 The fabrics

A series of angle-interlock woven fabrics with different structural parameters, as shown in Table 5.2, have been produced using the Saurer 100W dobby loom with maximum 22 heald frames, which has a loom speed of 160 picks/minute and the maximum width of 1.2m. A negative let-off mechanism was used in controlling the weaver's beam and balancing the warp yarn tension. Kevlar® 49 with 158 tex, the commonly used yarns for

ballistic protective applications, was used to make the angle-interlock woven fabrics [143].

Table 5.2 Fabric specifications

Fabrics	Fibre Type	Yarn density		Yarn count		Areal density (g/m²)	Weave structure
		Warp (ends/cm)	Weft (picks/cm)	Warp (tex)	Weft (tex)		
F18	Kevlar® 49	12	26	158	158	609.02	4-layer angle-interlock woven fabrics
F19	Kevlar® 49	12	28	158	158	640.58	
F20	Kevlar® 49	12	30	158	158	672.13	
F21	Kevlar® 49	12	32	158	158	703.69	
F22	Kevlar® 49	8	26	158	158	542.76	5-layer angle-interlock woven fabrics
F23	Kevlar® 49	8	28	158	158	574.31	
F24	Kevlar® 49	8	30	158	158	605.87	
F25	Kevlar® 49	8	32	158	158	637.42	
F26	Kevlar® 49	10	28	158	158	607.44	
F27	Kevlar® 49	10	30	158	158	639.00	
F28	Kevlar® 49	10	32	158	158	702.11	
F29	Kevlar® 49	12	26	158	158	609.02	
F30	Kevlar® 49	12	28	158	158	640.58	
F31	Kevlar® 49	12	30	158	158	672.13	
F32	Kevlar® 49	12	32	158	158	703.69	
F33	Kevlar® 49	12	34	158	158	735.24	

5.3.2 Experiments

These fabrics were ballistically tested in the clamped state for energy absorption at the room temperature using the firing apparatus. Before coming to the test result analysis, it is necessary to mention that features displayed in 2D woven fabrics such as yarn slippage, fibre fracture and cone formation, can also be identified in 3D angle-interlock woven fabrics during the ballistic test.

5.3.3 Some observations

Figure 5.10 (a) shows a typical sample after shooting when clamping has been removed. It can be seen that some of the primary yarns are broken whilst some others are pulled

towards the impact point where the projectile has penetrated the target fabric. The arrows signify the direction of primary yarn motion. This is similar to the situation where a single layer plain woven fabric is impacted on, where the longitudinal and transverse waves would be generated. Primary yarns stand the ballistic impact directly, which however could not consume a lot of kinetic energy and therefore exhibits fracture and pull-out as two typical localised damages in the central impact zone, as shown in Figure 5.10 (a). Another apparent phenomenon is the pulling of the primary yarns from the fabric edge, more serious than the situation for the plain woven fabrics. This indicates that the angle-interlock woven fabrics have lower gripping power to the constituent yarns because of the fabric structure. Thirdly, cone formation phenomenon is quite noticeable. As a matter of fact, the conic shape that is seen in Figure 5.10(a) is not the cone caused by the transverse movement of the projectile. It is rather a combination of the actions from the impact of the projectile, the sabot, and the oscillation of the fabric. The cone formation caused by the projectile takes place in a very short period after the impact (a few microseconds). The fabric works like a net to block the flying projectile, which performs a conical deformation towards backface of the target fabric; at the top of the cone localised damage takes place. Like other types of ballistic fabrics, fabric areas associated with the secondary yarns are not much affected by the impact. Measures need to be taken to get more of such areas to be involved in absorbing energy. Efforts are being made to improve the situation for all types of ballistic fabrics at the University of Manchester. The property of low shear rigidity of angle-interlock woven fabric is determined by its unique structure consisting of layers

of straight weft yarns bound by a single layer of warp yarns from back to face, as has been detailed in Chapter 4. Generally speaking, the angle-interlock woven fabric displays not only normal features of the energy absorption mechanisms but also new characteristics, e.g. low gripping of the yarns. However, as angle-interlock woven fabrics have a multi-layer of straight weft yarns, they should be able to take on the impact more directly by yarns than other types of fabrics if the gripping on yarns can be improved. This remains to be explored for future research.

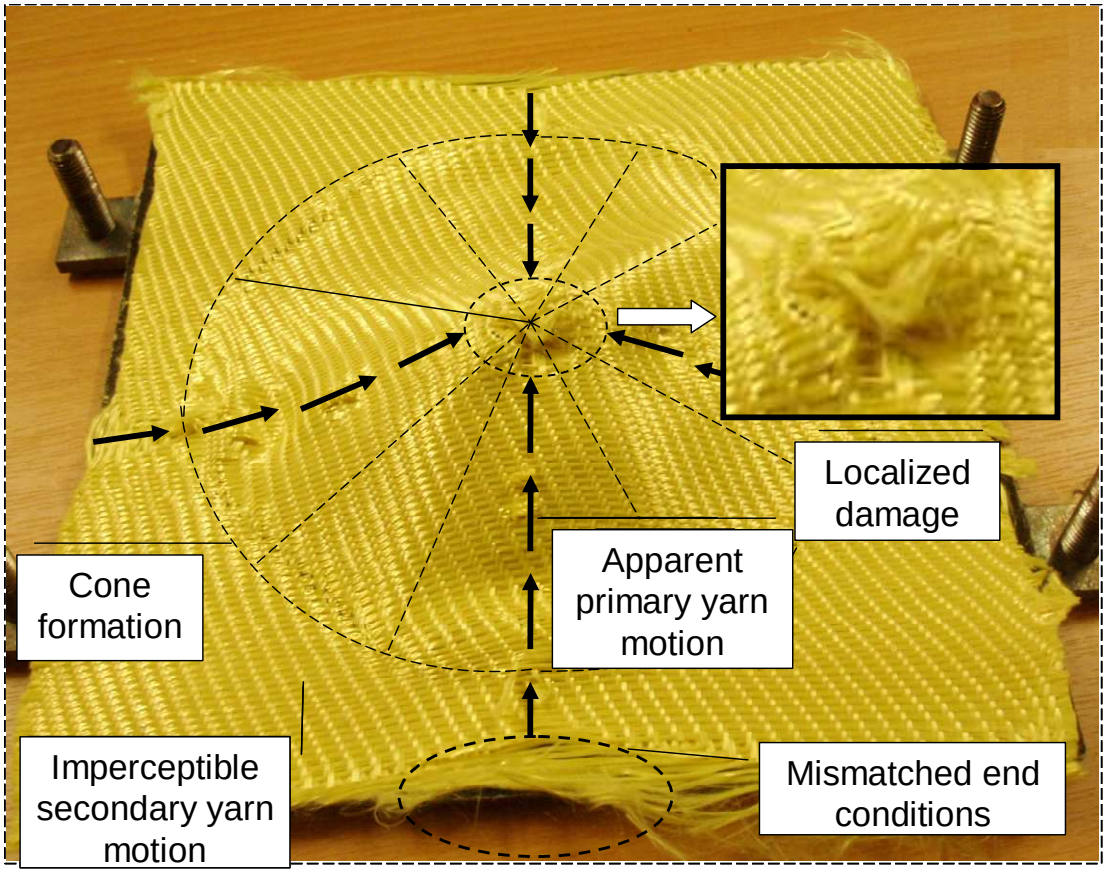

(a)

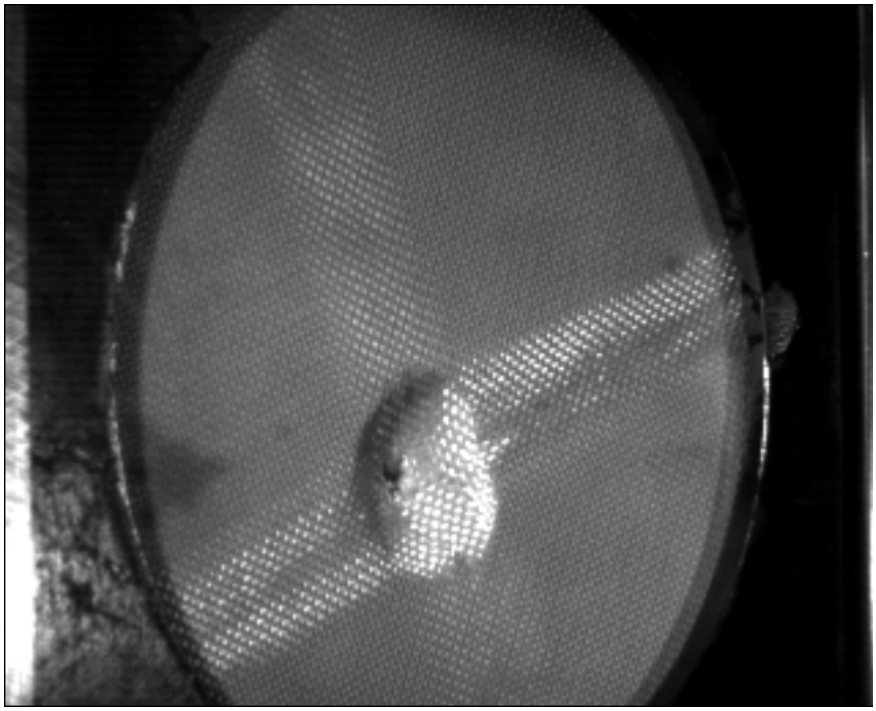

(b)

Figure 5.10 the impacted fabric (a) the final state (b) during the impact (snapshot)

5.3.4 Test results and analysis

5.3.4.1 Data processing

The original data obtained during the energy loss test are attached as Appendix A. The t_0, the time used by the projectile to travel through a pair of detectors before impact, and t_1, the time used to travel through the detectors after impact, were the original data caught during the energy loss test. Due to the importance of the data, the following actions were taken to eliminate the less meaningful data from the set.

1) For each sample group, the t_0 and t_1 were averaged respectively. Data were only selected if they were within ±10% of the average values;

2) The selected values for t_0 and t_1 were averaged again respectively. The average

data were employed to calculate the impact and exit velocities and the energy loss using Equations (5.2) and (5.1), respectively.

Table 5.3 Ballistic results

Fabrics	Areal density (g/m^2)	V_0 (m/s)	V_1 (m/s)	E_0 (J)	E_1 (J)	ΔE (J)	$\frac{\Delta E}{\text{Areal density}}$ ($J.g/cm^2$)
F18	609.02	483.04	439.99	123.63	102.57	21.06	345.80
F19	640.58	469.65	418.14	116.87	92.64	24.23	378.25
F20	672.13	486.04	437.20	125.17	101.28	23.89	355.44
F21	703.69	483.66	429.93	123.95	97.94	26.01	369.62
F22	542.76	466.58	422.24	115.35	94.47	20.88	384.70
F23	574.31	477.84	440.28	120.98	102.71	18.27	318.12
F24	605.87	494.51	451.05	129.57	107.80	21.78	359.48
F25	637.42	485.91	444.72	125.10	104.79	20.31	318.63
F26	607.44	501.07	447.10	133.03	105.92	27.11	446.30
F27	639.00	480.57	420.83	122.37	93.84	28.53	446.48
F28	702.11	476.75	417.93	120.43	92.55	27.88	397.09
F29	609.02	485.24	428.71	124.76	97.38	27.37	449.41
F30	640.58	513.47	473.62	139.70	118.85	20.85	325.49
F31	672.13	478.25	434.70	121.19	100.12	21.06	313.33
F32	703.69	492.04	429.01	128.28	97.52	30.76	437.12
F33	735.24	489.07	444.06	126.74	104.48	22.25	302.62

The results after data selection are shown in Table 5.3, where V_0, V_1, E_0, E_1 and ΔE represent the impact velocity, exit velocity, impact energy carried by the projectile, residual energy carried by the projectile, and the energy loss due to penetration, respectively. In order to eliminate the effect of the amount of fibre materials in each of the fabrics, the energy loss were normalized by the areal density for the purpose of comparisons.

This study aimed to examine the influence of structure on the energy loss. Structural parameters considered include the number weft yarn layer, weft density and warp

density of the angle interlock fabrics. The relationships are depicted in Figure 5.11.

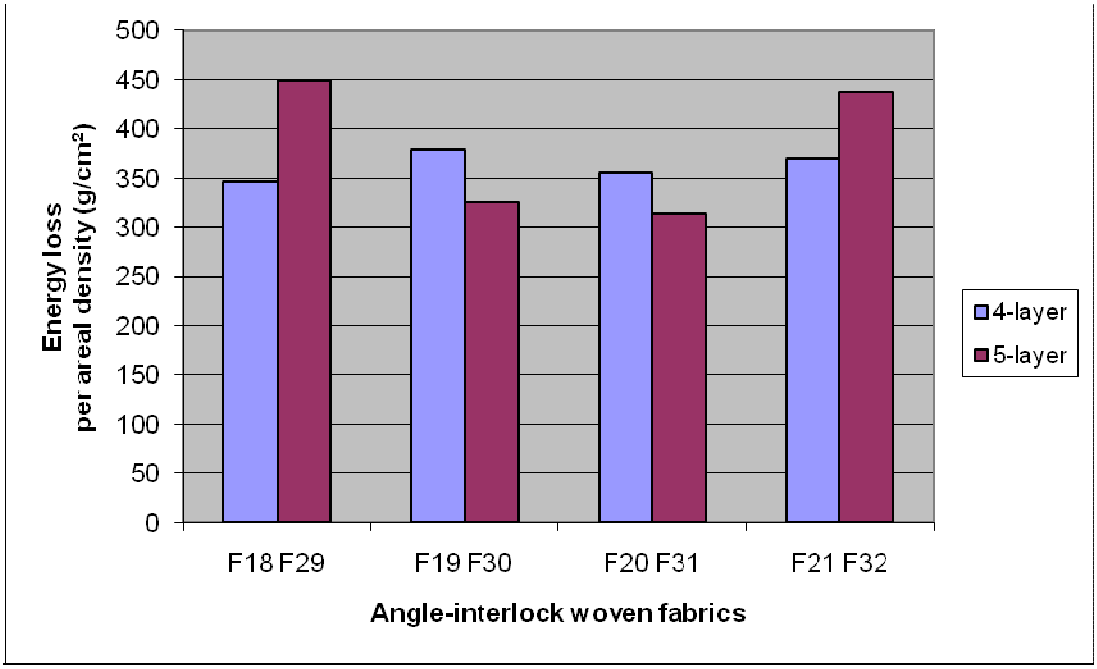

(a)

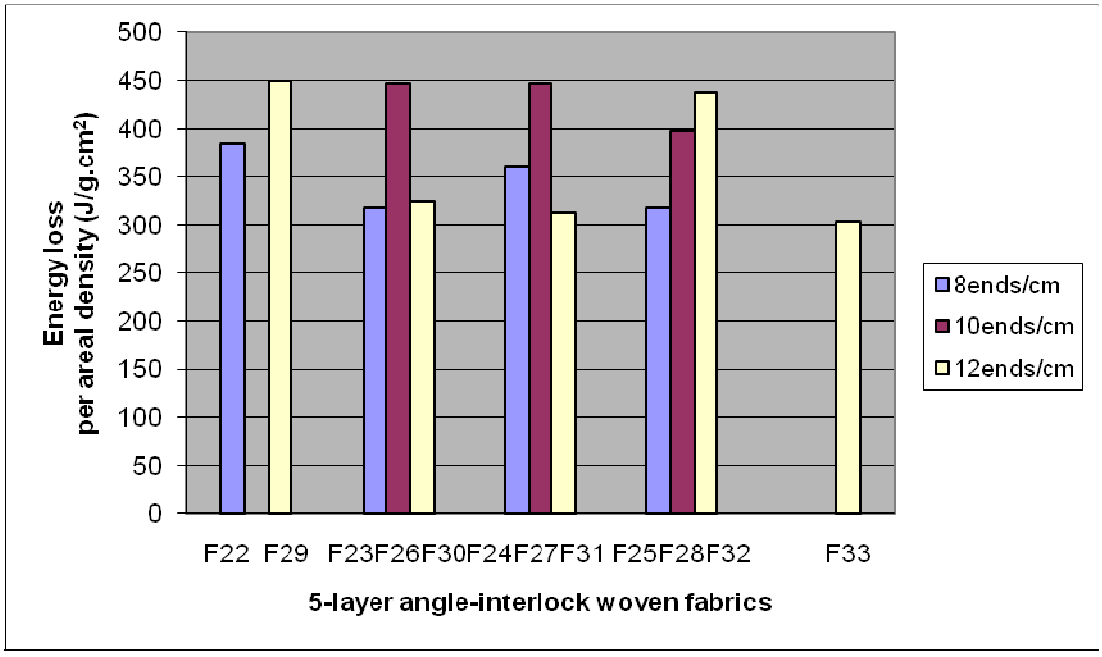

(b)

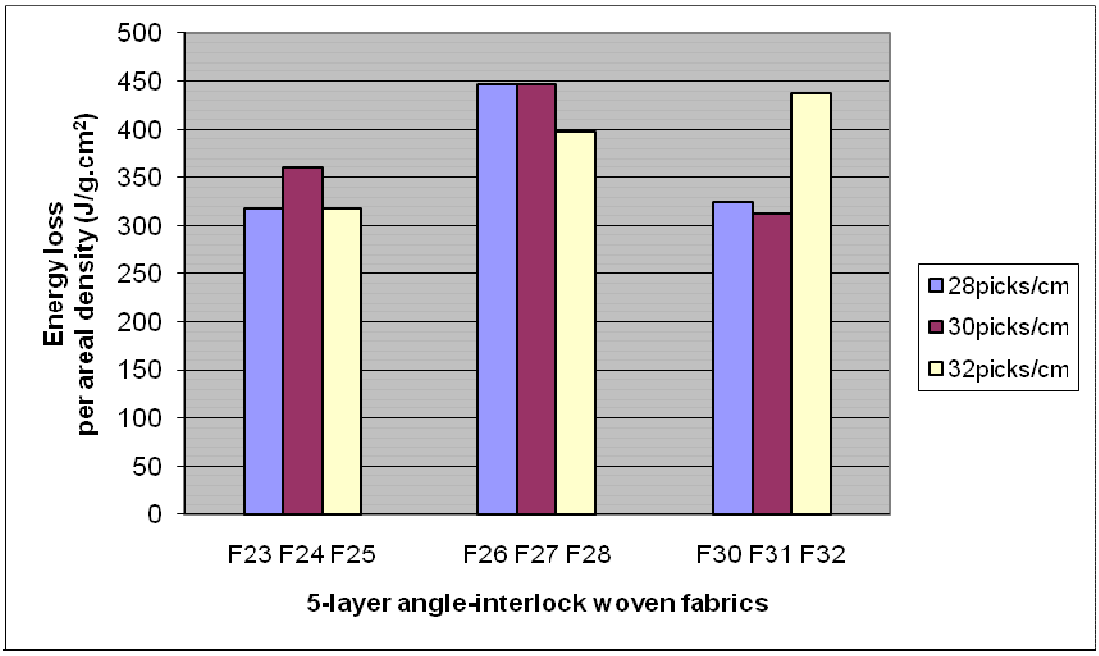

(c)

Figure 5.11 Energy loss normalized by areal density V.S. parameters: (a) weft layers; (b) weft densities; (c) warp densities

5.3.4.2 Analysis

It could be seen from Figure 5.11 that the trend in all cases is not clearly obvious. This section will try to give explanations from four different angles, which are (a) the clamping state; (b) yarns hit by the projectile; (c) the impact angle of the projectile; (d) the impact velocity.

Clamping

Fabric clamping is important as boundary conditions influence the ballistic performance of the fabrics. Fabrics were clamped for energy loss test, and the clamp held the fabric by four fastening screws in the corners of the clamp with needles evenly distributed in a circular arrangement, as shown in Figure 5.5. However, an angle-interlock woven fabric contains multiple layers of weft yarns leading to a thick fabric, and that requires more

clamping power, compared to the situation of clamping the single-layer 2D woven fabric. Figure 5.12 illustrates the clamping of the 5-layer angle-interlock woven fabric and the single layer plain woven fabric for comparison. The thickness of the former is almost five times than the latter, which indicates that the angle-interlock woven fabric requires much more clamping power to be stabilised and therefore it is more difficult to be clamped well. Additionally, the weft yarns in the angle-interlock fabric are straight and only interlaced with a single-layer of warp yarns. Therefore, the weft yarns are not well gripped by the fabric and hence easy to move. This makes tight clamping more difficult. The difficulty to offer the exact unified clamping state may be an important factor leading to the randomness of results.

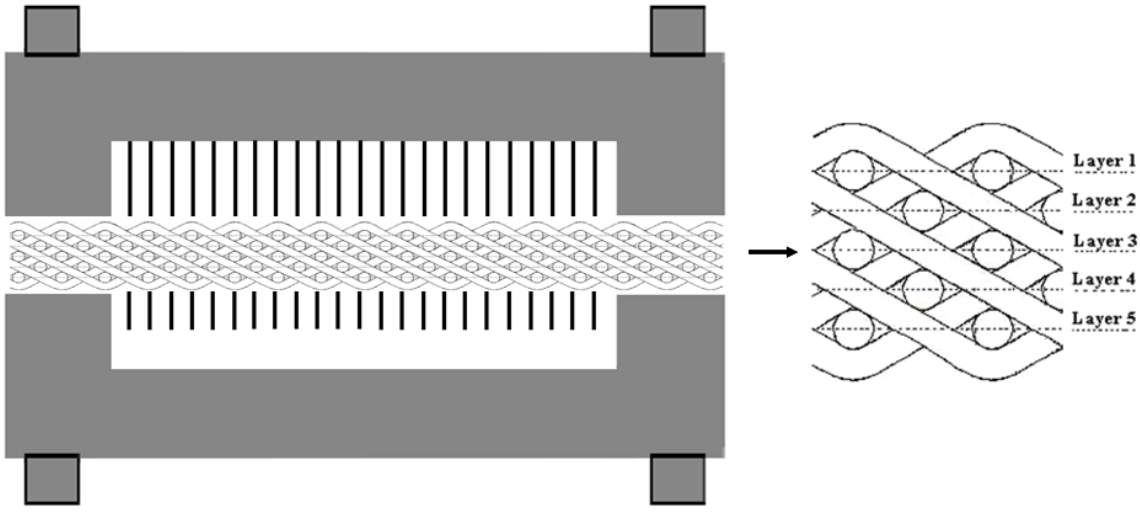

(a)

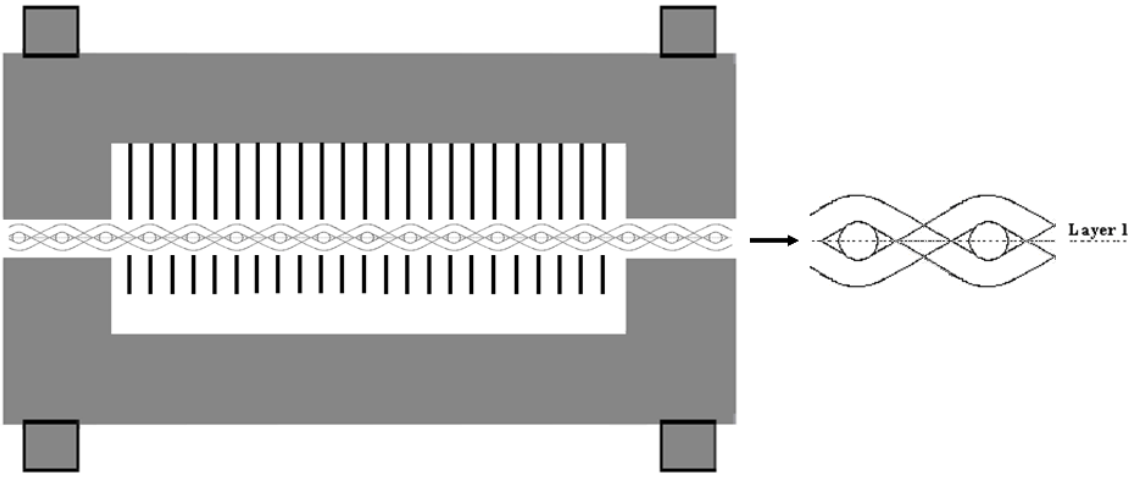

(b)

Figure 5.12 Clamping state: (a) 5-layer angle-interlock woven fabric; (b) plain woven fabric

Yarns hit by the projectile

The number of warp/weft yarns hit by the projectile may lead to the complication of energy absorption of the fabric. In a fabric the spot the projectile hits is composed of warp and weft yarns. The projectile may hit the yarns, the interlacements, or the gap between yarns. If the projectile hits quite a few yarns, the results will be quite complicated. In an ideal situation where the whole end area of the projectile touches the fabric, the numbers of warp and weft yarns hit by the projectile, denoted as N_e and N_p respectively, can be calculated as follows:

$$N_e = \frac{d_{pro}}{d_e} \tag{5.3}$$

$$N_p = \frac{d_{pro}}{d_{p_l}} \times n_l \tag{5.4}$$

where, d_{pro} is the diameter of the projectile; d_e is the distance between the neighbouring warp yarns; d_{pl} is the distance between the neighbouring weft yarns per

weft layer as the angle-interlock woven fabric has a multi-layer structure; and n_l is the number of weft layers. Figure 5.13 illustrates the impact area hit by the projectile on the angle-interlock woven fabric. The impacted fabric area is equal to the end area of the projectile. Therefore the diameter of the projectile d_{pro} would determine the length and width of the fabric which is impacted on. $\frac{d_{pro}}{d_e}$ and $\frac{d_{pro}}{d_{pl}}$ give the numbers of warp and weft yarns directly hit by the projectile. The latter value needs to multiply the number of weft layers, n_l, to obtain the total number of weft yarns influenced by the projectile as the thickness of the angle-interlock woven fabric is considered.

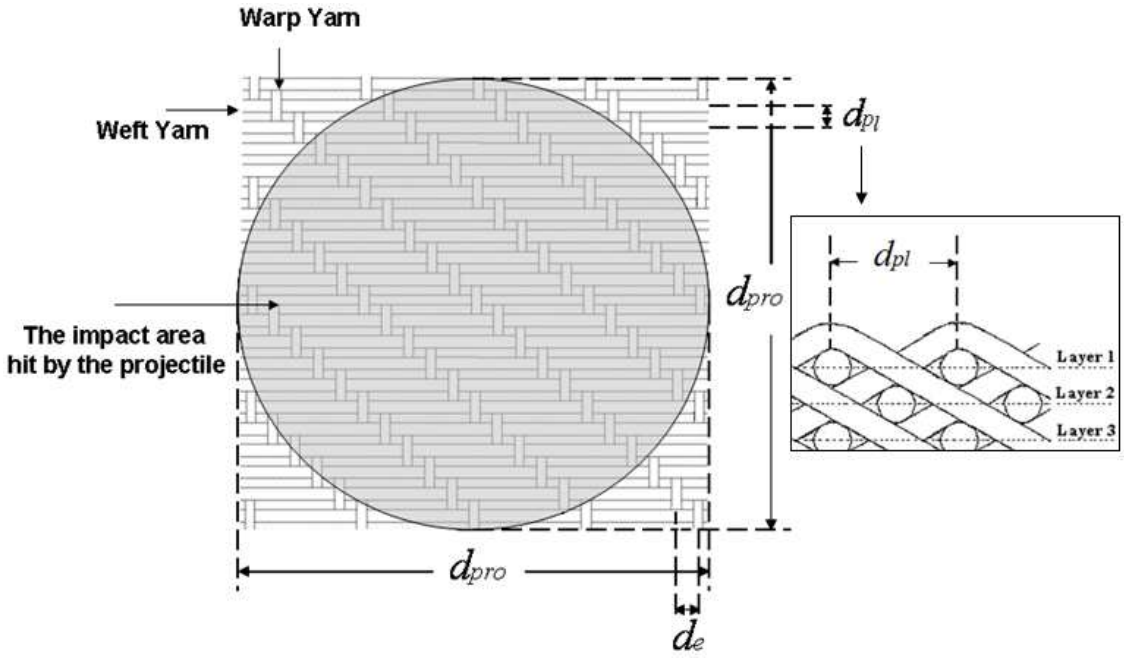

Figure 5.13 The impact area hit by the projectile

d_e and d_{p_l} could be achieved by:

$$d_e = \frac{1}{n_e} \tag{5.5}$$

$$d_{pl} = \frac{n_l}{n_p} \tag{5.6}$$

where n_e and n_p are the warp/weft density. Substituting (5.5) and (5.6) into (5.3) and (5.4) respectively leads to

$$N_e = d_{pro} \cdot n_e \tag{5.7}$$

$$N_p = d_{pro}.n_p \tag{5.8}$$

Taking 4-layer angle-interlock woven fabric with 12 ends/cm and 26 picks/cm as an example (the relative details are shown in Table 5.2), the number of warp and weft yarns covered by the end area of the projectile, N_e and N_p, can be easily calculated as 7 and 15, respectively.

This indicates that for this fabric, the projectile needs to work directly with 7 ends and 15 picks during the ballistic impact. More possibilities will be created when more yarns are under an attack. Failure of a yarn at a different location will cause a different reaction from the rest of the yarns. It can be said in general that the consideration of the numbers of warp and weft yarns hit by the projectile contribute to the uncertainty in the ballistic results.

The impact angle of the projectile

The above-mentioned analysis is considered under the ideal state where the flat end of the cylindrical projectile perfectly hits the target fabric for all the experiments, as shown

in Figure 5.14 (a). However, in real situations the projectile may impact on the fabrics in any orientation as indicated in Figure 5.14 (b); consequently, the randomness of the kinetic energy absorption by the fabric will occur. It is well accepted that the smaller the impact area, the larger the stress will be caused in the fabric when the identical force is applied to the fabric based on the definition of stress (a measure of the average amount of force exerted per unit area of a surface within a deformable object [144]):

$$\sigma = \frac{F}{A} \tag{5.9}$$

where σ is the stress

F is the total tensile or compressive force

A is the area where force acts upon

According to this principle, the force-exerted area is larger in Figure 5.14 (a) than in Figure 5.14 (b) since in the former case the end of the cylinder fully touches the fabric, which results in smaller stress and hence smaller strain in the fabric. More energy will have to be used to cause a bigger strain in the fabric in order to break the fabric. Consequently, the exit velocity will be lower and the energy loss will be larger based on Equation (5.1) when all other conditions are supposed to be unchanged. The different angles of projectile hitting the fabric would lead to the difference in energy loss.

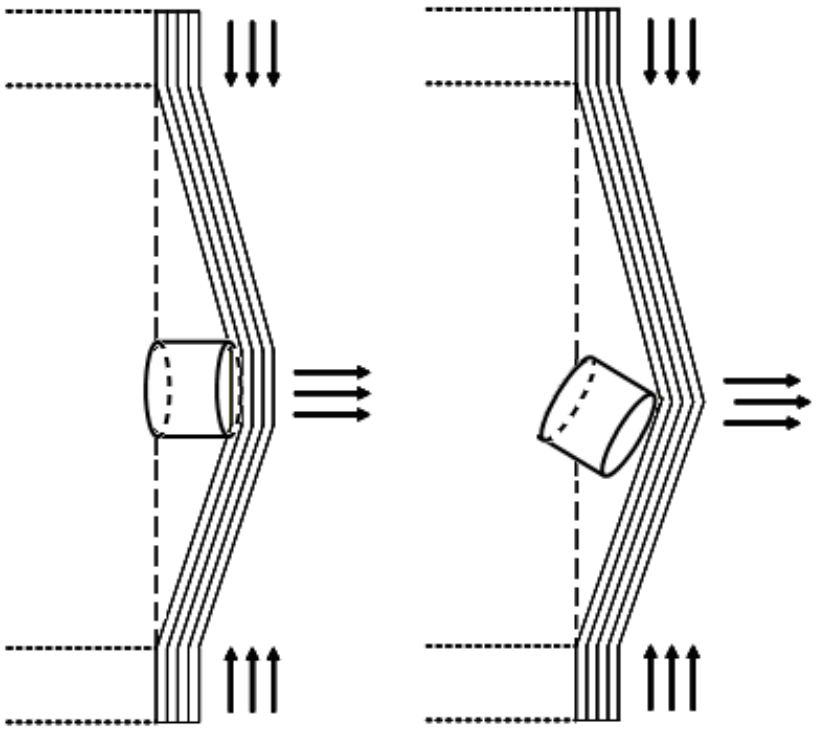

(a) **(b)**

Figure 5.14 Portions of projectile when impacting the fabric: (a) full end section; (b) edge segment

The impact velocity

The impact velocity may also have affected the results of the ballistic impact. During the impact test, it was seen that the impact velocity V_0 fluctuated from round to round of shootings, as demonstrated in Table 5.3. This is mainly due to the variation in the amount of explosive powder in the cartridges. It seems not likely to have exactly the same explosion every time. Therefore, keeping the impact velocity V_0 constant seems hard to achieve. As an attempt to eliminate the influence of the variation in velocity, the energy loss results normalised by the impact velocity V_0 are shown in Figure 5.15. Comparison between Figure 5.11(c) and Figure 5.15(c) does show that the projectile velocity influences the energy loss.

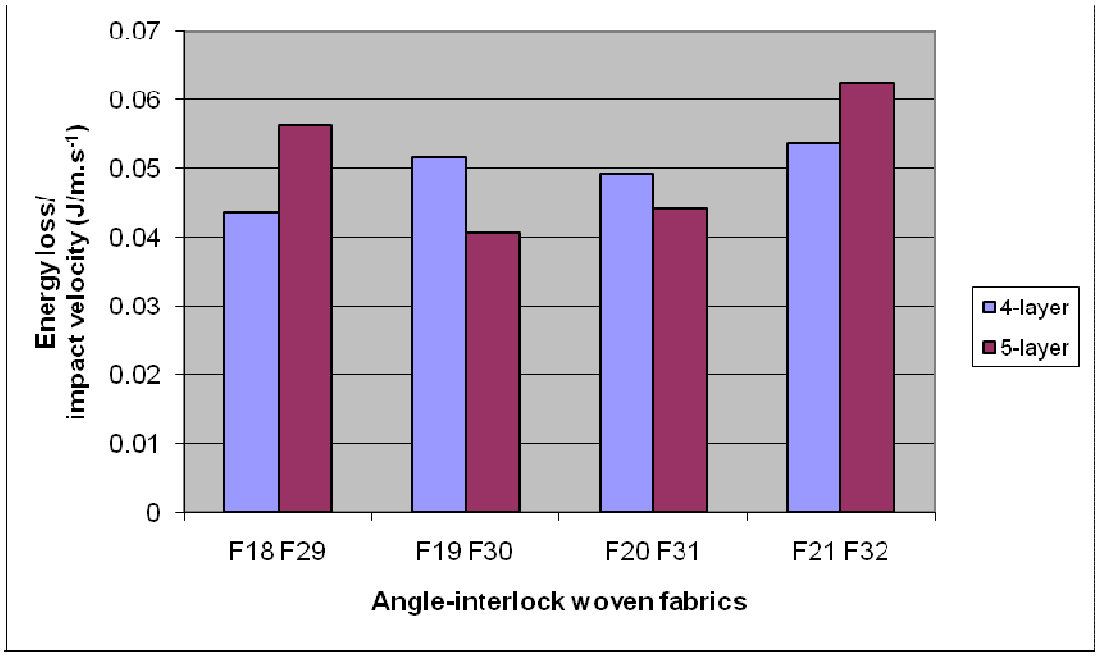
0.07
0.06
0.05
0.04
0.03
0.02
0.01
0
Energy loss/ impact velocity (J/m.s-1)
F18 F29
F19 F30
F20 F31
F21 F32
Angle-interlock woven fabrics
4-layer
5-layer

(a)

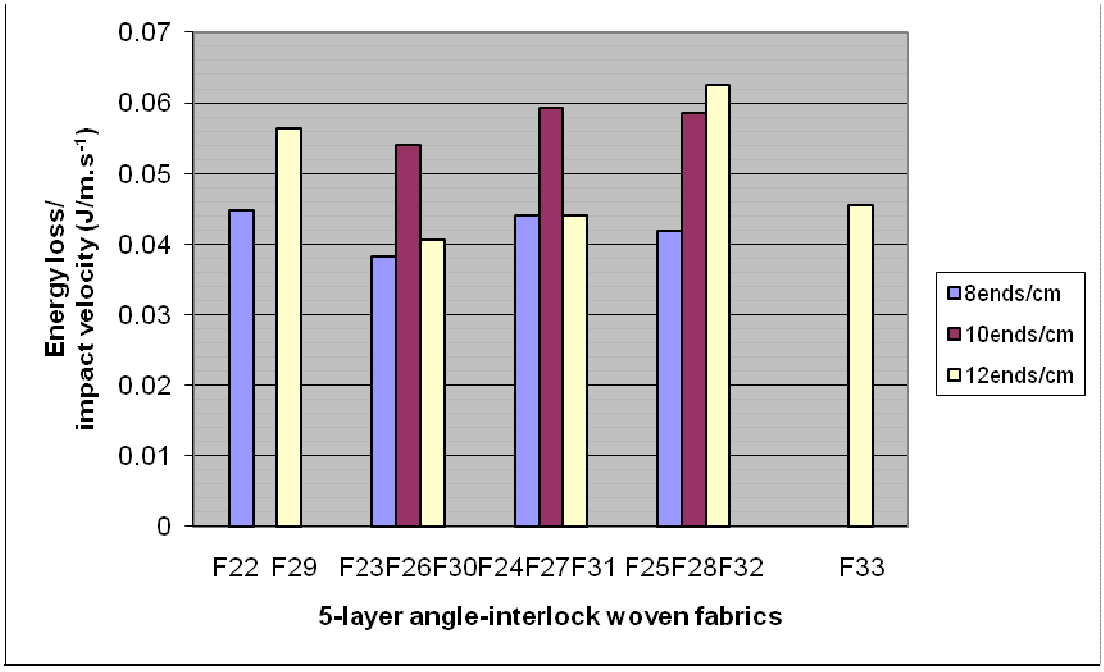
0.07
0.06
0.05
0.04
0.03
0.02
0.01
0
Energy loss/ impact velocity (J/m.s-1)
F22 F29
F23F26F30F24F27F31
F25F28F32
F33
5-layer angle-interlock woven fabrics
8ends/cm
10ends/cm
12ends/cm

(b)

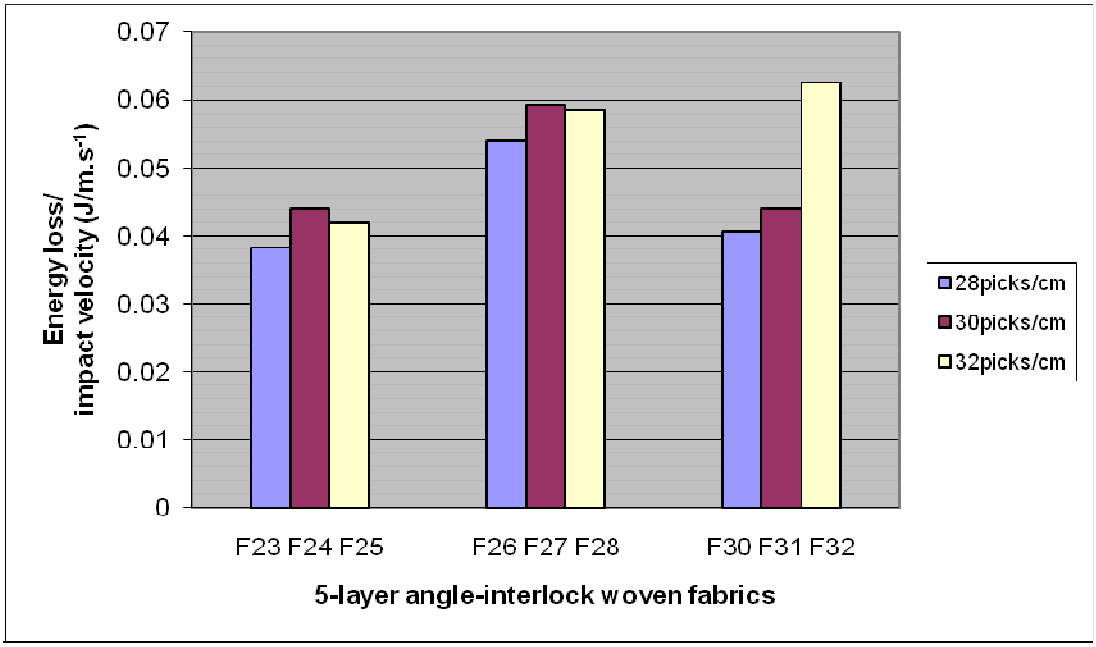

(c)

Figure 5.15 Energy loss normalized by impact velocity V.S. parameters: (a) weft layers; (b) weft densities; (c) warp densities

The reasons for the randomness of the energy loss results are quite complicated. Apart from the above-mentioned possibilities, the intrinsic factors could not be neglected, such as the yarn count, materials of the yarns, and weave structure which is considered to be fundamental. The structure of angle-interlock woven fabrics is composed of several layers of straight inserted weft yarns interlaced with a single layer of warp yarns from face to back. Low shear rigidity is its apparent character which indicates yarns are easy to move within the fabric under the impact. Besides, the angle-interlock woven fabric has a multi-layer structure; the thickness of the fabric could add more possibilities in ways energy is absorbed by the fabric. Further investigations may be required to address this issue.

5.4 Ballistic Evaluation of Angle-interlock Woven Fabric Panels

Figure 5.8 indicates that the angle-interlock woven fabrics, when compared to woven fabrics with other constructions, tend to have lower capability for absorbing the impact energy carried by the projectile. The reason for that can be attributed to the lower gripping power of the angle-interlock fabrics to their constituent yarns, based on single piece of fabric and on the size of the fabric samples (24cm × 24cm). However, it is of interest to know the performance of this type of fabrics when it is used in real size as a ballistic panel. This section reports on the evaluation of the ballistic performance of angle-interlock woven fabric panels according to the NIJ standard with the kind assistance from Armourshield Ltd in Greater Manchester.

5.4.1 Description of the ballistic test

Assisted by Armourshield Ltd, ballistic tests were carried out against the NIJ standard using their ballistic range, and the setup of the range is shown in Figure 5.16 (a), (b), and (c). 4- and 5- layer angle-interlock woven fabrics made from Kevlar® 49 of 1500 denier were layered up and placed at the target stand as shown in (b). These fabrics were woven on a conventional shuttle loom -'Arbon 100 W' made by Adolf Saurer™, which has a weft insertion rate of 160 picks/minute and the maximum width of 1.2 m. A negative let-off mechanism was assisted in controlling the warp beams and balancing the yarn tension. As a matter of fact, fabrics like these can be manufactured on most of the standard modern looms, regardless of the weft insertion methods and the let-off mechanism. The numbers of layers of angle-interlock fabrics were inserted into black plastic bags as would for other fabric panels, as shown in Figure 5.16 (d).

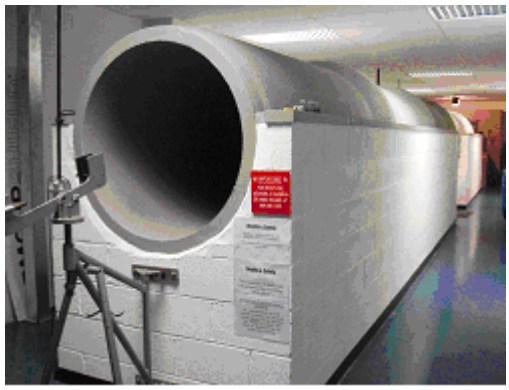

(a)

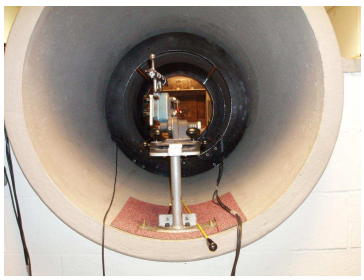

(b) **(c)** **(d)**

Figure 5.16 Shooting experiments: (a) ballistic range; (b) specimen prepared for shooting; (c) shooting position; (d) specimen after shooting

Certain numbers of layers of the angle-interlock fabrics with the same parameters were cut into the size of 35 × 35 cm^2 and sewn loosely together as would for other fabrics before putting into a black pocket as for the making of real body armour. The number of layers is calculated on the basis that the panel of sample fabrics has the same mass as the panel of standard fabrics. For the NIJ type II armour, a panel would consist of 25-32 layers of fabrics with 220 g/m^2 per layer. Therefore, based on the 'same mass' principle the number of layers of angle-interlock fabrics, N_s, can be calculated as follows.

$$N_s = \frac{W_{II} N_{II}}{W_s} \tag{5.10}$$

Where W_s is the areal density per layer for the angle-interlock fabric, W_{II} the areal density per layer for the standard fabric, and N_{II} the number of layers for the standard fabrics.

The number of layers of the angle-interlock woven fabrics for specimen can be determined from Equation (5.10) knowing the areal densities of the angle-interlock woven fabrics.

Before shooting, the fabric panel in the black bag was attached to the front of the target, backed with Roma Plastilina®, which is used to imitate the torso characteristics of a human and to measure the level of impact trauma from the projectiles. The indentation on the Roma Plastilina® after shooting, together with the number of layers of fabrics penetrated, determine the ballistic performance of a fabric. Roma Plastilina® should be warmed up to 37ºC, similar to human body temperature, and its softness is then measured by a weight drop test.

The ballistic test was carried out in a large, long, thick and solid concrete tube, divided into two parts to achieve the shoot range of 5 m and 15 m respectively. At the end of the tube, the box where the ballistic fabric panel was attached was located in the centre. Simultaneously, the relevant technical data for the impact test were recorded by the computer software.

5.4.2 Results and analysis

In this experiment, there were seven angle-interlock woven fabric panels for the ballistic performance test. One panel was used each time, and some of packages were shot at twice in order to compare the results with or without the additional protective assistance. The structural parameters of the fabrics and the data obtained through the test are listed in Table 5.4.

Table 5.4 Technical data for the impact tests

Threat Level	Calibre A	Bullet Type A	Backing Type	Drop Test
NIJ Type II	9 mm	9 mm FMJ	Roma Plastilina®	19 mm

Weft layers	Ends (per cm)	Picks (per cm)	Areal density (g/m² per layer)	Layers	Velocity (m/s)	Trauma (cm)	The number of penetrated layers
4	12	26	626.76	9	333.1 795.99	4.1 3.6*	4 0
4	12	28	664.84	9	347.72	3.7	4
4	12	30	704.41	8	335.75 345.96	4.1 2.7**	4 4
4	12	32	738.79	8	329.58 328.18	3.65 3.3***	5 4
5	12	28	668.65	9	332.27	4.4	4
5	12	32	733.98	8	336.56	3.6	4
5	12	34	768.93	8	350.2	4	4

3.6*: Bullet Type – 30.06 AP, TL 1012SC4 plate

2.7: Bullet Type – 9 mm FMJ, 3 × poly TP**

3.3*: Bullet Type – 9 mm FMJ, 2" diamond stitch**

According to the NIJ standard, a body armour panel passes the test if the panel stops the projectile from penetrating the panel and the depth of the backface signature (trauma) does not exceed 4.4 cm. It could be seen that all the panels made from angle-interlock fabrics satisfied the NIJ type II standard. Such a result is a significant finding as it provides evidence that the angle-interlock fabric offers adequate ballistic protection.

This indicates that the angle-interlock woven fabrics are qualified for ballistic protection.

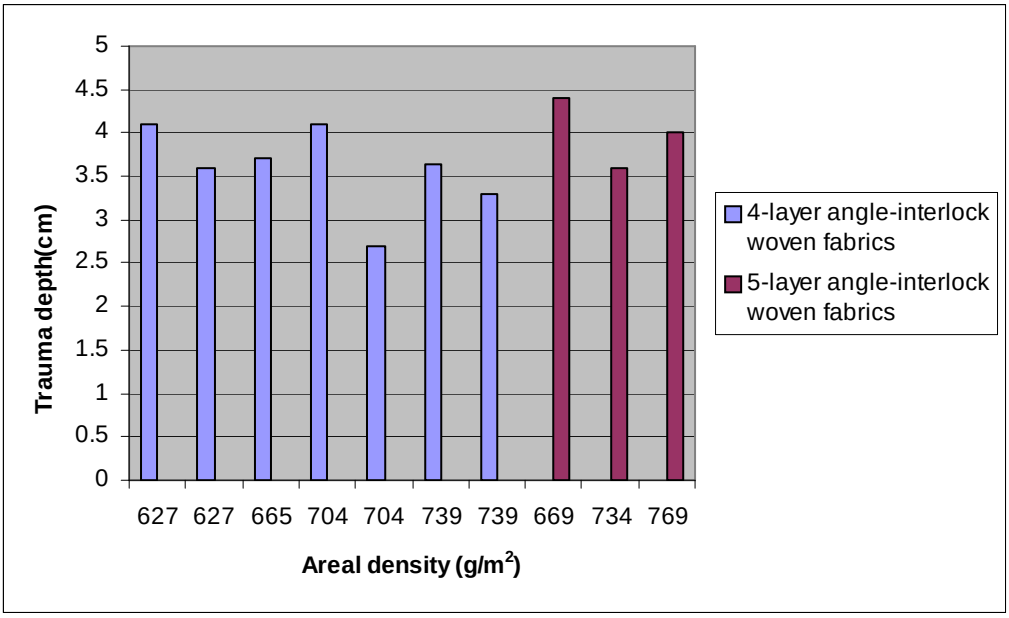

Table 5.17 Trauma depth V.S. areal density

Table 5.17 depicts the relationship between the fabric areal density and the trauma depth. It is observed that there is no obvious trend between the areal density and the trauma depth. Higher areal density doesn't indicate better ballistic performance. This may be due to the fact that the projectile can go easily through a loose woven fabric by piercing between the yarns, while then it can also penetrate easily tight woven fabrics by rupturing the yarns upon impacting. The 4-layer angle-interlock fabric with 12 ends/cm and 28 picks/cm and the 5-layer angle-interlock fabrics with 12 ends/cm and 32 picks/cm have shown the lowest trauma depths against the ballistic impact as they relate to the smallest trauma depths of 3.7cm and 3.6cm respectively.

In addition, increasing thickness of the angle-interlock woven fabrics seems to influence

on trauma depth, given the same warp and weft density under the same test standard. As shown in Figure 5.18, the trauma depths are different for 4-and 5-layer angle-interlock woven fabrics. But there is no clear trend between the thickness of the structure and the trauma depth, and more testing data from further investigation are needed to establish a conclusive relationship.

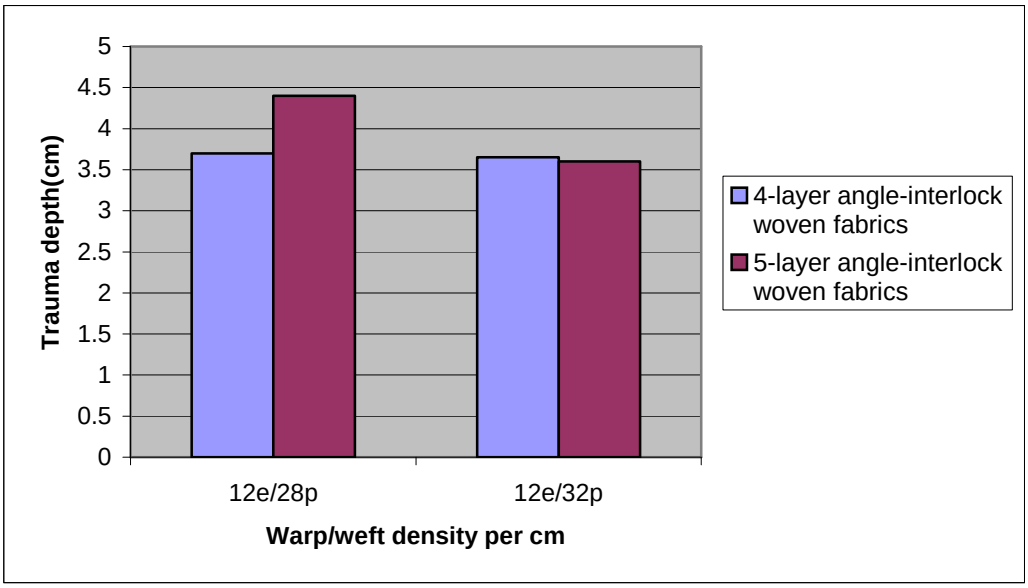

Figure 5.18 Warp/weft density V.S. trauma depth

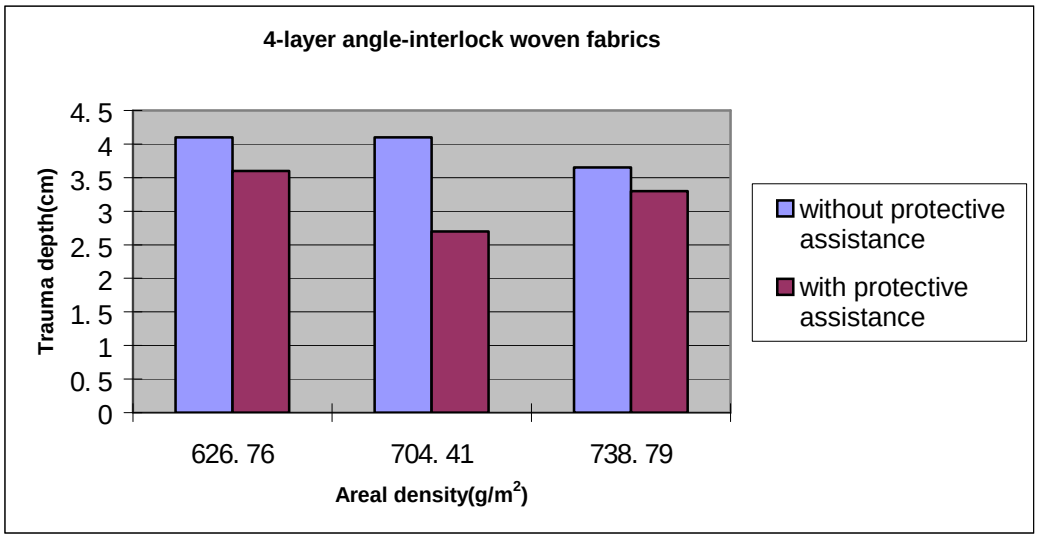

Figure 5.19 4-layer angle-interlock woven fabrics: trauma depth V.S. areal density

In the experiment, a type of thin plastic plate was also used among the layers of fabrics in some panels to see its influence on the trauma depth. The result is shown in Figure 5.19. Under the same condition, the trauma depth reduced with the protective assistance for all cases tested. In particular, the trauma depth reduced from 4.1cm to 3.6cm when the TL 1012SC4 plate was attached for the 4-layer angle-interlock fabrics with 12 ends/cm and 26 picks/cm and the areal density 626.76 g/m². More strikingly, the number of fabric layers penetrated was sharply reduced from 4 to zero. This suggests that incorporation of materials such as plastic plates improves the overall performance of panels against ballistic impact. It, however, remains to be further investigated as how such plastic plates can be applied into female body armour.

5.5 Remarks

This chapter reported the outcome from the ballistic test of the angle-interlock fabrics with the aim to validate the usefulness of the 3D woven fabrics for making female body armour. The overall ballistic performance of angle-interlock woven fabrics in comparison to other fabrics investigated for body armour application is quite low. Almost all other tested fabrics show stronger energy absorption capability than angle-interlock woven fabrics. Besides, the parametric study of the angle-interlock woven fabric is very complicated and currently no tendency could be found. Further investigations will be required. Nevertheless, the ballistic tests for fabric panels of angle-interlock woven fabrics demonstrate quite clear positive results. It has been clearly shown that all the angle-interlock woven fabrics tested meet or exceed the level

II performance defined in the NIJ standard and they are no less than the conventional fabrics used for ballistic protection, in terms of both the layers of penetration and the depth of the backface signature. Moreover, the 4-layer angle-interlock fabric with 12 ends/cm and 28 picks/cm and the 5-layer angle-interlock fabric with 12 ends/cm and 32 picks/cm showed better ballistic performance. In addition, it has shown that the incorporation of a thin plastic plate can dramatically reduce the trauma depth and the panel penetration. These findings will allow the angle-interlock fabrics to be used for making female body armour.

Chapter 6

Pattern Creation for Seamless Front Female Body Armour Panel using Angle-interlock Woven Fabrics

The angle-interlock woven fabric offers an option to make female body armour as it can form integrally the required dome shape without cutting or moulding because of its extraordinary mouldability. The ballistic impact testing has proved that the angle-interlock woven fabric provides no less ballistic performance than other commercially used fabrics according to the NIJ standard. Based on the extraordinary mouldability and the satisfactory ballistic performance, this chapter presents a mathematical model to determine the pattern geometry for the front panel of female body armour. The raised bust area was divided into seven different parts for the modelling, using the simplest surfaces possible. This mathematical model takes the body figure size and bra size as the input, and the output is the profile of the front pattern of female body armour. The front panel of female body armour could be quickly created on the basis of utilising this mathematical model, which may indicate that a novel approach for making seamless female body armour with satisfactory ballistic performance is established.

6.1 Key Problem

In the former research, it has been shown that the angle-interlock woven fabric has good mouldability as well as satisfactory ballistic performance. Based on these characteristics, it is of great interest to investigate the possibility of making female body armour from the angle-interlock woven fabrics. One key problem is the pattern making for the female ballistic vest, whose final configuration is three-dimensional and without cuts or folding, a problem which is described in some literature. Because of the fabrics capability in moulding, the front pattern of the female body armour will have to contain sufficient area so that when the fabric is domed up to accommodate the bust the body armour would come to the normal shape.

Therefore, an effort to establish a mathematical model for the determination of the boundary profile of the front panel for female body armour based on the use of the angle-interlock woven fabric is required. The excellent formability or mouldability of the angle-interlock woven fabric will be used for making the front panel of the female body armour.

Compared with the male, the female has more complicated curvaceous torso, which indicates difficulty to construct corresponding well-fitting mathematical model of body armour. A size 12 female torso mannequin is shown as an example in Figure 6.1, where it is obvious that suitable surface must be used to describe the bust area with accuracy. This indicates that more fabric is needed to cover the three-dimensional bust area when shaping the front pattern of the female body armour. In normal clothing pattern making, darts and folding are used to accommodate the female bust area, but for body armour

those techniques become inappropriate. Seeking the mathematical relationship between the bust area and the block projection is the purpose of this mathematical model.

Figure 6.1 Size 12 female mannequin

A mathematical model is supposed to agree with existing measurements within a specified accuracy and can be used with confidence to predict future observations and behaviour [145]. To develop a reasonable model, it is important to pay attention to features that reflect the observed phenomenon sufficiently and accurately, while the unnecessary features are neglected to avoid increased complexity and difficulties in solving the given problem. Therefore, the mathematical model for the front panel of female body armour is supposed to be simple enough to give useful information, but it should also be sophisticated enough to give the required information with sufficient accuracy.

6.2 Construction of Mathematical Model

The mathematical model for the front panel of the female body armour can be constructed by combining two components: the part without the bust-cup area and the

bust-cup part. The former is also known as the block projection, on which bust-cups of with different sizes are located. The modelling of the block projection and the shape of the bust area are described as follows.

6.2.1 Block projection

The block projection can be created on the basis of the classic coat block, which is suitable for close fitting coats and easy fitting over garments [146] The method for making the front block is used to generate the front panel block projection of the female body armour. The dart area is omitted as this block is meant to be the projection of the front panel. The area from the waistline to the hipline is also omitted because it is not necessary for the body armour vest to cover this area. Figure 6.2 shows how the projection block is created from the classic coat block. A half block is considered in pattern-making because of the pattern symmetry.

The Classic Coat Blocks

For close fitting coats and easy fitting overgarments.

MEASUREMENTS REQUIRED TO DRAFT THE BLOCK (example size 12)
Refer to the size chart (page 11) for standard measurements.

bust	88 cm	shoulder	12.25 cm
nape to waist	41 cm	back width	34.4 cm
waist to hip	20.6 cm	dart	7 cm
armscye depth	21 cm	chest	32.4 cm
neck size	37 cm	front shoulder to waist	41 cm

Important Note The easy fitting block has a reduced dart for less bust shaping. Reduce the standard dart measurement by half. The instructions for the easy fitting block are shown in brackets.

Square down from 0; square halfway across the block.
0–1 2 cm.
1–2 armscye depth plus 4 cm (6 cm); square across.
2–3 half bust plus 10 cm (15 cm) [i.e. for 88 cm bust; (88 ÷ 2) + 10 = 54 cm]. Square up and down, mark this line the centre front line.
3–4 = 0–2 (add 0.3 cm for each size 16, 18 and 20: add a further 0.8 cm for each of the remaining larger sizes.) Example for size 20, 3–4 = 0–2 plus 0.9 cm.
1–5 nape to waist measurement plus 0.5 cm; square across to 6.
5–7 waist to hip measurement; square across to 8.

Back
0–9 one fifth neck size plus 0.4 cm (0.8 cm); draw in back neck curve 1–9.
2–10 half the measurement 1–2; square out.
1–11 quarter armscye depth measurement; square out.
2–12 half back width plus 1.5 cm (4 cm); square up to 13 and 14.
14–15 2 cm; square out.
9–16 shoulder measurement plus 2 cm (3.5 cm).
These measurements include shoulder ease of 0.5 cm.

Front
4–17 one fifth neck size plus 0.2 cm (0.6 cm).
4–18 one fifth neck size plus 0.3 cm; draw in front neck curve 17–18.
17–19 dart measurement (half dart measurement). Joint point 19 to point 14.
19–20 the measurement 9–16 minus 1 cm.
20–21 1.5 cm (1 cm); join 19–21 with a slight curve.
3–22 half chest plus half the measurement 17–19 plus 1 cm (4 cm). Square up.
22–23 one third the measurement 3–18.
22–24 half the measurement 3–22 (square up 3 cm to mark bust point). Join 17–24 and 19–24 to form dart.
22–25 half the measurement 12–22; square down to 26 and 27.
Draw armscye as shown in diagram touching points 16, 13, 25, 23, 21; measurement of the curves:

		from 12	from 22
sizes	8–14	2.75 cm (3.25 cm)	2.25 cm (2.75 cm)
sizes	16–20	3.25 cm (3.75 cm)	2.75 cm (3.25 cm)
sizes	22–26	3.75 cm (4.35 cm)	3.25 cm (3.75 cm)

Note For simple shapes (i.e. kimono block) for mass production, equalize the side seam by making:
2–25 half the measurement 2–3; square down to point 26 on the waistline and 27 on the hipline.

Sleeve Draft the one-piece sleeve (page 22) or a two-piece sleeve (page 24) to fit armscye.

(a)

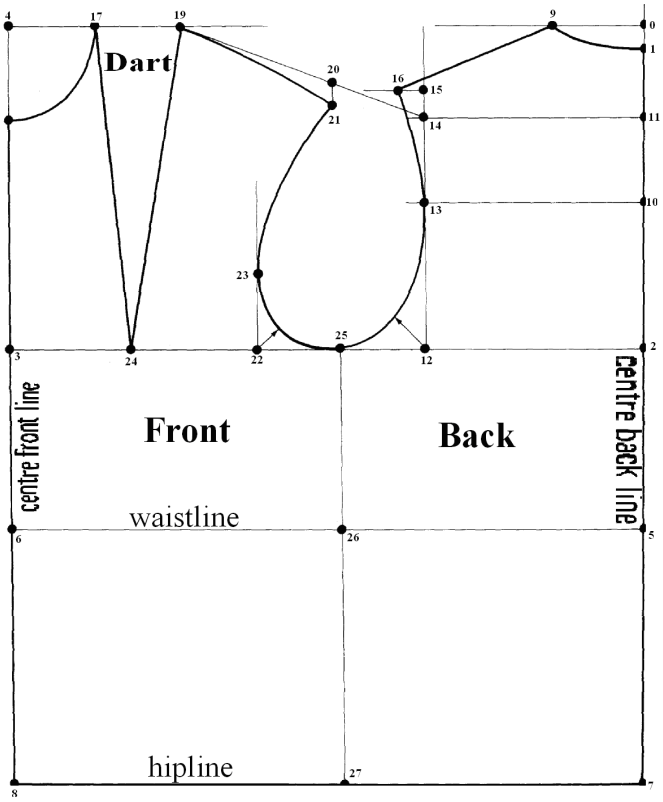

(b)

Omitting

- **The dart area**
- **The back area**
- **The area from the waistline to the hipline**

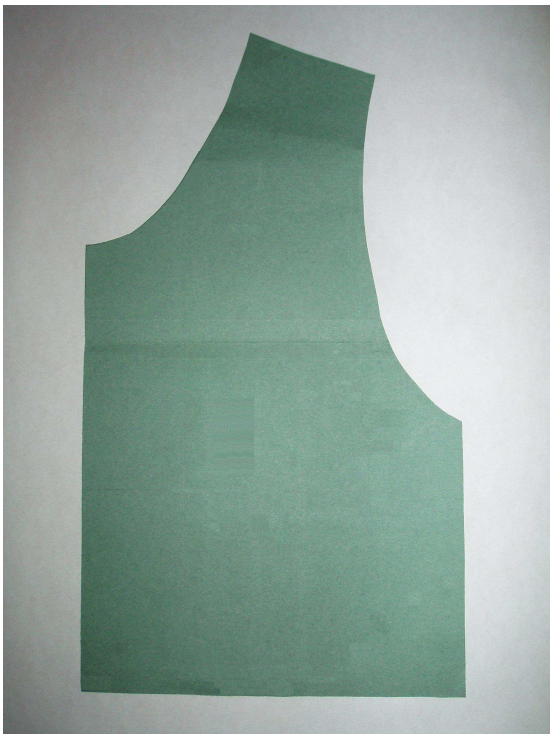

(c)

Figure 6.2 Block projection making: (a) procedure of making classic coat block [146]; (b) classic coat block design; (c) block projection

The block projection described above is based on size 12, and is treated as the base type in this work. Block projections of other sizes can be obtained by grading. Pattern grading is about identifying the coordinates of specific points on the pattern for a different size, which can be either larger or smaller. These points are moved following X and Y coordinates which tell the computer the direction of movement; measurements are given to identify the position of the new point. This coordinate movement is known as a grade rule. Grading rules are usually calculated to one-tenth of a millimetre. The amount of movement in the X direction is written first, followed by the Y direction, illustrated in Figure 6.3 [146].

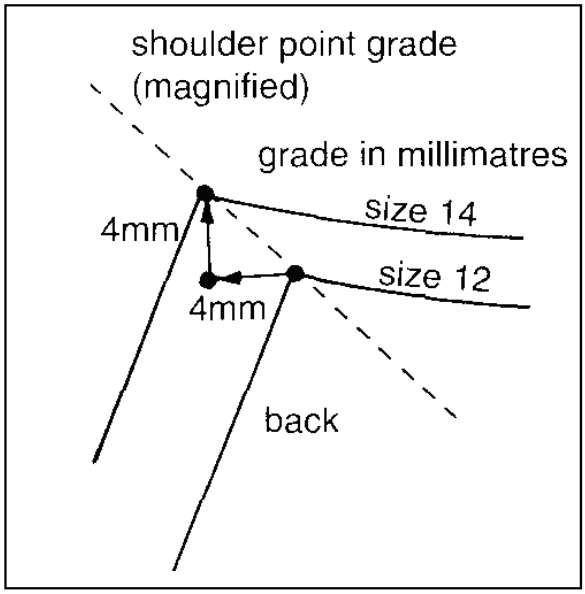

Figure 6.3 Grading method [146]

There are many grading rules to calculate the new position of specific points, but the basic principles are similar. In this situation, a series of key points are chosen to sketch the projection block for size 12. The coordinate origin is at the intersection of the bust line (X) and the central front line (Y), and this is shown in Figure 6.4(a). Figure 6.4(b) illustrates the graded projection blocks using the PAD software system (PAD Systems International Ltd, Hong Kong, China). The key points and their corresponding

coordinates for the pattern projection of size 12 are listed in Table 6.1. Table 6.2 shows the grading rules in order to achieve pattern projections of other sizes. It should be noticed that the increments among sizes are different determined by different regions. Therefore, the calculations after grading also varied. Different body measurements are used by UK and other European countries; their results after grading have been illustrated respectively in this context.

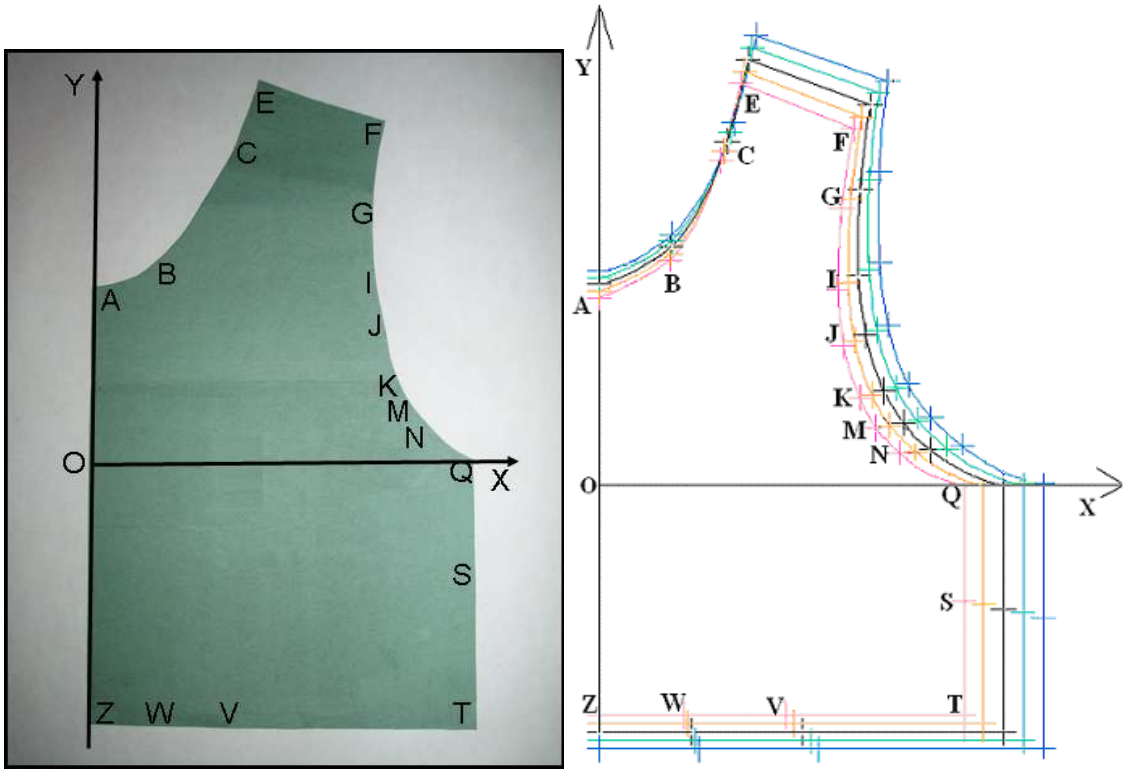

(a) **(b)**

Figure 6.4 Block projection: (a) marking key points; (b) grading

Table 6.1 Block projection: key points' position

Block Projection for Size 12		
Key Points	**Position**	
	X	**Y**
A	0	10.3
B	4.5	12.6
C	7.9	19.0
E	9.4	23.8
F	17.1	21.2

G	16.3	16.2
I	16.3	11.3
J	16.9	7.7
K	17.9	4.2
M	19.2	2.2
N	21.0	0.5
Q	21.75	0.0
S	21.75	-8.3
T	21.75	-15.8
V	12.8	-15.8
W	5.8	-15.8
Z	0	-15.8

Table 6.2 Block projection: coordinate movement (a) for UK sizing; (b) for European sizing
(a)

Key Points	Figure Size	Coordinate Change		Key Points	Figure Size	Coordinate Change	
		X	Y			X	Y
	8	0.00	-0.40		8	-0.03	-0.37
	10	0.00	-0.40		10	-0.03	-0.37
A	12	0.00	0.00	**B**	12	0.00	0.00
	14	0.00	0.40		14	0.03	0.37
	16	0.00	0.40		16	0.03	0.37
	8	-0.20	-0.56		8	-0.24	-0.70
	10	-0.20	-0.56		10	-0.24	-0.70
C	12	0.00	0.00	**E**	12	0.00	0.00
	14	0.20	0.56		14	0.24	0.70
	16	0.20	0.56		16	0.24	0.70
	8	-0.54	-0.70		8	-0.60	-0.55
	10	-0.54	-0.70		10	-0.60	-0.55
F	12	0.00	0.00	**G**	12	0.00	0.00
	14	0.54	0.70		14	0.60	0.55
	16	0.54	0.70		16	0.60	0.55
	8	-0.66	-0.41		8	-0.71	-0.30
	10	-0.66	-0.41		10	-0.71	-0.30
I	12	0.00	0.00	**J**	12	0.00	0.00
	14	0.66	0.41		14	0.71	0.30
	16	0.66	0.41		16	0.71	0.30
	8	-0.75	-0.20		8	-0.87	-0.15
	10	-0.75	-0.20		10	-0.87	-0.15
K	12	0.00	0.00	**M**	12	0.00	0.00
	14	0.75	0.20		14	0.87	0.15
	16	0.75	0.20		16	0.87	0.15
	8	-0.99	-0.11		8	-1.25	0.00
N	10	-0.99	-0.11	**Q**	10	-1.25	0.00
	12	0.00	0.00		12	0.00	0.00
	14	0.99	0.11		14	1.25	0.00

	16	0.99	0.11		16	1.25	0.00
S	8	-1.25	0.25	**T**	8	-1.25	0.50
	10	-1.25	0.25		10	-1.25	0.50
	12	0.00	0.00		12	0.00	0.00
	14	1.25	-0.25		14	1.25	-0.50
	16	1.25	-0.25		16	1.25	-0.50
V	8	-0.54	0.50	**W**	8	-0.24	0.50
	10	-0.54	0.50		10	-0.24	0.50
	12	0.00	0.00		12	0.00	0.00
	14	0.54	-0.50		14	0.24	-0.50
	16	0.54	-0.50		16	0.24	-0.50
Z	8	0.00	0.50				
	10	0.00	0.50				
	12	0.00	0.00				
	14	0.00	-0.50				
	16	0.00	-0.50				

(b)

Key Points	Figure Size	Coordinate Change		Key Points	Figure Size	Coordinate Change	
		X	Y			X	Y
A	8	0.00	-0.20	**B**	8	-0.10	-0.35
	10	0.00	-0.20		10	-0.10	-0.35
	12	0.00	0.00		12	0.00	0.00
	14	0.00	0.20		14	0.10	0.35
	16	0.00	0.20		16	0.10	0.35
C	8	-0.16	-0.44	**E**	8	-0.20	-0.50
	10	-0.16	-0.44		10	-0.20	-0.50
	12	0.00	0.00		12	0.00	0.00
	14	0.16	0.44		14	0.20	0.50
	16	0.16	0.44		16	0.20	0.50
F	8	-0.45	-0.50	**G**	8	-0.49	-0.41
	10	-0.45	-0.50		10	-0.49	-0.41
	12	0.00	0.00		12	0.00	0.00
	14	0.45	0.50		14	0.49	0.41
	16	0.45	0.50		16	0.49	0.41
I	8	-0.54	-0.32	**J**	8	-0.57	-0.26
	10	-0.54	-0.32		10	-0.57	-0.26
	12	0.00	0.00		12	0.00	0.00
	14	0.54	0.32		14	0.57	0.26
	16	0.54	0.32		16	0.57	0.26
K	8	-0.60	-0.20	**M**	8	-0.69	-0.15
	10	-0.60	-0.20		10	-0.69	-0.15
	12	0.00	0.00		12	0.00	0.00
	14	0.60	0.20		14	0.69	0.15
	16	0.60	0.20		16	0.69	0.15
N	8	-0.79	-0.11	**Q**	8	-1.00	0.00
	10	-0.79	-0.11		10	-1.00	0.00

	12	0.00	0.00		12	0.00	0.00
	14	0.79	0.11		14	1.00	0.00
	16	0.79	0.11		16	1.00	0.00
S	8	-1.00	0.25	**T**	8	-1.00	0.50
	10	-1.00	0.25		10	-1.00	0.50
	12	0.00	0.00		12	0.00	0.00
	14	1.00	-0.25		14	1.00	-0.50
	16	1.00	-0.25		16	1.00	-0.50
V	8	-0.50	0.50	**W**	8	-0.12	0.50
	10	-0.50	0.50		10	-0.12	0.50
	12	0.00	0.00		12	0.00	0.00
	14	0.50	-0.50		14	0.12	-0.50
	16	0.50	-0.50		16	0.12	-0.50
Z	8	0.00	0.50				
	10	0.00	0.50				
	12	0.00	0.00				
	14	0.00	-0.50				
	16	0.00	-0.50				

6.2.2 Block for the bust area

After making the block projection, the bust area for female body armour is geometrically modelled with the assistance of the Rhinoceros software (McNeel, Seattle, USA). Three models have been considered, which are explained below.

6.2.2.1 Model One

The two-dome-shaped model for the bust area is illustrated in Figure 6.5, with (a) showing the physical shape and (b) the flattened pattern shape. In this model, the flattening of the domes is carried out under the assumption that the material for the domes is spread out in the radial directions. It is obvious that this model is not feasible because of the strange shape. In addition, the formation of the two domes would create potential problems in pattern making, this being illustrated in Figure 6.5 (b) showing where there is a need for excessive amount of fabric between the two domes.

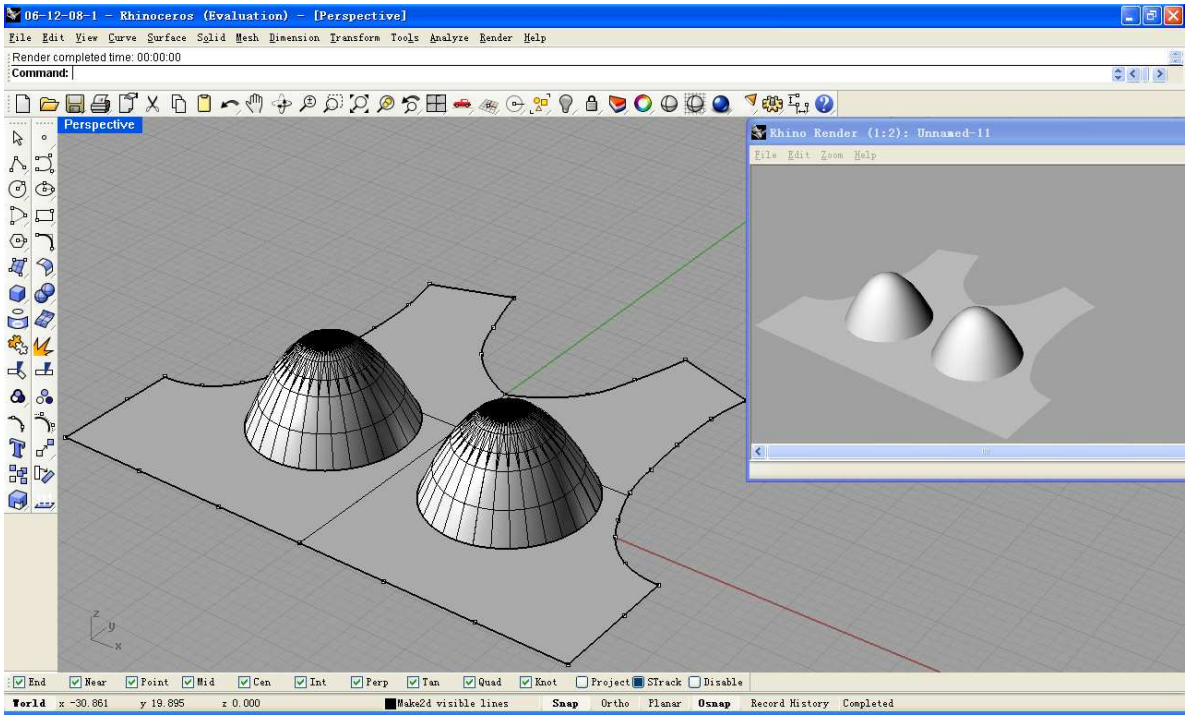

(a)

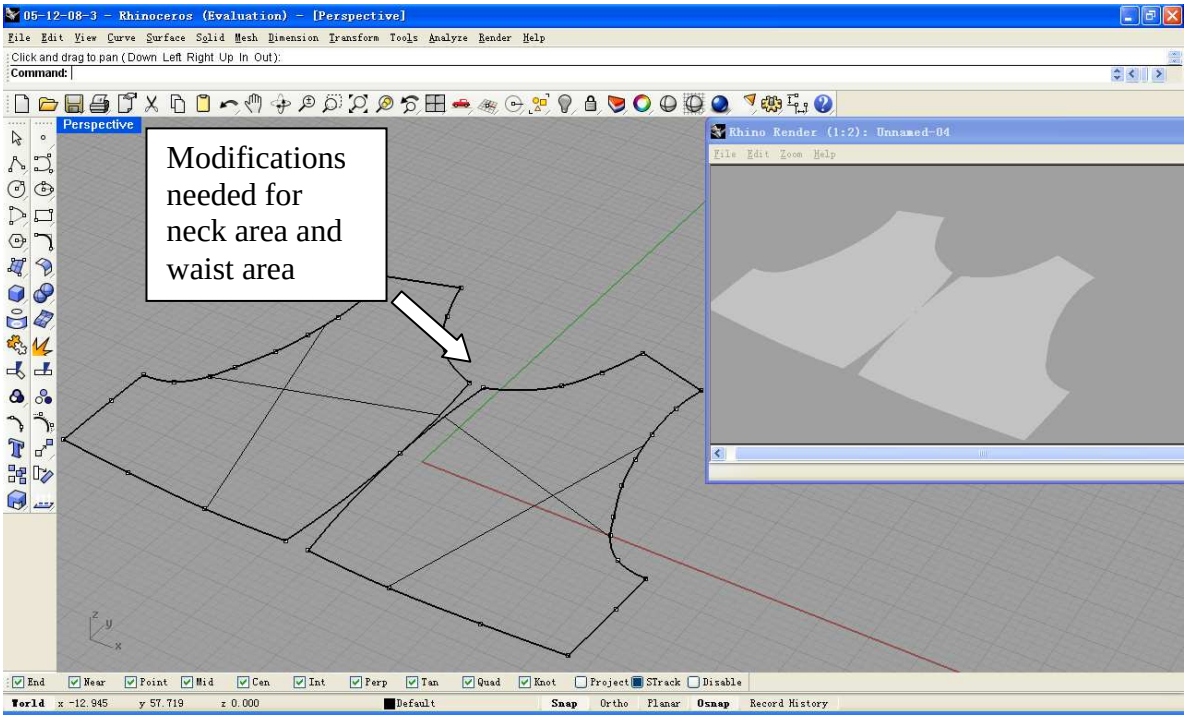

(b)

Figure 6.5 Model One: (a) 3D shape: (b) shape after pressed

6.2.2.2 Model Two

To address the extra fabric requirement issue, the bust area is considered as an entirety, created by linking the two domes in the second model, which is shown in Figure 6.6. However, it is easy to see that the problem for this model is that it over-simplifies the bust surface. The surface of the top half for the linked-dome has been proven to be too steep to be practical for real body armour. In this model, the flattening is also assumed to be done by distributing the raised portion of materials in the radial directions. Figure 6.6 (c) shows the inaccuracy in the marked region *ABCD*, where excessive material is included because of the way of calculation.

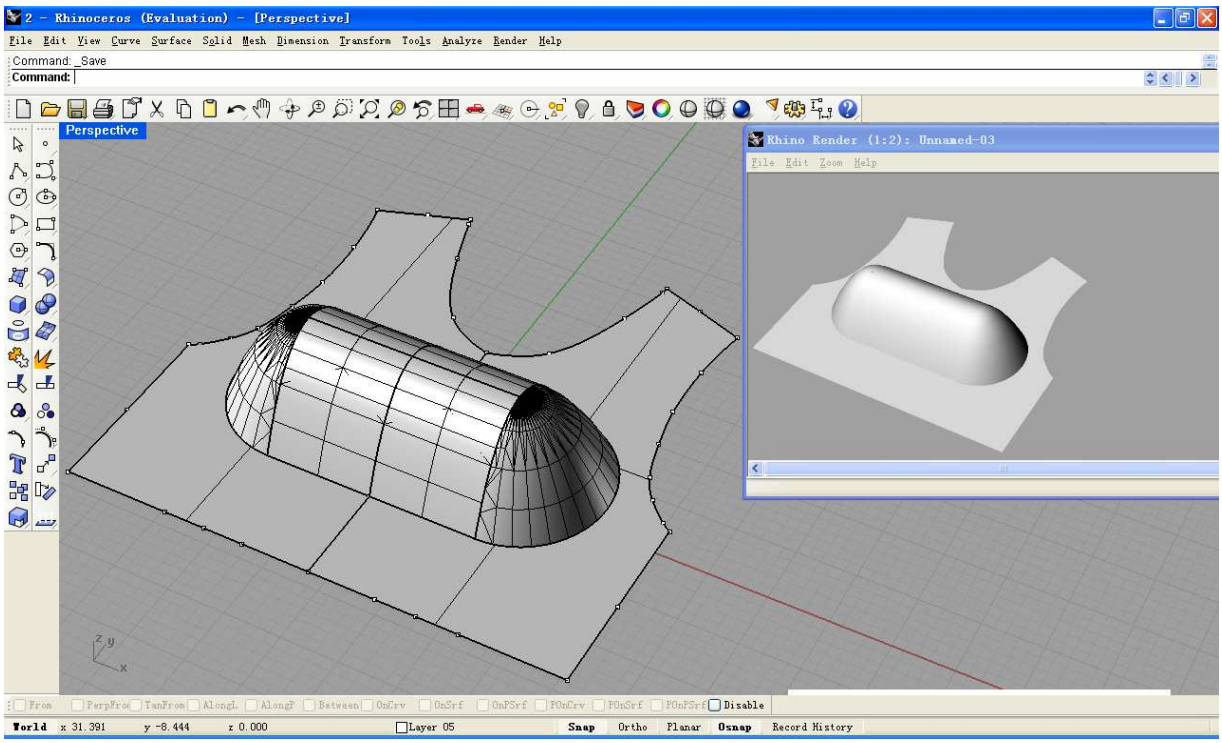

(a)

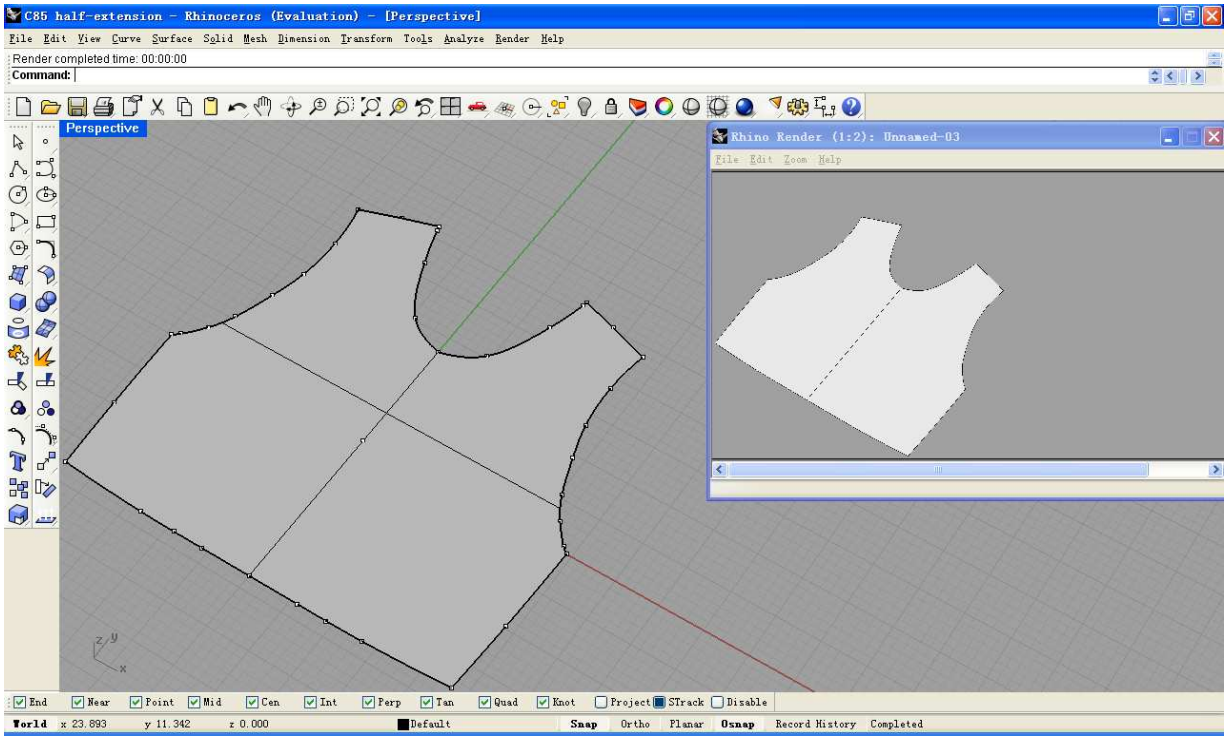

(b)

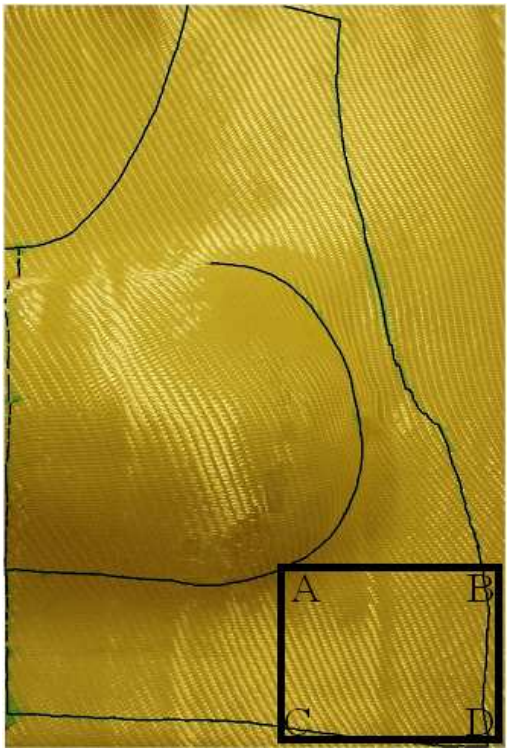

(c)

Figure 6.6 Model Two: (a) 3D shape; (b) shape after pressed; (c) practical effect

6.2.2.3 Model Three

To overcome the drawbacks of the previous models, a simple but more realistic model for the front panel for female body armour has been established based on the observation of the mannequin. Observing the mannequin from the side view, the upper half of bust area can be roughly represented using a triangular prism which is joined with lower half of the bust area. The angle between the slope of the breast and the vertical line going through the body is approximately 33° based on measurement, as shown in Figure 6.7. Based on observation and measurement, the bust area is divided into 7 portions in the establishment of the geometrical model, which are

- a triangular prism representing the upper half of the bust area;
- a quarter of cylinder for the lower half of the bust area;
- two one-eighths of a sphere at ends of quarter of cylinder;
- two quarters of a cone surface at the ends of the triangular prism; and
- the flat area that makes up the rest of the front panel.

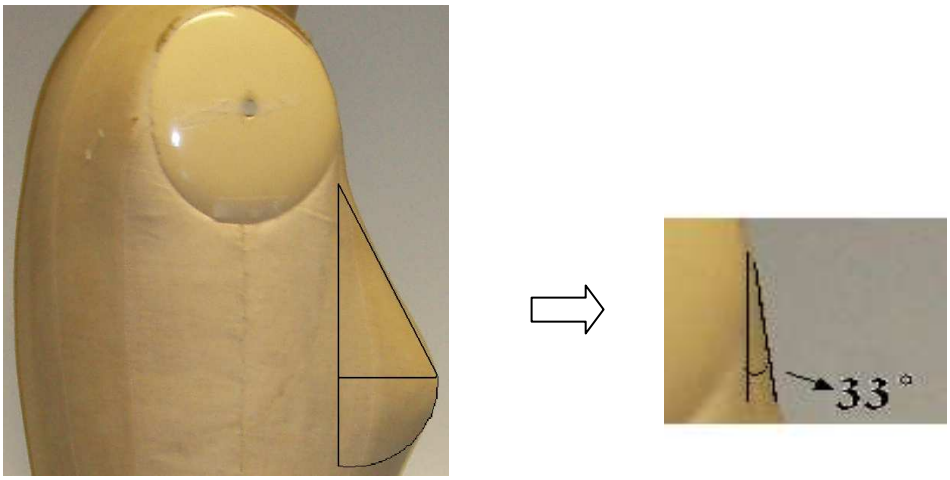

Figure 6.7 Bust measurement

As observed from the experiments, it was found that the dome forming of the angle-interlock fabrics comes mainly from the contribution of fabric in the warp and weft

directions, whereas the contribution from the other directions is not significant, and this has been indicated in Figure 6.6 (c).

This can be explained from the fact that the angle-interlock structures consist of layers of straight weft yarns and a single set of warp yarns which locks the layers of weft yarns together. The cross-over points in the fabric are only between the warp yarns and the top and the bottom layers of weft yarn, leading to low friction against fabric shear which is an important element in fabric draping and moulding. In addition, the limited interlacement density in the angle-interlock fabric creates more room than other 3D woven fabrics for the yarns which allows the fabric to be sheared to a greater extent. Together, these lead to low shear modulus of the angle-interlock fabrics. It has been proven that the smaller the shear modulus, the more mouldable the fabric [104]. The formation of double curvature would require a larger area of fabric to form the surface. As has shown earlier, such extra fabric area will be provided mainly in the warp and weft direction, and the fabric region between the warp and weft direction will be sheared to suit the dimension change. In comparison to the fabric area requirement in the warp and weft direction, that in the oblique direction is much smaller, and this can be seen from the observation. Therefore, in model three, only the fabric area contribution will be considered during the formation of double curvature in the warp and the weft directions, ignoring the contribution from the oblique direction. According to this assumption, the pattern block will only extend in the warp and weft and weft directions during the flattening process. Figure 6.8 is the illustration of this model showing the shape of the bust area. The determination of the flattened shape is explained in the next section.

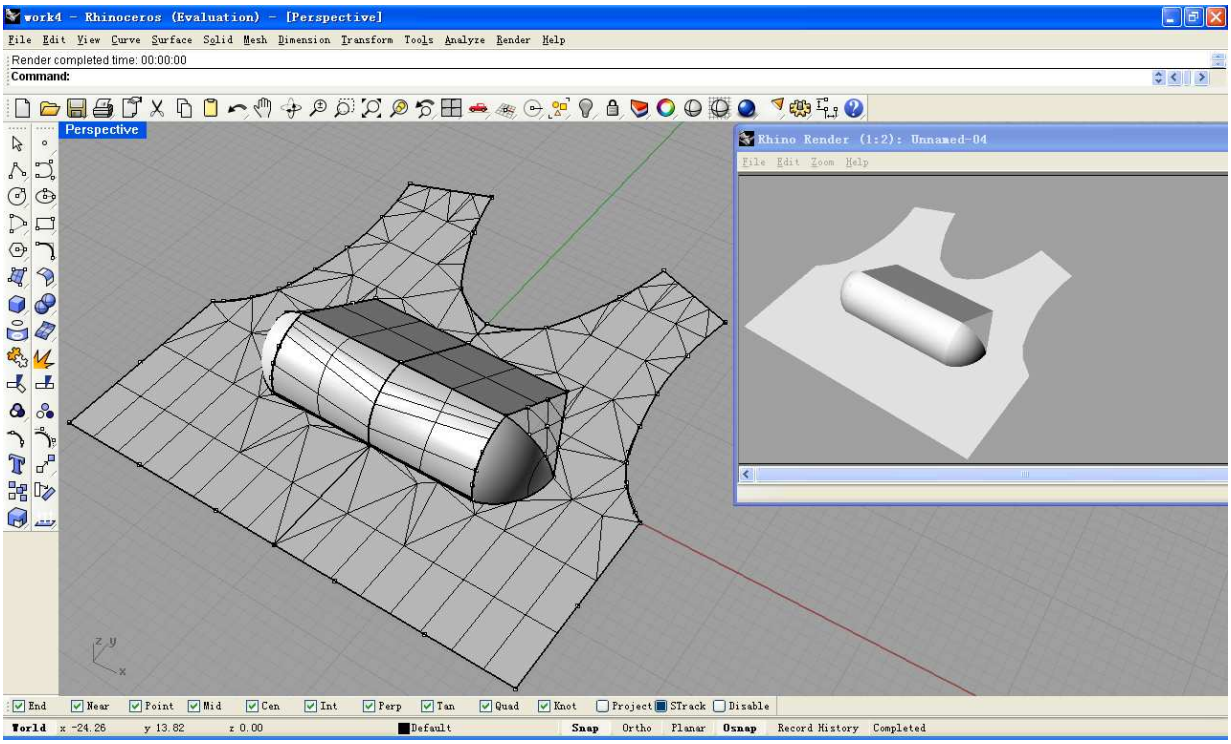

(a)

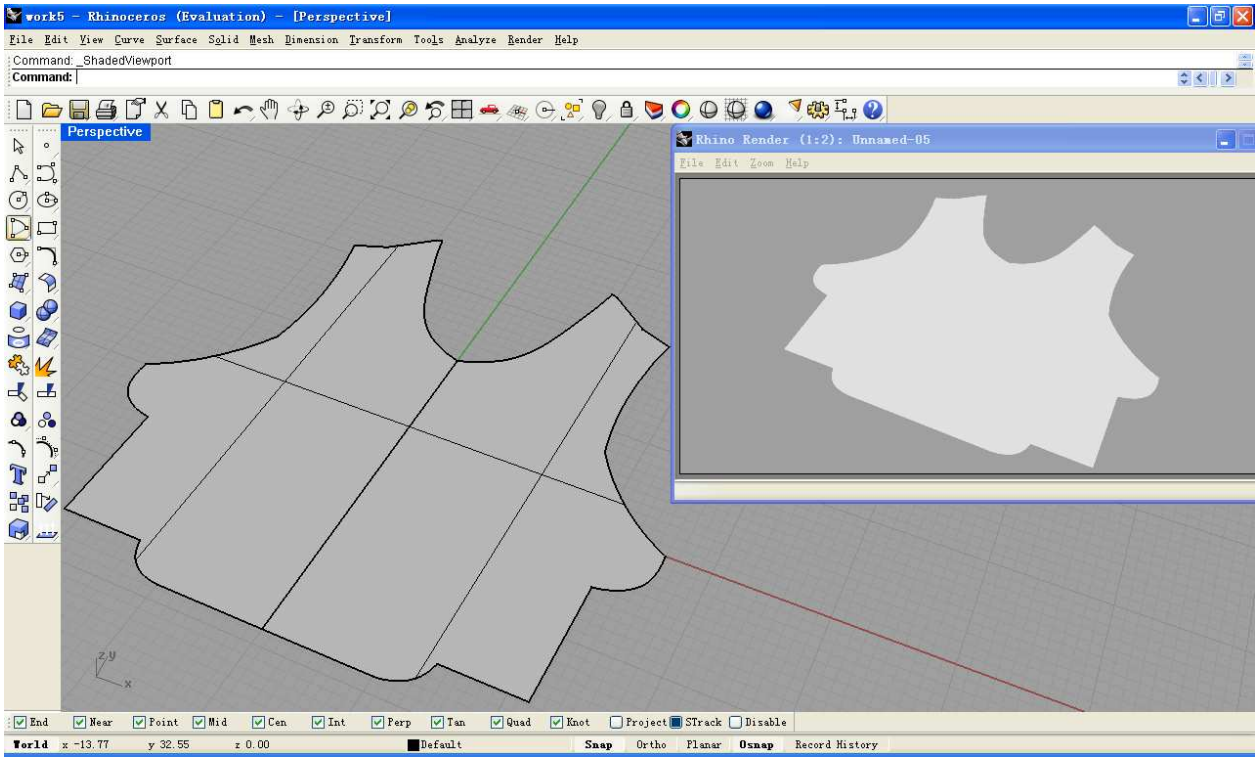

(b)

Figure 6.8 Model Three: (a) 3D shape; (b) shape after pressed

6.3 Establishment of a Mathematical Model for Pattern Generation

The mathematical model of half of the front panel of female body armour for size 12 based on a standard mannequin is to be created in order to generate the front pattern shape. The solid lines in Figure 6.9 sketch the projection block, called Block BB (block before flattening), and the dashed lines sketch the block after Block BB is flattened, named as Block BA (block after flattening). In Figure 6.9, U_2 is the point where the tip of the nipple is located, and U_1 is its projection on the pattern plane. U_1U_2 is the height of the breast, whose value is H. In this model which represents a half of the front panel, the bust area is described geometrically by four simple shapes joining together. These are (i) a triangular prism for the upper half of the bust area, (ii) a quarter of cylinder for the lower half of the bust area, (iii) a one-eighth spherical segment at the end, and (iv) a connection area between the triangular prism and the spherical end. Crossing at point U_1, line $U_3"U_4"$ and the X-axis divide the bust area into these four parts. These four parts shared the same height H that is equal to the height of the breast, $\frac{2L}{\pi}$.

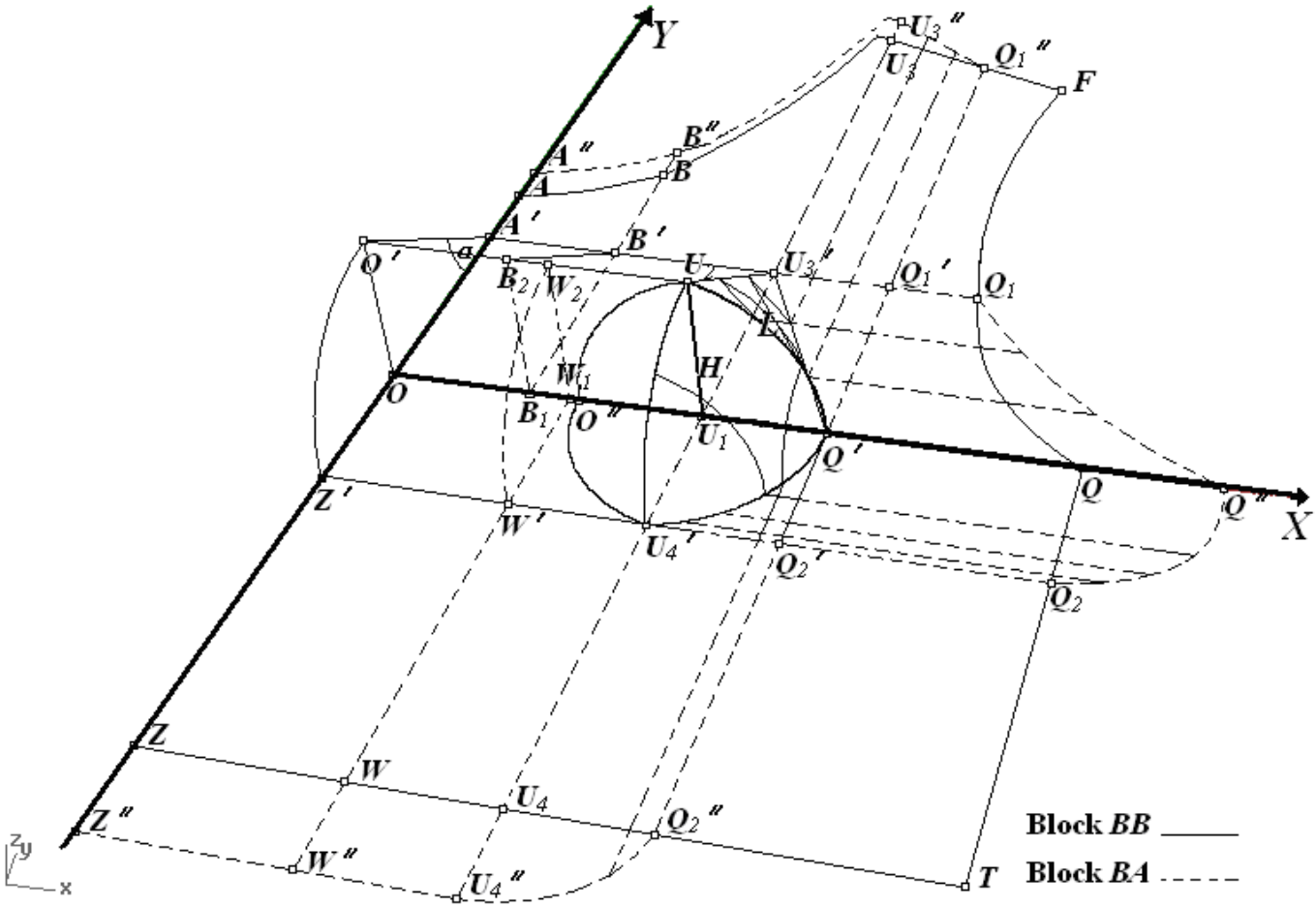

Figure 6.9 Mathematical model of half front panel of female body armour

6.3.1 Geometric data for breast

Before calculation, an important factor worth noting is that the breast has irregular shape. The curve lengths between the nipple and root of the breast in various directions are different [147]. As shown in the Figure 6.10 the curve lengths between the nipple point and the root points at the central, bottom and side positions are named as *arcDB*, *arcDC* and *arcDS*， and it is clear that $arcDS > arcDC > arcDB$.

To simplify the model in this situation without affect the accuracy too much, the breast is assumed to be a partial spherical surface, and the arc lengths from the nipple to the

root plane in different directions are the same. Under this assumption, the length of *arcDC* will be used as the curve length since it is the medium value among *arcDB*, *arcDC* and *arcDS*. *L* is used to represent this length in this context.

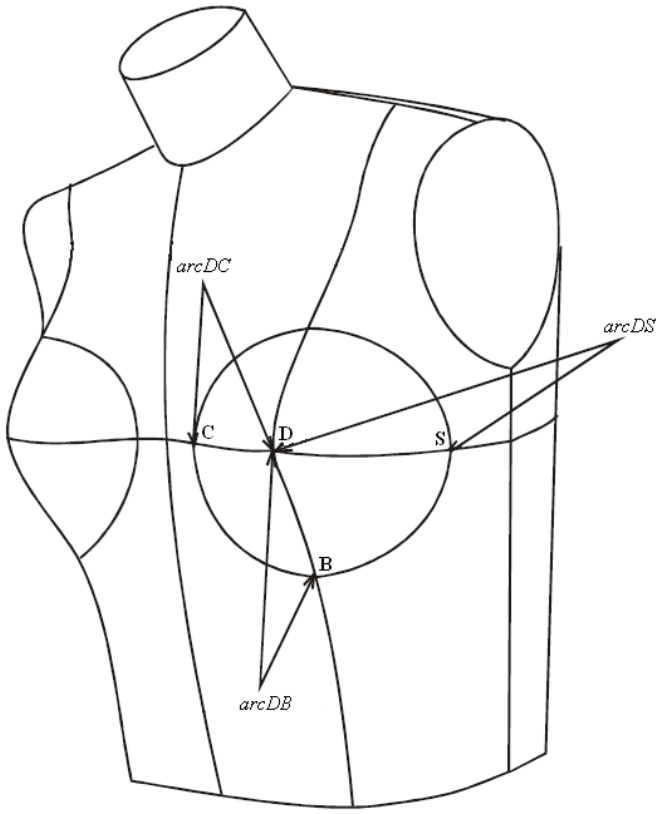

Position	Band Size / Cup Size	70 (cm)	75 (cm)	80 (cm)	85 (cm)	Increment (cm)
arcDB	A	6.5	6.9	7.3	7.7	0.4
	B	6.9	7.4	7.9	8.4	0.5
	C	7.3	7.9	8.5	9.1	0.6
arcDC	A	7.1	7.6	8.1	8.6	0.5
	B	7.5	8.1	8.7	9.3	0.6
	C	7.9	8.6	9.3	10	0.7
arcDS	A	7.5	8	8.5	9	0.5
	B	7.9	8.5	9.1	9.7	0.6
	C	8.3	9	9.7	10.4	0.7

Figure 6.10 Geometric data for breast [147]

6.3.2 Mathematical equations

In Figure 6.9, the dashed lines and curves form the block shape, block BA, when the bust area is flattened. Block BA is obtained by extending Block BB (block before flattening) according to the calculated shifts of the key points. The equations to demonstrate the corresponding relationships between the original coordinates (X_{OP}, Y_{OP}, Z_{OP}) of the key points on the edge of the pattern and the corresponding after-flattening coordinates (X_{FP}, Y_{FP}, Z_{FP}) of these points will be described as follows. In this model, the raised parts above the curve *O'U*$_2$*Q'* will contribute upwards, and the parts below that will contribute downwards.

6.3.2.1 Portion 1 triangular prism representing the upper half of the bust area

In this portion, the triangular prism segment would influence on the key points on the top edge of the pattern by enlarging their coordinate values in the Y-axis direction and no change will be made in the X-axis direction as this triangular prism segment only influences the length of the block when pressed. The relationship between the triangular prism and the pattern shape is shown in Figure 6.11. For example, B'' represents the after-flattening coordinate of the key point B. The line B_1B'' is parallel to Y-axis and intersecting X-axis at the point B_1. The line B_1B_2 is parallel to H, the height of the bust. The value of B'' is achieved by extending the length of the line B_1B on which the segment B_1B' is replaced by B_2B' when the block is pressed to be flat.

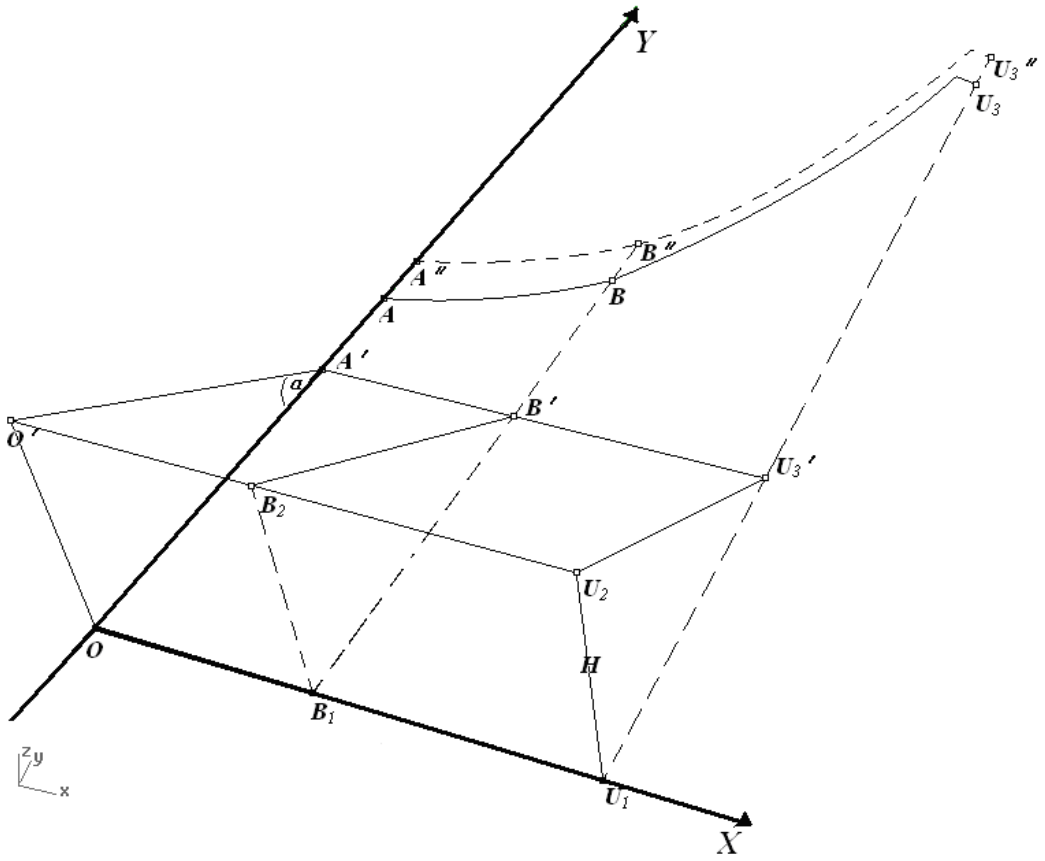

Figure 6.11 Triangular prism segment

Annotating B and B'' as $(X_{B,}Y_B,0)$ and $(X_B'',Y_B'',0)$ respectively, it could be easily achieved that $X_B''=X_B$ and $Y_B''=Y_B-B_1B'+B_2B'$. Additionally, B_1B' equals to OA', and B_2B' equals to $O'A'$ as in $\Delta O'OA'$, $\frac{O'O}{OA'}=\tan\angle\alpha$ and $\frac{O'O}{O'A'}=\sin\angle\alpha$, where $O'O=H$. Y_B'' could be expressed as $Y_B''=Y_B-\frac{H}{\tan\alpha}+\frac{H}{\sin\alpha}$.

Therefore, for an arbitrary point on the top edge of the pattern, coordinate change will only happen in the *Y*-direction and could be expressed as below:

$$\begin{cases} X_{FP}=X_{OP} \\ Y_{FP}=Y_{OP}-\frac{H}{\tan\alpha}+\frac{H}{\sin\alpha} \\ Z_{FP}=Z_{GP} \end{cases} \tag{6.1}$$

where in this case, $H = \frac{2L}{\pi}, \alpha = 33°$. The value of α is the value for angle $<B_1B'B_2$ and is measured from the female mannequin, as shown in Figure 6.7.

6.3.2.2 Portion 2 cone surface at the end of the triangular prism

The bisection method is applied to the connection area between the triangular prism segment and the spherical segment. The bisection method is defined as a root-finding algorithm which repeatedly divides an interval in half and then selects the subinterval in which a root exists [148]. The flattening of this surface (represented by the triangular mesh in Figure 6.12) will cause dimension change in the pattern in both *X* and Y directions.

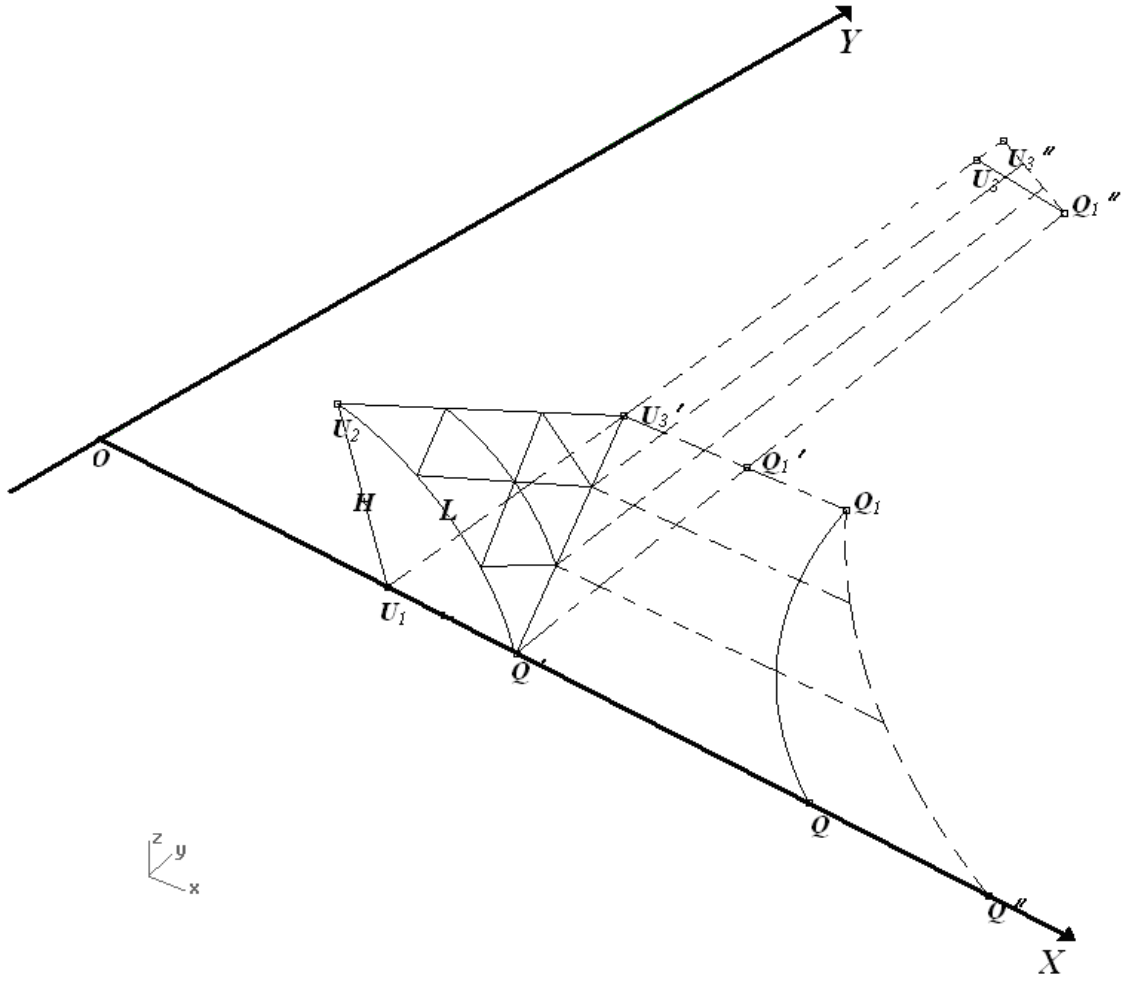

Figure 6.12 Cone surface segment

In Figure 6.12, $U_3'Q'$ and $U_3'U_2$ are divided into three equal segments respectively. Therefore, the curves on the mash in X direction are supposed to reduce proportionally from $arcU_2Q'$ to the point U_3', namely their length are $arcU_2Q'$, $\frac{2}{3}arcU_2Q'$ and $\frac{1}{3}arcU_2Q'$. Therefore, in order to get after-flattening points, the original key points need to move along X direction with the distances $(arcU_2Q'–U_1Q')$, $\frac{2}{3}(arcU_2Q'–U_1Q')$ and $\frac{1}{3}(arcU_2Q'–U_1Q')$ respectively. Because $sectorU_1U_2Q'$ is known as the cross-section of the breast which is assumed as 1/8 sphere, it is easy to get the formula $U_1Q' = U_1U_2 = \frac{2}{\pi}arcU_2Q'$. Additionally, knowing $arcU_2Q' = L$ and $U_1Q' = H$ where L and H are defined as the curve length and the height of the breast respectively, the above-mentioned distances could be represented as $(L - \frac{2}{\pi}L)$, $\frac{2}{3}(L - \frac{2}{\pi}L)$ and $\frac{1}{3}(L - \frac{2}{\pi}L)$ respectively.

The similar method is applied to get after-flattening coordinates in Y direction. Generally speaking, when flattening, the influence of points on the edge of the pattern in the X direction will be：

$$\begin{cases} X_{FP} = X_{OP} + n(L - \frac{2}{\pi}L) \\ Y_{FP} = Y_{OP} \\ Z_{FP} = Z_{OP} \end{cases} \tag{6.2}$$

and in the *Y* direction the influence will be：

$$\begin{cases} X_{GP} = X_{OP} \\ Y_{GP} = Y_{OP} + n(\dfrac{2L}{\pi \sin\alpha} - \dfrac{2L}{\pi \tan\alpha}) \\ Z_{GP} = Z_{OP} \end{cases} \tag{6.3}$$

where *n* takes value of 1, 2/3 or 1/3 as the surface is divided in 3 sections in both *X* and *Y* directions. Obviously, more precise result could be achieved theoretically when more intervals are used, but for pattern making the 3-section division give sufficient accuracy. In equation (6.2) and (6.3), *L* is the arc length from the nipple to the bust root which in this model has been assumed to be equal from the nipple to any other point on the bust root.

6.3.2.3 Portion 3 One-eighth spherical segment

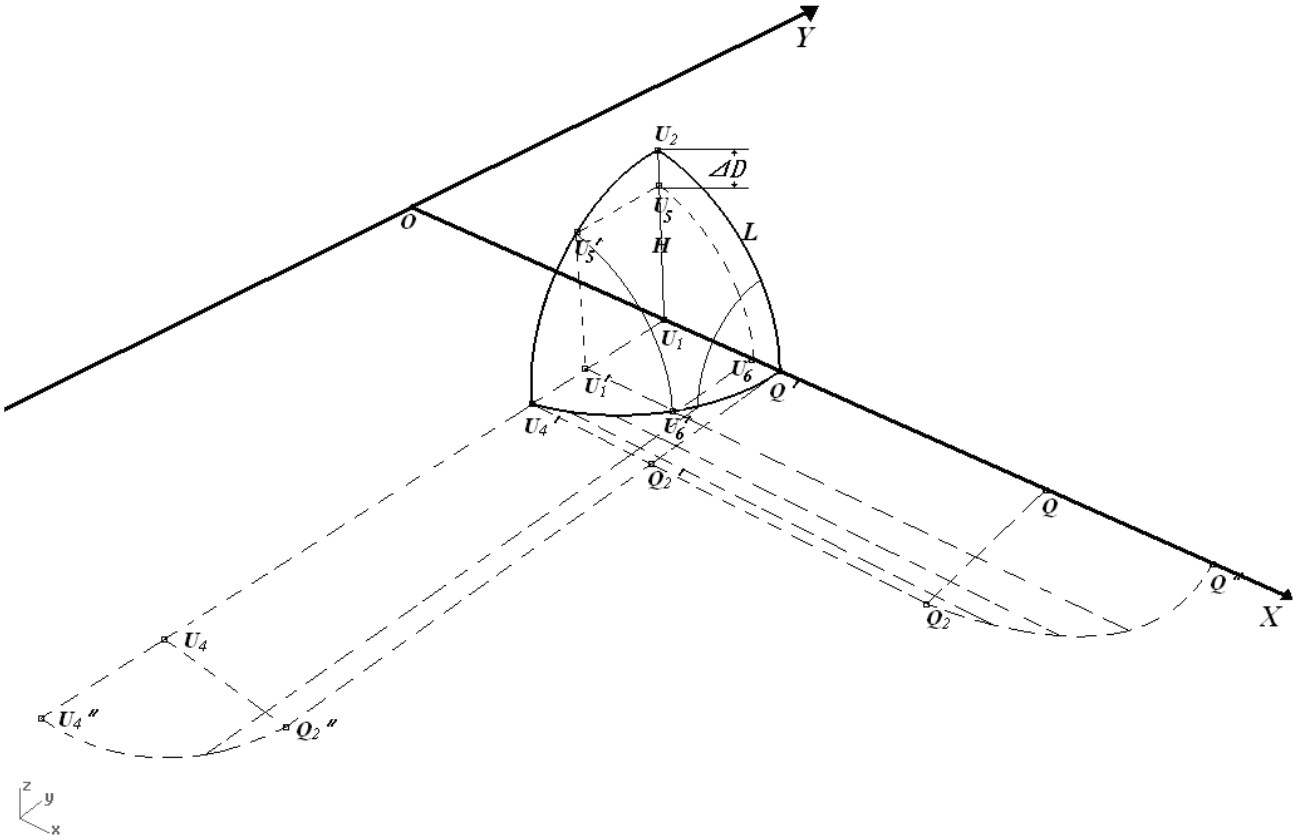

Figure 6.13 Spherical segment

Flattening of this portion of the bust area would also affect the edges in both *X* and *Y* directions. Step length is made along the height of the spherical segment, annotated as ΔD. Among each step length, small curves duplicating the curve of breast could form both in plane U_2U_1Q' and $U_2U_1U_4'$. The surface of the spherical segment could be treated as the result of extracting these curves from the planes.

Using $arcU_5U_6$ in the plane U_2U_1Q' as an example to illustrate the influence of the flattening in *X* direction, it can be easily calculated that $arcU_5U_6 = \frac{1}{2}\pi(H - \Delta D)$ as $\mathrm{sec}torU_5U_1U_6 \cong \mathrm{sec}torU_2U_1Q'$ in which $\mathrm{sec}torU_2U_1Q'$ is considered as a cross-section

of 1/8 sphere. Therefore, the corresponding extraction $arcU_5'U_6' = \frac{1}{2}\pi(H - \Delta D)$. When flattening the block, $arcU_5'U_6'$ would replace its projection line $U_1'U_6'$ and its subtraction indicates the extent of the flattening in *X* direction., i.e., the *X* value of original coordinates of the key points needs to enlarge in order to achieve the corresponding after-flattening coordinates.

The influence of flattening in *X* direction could be represented by the following equation:

$$\begin{cases} X_{FP} = X_{OP} + (H - \Delta D)(\frac{1}{2}\pi - 1) \\ Y_{FP} = Y_{OP} \\ Z_{FP} = Z_{OP} \end{cases} \quad (6.4)$$

where $H = \frac{2L}{\pi}$ and ΔD is the step length from the centre of the sphere along the height.

Similar method would be applied for investigating the influence of flattening in *Y* direction. The equation could be represented as follows:

$$\begin{cases} X_{FP} = X_{OP} \\ Y_{FP} = Y_{OP} + (H - \Delta D)(\frac{1}{2}\pi - 1) \\ Z_{FP} = Z_{OP} \end{cases} \quad (6.5)$$

where $H = \frac{2L}{\pi}$ and ΔD is the step length from the centre of the sphere along the height.

6.3.2.4 Portion 4 a quarter of cylinder for the lower half of the bust area

When flattening this portion of the bust area, changes of the pattern edge will only be caused in of the pattern edge in *Y* direction. Because this portion represents the lower breast, it is such arranged that the points on the lower edge of the pattern move downwards during flattening. The positive direction of *Y* axis is upwards; therefore the 'growth' of the lower edge of the pattern is a negative one, which in this case is $L - H$. Equation (6.6) represents the relationship between the original and the after-flattening coordinated of points on the lower edge of the pattern.

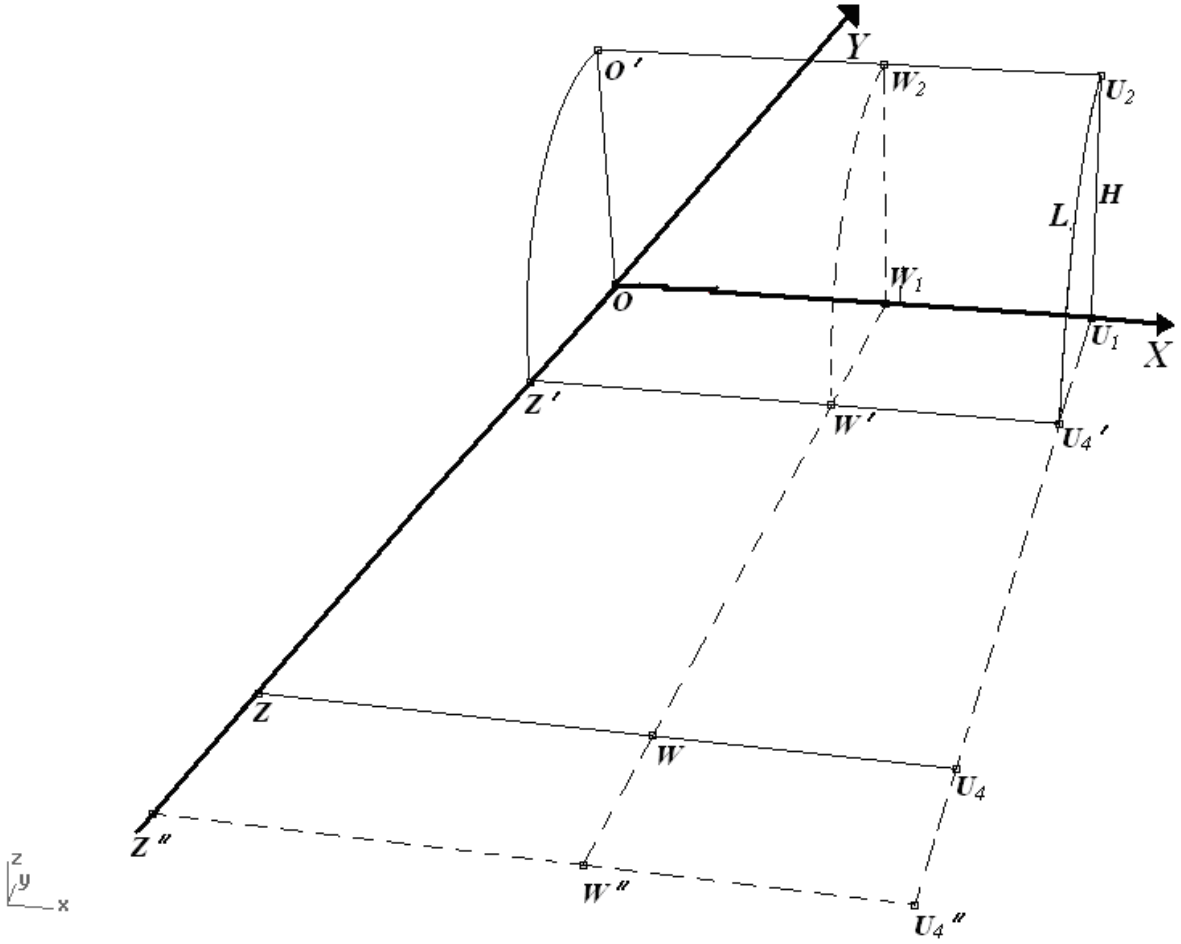

Figure 6.14 One-quarter-cylinder segment

$$\begin{cases} X_{FP} = X_{OP} \\ Y_{FP} = Y_{OP} + H - L \\ Z_{FP} = Z_{OP} \end{cases} \tag{6.6}$$

6.3.2.5 Portion 5 rest segment

In this simplified scenario, the rest of the pattern is not affected by the 3D pattern flattening process, and therefore the corresponding points are unchanged. It needs to be mentioned here that practically all parts of the fabric are affected to some extent because the fabric is a continuous material which facilitates deformation/strain to be distributed. In this simplified model, it is assumed that there will be no dimensional change as the change in such areas is much smaller than caused by flattening other parts as aforementioned. This is reflected in Equation (6.7).

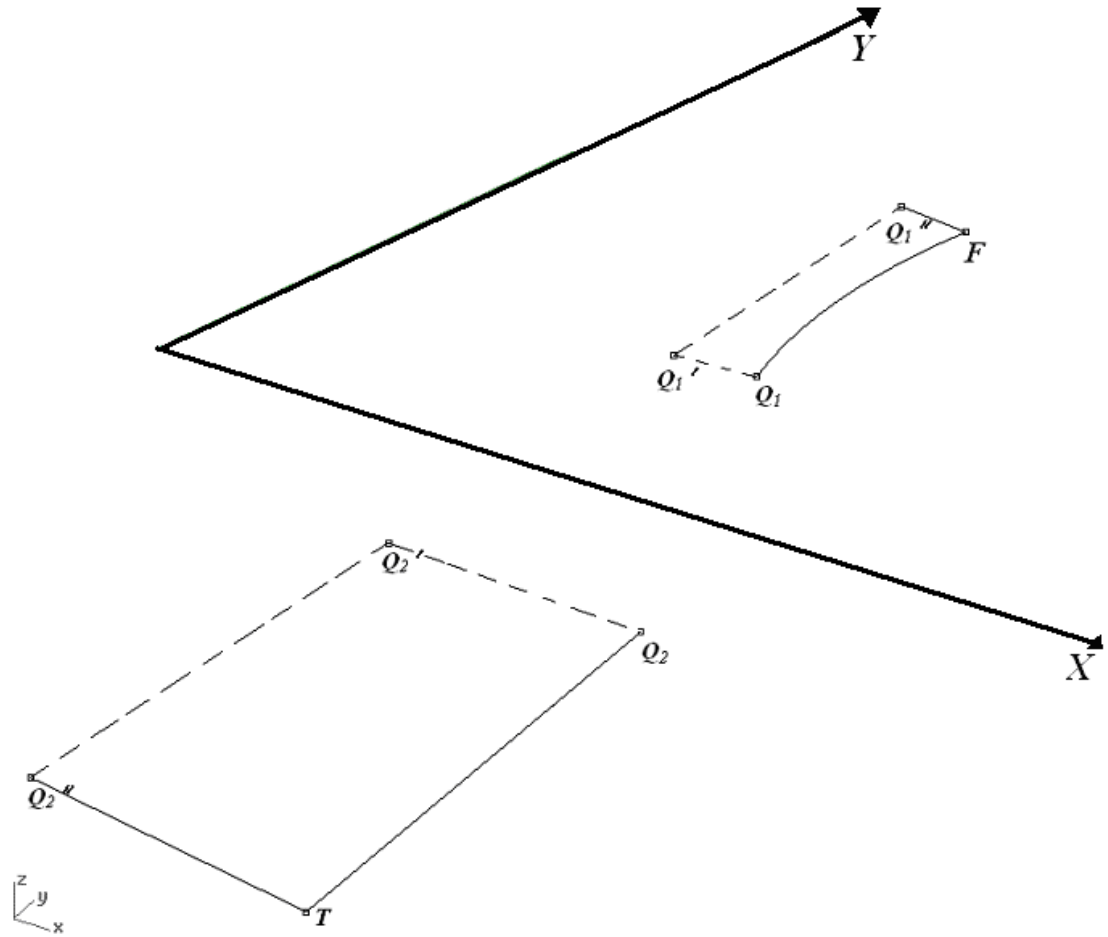

Figure 6.15 Rest segment

$$\begin{cases} X_{FP} = X_{OP} \\ Y_{FP} = Y_{OP} \\ Z_{FP} = Z_{OP} \end{cases} \tag{6.7}$$

6.3.3 Model modification

According to the model described above, the calculated profile of pattern for the front panel of the female body armour is shown in Figure 6.16 (a), where it is obvious that there are places where the curve is not continuous. This is caused by the simplified assumption that the raised fabric will only be distributed along the warp and weft directions when flattened. To reduce the error, the calculated pattern profile is modified

by connecting the vertex points by a simple curve. For instance, an asymptote is drawn between points *Q"* and *T* and points U_4*"* and *T*. The modified pattern profile is shown in Figure 6.16 (b) for body size 12 with bra size 75B.

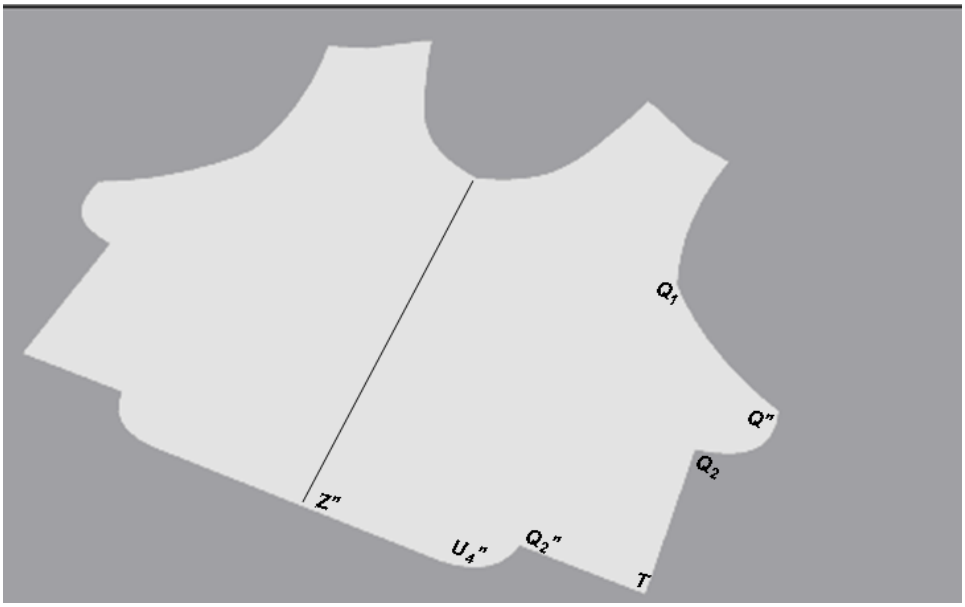

(a)

(b)

Figure 6.16 Modification of the calculated pattern profile: (a) the calculated; (b) the modified

6.4 Verification of the Model

To verify the correctness of the mathematical model, a simple experiment was carried out. Using the mode described above, a pattern for the front panel of female body armour was created and drawn on an angle-interlock fabric. Figure 6.17(a) shows the front panel pattern after shaping, and (b) the comparison of the block projection to the raised pattern. As can be seen, the calculated pattern in Figure 6.16(b) has an irregular boundary because of the consideration of the doming up for the bust. When the angle-interlock fabric has been domed up as shown in Figure 6.17(a), the boundary curve retracts to almost the normal shape for a front panel pattern. The comparison shown in Figure 6.17(b) indicates a satisfactory agreement between the raised pattern and the projection block, despite minor disagreements in some places.

(a)

(b)

Figure 6.17 Validation of the front panel of female body armour: (a) 3D shape; (b) comparison

6.5 Multi-layer Front Panel of Female Body Armour

The relationship between the thickness of fabrics and the pattern block for different layers of fabrics needs to be investigated for the purpose of manufacturing the whole front panel of female body armour. One ballistic panel normally contains multiple pieces of fabrics, which indicates that the outer layer is larger than the inner layer while still keeping uniformity in the design as the contour surface induced by the female torso needs to be fully covered. The pattern block of the outer layer can be achieved by grading that of the inner layer if the intervals (named as N_i) between them is known. N_i is equal to the increment of the bust girth. N_i exists because of the thickness of fabrics (named as N_t). N_t is obtained via measurement. Therefore, N_i can be calculated if the mathematical relationship between N_i and N_t is known. Figure 6.18 is the cross-section of the mannequin viewed from the top of the head. The dotted line indicates the bust girth (named as l) which is used to make the original block for the first layer of the multi-layer garment. The full line indicates the new bust girth (named as L) when the

second layer is added. The gap (marked as the shadowed area) between l and L is unchanged at any point because this gap is actually formed by the thickness of fabrics, N_t.. Therefore, keeping l , L and N_t unchanged, their mathematical relationships could be considered on the assumption that they make a concentric circle, as shown in Figure 6.19.

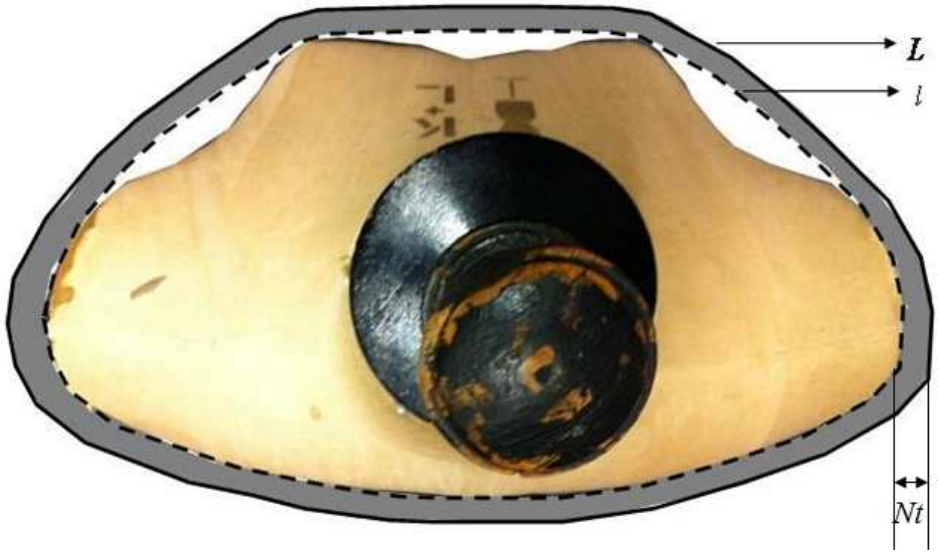

Figure 6.18 Cross-section of mannequin viewed from the top of the head

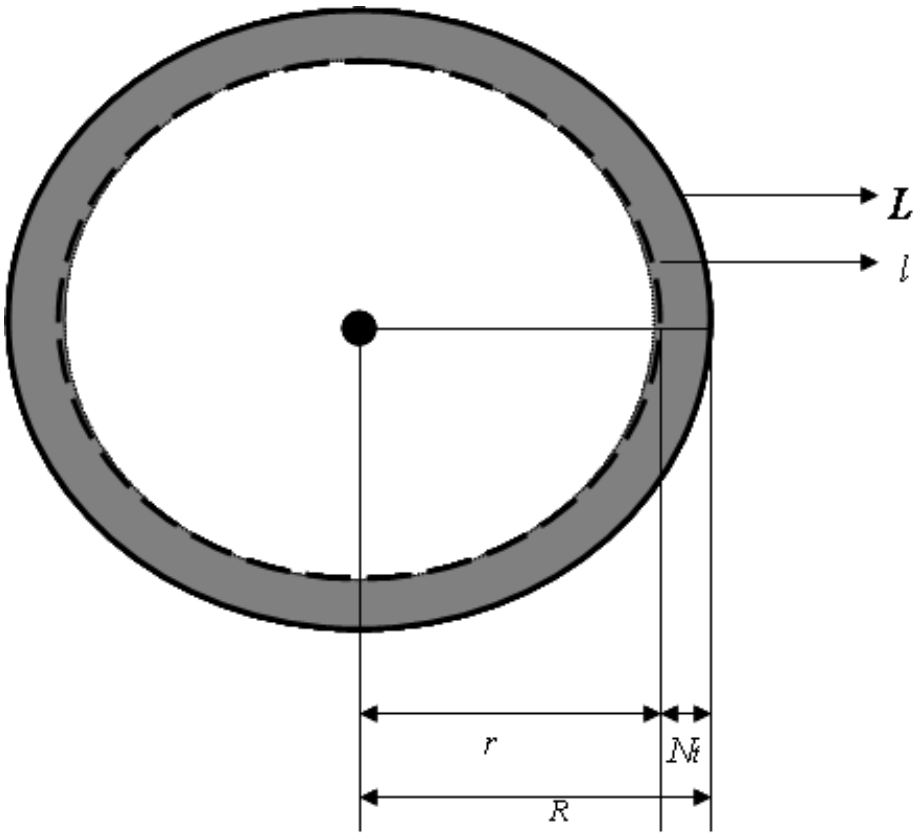

Figure 6.19 Concentric circle composed of l , L and Nt

In Figure 6.19, l is the perimeter of the inner circle, which could be expressed as:

$$l = 2\pi r \tag{6.8}$$

where r is the radius of the inner circle. r could then be expressed as:

$$r = \frac{l}{2\pi} \tag{6.9}$$

L is the perimeter of the outer circle, which could be expressed as:

$$L = 2\pi R \tag{6.10}$$

where R is the radius of the outer circle and could be achieved by $r + N_t$. As known $r = \frac{l}{2\pi}$, the equation for L can be converted into

$$L = l + 2\pi N_t \tag{6.11}$$

Equation (6.11) minus (6.8) indicates $L - l$ which means the increment of bust girth between the first layer and the second layer, in other words, the intervals, N_i. Therefore, the mathematical relationship between N_i and N_t can be achieved as:

$$N_i = 2\pi N_t \tag{6.12}$$

Equation (6.12) means that the ratio between the intervals and the thickness of fabrics is $2\pi : 1$. The thickness of angle-interlock woven fabrics used in this research is around 0.3cm. Therefore, the corresponding intervals between the outer layer and inner layer of fabrics could be calculated around 2cm according to Equation (6.12). Table 6.3(a) illustrates the coordinate movements of original block projection with 2cm intervals graded by PAD system, (b) the coordinate values of new block projection and (c) the illustration of new block projection. The pattern blocks for more (larger) outer layers may also be achieved using this ratio for grading. As just the number of layers increases, the thickness of fabrics is increased by the same amount (2cm) for each layer.

Table 6.3 New block projection: (a) the coordinate movements with 2cm intervals; (b) the coordinate values, (c) the illustration

(a)

Original key points	Coordinate Change		Original key points	Coordinate Change	
	X	Y		X	Y
A	0.00	0.16	B	0.01	0.15
C	0.08	0.22	E	0.10	0.28
F	0.22	0.28	G	0.24	0.22
I	0.26	0.16	J	0.28	0.12
K	0.30	0.08	M	0.35	0.06
N	0.40	0.04	Q	0.50	0.00
S	0.50	-0.10	T	0.50	-0.20
V	0.22	-0.20	W	0.10	-0.20
Z	0.00	-0.20			

(b)

Key Points	Coordinate values	
	X	Y
A_n*	0.0	10.5
B_n	4.5	12.7
C_n	8.0	19.2
E_n	9.5	24.1
F_n	17.3	21.5
G_n	16.5	16.4
I_n	16.6	11.5
J_n	17.2	7.8
K_n	18.2	4.3
M_n	19.5	2.3
N_n	21.4	0.5
Q_n	22.3	0.0
S_n	22.3	-8.4
T_n	22.3	-16.0
V_n	13.0	-16.0
W_n	5.9	-16.0
Z_n	0.0	-16.0

An*: key points for new block projection after 2cm intervals

(c)

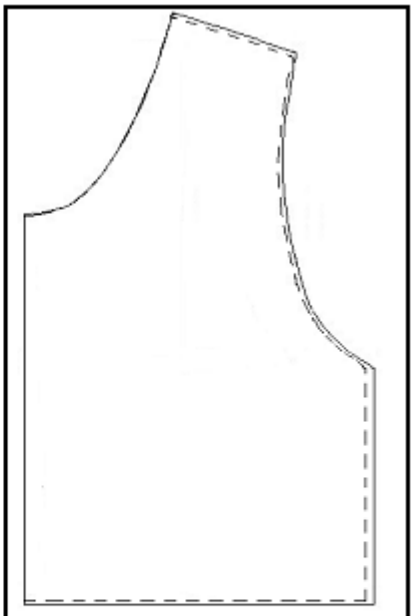

****The new block projection indicated by the full line is graded from the original block projection indicated by the dotted line.**

After the new block projection has been produced, the pattern block with the bust-cup part can be designed using the same mathematical modelling detailed in section 6.3. Figure 6.20 shows the front panel pattern of body size 12 with bra size 85C after shaping.

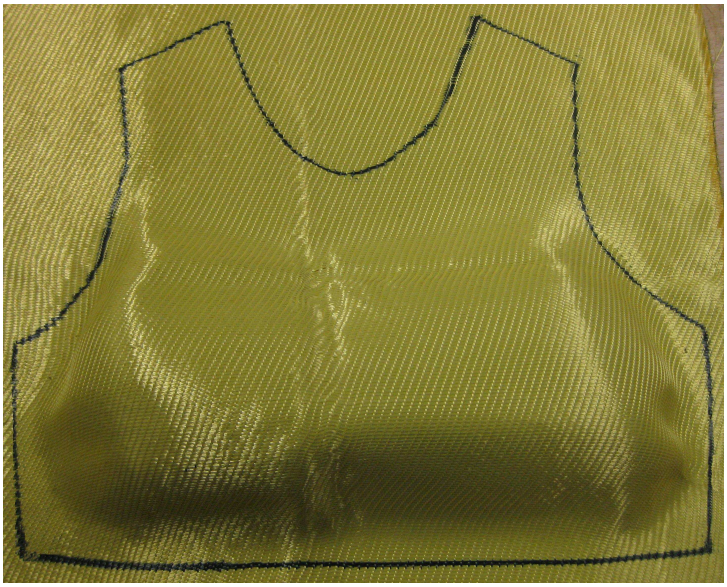

Figure 6.20 the front panel pattern of body size 12 with bra size 85C after shaping

Based on the new pattern block, the outer layer of appropriately-profiled angle-interlock ballistic fabrics can be produced which is subtly graded to fit the inner layer to make a two-layer front panel of female body armour. Figure 6.21 shows the result: (a) top view: the outer layer entirely fits the inner layer; (b) side view: two neighbouring layers of fabrics are laid together very closely; (c) 3D view: the inner layer of front panel of female body armour has already been shaped, which is demonstrated by peeling off a corner of the outer layer and a half of the outer layer.

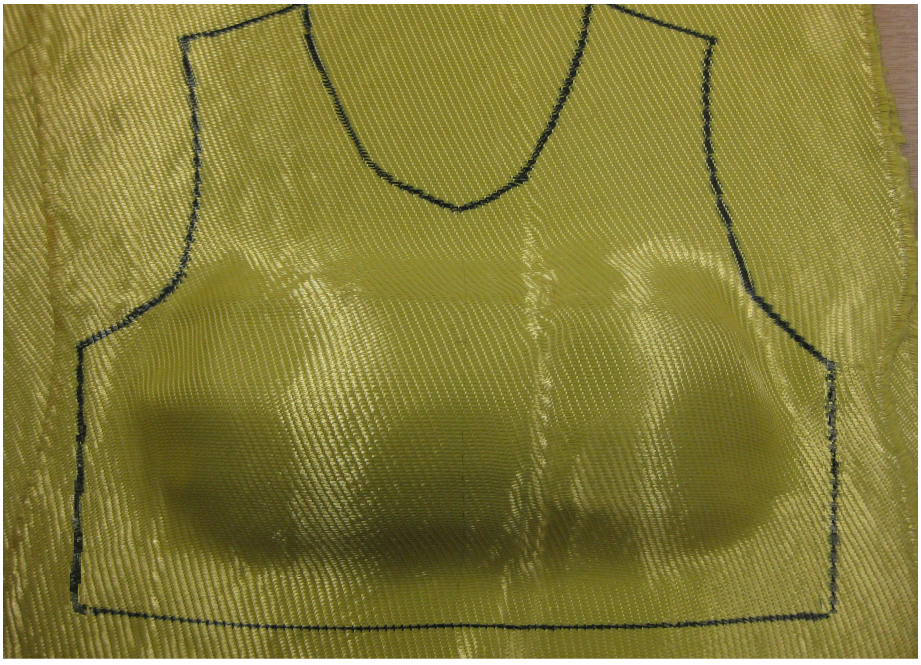

(a)

(b)

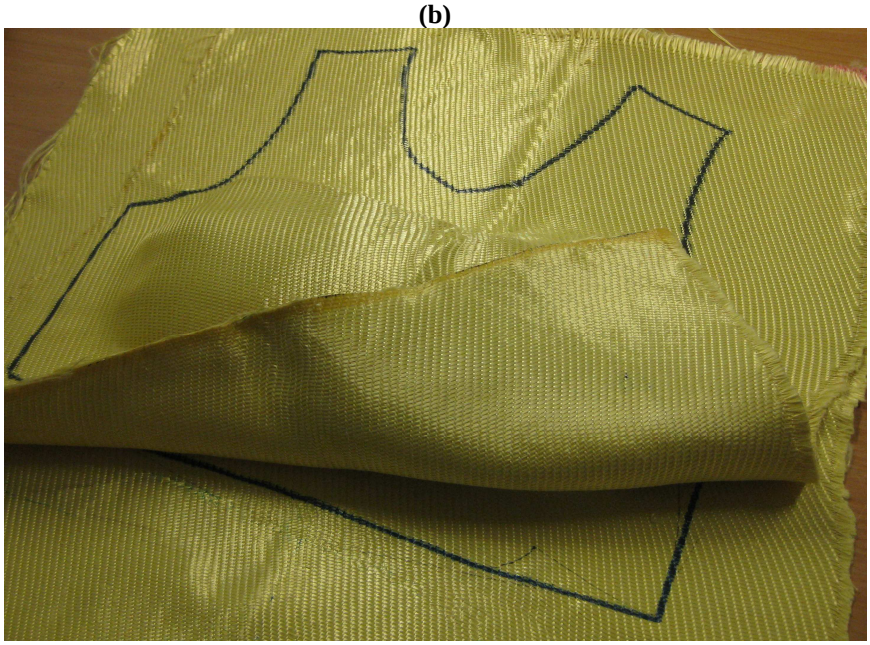

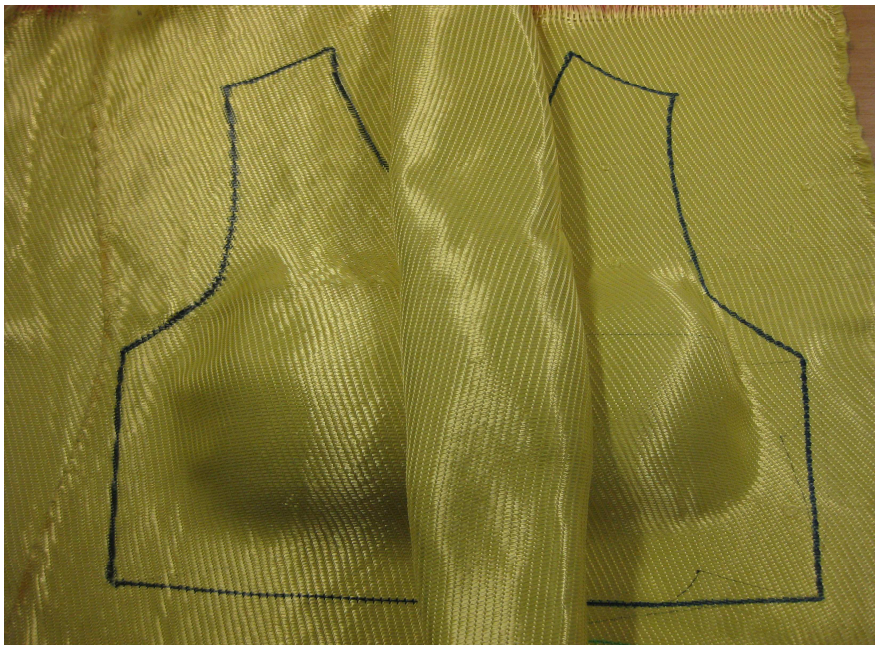

(c)

Figure 6.21 Two-layer front panel of female body armour: (a) top view; (b) side view; (c) 3D view

6. 6 Remarks

Based on the ballistic evaluation of angle-interlock fabrics which was reported in the former research, this chapter is an attempt to set up mathematical relations to calculate the flattened pattern shape. The use of angle-interlock fabric for female body armour will diminish the drawbacks such as wrinkles and fabric discontinuity which negatively influence ballistic protection. In order to create the front panel pattern correctly, this section has described the establishment of a mathematical model which calculates the boundary curve of the pattern by taking into consideration of the body size and bra size. In the successful model, the bust area is represented by some simple geometrical shapes. When flattened, the fabric material is assumed to distribute mainly in the warp and weft directions. A modification procedure has been put forward to improve the accuracy of the pattern profile. The experimental results have shown satisfactory accuracy of the pattern shape for the front panel of female body armour, which leads to the correct shape of the final domed front panel, despite some minor disagreements. This model is ready to be implemented into computer programmes specialised for designing female body armour using the type of fabrics described based on the wearer's body and bra sizes. Moreover, the mathematical relationship between the thickness of fabrics and the pattern block for different layers of fabrics also has been solved and correspondingly, the multi-layer front panel of female body armour could be created using this work.

Chapter 7

Conclusions and Future Work

7.1 Conclusions

The main objective of this research was to develop a novel type of female body amour panel with the fibre continuity for wearing comfort and for protection performance against impact in contrast to the current methods such as cutting and sewing. The new fabric used for making the front panel must therefore possess two features, i.e., (i) the three-dimensional dome shape so as to fit the curved female torso and (ii) performance against ballistic impact comparative to the fabrics used for normal body armour. The work carried out and the achievements are concluded as follows.

(a) Investigation of dome formability of dome-shaped fabric

A series of dome-shaped fabrics have been successfully produced on a shuttle loom with the assistance of a commercial CAD/CAM programme, ScotWeave. The principle of honeycomb weaves was adopted to produce dome-shaped fabrics with weaves with different float lengths arranged in a concentric sequence. The dome depth of such fabrics was noticeable. Investigations were carried out on the relationship between the parameters of the dome-shaped fabric and the dome depth.

(b) Mouldability of angle-interlock woven fabrics

Previous work demonstrated that the angle-interlock woven fabrics are mouldable. Angle-interlock woven fabrics with different structural parameters were designed and produced from Kevlar® yarns. The mouldability of angle-interlock woven fabrics were theoretically explored and practically measured. The results indicated that the angle-interlock woven fabrics can shape larger deformation depth than the dome-shaped fabrics and therefore it is more suitable for making curvaceous female body armour, subject to satisfactory performance against ballistic impact.

(c) Evaluation of angle-interlock woven fabrics for ballistic performance

Two methods were used to evaluate the ballistic performance of the angle-interlock fabrics. The first is the parametric study for energy absorption using the in-house firing range and compartive study against the commonly used fabrics for ballistic protection. The studies revealed that whilst the structural parameters of angle-interlock fabrics do not have a clear influence on the ballistic performance, this type of fabrics tends to be less energy absorbent than other various fabrics because of the weaker gripping power on the constituent yarns in the angle-interlock fabrics. The second method used to evaluate the ballistic performance of the angle-interlock fabrics is the NIJ level II test carried out in a collaborating company. All the panels made from angle-interlock fabrics passed the aimed level II criteria according to the NIJ standard. It showed that the angle-interlock fabrics is not less protective than the existing body armour fabrics based on the same amount of materials. This, in conjunction with the good moudability, obviously shows that the angle-interlock woven fabrics are acceptable for making female body armour.

(d) Mathematical modeling for the front panel of female body armour

The angle-interlock fabrics are a type of fabric that is mouldable. In pattern making for the front panel of female body armour, it is important to have the correct pattern profile so that when the fabric is raised to form the dome, the pattern periphery conforms with the body armour design. A mathematical model was developed to generate the shape of the front panel of female body armour based on the use of angle-interlock woven fabrics. The mathematical model was constructed by combining two components: the part without the bust-cup area and the bust-cup part. The former was also known as the block projection, on which bust-cups with different sizes were located. This was created on the principle for making clothing blocks, and different sizes can be achieved by grading. The results for UK sizing and European sizing have been demonstrated with the assistance of the PAD software system. In the optimal model, the bust area was divided into 7 portions including a triangular prism, a quarter of cylinder, two one-eights of a sphere at ends of quarter of cylinder, two quarters of a cone surface at the ends of the triangular prism, and the flat area that makes up the rest of the front panel. Mathematical equations were set up to calculate the contribution to the pattern profile for each of the 7 portions. Experimental results showed a good agreement with the outcome from the mathematical modeling. With this mathematical model, the front panel of female body armour is able to be designed based on figure size and bra size. As the ballistic panel is composed of many layers, the outer layer is larger than the inner layer but the same as that in the design when covering the contour female torso. The mathematical relationship between the thickness of fabrics and the pattern block for different layers of fabrics also has been investigated, which indicates that the whole multi-layer front panel of female body armour can been produced.

7.2 Future Work

It has been shown that angle-interlock woven fabrics can be an effective alternative in the application of female body armour as they have good mouldability and satisfactory ballistic protection in this project. However, there are still some aspects that require further research; important work is listed as follows.

(a) A finite element model is required in order to eliminate experimental errors in the ballistic shooting tests. The analysis of computational simulation may provide valuable information to reflect the response coupling between the fabric specimens and the projectile. Additionally, no bulky fabric specimens are required.

(b) The next important aspect is the implementation of the mathematical model of the front panel of female body armour into the computer programs. After the body and bra size are input into the software, the profile of the front panel of female body armour will be calculated as the output automatically. With this software configuration, high efficiency in pattern creation can be demonstrated.

(c) The last but not the least point is the manufacture and ballistic testing of the front panel of female body armour. The whole front panel needs to be produced and then its ballistic performance is required to be further investigated.

References

[1] Home Office, Crime in England and Wales 2008/09 (a summary of the main findings), 2009.

[2] Home Office, Controls on Firearms (a Consluation Paper), 2004.

[3] Department of Justice, Violent Crime Rate Remined Unchanged While Theft Rate Declined in 2008, 2009.

http://www.ojp.usdoj.gov/newsroom/pressreleases/2009/BJS09131.htm, (2009).

[4] Dennard, J., Hyosung's Creora® Fibre Finds Many Applications, *Textile Worl*d, 2003. **153**(3): p.54.

[5] Jack Ellis Body Protection Company, Gulf Success, *Textile Month*, 2003. **2003**(8): p.34.

[6] Larrivee, M.N., Protective Materials for Soldiers: The Most Demanding Textile Customers, *International Fibre Journal*, 2006. **21**(2): p.42-43.

[7] Stull, J.O., Standards of Protection, *Textile Asia*, 1995. **26**(6): p.111-117.

[8] Daniel, B., Bulletproof Vests, *Textile Journal: La Revue du Textile*, 2005.**122**(2): p.24-30.

[9] Navel Research Laboratory, Full-body Protection, *Industrial Fabric Products Review*,2005. **90**(4): p.10.

[10] Majumdar, D., Srivastava, K.K., Purkayastha, S.S., Pichan, G. and Selvamurthy, W., Physiological Effects of Wearing Heavy Body Armour on Male Soldiers, *International Journal of Industrial Ergonomics*, 1997. **20**(2): p.155-161.

[11] Ashcroft, J., Daniels, D. J. and Hart, S.V., Selection and Application Guide to Personal Body Armour NIJ Guide 100–01 (Update to NIJ Guide 100–98), *U.S. Department of Justice (Office of Justice Programs, National Institute of Justice)*, 2001.

[12] *http://www.twaron.com/pdf/ladies-vest-leaf.pdf*, (2006).

[13] *http://www.mod.uk/defenceinternet/factsheets/womeninthearmedforces.htm*, (2006).

[14]*http://www.army.mil/-news/2007/03/26/2405-womens-history-month-reminds-female-soldiers-how-far-theyve-come/*, (2007).

[15] Cork, C.R., Narrow Fabrics-Ballistic Opportunities, *Textiles Magazine*, 2006. **33**(2): p.16-18.

[16] Rodie, J.B., Life-Saving Fabrics, *Textile World*, 2009. **159**(3): p.22-24.

[17] CSIRO Textile & Fibre Technology Company, CSIRO Spins the Tubes, *Textile Month*, 2005. **2005**(3): p.14-15.

[18] Michael, M., Tailored Resistance, *Nonwovens Report International*, 2005. **2005**(10) : p.27.

[19] TEIJIN Twaron BVE. I.du Pont de Nemours & Co., Layers of Resistance, *Future Materials*, 2005.**2005**(2): p.20-21.

[20] Ballistics Technology Team at the U.S. Army Soldier Systems Centre, Pushing the Ballistic Boundaries, *Future Materials*, 2005. **2005**(2): p.8-9,

[21] Ballistics Technology Team at the U.S. Army Soldier Systems Centre, Light Armour, *Textile Horizons*, 2004. **2004**(10): p.10.

[22] DSM Fibre Intermediates Company and BEKAERT Fibre Technologies Company, A Vest Combining Bullet and Stab Protection, *TUT: Textiles a l'Usage Technique*, 2005. **58**(4) : p.9.

[23] BSST GmbH Company and Ten Cate Advanced Composites Company, Triple Threat Protection, *Textile Horizons*, 2006. **2006**(7-8): p.21.

[24] Ian, H., Breathability, Protection and Comfort, *International Dyer*, 2006. **191**(8): p.26-27.

[25] Walker, C. A., Gray, T. G. F., Nichol, A. C. and Chadwick, E. K. J., Evaluation of Test Regimes for Stab-resistant Body Armour, *Proceedings of the Institution of*

Mechanical Engineers, Part L: Journal of Materials: Design and Applications, 2004. **218**(4): p.355-361.

[26] Dyer, P.A. and Ohio, H.H., *U.S. Pat. No.5, 020, 157*, 1991.

[27] Mellian, S.A. and Mass, W., *U.S. Pat. No.4, 183, 097*, 1980.

[28] Carothers, J.P., Body Armour, A Historical Perspective, USMC CSC 1988.

[29] Chen, X. and Chaudhry, I., Ballistic Protection-Textiles for Protection, *the Textile Institute*, 2005. p.532-554.

[30] *http:// inventors.about.com/od/bstartinventions/a/Body_Armor.htm*, (2010).

[31] *http://www2.dupont.com*, (2010).

[32] Gadow, R. and Niessen K.V., Lightweight Ballistic with Additional Stab Protection Made of Thermally Sprayed Ceramic and Cermet Coatings on Aramid Fabrics, *International Journal of Applied Ceramics Technology*, 2006. **3**(4): p.284–292.

[33] Dingenan, J.P. and Verlinde, A., Nonwovens and Fabrics in Ballistic Protection, *Technical Textiles International*, 1996. p.10-13.

[34] Riewald, P.G., Yang, H.H. and Shaughnessy, W.F., Lightweight Helmet from a New Aramid Fibre, *Du Pont Fibers*,1991.

[35] Weatherall, J., Rappaport M. and Morton J., Outlook for Advanced Armour Materials, *National SAMPE Technical Conference Advanced Materials: Looking Ahead of the 21st Century*, 1990. p.1070-1077.

[36] *http://en.wikipedia.org/wiki/Ballistic_vest*, (2010).

[37] Ashcroft, J., Daniels, D. J. and Hart, S.V., Selection and Application Guide to Personal Body Armor NIJ Guide 100–01 (Update to NIJ Guide 100–98), *U.S. Department of Justice (Office of Justice Programs, National Institute of Justice)*, 2001.

[38] *http://www.praetorianasc.com*, (2010).

[39] Jacobs, M.J.N. and Van Dingenen, J.L.J., Ballistic Protection Mechanisms in Personal Armour, *Journal of Materials Science*, 2001. 36: p.3137-3142.

[40] Yang, H.H., Kevlar Aramid Fibre, *John Wiley & Sons Ltd*, 1993. p.3-14.

[41] *http://en.wikipedia.org/wiki/kevlar*,(2010).

[42] Ashok, B., Lightweight ballistic composites: military and law-enforcement applications, *Woodhead Publishing in materials*, 2006. p.216.

[43] *http:// en.wikipedia.org/wiki/UHMWPE*,(2010).

[44] *http://en.wikipedia.org/wiki/zylon*,(2010).

[45] Croft, J., Longhurst, D., HOSDB Body Armour Standards for UK Police Part 1: General Requirements, *Home Office Scientific Development Branch*, 2007.

[46] Croft, J., Longhurst, D., HOSDB Body Armour Standards for UK Police Part 2: Ballistic Resistance, *Home Office Scientific Development Branch*, 2007.

[47] Higgins, K.M., Lord, C.K., Lightsey, S.L. and Malley, K., Ballistic Resistance of Personal Body Armour NIJ Standard-0101.04, *National Institute of Justice, Office of Science and Technology*, 2001.

[48] *http://www.armourshield.com/ballistic%20standards.html*,(2009).

[49] Croft, J., Longhurst, D., HOSDB Body Armour Standards for UK Police Part 3: Knife and Spike Resistance, *Home Office Scientific Development Branch*, 2007.

[50] Milliken & Company, Comfort and Protection, *Future Materials*, 2007. **2007**(11):p.26.

[51] Tencate & Company, Military Safegaruds, Future Materials, 2008. **2008**(11): p.7.

[52] Kumar, S., Gupta, D.S., Singh, I. and Sharma, A., Behaviour of Kevlar/Epoxy Composite Plates under Ballistic Impact, *Journal of Reinforced Plastics and Composites*, 2009. **0**(00/2009): p.1-17.

[53] Williams I., Reinforcing Materials for Body Armour, GB2433192A, *UK Patent Application*, 2007.

[54] Robert A., Body Armour, GB2457640A, *UK Patent Application*, 2009.

[55] Christine, M.P. and Stephen, H.C., Risky Talk: Framing the Analysis of the Social Implications of Nanotechnology, *Bulletin of Science, Technology and Society*, 2007.**27**(5): p.349-366.

[56] Cunniff, P.M., a Semi-empirical Model for the Ballistic Impact Performance of Textile-based Personnel Armour, *Textile Research Journal*,1996. **66**(1): p.45-59.

[57] Cardi., A.A., Adams, D. and Walsh, S., Ceramic Body Armour Single Impact Force Identification on a Compliant Torso using Acceleration Response Mapping, *Structural Health Monitoring*, 2006. **5**(4): p.335-372.

[58] Gillespie, J.W., Monib, A.M. and Carlsson, L.A., Damage Tolerance of Thick-section S-2 Glass Fabric Composites Subjected to Ballistic Impact Loading, *Journal of Composite Materials*,2003. **37**(23): p.2321-2147.

[59] Lee, B.L., Song, J.W. and Ward, J.E., Failure of Spectra® Polyethylene Fibre Reinforced Composites under Ballistic Impact Loading, Journal of Composite Materials, 1994. **28**(13): p.1202-1225.

[60] Ji, K.H. and Kim, S.J., Dynamic Direct Numerical Simulation of Woven Composties for Low-velocity Impact, *Journal of Composite Materials*, 2007. **41**(2): p.175-200.

[61] Petterson. D.R., Stewart, G.M., Odell, F.A. and Maheux, R.C., Dynamic Distribution of Strain in Textile Materials under High-speed Impact: Part I: Experimental Methods and Preliminary Results on Single Yarns, *Textile Research Journal*, 1960. **30**(6): p.411-421.

[62] Cheng, M., Chen, W. and Weerasoriya, T., Mechanical Properties of Kevlar KM2 Single Fibre, *Journal of Engineering Materials and Technology*, **127**(4): p.197-203.

[63] Dillon, J.H., Current Problems and Future Trends in Synthetic Fibres, *Textile Research Joural*,1953. **23**(5): p.298-312.

[64] Rao, M.P., Nilakantan, G., Keefe, M., Powers, B.M. and Bogetti, T.A., Global/Local Modeling of Ballistic Impact onto Woven Fabrics, *Journal of Composite Materials*, 2009. **23**(5): p.445-467.

[65] Nasr-Isfahani, M., Amani-Tehran, M. and Latifi, M., Simulation of Ballistic Impact on Fabric Armour using Finite-element Method, *the Textile Institute*, 2009.**100**(4): p.314-318.

[66] Iremonger, M.J. and Went, A.C., Ballistic Impact of Fibre Composite Armours by Fragment-simulating Projectiles, *Journal of Composites*, 1996. **27A** (1996): p.575-581.

[67] Termonia, Y., Impact Resistance of Woven Fabrics, *Textile Research Journal*, 2004. **74**(8): p.723-729.

[68] Susich, G., Dogliotti, L.M. and Wrigley, A.S., Microscopical Study of a Multilayer Nylon Body Armour Panel after Impact, *Textile Research Journal*, 1958. **28**(5): p.361-377.

[69] Cheng, M. and Chen, W.N. Modelling Transverse Behaviour of Kevlar KM2 Single Fibres with Deformation-induced Damage, *International Journal of Damage Mechanics*, 2006. **15**(4): p.121-132.

[70] Petterson, D.R. and Stewart, G.M., Stress-strain Curves from Strain-Position Distributions, 1960. **30**(6): p.422-431.

[71] Lee, B.L., Walsh, T.F., Won, S.T., Patts, H.M., Song, J.W. and Mayer, A.H., Penetration Failure Mechanisms of Armour-grade Fibre Composites under Impact, *Journal of Composite Materials*, 2001. **35**(18): p.1605-1633.

[72] Lim, C.T., Tan, V.B.C and Cheong, C.H., Perforation of High-strength Fabric by Projectiles of Different Geometry, *International Journal of Impact Engineering*, 2003. **28**(2003): p.207-222.

[73] Freeston, W.D. and Claus, W.D., Strain-wave Reflections during Ballistic Impact of Fabric Panels, *Textile Research Journal*, 1973. **43**(6): p.348-351.

[74] Montgomery, T.G., Grady, P.L. and Tomasino, C., the Effects of Projectile Geometry on the Performance of Ballistic Fabrics, *Textile Research Journal*, 1982. **52**(7): p.442-450.

[75] Silva, M.A.G., Cismasiu, C. and Chiorean, C.G., Numerical Simulation of Ballistic Impact on Composite Laminates, *International Journal of Impact Engineering*, 2005. **31**(3): p.289-306.

[76] Hayhurst, J.C., Livingstone, I.H., Clegg, A.R. and Fairlie, G.E., Numerical Simulation of Hypervelocity Impacts on Aluminum and Nextel/Kevlar Whipple Shields, Hypervelocity Shielding Workshop, Texas, USA.

[77] Akdemir, A., Candan, C. and Sahin, O.S., Effects of Production Parameters and Conditioning upon Ballistic Characteristics of Para Aramid Light Armours, *Journal of Composite Materials*, 2008. **42**(19): p.2051-2061.

[78] Simons, J., Erlich, D. and Shockey, D., Finite Element Design Model for Ballistic Response of Woven Fabrics, *19th International Symposium of Ballistics*, Interlaken, Switzerland.

[79] Clegg, R., Hayhurst, C., Leahy, J. and Deutekom, M., Application of a Coupled Anistropic Material Model to High Velocity Impact Response of Composite Textile Armor, *18th International symposium on Ballistics*, 1999. p.791-798.

[80] Riewald, P.G., Folgar, F., Yang, H.H. and Shaughnessy, W.F., Lightweight Helmet from a New Aramid Fibre, 23rd International SAMPE Technical Conference.

[81] Colakoglu, M., Experimental and Numerical Investigations on the Ballistic Performance of Polymer Matrix Composites used in Armour Design, *Applied Composite Materials*, 2007. **14**(1): p.47-68.

[82] Lim, C.T., Tan, V.B.C and Cheong, C.H., Perforation of High Strength Double Ply Fabric System by Varying Shaped Projectiles, *International Journal of Impact Engineering*, 2002. **27**(6): p.577-591.

[83] *http://www.teijinaramid.com*, (2010).

[84] *http://www.dyneema.com*, (2010).

[85] *http://www51.honeywell.com*, (2010).

[86] Altmann, J., Military Use of Nanotechnolgy: Perspectives and Concerns, *International Peace Research Institute,* 2004.**35**(1): p.61-79.

[87] *http://news.bbc.co.uk/1/hi/sci/tech/7038686.stm,* (2009).

[88] Sinnppoo, K., Arnold, L. and Padhye, L., Application of Wool in High-velocity Ballistic Protective Fabrics, *Textile Research Journal,* 2010. **80**(11): p.1083-1092.

[89] Marsyahyo, E., Jamasri, Rochardjo, H.S.B. and Soekrisno, Preliminary Investigation on Bulletproof Panels made from Ramie Fibre Reinforced Composites for NIJ Level II, IIA and IV, *Journal of Industrial Textiles,* 2009. **39**(1): p.13-26.

[90] Shockey, D.A., Erlich D.C., Simons J.W., Lightweight Fragment Barriers for Commercial Aircraft. In: Proceedings of the 18th International Symposium on Ballistics, San Antonio, Texas, 15-19 November 1999. p.1192-1199.

[91] Cunniff, P.M., An analysis of the System Effects of Woven Fabrics under Ballistic Impact. *Textile Research Journal,* 1992. **62**(9): p.495-509.

[92] Cork, C.R. and Foster, P.W., the Ballistic Performance of Narrow Fabrics, *International Journal of Impact Engineering,* 2007. **34**(3): p.495-508.

[93] Chitrangad. Hybrid Ballistic Fabric, *U.S. Pat. No.5,187,003,* 1993.

[94] Karahan, M., Kus, A. and Eren, R., an Investigation into Ballistic Performance and Energy Absorption Capabilities of Woven Aramid Fabrics, *International Journal of Impact Engineering,* 2008. **35**(2008): p.499-510.

[95] Armellino, R.A. and Armellino, S.E., Ballistic Material for Flexible Body Armor and the Like, US Patent 4522871, 1985.

[96] Harpell, G.A., Palley, I., Kavesh, S. and Prevorsek, D.C., Ballistic-resistant Fine Weave Fabric Article, US Patent 4737401, 1988.

[97] Dunbavand, I.E., Flexible Armour, *U.S. Pat. No. 4,608,717,* 1986.

[98] Karahan, M., Kus, A. and Eren, R., an Investigation into Ballistic Performance and Energy Absorption Capabilities of Woven Aramid Fabrics, *International Journal of Impact Engineering,* 2008. **35**(2008): p.499-510.

[99] Bilisik, A.K. and Turhan, Y., Multidirectional Stitched Layered Aramid Woven Fabric Structures and their Experimental Characterization of Ballistic Performance, *Textile Research Journal,* 2009.**79**(7): p.1331-1343.

[100] Howard, T.L., Application of Multi-component Materials for Improvements in Ballistic Portection, *International Textile Bulletin,* 2001.**62**(9): p.495-509.

[101] Lou, C.W., Lin, C.W., Hsu, C.H., Chen, J.M., Lin, J.H. and Meng, H.H., Process and Bullet-resistant Buffer Effect of an Elastic Cushioning Structure Made of Polyamide Non-woven Fabric and Chloroprene Rubber, *Textile Research Journal*, 2008. **78**(3): p.258-263.

[102] Lin, J.H., Novel Compound Cushion Layer for Reinforcement of Ballistic Resistance, *Textile Research Journal*, 2005. **75**(5): p.431-436.

[103] Ahmad, M.R., Ahmad, W.Y., Salleh, W.J. and Samsuri, A., Performance of Natural Rubber Coated Fabrics under Ballistic Impact, *Malysian Polymer Journal*, 2007. **2**(1): p.39-51.

[104] Gadow, R. and Niessen, K.V., Lightweight Ballistic with Additional Stab Protection Made of Thermally Sprayed Ceramic and Cermet Coatings on Aramid Fabrics, *International Journal of Applied Ceramic Technology*, 2006. **3**(4): p.284-292.

[105] Rosset, W.S., Patterned Armour Performance Evaluation for Multiple Impacts, *Army Research Laboratory ARL-TR-3038*, 2003.

[106] *http://www.cosmoworlds.com/photobase/news/textiles_intelligencemilitary_*

clothing-01092009.html, 2009.

[107] Rao, K.N. and Singh, D., Impact Resistance Behavior of Polymer Nanocomposite Transparent Pane*ls, Journal of Composite Materials*, 2009. **43**(2): p.139-151.

[108] Lee, B.W., Kim, I.J. and Kim, C.G., the Influence of the Particle Size of Silica on the Ballistic Performance of Fabrics Impregnated with Silica Colloidal Suspension, *Journal of Composite Materials*, 2009. **0**(0): p.1-20.

[109]*http://www.americansecurity.net/main.php?obj=prod&action=VIEW&id=6218e2dc0e47795bac2d3a7bcca7f576&sess3=7aad3c4d826c850b11547760254a2962,2006,(2006).*

[110] *http://www.chiefsupply.com/sizingchart/Second-Chance-Female.pdf,* (2006).

[111] *http://pacabodyarmor.com/pdf/TruFit2-low.pdf,* (2006).

[112] *Http://www.freepatentsonline.com/4183097.html,* (2006).

[113] *http://www.connectstores.com/mc/sp_35176.html,* (2006).

[114] Amirbayat, J. and Hearle, J.W.S., the Anatomy of Buckling of Textile Fabrics: Drape and Conformability, *Journal of Textile Institute*, 1989. **80**(1): p.51-70.

[115] Busgen, A., Woven 3 Dimensional Shapes - Update and Future Prospects for New Weaving Techniques, *Melliand English*, 1999. p.131.

[116] Tayyar, A.E., Weaving and Evaluation of Dome-shaped Fabrics, PHD Thesis, UMIST, 2002.

[117] Nie, J.B., Lu, S.Y. and Chen, X., Woven Structure and Design, *China Textile Press,* 2004.

[118] Atides, D.G., Woven Structure and Design-Part 1 Single Cloth Construction, *Wira Technology Group Ltd*., 1986.

[119] Chen, X., Lo, W.Y., Tayyar, A.E. and Day, R. J., Mouldability of Angle-interlock Woven Fabrics for Technical Applications, *Textile Research Journal*, 2002. **72**(3): p.195-200.

[120] Naik, N.K., Azad, S.K.N.M. and Prasad, P.D., Stress and Failure Analysis of 3D Angle Interlock Woven Composites, *Journal of Composite Materials*, 2000. **36**(01/2002): p.95.

[121] Ellison, R., Investigation into Bullet Resistant Vests for Female Police Officers, Bachelor Degree Dissertation, University of Manchester, 2002.

[122] Kamiya, R., Cheeseman, B.A., Popper, P. and Chou, T.W., Some Recent Advances in the Fabrication and Design of Three-dimensional Textile Performs: a review, *Composites Science and Technology*, 2000. **60**: p.33-47.

[123] Tan, P., Tong, L.Y., and Steven, G.P., Micromechanics Models for Mechanical and Thermo Mechanical Properties of 3D Through-the-thickness Angle interlock Woven Composites-Part A, *applied science and manufacturing,* 1999. **30A**(5): p.637-648.

[124] Cox, B.N., Dadkhah, M.S., Inman, R.V., Morris, W.L. and Zupon, J., Mechanisms of Compressive Failure in 3D composites, *Acta Metal Mater,*1992**. 40**(12): p.3286.

[125] Roedel, C., Innovation and Analysis of Police Riot Helmets with Continuous Textile Reinforcement for Improved Protection, PHD thesis, University of Manchester,2008.

[126] Sun, B.Z., Gu, B. H. and Ding, X., Compressive Behaviour of 3-D Angle-interlock Woven Fabric Composites at Various Strain Rates, *Polymer Testing*, 2005. **24**(2005)**:** p.447-454.

[127] Sheng, S.Z. and Hoa, S.V., Modelling of 3D Angle-interlock Woven Fabric Composites, *Journal of Thermoplastic Composite Materials,* 2003. **16**(1): p.45-58.

[128] Nie, J.B., Lu, S.Y and Gu, B.H., Fractional Formula Description of Angle-interlock Woven Fabric Construction, *Journal of Industrial Textiles*, 2006**. 36**(2): p.125-132.

[129] Chen, X. and Potiyaraj, P., CAD/CAM of Orthogonal and Angle-interlock Woven Structures for Industrial Applications, *Textile Research Journal,* 1999. **69**(9): p.648-655.

[130] Chen, X., Knox, R.T., McKenna, D.F and Mather, R.R, Relationship between Layer Linkage and Mechanical Properties of 3D Woven Textile Structures, VTT Symposium 133, Textiles and Composites'92,*Technical Research Centre of Finland Espoo,* 1992. **92**(133): p.166-172.

[131] Chen, X., Gisbert, M.S., Paya, J. and Sellabona, P.M., Experimental Studies on the Structure and Mechanical Properties of Multilayer and Angle-interlock Woven Structures, *Journal of Textile Institute,* 1999.**60**(1): p.91-99.

[132] Hearle, J.W.S., Grosberg, P. and Backer, S., Structural Mechanics of Fibers, Yarns, and Fabrics, 1st Edition, *New Work: Wiley-Interscinece,* 1969.

[133] Prodromou, A.G. and Chen, J., On the Relationship between Shear Angle and Wrinkling of Textile Composite Preforms, *Composites: part A*, 1997. **28**(A): p.491-503.

[134] Van West, R., Pipes, R.B. and Keefe, M., A Simulation of the Draping of Bidirectional Fabrics over Arbitrary Surfaces, *Journal of Textile Institution,*1990. **81**(4): p.448-460.

[135] McBride, T.M. and Chen, J., Unit-cell Geometry in Plain-Weave Fabrics during Shear Deformations, *Composite Science and Technology*, 1997. **57**(3): p.345-351.

[136] Liden, E., Berlin, R., Janzon, B., Schantz, B. and Seeman, T., Some Observations relating to Behind-body Armour Blunt Trauma Effects caused by Ballistic Impact, *Journal of Trauma*, 1988. **28**(1): p.s145-148.

[137] Cantwell, W.J. and Morton, J., the Impact Resistance of Composite Materials - a Review, *Composites,* 1991. **22**(5): p.347-362.

[138] John E. Kirkwood, J.E., Keith M.Kirkwood, K.M.,Young Sil Lee, Y.S., Ronald G. Egres, R.G., Wagner, N.J. and Wetzel, E.D., Yarn Pull-out as a Mechanism for Dissipating Ballistic Impact Energy in Kevlar KM-2 Fabric Part II Predicting Ballistic Performance, *Textile Research Journal*, 2004.**74** (11): p.939-948.

[139] Naik, N.K., Shrirao, P. and Reddy, B.C.K., Ballistic Impact Behaviour of Woven Fabric Composites: Formulation, *International Journal of Impact Engineering*, 2006. **32**(9): p.1521-1552.

[140] Backman, M. E. and Goldsmith, W., the Mechanics of Penetration of Projectiles into Targets, *International Journal of Engineering Science*, 1978. **16**(1): p.1-99.

[141] Reedy, J.N., Impact on Laminated Composite Plates: a Review of Recent Computational Developments. Computational Aspects of Penertraton Mechaics, Proc. of the Army Research Office Workshop on Comp. Asp, of Penetration Mechanics, 1983.

[142] Grosicki, Z., Watson's Advanced Textile Design: Compound Woven Structures, 4th Edition, *Butterworth & Co. (publishers) Ltd*, 1977.

[143] Jacobs, M.J.N. and Van Dingene, J.L.J., ibid, 2001. 36: p.3137.

[144] *http://www.absoluteastronomy.com/topics/stress*,(2009).

[145] Tayler, A. B., Mathematical Models in Applies Mechanics, Oxford University Press, 1986.

[146] Aldrich, W., Metric Pattern Cutting, 4th Edition, Blackwell Publishing, 2006.

[147] Sun, L., Research on the Methods of Brassiere's Pattern Design, Msc thesis, Suzhou University, China, 2006.

[148] Mackerle, J., Finite Element Analysis and Simulation of Manufacturing Processes of Composites and Their Mechanical Properties: a Bibliography (1985-2003), Computational Material Science, 2004. **31**(3-4): p.187-219.

Appendix A: original data obtained during the energy loss test

Fabrics	Fabric1		Fabric2		Fabric3		Fabric4		Fabric5		Fabric6	
	t_0*	t_1**	t_0	t_1	t_0	t_1	t_0	t_1	t_0	t_1	t_0	t_1
4LAI12×26	0.981	0.831	0.962	0.801	1.017	0.931	0.958	0.79	0.991	0.869		
4LAI12×28	1.03	0.916	0.962	0.826	1.072	0.919	1.129	0.983	0.939	0.802	0.931	0.776
4LAI12×30	0.957	0.828	0.942	0.778	0.905	0.776	1.009	0.977	1.054	0.986	1.054	0.986
4LAI12×32	1.046	0.967	0.952	0.801	0.912	0.754	0.977	0.846				
5LAI8×26	1.103	1.093	0.948	0.797	1.081	0.904	0.932	0.771	0.993	0.871		
5LAI8×28	0.956	0.823	0.994	0.858	0.94	0.768	1.027	0.837	1.001	0.825		
5LAI8×30	0.915	0.745	1.023	0.929	0.919	0.767	0.934	0.789	0.999	0.835		
5LAI8×32	0.927	0.784	0.894	0.741	1.022	0.812	1.026	0.919				
5LAI10×28	0.944	0.812	0.945	0.815	0.925	0.802						
5LAI10×30	0.867	0.731	1.04	1.016	1.02	0.955	0.9	0.737	0.985	0.862		
5LAI10×32	1.023	0.993	0.946	0.782	0.914	0.778	0.995	0.886	1.045	0.874	0.992	0.884
5LAI12×26	0.956	0.824	0.968	0.838	0.907	0.76	1.101	1.053	0.936	0.799	1.076	1.001
5LAI12×28	0.903	0.756	0.856	0.705	N/A	0	0.987	0.832				
5LAI12×30	N/A	0	0.985	0.877	N/A	0	0.99	0.817	1.017	0.849	0.939	0.788
5LAI12×32	0.924	0.799	0.978	0.875	N/A	0	0.974	0.875	0.968	0.855	0.932	0.815
5LAI12×34	0.932	0.767	0.993	0.841	0.968	0.873	0.958	0.795	0.954	0.8		

t_0*: the time used by the projectile to travel through a pair of detectors before the impact
t_1: the time used by the projectile to travel through a pair of detectors after the impact**